BEHAVIOUR OF UNSTIFFENED COLUMN WEBS IN BOLTED BEAM-TO-COLUMN CONNECTIONS IN BUILDING FRAMES

Grant Keith Youngson

A thesis submitted in partial fulfilment of the requirements of the University of Abertay Dundee for the degree of Doctor of Philosophy

December 2002

I certify that this thesis is the true and accurate version of the thesis approved by the examiners.

Signed [redacted] .. Date 16 June '03

Director of Studies

Acknowledgements

Unfortunately during the course of this research I have had to battle through 2 long and difficult illnesses and therefore this acknowledgement section has extra importance for me as without the support of the people and organisations below I would never have been able to complete this research.

I would therefore like to express my sincere gratitude to my supervisors Dr B. Bose (who sadly has had to retire through serious illness) and Prof. S. Sarkar, for their guidance, encouragement and assistance throughout the course of this investigation. Without their support, it would have been impossible to accomplish the task successfully.

The author would also like to acknowledge the University of Abertay Dundee for providing financial support for the project.

The author would also like to thank all the technical staff of the School of Science and Technology, Messers Husband, Wallace and Thomson for their much valued help and co-operation.

On a more personal level a special thanks goes to my wife for her support and understanding during these stressful times and to my parents for their words of advice and wisdom. Finally thanks also goes to the staff at Ninewells Hospital, Dundee.

Behaviour of Unstiffened Column webs in Bolted Beam-to-Column Connections in Building Frames

Grant Keith Youngson , B. Eng (Hons)

ABSTACT

From various surveys, steel bolted end plate connections are used widely in construction projects throughout the UK. The most popular connections are flush end plated ones with extended end plated ones just behind in popularity. These connections are chosen over other connections types mainly due to their ease of construction and fabrication.

The main objectives of this project was to develop a design philosophy to predict column web failure moments based on a series of full scale tests (flush and extend end plates) carried out at the University of Abertay Dundee.

Buckling of the column web was observed in a large number of the bolted beam-to-column connections tested.

Three dimensional finite element prediction models were developed using the software package ABAQUS, these consisted of 3 flush end plates and 4 extended endplates connections.

Investigation of Eurocode 3-Annex J was also undertaken with emphasis on the 7 connections that failed by column web buckling.

Comparison between the three different prediction methods were investigated, this involved comparing physical test, Eurocode 3 and finite element results (ABAQUS)

List of Tables

List of Figures

Notation

3D CMMP	3D Solid Combined Modified Material Properties
3D SMMP	3D Solid Modified Material Properties
3D SNMMP	3D Solid Non Modified Material Properties
a_b	size of the weld
A	Cross sectional area
A_s	tensile stress area of bolt
A_{vc}	shear area of the column
b_{eff}	effective width of an equivalent T-stub
[B]	Strain Shape function
$B_{t,Rd}$	Tension resistance of bolt
d	diameter of bolt
d_c	depth of column web
[D]	Elastic matrix
e	distance between the bolt and the edge of T-stub
E	Young's modulus of elasticity
EEP	Extended End Plate
F	the relative motions of material particles in the infinitesimal neighbourhood of the material particle that was at X in the reference configuration
FEP	Flush End Plate
fy	Yield strength
$F_{c,fb,Rd}$	design resistance of the beam flange and web in compression
$f_{y,wc}$	yield strength of column web
$F_{c,wc,Rd}$	design resistance of the column web in compression
$F_{t,Rd}$	design tension resistance of an equivalent T-stub flange or end plate
$F_{t,wc,Rd}$	Column web in tension
f_{ub}	ultimate tensile strength of the bolt
h_b	depth of beam
h_r	distance between bolt row r and the centre of compression
h_c	depth of column
[J]	Jacobian matrix
keff,r	effective stiffness coefficient for bolt row r
keq	equivalent stiffness coefficient
k_i	stiffnes of joint element
k_{ir}	stiffness coefficient representing component I relative to bolt row r
$[K^{(e)}]$	Element Stiffness matrix
L	Length of beam
L_b	elongation length of the bolt
l_{eff}	effect length of an equivalent T-stub
m	clear distance between the bolt and the web/flange of T-stub
$M_{c,Rd}$	design moment resistance of the connection
$M_{j,Rd}$	moment resistance of the connection
$M_{pl,1,Rd}$	design plastic moment of resistance for mode 1
$M_{pl,2,Rd}$	design plastic moment of resistance for mode 2
n	e_{min}, n has to be less than 1.25x m

[N]	Column matrix relating to the shape function
$\vec{P}_b^{(e)}$	Vector of element nodal forces produced by body forces
$\vec{P}_i^{(e)}$	Vector of element nodal forces produced by the initial strain
$\vec{P}_s^{(e)}$	Vector of element nodal forces produced by surface forces
ρ	reduction factor
$\vec{Q}^{(e)}$	vector of nodal displacement
r	Part of a co-ordinate system(Natural co-ordinates)
rc	root radius
R	rigid body rotation of the principal direction of strain
s	this is related to type of section either I or H section
S	Part of a co-ordinate system(Natural co-ordinates)
S	Part of a co-ordinate system
S_j	rotation stiffness
$S_{j,ini}$	initial rotation stiffness
t	Part of a co-ordinate system (Natural co-ordinates)
t_{fc}	thickness of the column flange
t_p	thickness of the end plate
t_{fb}	thickness of the beam flange
t_{wb}	thickness of the beam web
t_{wc}	thickness of the column web
u, u_i	Displacement in the x direction
v,v_i	Displacement in the y direction
ν	Poisson's ratio
V	the deformation of the material particles at X
$V_{wp,Rd}$	design shear resistance of a column web panel
w,w_i	Displacement in the z direction
x, X	Part of a co-ordinate system
Y_{MO}	resistance of class 1, 2 or 3 cross-section
Y_{mb}	factor of safety for bolt usually 1.25
z	lever arm
z, Z	Part of a co-ordinate system
β	transformation parameter
ε	Strain
ϕ	Rotation
Ψ	coefficient related to the type of connection being tested
μ	stiffness ratio
σ	Stress
Ω	Stretch ratio
[λ]	(Transformation matrix)

Table of Contents

Introduction

Chapter 1

1.0 Introduction

This report will detail the bolted flush (FEP) and extended end plate (EEP) connections that are generally used in steel construction, examine their behaviour, investigate the ability of Eurocode 3 recommendations and the finite element model using Abaqus to accurately simulate the behaviour.

The research specifically investigates the ability of the analytical techniques to predict the buckling failure that was evident in 7 of the 18 full scale laboratory tests previously undertaken at the University of Abertay Dundee (Bose 1993, Bose 1994 and Wang 1996)

This buckling failure was unexpected as the connections were symmetrically loaded and design concepts (British Standard Institution, 1985) indicate crushing of the column should occur as the normal failure mode (Bose and Hughes, 1995).

1.1 Aims and Objectives of Study

The main aims of this study was to investigate the behaviour of semi rigid end plate connections and to evaluate the different analytical models in existence. The objectives were therefore as follows:

1. To conduct an in depth investigation of Eurocode 3- Annex J and the concepts behind semi rigid design philosophy.
2. To develop numerical models to predict the behaviour of 7 semi rigid end plate connections that failed by buckling.
3. To develop an understanding of T-Stub modelling and compare models with experimental results.
4. To compare numerical model predictions with the failure nodes of the 7 physical tests
5. To compare numerical model predictions with those of Eurocode 3 – Annex J.
6. To study the limitations of software in relation to modelling full-scale semi-rigid end plate connections.

1.2 Methodology Adopted

1. To investigate current on- going research: this involved literature reviews and meetings with other researchers in Europe to collaborate in on-going research studies.
2. Initially working with T-Stub models to both understand the workings of the finite element software (ABAQUS) and increase experience in finite element design concepts. This allowed methodologies to be tested before developing models for full scale connections.
3. Development of shell models to understand how large complex models are constructed. This involved determining how loading was to be applied and construction of various components were to be implemented.

1.3 Structure of Report.

It was considered appropriate that a report which examines the behaviour of bolted end plate connections and the different analytical tools to predict the behaviour should include general information on Bolted End Plate Connections (Chapter 2).

The background to the development of bolted end plate connections, analytical tools and the current research is then summarised in the literature review (Chapter 3). The report continues with a review of the full scale laboratory tests that were examined during this research (Chapter 4).

The report then details the two different analytical techniques that were investigated in depth, specifically Eurocode 3 (Chapter 5) and finite element modelling (Chapter 6). The construction of a basic finite element model using Abaqus is detailed in Chapter 7 followed by information on the full scale models (Chapter 8) and information of the problems associated with using Abaqus (Chapter 9).

The results obtained during the research are evaluated in Chapter 10 with the conclusions and recommendations for future work summarised in Chapter 11.

Introduction to Bolted End Plate Connections

Chapter 2

2.0 Introduction

Bolted connections are used widely within the construction industry according to a local survey (Tayside, Scotland) carried out by Marshall (Marshall, 1993) for many types of applications, from bridges to portal frames. The main interest to this researcher are steel bolted end plate connections, which can withstand loadings that cause shear and moments. The different types of connections that can be used in the construction industry will be discussed later in this chapter.

From the 1950's, a better understanding of bolted connections had developed through extensive full-scale testing. Physical testing in the past was the only recognised way of being able to determine the ultimate strength of bolted end plate connections, but this was very costly to implement. A way had to be found to reduce this reliance on testing and thus make bolted connections more popular within the construction industry.

Before the development of the bolted connection, rivets were the most commonly used medium for connections. Rivets had major disadvantages, not just in materials required (many rivets) but the fire hazards, as the rivets had to be red hot before placement; specialised machinery was therefore needed. The personnel would also have to be specially trained to use the machinery thus incurring considerable extra costs in the building of the structure.

2.1 Bolted End plate Connections

With the renewed interest in bolted connections, (because of their ease of construction and cost) more efficient and economical methods for the design of bolted end plate connections had to be examined.

The end plate " must be of sufficient thickness to transmit the necessary force. Also it must not be so stiff otherwise the predominate failure mode is by bolt fracture" [P38 (Tong,1985)]

The perceived advantages of bolted end plate connections over other types of connections, T-stub angle and rivet connections (Wang, 1996) are shown below:-

1. Saving in material weight and fabrication costs.

2. Reduced number of detail pieces to handle.
3. Alignment with connecting members not affected by variations in the depth of the beams used.
4. Workmanship is simpler when all drilling is confined to plates which are then welded to beams i.e. faster to erect.
5. Less specialised construction personnel required and therefore a reduction in construction overheads.

2.2 Classification of Connections

There are three types of connection that exist and the following is a brief description of each

2.2.1 Rigid Connections

A large proportion of moment in a span is taken by the connection with very little transferred to the beam (Figure 2.1). The beams are consequently smaller than those with pinned connections, but have to be of sufficient strength that they do not fold under their own weight.

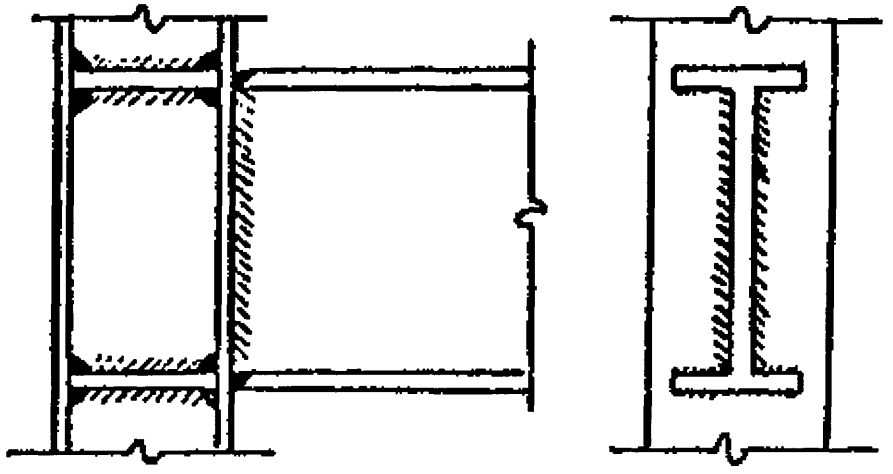

Figure 2.1: Example of Rigid Connection, Directly welded connection with stiffeners (Marshall, 1993)

2.2.2 Flexible (Pinned) Connections

Very large beams are used to withstand the moments applied, very little of the moment being transferred to the end connections. Pinned connections are the opposite of the fully rigid connection. (Figure 2.2)

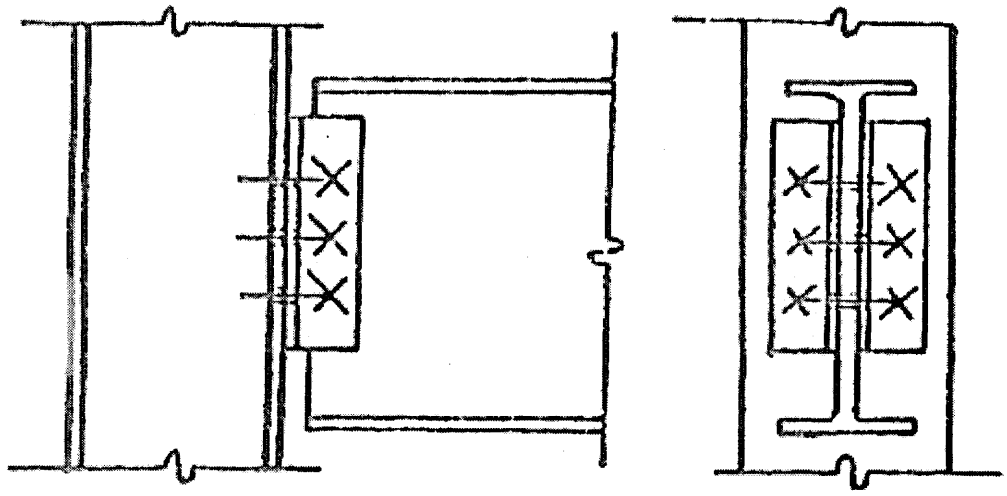

Figure 2.2: Example of Flexible connection, Angle Web Cleat (Marshall, 1993)

2.2.3 Semi-Rigid Connection

The applied moment in a span is shared between the beam and the connection, thus distribution of the load occurs. (Figure 2.3)

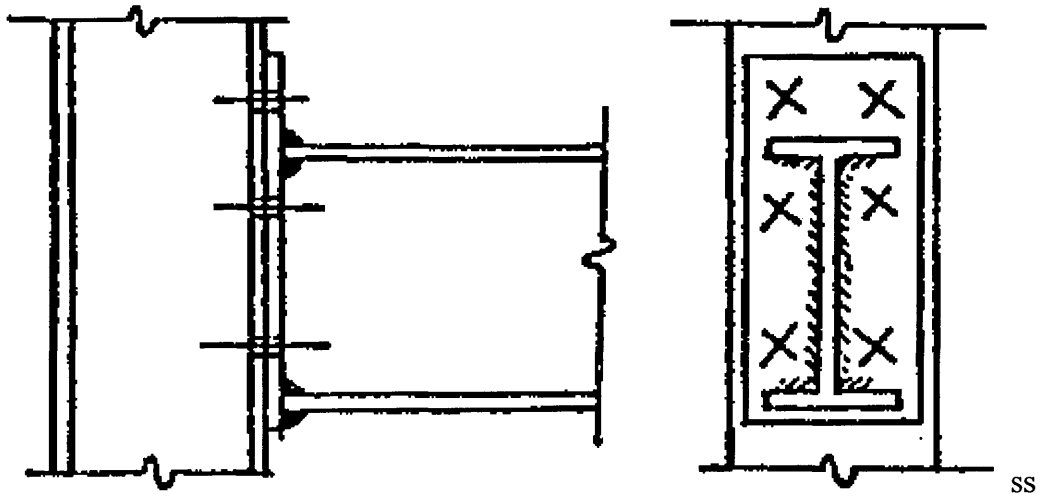

Figure 2.3: Example of Semi Rigid connection, Extended end plate connection (Marshall, 1993)

Semi-Rigid connections combining the benefits of rigid and flexible types are at present the most popular type of connection. The main difficulty with semi-rigid connections has been developing a safe design method that is both easy to use and understand and cost effective. The contribution by the individual components of the connection to the stiffness and moment resisting characteristics is very complex as many researchers have found out.

2.3 Failure of Bolted End Plate Connections

Bolts and welds within the connection generally behave in a brittle manner; this type of failure is unwanted by the designer as very little warning to failure is present. A balance therefore has to be made between the various components, of major importance being the endplate and specifically the thickness of the endplate. Thick end plates can cause failure in the bolts with very little bending in the end plate causing higher stresses to develop in the bolt and thereby increasing the possibility of bolt failure. Thin end plates cause relatively smaller stress in the bolt but the displacement and rotation in the end plate would be high thus restricting their use in all but the most specialised situations.

Semi-rigid connections can fail at loads significantly smaller than the theoretical loads predicted by the various design methods due to the failure of the column web (buckling). The usual solution is to place stiffeners near the points of loading on the column flange i.e. where the bolts are placed; this however incurs an increase in costs. The placement of the stiffeners can be complicated and time consuming to fit; the cost of the extra material and associated fabrication also cannot be discounted.

2.4 Types of Semi-Rigid Bolted End Plates

The two main types of semi-rigid connections that are commonly used in the industry (Marshall ,1993) are:-

1. Flush end plate (FEP),
2. Extended End Plate (EEP)

2.4.1 Flush End Plate

FEP (Figure 2.4) connections are normally used to withstand small to medium loadings. There is little extension of the end plate past the beam flange and the bolts

are within the confines of the beam flange. Therefore only small lever arms are present and thus smaller restraining moments are produced.

2.4.2 Extended End Plates

When high strength and greater stiffness are required, the normal option would be the EEP (Figure 2.5). The end plate extends past the beam flange on the tension side to allow bolts to be placed outside the confines of the beam flanges. The bolts on the extended part of the connection supply a considerable restraining moment due to the increased lever arm. Bolt row 1 normally applies the highest restraining moment due to the high lever arm [bolt row 1 is normally taken as the furthest from the centre of the beam]. This is the bolt row that is affected most by the applied load i.e. higher stresses are induced within the bolt and normally it is the first row that fails in the connection.

In end plates connections, both flush and extended, moments are transferred by the interaction between the column, beams and bolts. This produces a combination of tensile and compressive forces within the connection. The interaction between the various components, specifically the end plate and column flange is very complex and difficult to understand.

Over the last 10 years, much development work has been on going in order to produce a unified approach to the design of semi-rigid bolted connections.

As the Europe-wide construction industry is becoming more integrated, the designers schooled in the various partner countries must be able to work anywhere in Europe. The main concern for the designer is the multitude of codes that exists for connection design which are all slightly different in minor but important details such as factor of safety etc.

Therefore a united strategy has been formulated to produce one European Code, Eurocode 3 (British Standard Institution , 1995), see Chapter 5 for details of Eurocode 3-Annex J. Eurocode 3 exists as a draft at present until the engineers in each country involved resolve the various problems inherent to such an undertaking.

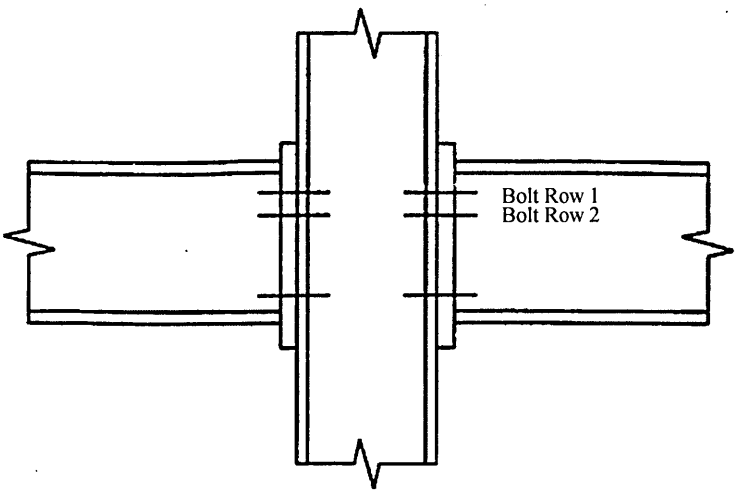

Figure 2.4: FEP

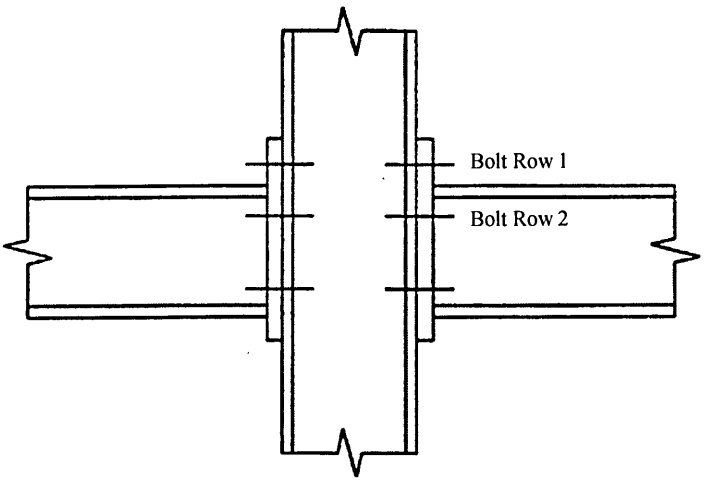

Figure 2.5: EEP

Literature Review

Chapter 3

3.0 Mankind and Construction

Throughout the ages, man has been inspired to create. Engineering design has always been at the forefront of evolution from the pre-history to modern times e.g. the Great Wall of China or the Pyramids in Egypt to the Millennium Bridge in the 21st Century. These all relied on the application of engineering and innovative techniques to solve the challenges that arose.

Conurbations arose and over time new and better building materials evolved from the traditional stone and wood, progressing to iron and bronze. Today, there are various grades of steel available and it is one of the main structural materials in most large scale constructions. Because of the improved and advanced properties of this material, buildings have become bigger, more slender, more complex, arguably more cost-effective and by and large, better. In order to utilise these materials to their full potential a better understanding of how the whole structure behaves, the interaction of the component elements and the overall stability have become of paramount importance in order that the designs can be both structurally sound and economically viable and to ensure the continual evolution of building design.

The stability of the structure depends on the integrity of the design, the component elements and their connections, which means that the holistic approach to the design must be supported by the detailed design of the elements involved. For a steel building structure this will mean a high standard of design of both the large components such as floor, beam and column elements, right down to individual bolts in the connection. Considerable research and resources have been poured into providing a better understanding of structural behaviour of the connection. One such aspect is the bolted connection widely used in the steel construction industry (Marshall, 1993). Structural connections are employed in a myriad of applications from bridges and portal frames to high rise buildings.

Detailed investigations by previous researchers (Sherbourne, 1961; Douty and McGuire, 1965; Bailey, 1970) have shown that understanding the behaviour of

connections is vital to the successful completion of any design project. This current research further explores the importance of these connections and the means and methods employed to improve the design of connections and their stability.

The main interest to the researcher is the bolted end-plate beam to column connections as illustrated in figure 3.1, which can withstand the most commonly occurring loading such as wind, dead and imposed loads in the static domain. This chapter details why this type of connection has been the focus of this research.

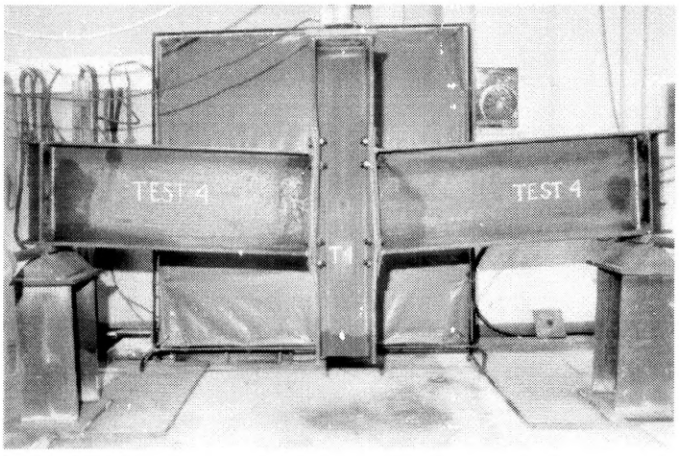

Figure 3.1: Example of a steel bolted connection

Bolted connections were the subject of extensive testing programmes (Graham et al. 1959; Schultz, 1959) in the 1950's. In that time full scale testing was the only recognised way of being able to determine the ultimate load capacity of bolted end plate connections. This test method allowed the designers to see the end result of their design. However the costs involved meant that an alternative technique had to be found to reduce this cost in order for bolted connections to be a viable option within the construction industry.

The motivation for the determination of alternative test methods was that the riveted connections prevalent at the time had several major disadvantages. Specifically:

- Fire hazards, rivets had to be red hot before placement.

- Requirement of specialised machinery
- Requirement of experienced personnel
- Uncertainty of the quality

In comparison bolted connections were easier to construct, with the exception of the costly testing techniques utilised, they involved a lower cost. Therefore if a suitable testing technique could be found they would be economic.

Bolted end plate connections have several advantages over other types of connections (Wang, 1996) and these are as below:

- Saving in material weight and fabrication costs.
- Reduced number of detail pieces to handle.
- Alignment with connecting members not affected by variations in the depth of the beams used.
- Workmanship required is simpler where drilling is confined to the end plates which are then welded to beams
- Therefore the erection is simpler and faster.
- Less specialised construction personnel required and therefore a reduction in construction overheads.

These advantages illustrate why bolted end plate connections are an important building component and in order to optimise their use, it is necessary to fully understand all the characteristics of the different end plate types (Detailed in section 3.1 below)

3.1 Classification of Bolted End Plate Connections

There are three classifications of bolted end plate connection that are presently in use and the following is a brief description of each:

At present several different types of bolted end plate connections exist (figure 3.2).

Figure 3.2a: shear beam-column connection used in the Ottawa Palladium structure

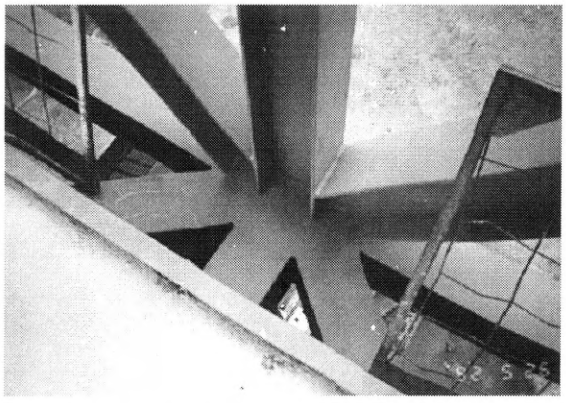

Figure 3.2b: moment connection used in the steel bridge linking the two wings of the Ottawa City Hall extension

Figure 3.2: Various types of connections

3.1.1 Rigid Connections: The columns are generally stiff and the connection details allow large moments to be taken by the column- beam connection and then transferred to the beam ends resulting in relatively small moments being transferred to the beam span. (Figure 3.3a) The beams are usually lighter in a rigidly connected

frame when compared with beams in a pinned connection with the proviso that they have sufficient strength so as not fail under their own weight.

3.1.2 Flexible (Pinned) Connections: These connections occur in structures when very large beam sections are used to withstand the moments applied and very little of the moment is allowed to be transferred to the end connections. These connections are used in fully braced frames which do not require moments to be carried by the joints. Pinned connections are the opposite of the fully rigid connections. (Figure 3.3b).

3.1.3 Semi-Rigid Connection: As the name suggests in this type of connection the moments are more evenly shared between the ends and the span of the beams and therefore the sizes of the beams and the columns are more evenly balanced. (Figure 3.3c)

Figure 3.3a: Model of fixed end connections

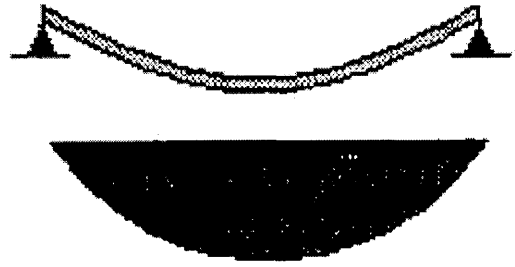

Figure 3.3b: Model of pinned connections

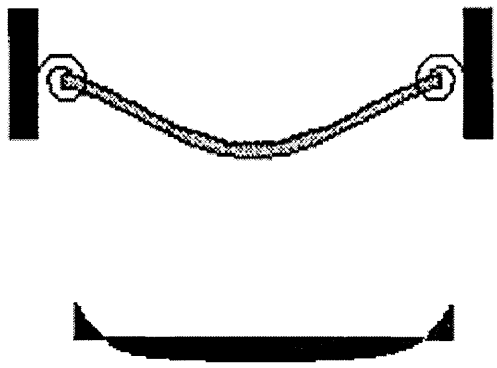

Figure 3.3c: Model of semi-rigid connections

Figure 3.3: Models of the various types of connections

Semi-rigid connections are the most popular type of connection with the structural designers and architects, as they offer greater freedom in the choice of structural configuration combining the benefits of rigidity and flexibility. However, the main difficulty with semi-rigid connections has been in the development of a safe design method that is easy to understand and use, and ultimately is cost effective.

A semi-rigid connection comprises:

- column: flanges, web
- beams: flanges, webs
- end plates
- bolts (number of bolts depends on the type of connection, normally 8 bolts)
- welds.

The mode of contribution by the individual components of the connection to the stiffness and moment resisting characteristics is very complex as many researchers have observed (Jaspart and Maquoi, 1994; Eurocode 3 (British Standard Institution), 1995) (see later in the chapter for more detailed discussions).

3.1.3.1 Types of Semi-Rigid Bolted End Plate Connections

The two main semi-rigid connections that are commonly used in the industry (Marshall, 1993) are:

- Flush end plate (FEP), and
- Extended end plate (EEP).

(a) Flush End-Plate Connections

Please refer to Chapter 2, section 2.4.1 for details

(b) Extended End-Plates Connections

Please refer to Chapter 2, section 2.4.2 for details

Within the beam-column connections, both flush and extended plates, moments are shared between the column, beams and bolts. This produces a mixture of tensile and compressive stresses within the column. The interaction between the various components, specifically the end plate and column flange, is extremely complex.

Over the last decade much development work has been on going in order to produce a unified approach to the design of semi-rigid bolted connections(Toma et al. 1993; Kishi et al. 1993).

The work at the University of Abertay Dundee has for many years centred on the behaviour of semi-rigid steel bolted connections; therefore, considerable experimental data and experience have been accumulated within the University. Substantial experimental work involving full-scale load testing to failure was carried out, for individual research and consultancy and this work has been discussed elsewhere (Bose and Hughes, 1995; Bose et al. 1995; Bose et al. 1997; Wang, 1996)

As a consequence of understanding the behaviour of the connections the researchers appreciate that improvements to the complicated design codes must be instigated. Having become acquainted with the background of experimental and theoretical research, it was concluded that improvements had to be sought to further expand the knowledge base, understanding and applicability of the methods.

Therefore a holistic design approach was required, in order to understand the behaviour and contribution of each element in the connection.

As the Europe wide construction industry is becoming more integrated, the designers schooled in the various countries have to be able to work anywhere in Europe. In the structural industry, the main concern for the designer is the multitude of codes that exists for connection design. Each code differs from the other in minor but important details and this fact has been the main hindrance in the integration. After considerable deliberations over the years a strategy has now been formulated to produce one unified European Code, Eurocode 3 (British Standard Institution, 1995).

Designers presently are using the code in conjunction with existing national codes and improvements are currently in hand. This code is based on a wide ranging design philosophy. The new concept of component method (each connection is seen as individual components that will behave in a certain manner depending on loading conditions) is introduced by Eurocode 3- Annex J, which is based on the well founded principles of yield line analysis.

3.2 Yield Line Method of Analysis

Full scale physical testing was the standard recognised method of predicting the behaviour of bolted endplate connections, due to the complicated interactions that are inherent in these types of connections.

However, as complex connections became more widely used, it was necessary to determine ways to predict their behaviour without resorting to expensive and time consuming physical tests. Additionally, the high costs involved in physical testing increases as one attempts to cover every eventuality.

The method that was eventually adopted was the yield line analysis method, based on the original method proposed by Johansen (British Standard Institution, 1998) for the design and analysis of reinforced concrete flat floor slabs. Yield Line analysis is based on the principle that a flat structural surface under transverse loading produces a yield surface consisting of a pattern of yield lines, where the yield line is defined as: *"a continuous formation of plastic hinges along a straight line"* (British Standard Institution, 1998, P294).

The yield line method is an upper bound solution and therefore has to be viewed with caution in that all the possible mechanisms of failure must be investigated so that the predicted failure mode is accurate. Many authors have researched the use of yield line analysis for steel bolted connections, usually in conjunction with other methods, such as the finite element analysis, and the following review is conducted to investigate this development.

Schutz's (Schutz, 1959) investigations of the behaviour of steel connections using T-Stubs (Figure 3.4) centred on the development of the theory of "prying forces". A simple procedure was developed for examining the prying force, and physical tests were used as a comparison for the design. This theory related to the interaction between the deformed end plate and the column flange due to the loading applied; this investigation included 6 physical tests. The testing of the connections involved 6 full scale connections, with load applied vertically to the column, as in figure 3.5. The author hoped that the information obtained during the tests would lead to a better understanding of connection behaviour. After comparing the experimental results with those predicted by the theory, Schutz concluded that this method of design produced acceptable results and the connections were both easier to construct and more economical than that produced using existing codes.

Douty et al (Douty and McGuire, 1965) took Schutz's designs a stage further and investigated end plate connections. The authors carried out 7 full scale tests. The relationship between the bolts and the thickness of the end plate was also studied. The authors concluded that:

"the elongation of the lowest bolt row was less than the fracture value at the time the upper row entered the ultimate load plateau"[(Douty and McGuire, 1965) P121], where, the upper bolt row is the row above the beam flange and the lower one is the bolt row below the beam flange (See Chapter 2 figure 2.5). Even although the authors recognised that the number of tests were few, they hypothesised that: "the bolts and the part of the end plate symmetrical about the tension flange of the beam may be treated as an equivalent T-stub " [(Douty and McGuire, 1965) p126]. This approach

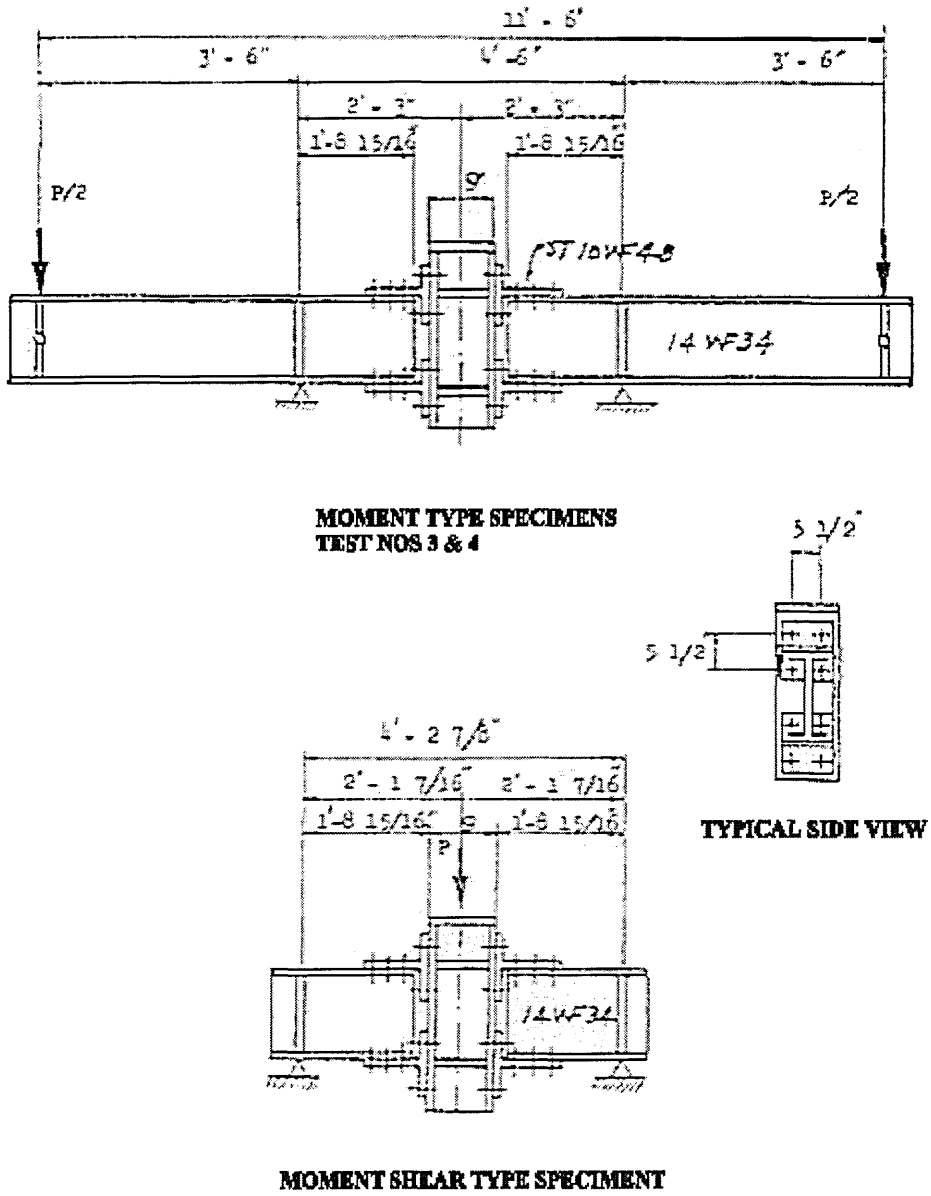

Figure 3.4: Schutz (Schutz, 1959) detailing example test specimens used.

has now become a standard method in analysing bolted end plate connections, i.e. end plate connection designed as an equivalent T-stub (figure 3.6). Their study was related to Schutz's and comparing the results, they concluded that the thickness of the

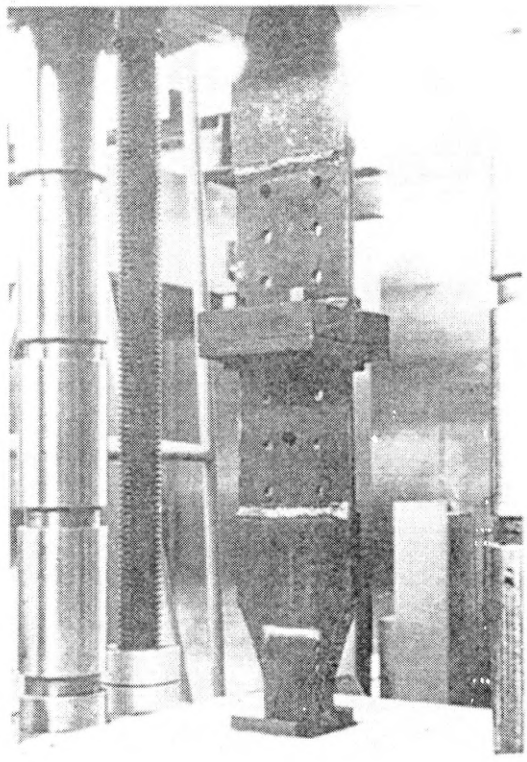

Figure 3.5: Detailing how Schutz (Schutz, 1959) carried out testing of T-Stub connections.

beam flanges plays an important part in the development of the prying force. They further concluded that EEPs are structurally more efficient due to the greater lever arm inherent in the configuration.

Mann (Mann, 1968) reported on this investigation into plastic design of end plate connections and the failure of exterior connections. This research utilised yield line method of analysis (figure 3.7) to determine the failure of exterior (figure 3.8a) connections. Mann stated that : "ideally the greater part of the rotation should occur in the yielded portion of the adjoining beam and in deformation of the column flanges where risk of brittle failure is small" [p73 (Mann, 1968)] The author noted from the investigation that failure of the connection was imminent with the on-set of yielding in the end plate.

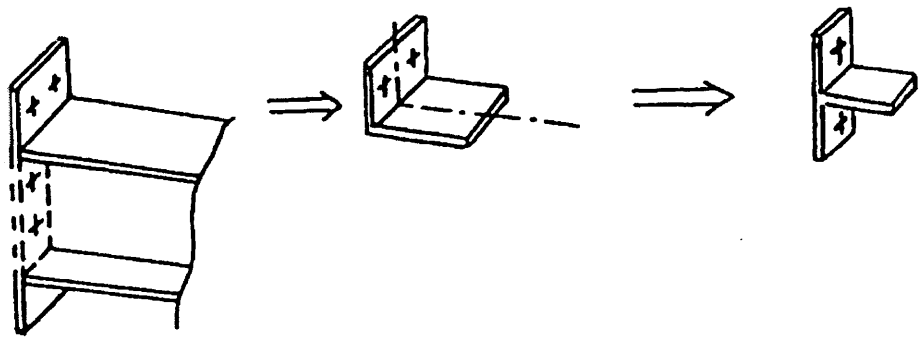

Figure 3.6a: Modelling an Extended plate as separate T-stubs, as defined in Eurocode 3-Annex J (British Standard Institution, 1995).

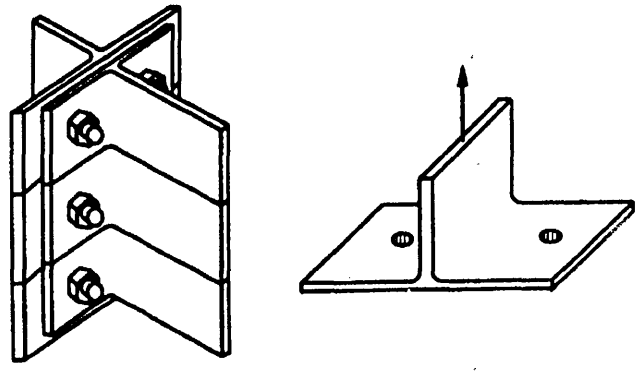

Figure 3.6b: A connection modelled as a series of T-stub's

Figure 3.6: Various T-stub models

Mann and Surtees (Surtees and Mann, 1970) tested 6 connections to provide a basis for their design method. Various objectives were set out at the outset of the tests in order that different aspects of connection behaviour could be observed and noted. Two different methods of measurement were used to ensure the accuracy of the results:

- optical: using mirrors attached to various areas of the section
- mechanical: dial gauges.

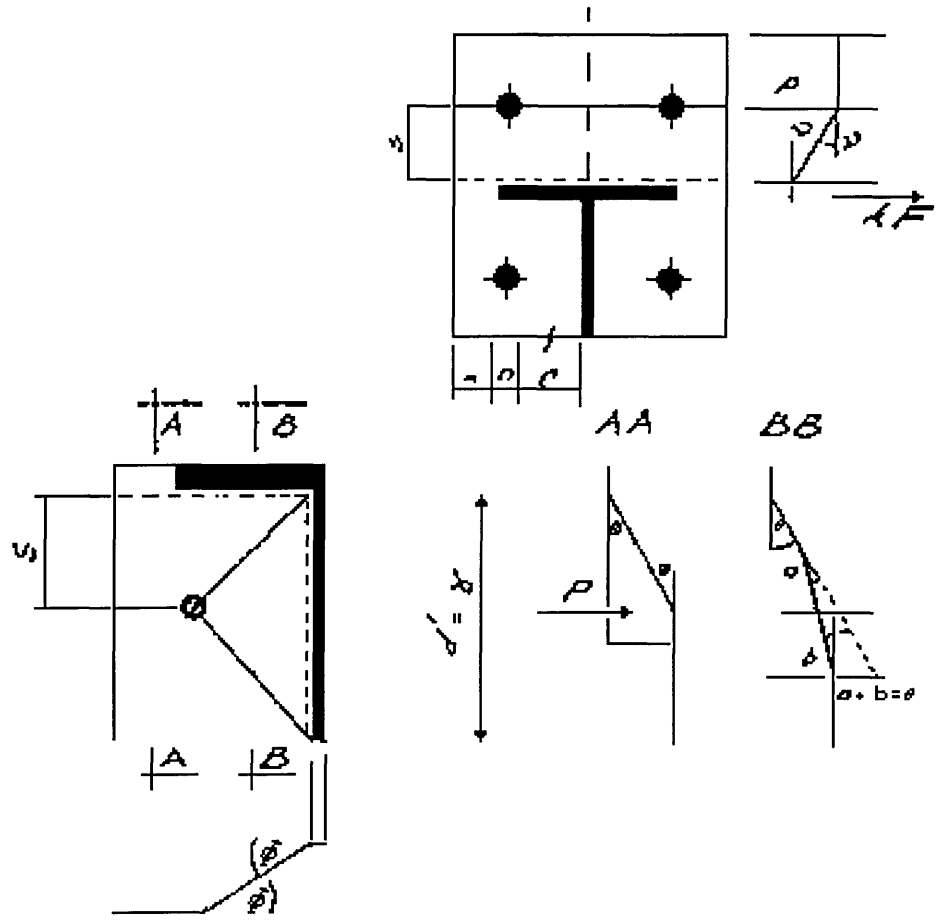

Figure 3.7: Details of the yield lines adopted by Mann (Mann, 1968)

Carbon paper was used between the column flange and the end plate in order to obtain the final contact imprint representing the pressure distribution at failure.

The authors produced a table detailing the contribution of the various elements that affect the rotation of the connection:

The hinge locations formed during the test are detailed in figure 3.9. This figure was subsequently used to determine the yield line patterns. The design method produced related to multi-storey frames. The authors had investigated the failure of exterior end

.

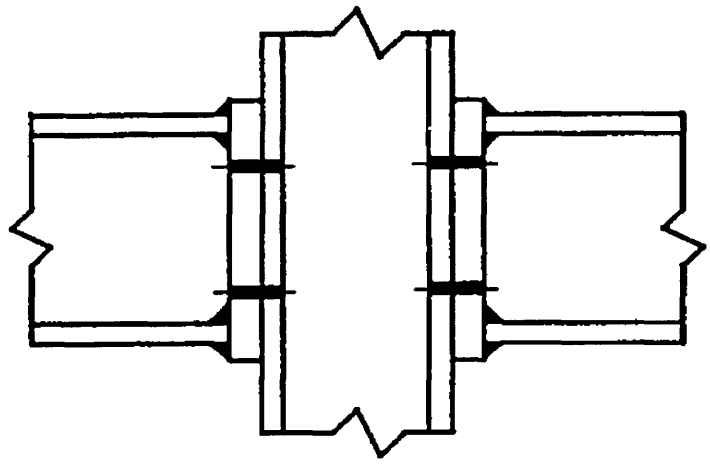

Figure 3.8a: Example of interior bolted connection

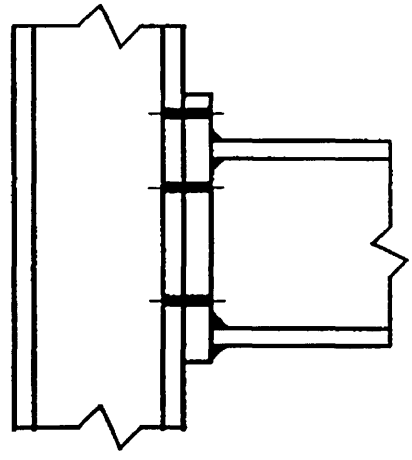

Figure 3.8b: Example of exterior bolted connection

Figure 3.8: Details of different types of connections

plate connections and therefore the column web shear played an important part in the design of their connections. The other conclusions drawn related to any bolted end

Element contribution to overall rotation of connection	% Contribution to total rotation
Shear deformation in column web	50
End plate flexure	18
column flange flexure	17
Tensile strain in column web	6
Compressive strain in column web and stiffener	9

Table 3.1: Contribution of the elements to the joint rotation

plate connection, especially the rotation required in the connection to allow the full plastic moment to be attained.

At about the same time, Chen and Oppenheim (Chen and Oppenhiem, 1970) examined the equations that were presented in the ASIC specification (American Institute of Steel Construction, 1969) relating to column web. They wanted to verify the effect of "column web depth-to thickness ratio" and its relationship to instability. The authors carried out a series of 9 tests to examine this effect. Yield patterns were detailed with specific emphasis on where the maximum distortions developed. The authors concluded that the existing codes at the time (American Institute of Steel Construction, 1969) were sufficient for safe design, maybe even conservative.

Stockwell's (Stockwell, 1974) investigations centred on using yield line analysis to predict the behaviour of the column web in welded beam connections. Various design assumptions were also stated by the author in order that yield line analysis could be used. Specifically:

1. Nominal size is assumed for beam groupings
2. The assumed yield pattern as shown in figure 3.10 and all lines are stressed to f_y of the column.
3. The sum of the length of lines 4 and 5 is assumed to equal the length of line 3 and the individual angles in between are assumed to be the same. (figure 3.10)
4. The web surface enclosed by lines 1 and 4 remains plane (figure 3.10)

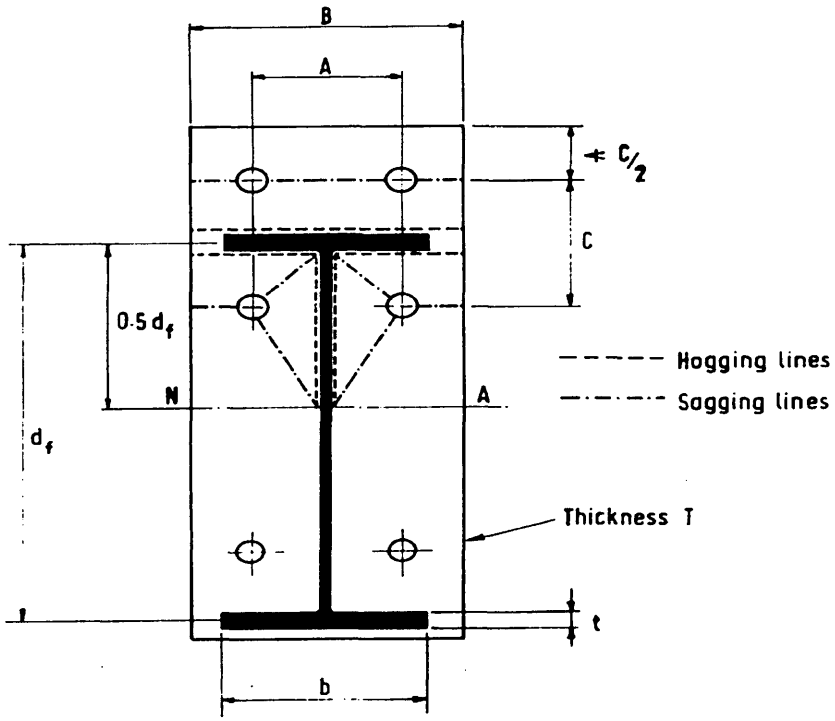

Figure 3.9: Location of Hinges as adopted by Surtees (Surtees and Mann, 1970)

The design method with emphasis on producing design curves was explained in detail which related column web thickness to moment capacity.

A detailed analysis using the yield line method was also carried out by Zoetemeijer(Zoetermeijer, 1974) on bolted beam to column connections. Two different methods of failure were discussed: bolt failure, and collapse resulting from the full plastification of the column flanges. 28 tests were carried out to verify the design method proposed by the author, both for the T-stub model and the effective length of the column that should be used in design modelling. The discussion relating to the effective length of the column centred on allowing the behaviour of the connection to fully develop. Therefore one of the two collapse mechanisms must be allowed to form (figure 3.11), bolt failure (mechanism 1) or collapse which results from failure of the flanges (mechanism 2). Plastic method of analysis was used to

derive the equations for the T-stub behaviour and three mechanisms of failure were discussed by the author:

- flange failure
- bolt failure
- combination of the two above

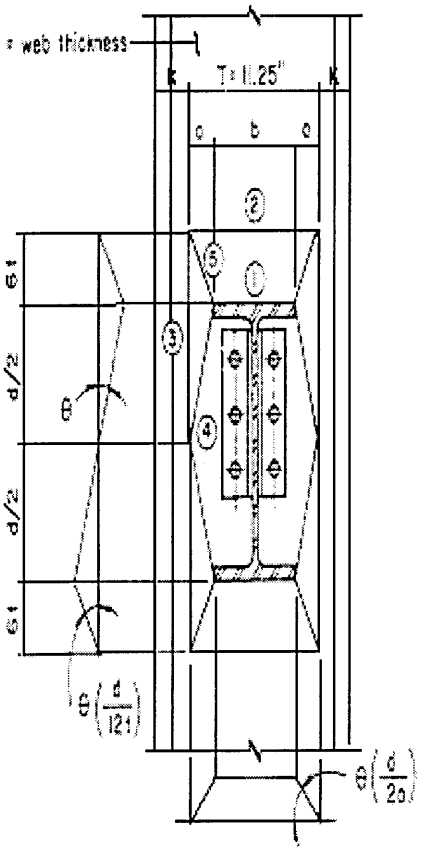

Figure 3.10: Yield pattern as defined by Stockwell (Stockwell, 1974)

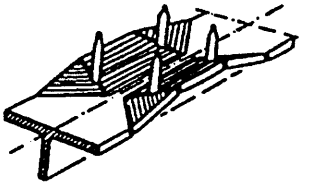

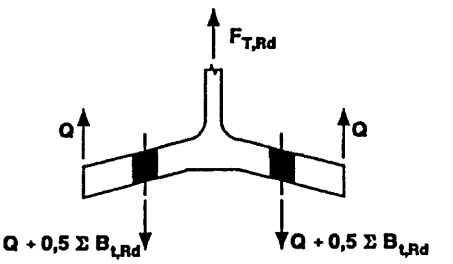

Figure 3.11a: Mode 1: Bolt failure with yielding of the flange

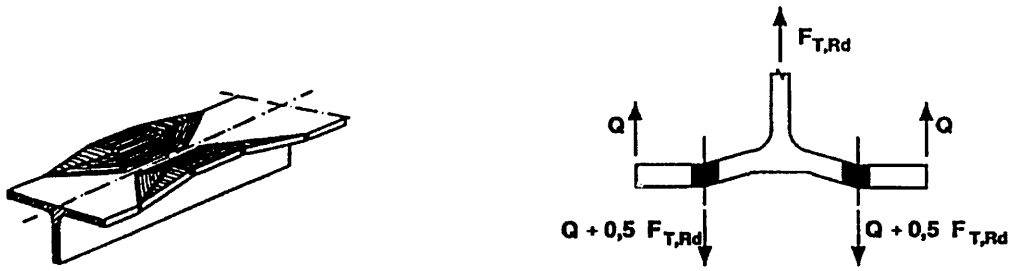

Figure 3.11b: Mode 2: Bolt failure with complete yielding of flange

Figure 3.11: Showing mode 1 and mode 2 failures

The author concluded that "one is free to choose the desired collapse mechanism and consequently the plate thickness and bolt diameter within certain limits"[(Zoetermeijer, 1974, P13]

He advocated the use of common sense and experience in choosing a particular combination, i.e. not to make the plate too thick, otherwise bolt strains would be too high, and not to make the plate too thin. A further recommendation was the use of standard size bolts in the plate, otherwise problems will result with the T-stub itself, which could lead in turn to shearing due to the bolt being too strong for a thin end plate.

The behaviour of bolted end plate connections was of major interest to Agerskov (Agerskov, 1976; Agerskov, 1977). In conjunction with the analytical study, the author tested 19 connections to verify the results. The analytical study centred on where and how the yielding of certain areas occurred. Agerskov discusses the effect of prying in bolted connections using the now standard method of equivalent T-stubs. Several conclusions were drawn by the author including how the prying force would increase, with the increase in any or all of the following:

1. the distance from the bolt line to the toe of the fillet;
2. the bolt diameter ; and
3. the yield stress of bolt material.

These test results were also compared with the existing American National codes and the code recommendations were found tc be very conservative. The author suggested that the simple design procedure developed by him was sufficient for safe and economic connections.

Morris and Packer (Morris and Packer, 1977) developed a modified version of the yield line theory based on curved yield lines (figure 3.12), with comprehensive derivations of yield line patterns dealing principally with the failure of column flanges were discussed. The design method proposed related to interior connections with balanced loads i.e. no shear distortion. To take account of the prying action, the bolt load was increased by 33 %, as there was no inclusion of this in the equations developed by the authors.

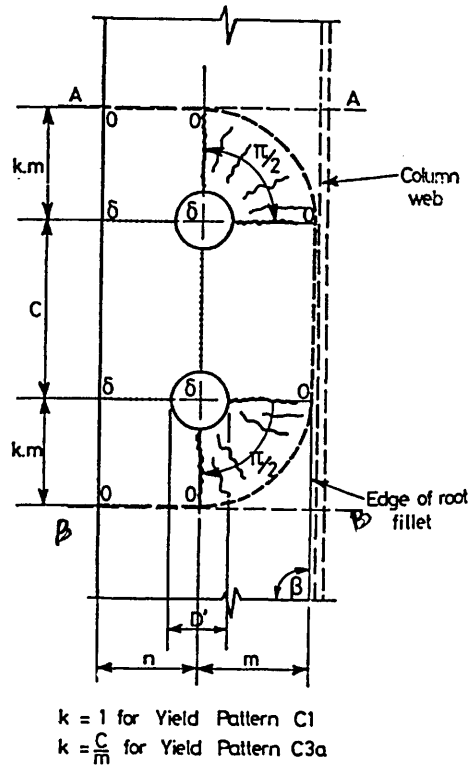

Figure 3.12: Curved yield pattern adopted by Morris (Morris and Packer, 1977)

Based on the results of several research programmes, Mann and Morris (Mann and Morris, 1979) attempted to establish a better understanding of EEP design. The effect rotation has on the development of the forces within a connection was considered to

be of paramount importance. They established that there were certain requirements for plastic conditions to occur: "First, they must be strong enough to withstand hinge moments and second, they must provide adequate hinge rotations while sustaining these moments [Mann and Morris, 1979, p512]". The authors also suggested modifications to other existing design methods particularly that by Surtees and Mann (Surtees and Mann, 1970). The basis of these recommendations was to improve the yield line method first developed by the above researchers. Figure 3.13 shows the modified yield line pattern developed by Mann and Surtees for both end plates and column flanges. The column flange patterns were curved to give a lower bound solution for the analysis. A simple design method was developed which the authors hoped would allow the designer to have a better understanding of connection design and thus increase economies in the design of these type of connections.

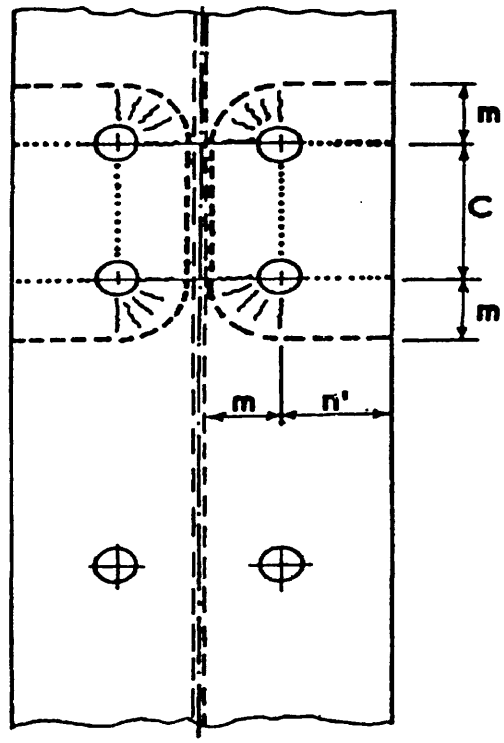

Figure 3.13: Yield pattern adopted by Mann and Morris (Mann and Morris, 1979)

With the introduction of new connections, detailed investigations to understand the behaviour of semi-rigid connections became vital. The investigation by Zoetemeijer (Zoetermeijer, 1981) was just such a study. Yield line analysis was used, based on earlier research carried out by Douty (Douty and McGuire, 1965), with special emphasis on the plastic design assumptions required.

The method developed by Zoetemeijer related the following to connection behaviour:

- Strength
- Stiffness
- Deformation capacity

The author recognised that only through a comprehensive test programme could this be achieved and therefore 38 tests were carried out in support of the analytical approach. Many yield line patterns were analysed in order to obtain the lowest failure loads and design charts were produced which were to be used only as a guide. The author stated that, no matter what the results produced in any of the theoretical calculations, physical tests were also required to backup the results due to the complex nature of semi-rigid connections.

As design methods were becoming more complex and researchers found ways to improve the accuracy of their models, an easier way to understand the process was required in order that designers could use these new design concepts. Yee and Melchers (Yee, L. and Melchers, 1984) assembled a method that they felt was suitable for this approach producing moment-rotation curves for bolted connections. The authors knew that extensive testing to validate all the different designs would be unrealistic on cost terms alone. They stated: " It seems more appropriate to obtain the moment-rotation curves through the use of mathematical models" [(Yee, L. and Melchers, 1984, P615]

The failure of bolted end plate connections were studied and the authors concluded that the following failure modes could occur in semi-rigid connections:

1. Bolt failure (tension)
2. Formation of end plate plastic mechanism

3. Formation of column flange plastic mechanism
4. Shear yielding of the column [exterior connections]
5. Web buckling
6. Web crippling

The different failure modes were related in terms of tension and compression forces within the flanges. Some failure modes are only relevant to compression and others to tension [Such as web buckling and column flange failure respectively]. The use of curved yield line patterns allowed the lowest failure load to be obtained for a future design method. To verify the new model, 16 specimens were tested to acquire the moment-rotation data. Reasonable predictions were obtained with the model, and the authors stated: "It was found that the moment-rotation curves are predicted within acceptable limits by the model provided that the connections are properly designed for strength criteria"[(Yee, L. and Melchers, 1984, P633]

With the myriad of connections available to the designer and all the different methods available for designing them, a standard method of design was required to encompass all the different facets. A new approach was required. Maquoi and Jaspart (Jaspart and Maquoi, 1994) attempted to do this by introducing the concept of component method by splitting the connection into its components.

The component method of analysis can be summed up by the following quote. "A joint is generally considered as a whole and is studied accordingly; the originality of the component method is to consider any joint as a set of individual basic components" (Jaspart and Maquoi, 1994, P1) To link the various design models together, other researchers' work was discussed and their design philosophies were used, such as Douty (Douty and McGuire, 1965) and Yee et al(Yee, L. and Melchers, 1984). These design methods all relied on yield line theory and the assumption that the column flange and the end plate in bending act as equivalent T-stubs connected together.

Connection behaviour was broken down in to 4 main sections:

- Initial stiffness
- The design resistance

- The strain-hardening stiffness
- The ultimate resistance

This method formed the basis for Eurocode 3-Annex J (British Standard Institution, 1995), which is discussed in greater detail within Chapter 5.

The paper by Bose and Hughes (Bose and Hughes, 1995) used the data from tests carried out at the University of Abertay Dundee to verify standard ductile connections (Bose, 1993; Bose, 1994). Specific areas of connection design and behaviour were investigated by the authors including failure due to column web buckling and the ductility of connections. Values were suggested concerning the minimum rotations required for plastic analysis and thus allow redistribution to take place between components within the connection. Conclusions concerning the rotation capacity of the overall connection were discussed with emphasis on large beams. Some of the connections with larger beams failed to achieve the capacity that was considered acceptable by the authors. The minimum rotation that could be seen as acceptable for plastic analysis was 0.03, this value being based both on their results and other researchers conclusions (Surtees and Mann, 1970).

A follow-up paper by Bose et al (Bose et al. 1995) compared the results of 18 tests (Bose, 1993; Bose, 1994) with Eurocode 3- Annex J(British Standard Institution, 1995). All aspects of the connection behaviour were investigated, including failure modes, rotation capacity and stiffness and these were compared with the Eurocode 3 Annex J results. The accuracy of the prediction method of Eurocode 3 was also considered, with discussions relating to the behaviour of the column web and how this could fail. The authors noted that the code did not take account of buckling behaviour within its remit, which was observed when comparisons were made with experimental and theoretical results. They observed that the rotation capacity of the connection derived within Eurocode 3 was incomplete in its assumptions, stating that if failure occurs in a particular component [e.g. column web], then the connection was deemed able to achieve sufficient rotation. The authors mention Surtees's (Surtees and Mann, 1970) paper and follow through a method for determining 0.03 [rotation] as sufficient for plastic hinges to form.

In the paper by Shi et al(Shi and Wong, 1996), modelling of end plate connections was proposed in which the authors investigated the moment-rotation characteristics. The authors used Eurocode 3 as the basis for their design method using equivalent T-stubs. The model developed by the authors did not require calibration to determine the moment-rotation characteristics of the connection. The design method produced results that were within 10% of those using Eurocode 3-Annex J.

As can be seen from the above there have been many researchers involved both in the past and present in the design of end plate connections. Their goals were to understand the behaviour and develop a better method for the design of bolted end plate connections. With the introduction of Eurocode 3 Annex J, even with its flaws, a standard method of design is now almost present, which will supersede all other existing methods in its ease of use as it presents a step by step method that can be followed through.

Yield line analysis gives the designer a powerful tool to aid understanding and design of connections, but there are still problems inherent in the understanding of the overall behaviour of the connection. This is mainly due to the complexity of component interactions that cause failure in semi-rigid connections as detailed in 3.2.1.. Theoretical methods are insufficient in describing the failure behaviour of steel bolted semi-rigid connections.

3.2.1 Failure of Semi-rigid End Plate Connections

From research by various individuals (Marshall, 1993), some of the components in semi-rigid connections have a greater impact on the behaviour of the connection than the others.

The main components that appear to affect the connection behaviour are:

- Size and grade of bolts.
- Thickness of end plate.
- Column type and size.

With new types of high strength steel being used in some of the components in conjunction with semi-rigid connection, brittleness of the steel itself begins to play an

important part in the design characteristics of the connection. Bolts and welds within the connection behave in a brittle manner. This type of failure is sudden and catastrophic, with little external evidence of impending failure.

The end plate itself, which is used to transfer the stresses and strains between the various components can significantly affect the performance of the overall connection. It has been found that the thickness of the end plate can significantly influence the eventual behaviour of the connection. The end plate " must be of sufficient thickness to transmit the necessary force. Also, it must not be too stiff otherwise the predominant failure mode will be by bolt fracture" (Tong, 1985, P38)

As new types of columns start to be used within semi-rigid connection design, new and more complex interaction patterns are emerging. One of the most complex problem that has been encountered is the failure of the column web by buckling and research into this field is currently on-going. As buckling failure is complex to model, other methods of analysis were also utilised in conjunction with recognised standard methods.

"With the advent of the electronic digital computer, however, engineers realised that the solution of a large number of simultaneous equations no longer posed an insurmountable problem and this prompted a return to fundamental methods of analysis"(Rockey et al. 1998, P2)

Finite element modelling was thus developed and used to help with the development of new design methods for semi-rigid connections.

3.2.2 Review of Buckling in Column Webs

Despite the on-going research into semi-rigid bolted connections over many years by several researchers in different countries very little is understood about the true nature of column web failure. This is usually seen as something that happens occasionally but the results from tests carried out by Bose (Bose and Hughes, 1995) prove otherwise. With the failure of the column web, plastic design assumptions can be affected, as sufficient rotation capacity may not have been achieved due to this premature failure. Researchers have investigated various aspects of column behaviour.

One of the first investigations centred on the welded beam to column connections, which have less individual components and thus are easier to analyse. Graham et al (Graham et al. 1959) were interested in understanding the column web behaviour and the effect stiffeners have on this behaviour. They carried out 10 tests on interior connections. During the study, rotation capacity was felt to be an " important feature in the plastic analysis of structures since it expresses the ability of the connection to sustain a full plastic moment through the required hinge angle" (Graham et al. 1959, P1) The authors also carried out simplified testing (figure 3.14), which allowed additional tests to be readily undertaken, 11 in this case. However, this type of testing has limitations, especially the effect the other components have on the behaviour of the column web, e.g. effect of the beam web.

Based on the modified tests, as shown in Figure 3.14. which reduced the cost considerably and simplified the monitoring, a design method was suggested with an emphasis on column web design. Idealised compression zones within the column web were also developed. With a better understanding of the column web the authors concluded that stiffeners may not be necessary.

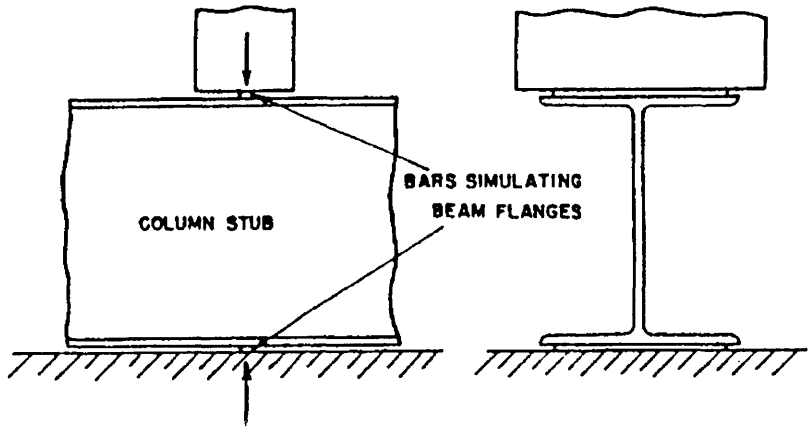

Figure 3.14: Testing rig as used by Graham et al (Graham et al. 1959)

Sherbourne (Sherbourne, 1961) discussed the best method of using bolted beam to column connections with relevance to current practices at the time, with specific

emphasis on the how and where they are used. In order to advance the understanding of bolted connections, the author also instigated a test programme of 5 full scale bolted beam to column connections. No two tests used similar components in the hope of obtaining as wide a range of behaviour results as possible; some used stronger end plates, others used column stiffeners. This approach was required due to the limited number of specimens that could be tested and thus the author hoped to gain an overall picture of different connection behaviour. The design method produced reflected this, and it lead to conservative estimates of the load carrying capacity of the bolts, the end plates and the column stiffening. The researcher commented that "For the connection design to be most efficient the component parts must be proportioned so that they reach the required strength and all yield simultaneously" (Sherbourne, 1961, P210) and suggested that

- thickness of the end plate could affect the rotation capacity of the connection; and
- the use of stiffeners, specifically a thin stiffener is more cost effective and is usually sufficient to prevent out of plane movement.

Two papers by Bose et al (Bose et al. 1972; Bose et al. 1972) reported how the column web behaved and various recommendations were made including an improved design philosophy. The authors stated that the behaviour of bolted beam to column connections can be broken down into three areas:

- local buckling of the beam web;
- strength of welds and fasteners; and
- the strength and stability of the column web.

Finite element analysis was used due to the complex nature of connection behaviour. The authors knew that basic plastic theory methods were insufficient in describing the overall behaviour of steel bolted beam to column connections. The development of finite element techniques will be discussed later, but suffice it to say that the authors used non-linear buckling analysis and used eigenvalue extraction to obtain the critical behaviour of the structure. The authors found that finite element analysis produced sufficiently accurate results when compared with experimental results, which gave the

designer a "crude approximation to the real behaviour". Finite element modelling was stated as being "sufficiently accurate and very economical".

The follow-up paper by Bose et al (Bose et al. 1972) centred mainly on how to improve existing design methods with the authors producing their own design recommendations. In conjunction with the design, full-scale testing was also carried out to verify the new design method. Both interior and exterior connections were tested, with the main interest of the research being dedicated to improving the knowledge of column web behaviour. The design of the column web according to the authors: "reduces essentially to the determination of two quantities: the capacity of the unstiffened web in resisting beam flange forces, and the additional capacity that may be developed by welding plate stiffeners to the web" (Bose et al. 1972, P282) The authors recommended changes to the current North America codes at the time, which centred on the behaviour of the column web.

Chen and Oppenheim (Chen and Oppenhiem, 1970) tested various connections and used the AISC codes to verify their solutions. Improvements to the code were also suggested by the authors. The web depth to thickness ratio with regard to the yield stress was found to be very important during the tests.

Chen and Newlin (Chen and Newlin, 1973) in the 70's investigated the strength a column web could develop in resisting compression forces, and based on these tests they observed: " It was also observed that this local yielding does not spread throughout the compression panel until just prior to ultimate load when the panel begins to buckle" (Chen and Newlin, 1973, P1981) The authors discussed a modification to the existing AISC design procedure, which mainly centred on how and when to use stiffeners.

Kalyanaraman et al (Kalyanaraman et al. 1976) investigated column buckling and stability; they concluded that the ultimate load can be much larger than the local buckling load. Several analytical methods for determining local buckling in the column were investigated. These were then compared with the experimental results in order to verify the effect of local and overall buckling on column stability.

A comprehensive study of failures of column webs in bolted connections was undertaken by Sherbourne and Murthy (Sherbourne and Murthy, 1978) utilising finite element analysis techniques. They hoped to "arrive at simple design equations affecting the strength and stability of column webs". Only one half of a connection was modelled using symmetry, and the authors used the basics of Bose's (Bose et al. 1972) work for the finite element analysis. These analytical results compared reasonably well with the experimental results. The authors concluded that an ideal section was:

" one which would promote buckling and yielding at the same time" (Sherbourne and Murthy, 1978, P484)

Compression strength of column webs were analysed by Hendrick and Murray (Hendrick and Murray, 1984). The authors wanted to verify if the provision in the existing AISC code at that time were suitable. To this end they carried out three different studies encompassing analytical, numerical and physical methods of analysis. The analytical method centred on the use of yield line analysis, the numerical study used finite element techniques, and to verify the results 6 physical tests were also carried out. The author's research attempted to build on the understanding of column web behaviour and modifications to the existing AISC code for the column web strength were also discussed. The various design methods used, namely analytical study and experimental study, were used in verifying the strength of the column web and as such were in "general agreement".

Sherbourne and El-Ghazaly (Sherbourne and El-Ghazaly, 1986) examined plastic buckling in symmetrical stiffened steel connections. Modelling was carried out to predict the behaviour of the web and different finite element models were created to test various hypotheses, namely how the web would behave and the stresses and strains that would develop.

The authors stated that the use of stiffeners to reinforce the column web, would allow connections to withstand higher loads and the relationship between the column web and column stiffeners in terms of load carrying capacity was highly non-linear.

A follow-up paper by Sherbourne and El-Ghazaly (El-Ghazaly and Sherbourne, 1987) used similar methods as employed in their first paper (Sherbourne and El-Ghazaly, 1986), to analyse the behaviour of welded steel beam to column connections. The design equations derived related to the behaviour of the column web. The method was both conservative and uneconomic, but it gave the designer an idea of the strength of various components.

With the trend of conducting physical tests of connections any design modifications would incur extra cost in terms of additional re-testing. Other approaches were required, and in order to evaluate this, researchers investigated the area of mathematical modelling. This method was inexpensive in terms of cost, but involved solving many multiple simultaneous equations and considerable analysis time was therefore required.

However, with the introduction of high powered computers, and utilising this method of analysis, the problem was considered no longer of such magnitude. As a result finite element analysis has become " widely accepted by the engineering professions as an extremely valuable method of analysis" (Rockey et al. 1998)

3.3 Finite Element Analysis for Bolted Connections

"The limitations of the human mind are such that it cannot grasp the behaviour of its complex surroundings and creations in one operation. Thus the process of subdividing all systems into their individual component or element, whose behaviour is readily understood, and then rebuilding the original system from such components to study its behaviour is a natural way ....." (Zienkiewicz, 1998, P1)

To carry out finite element modelling a simulation of the actual connection is run on the computer generated model; this involves applying load, temperature and/or displacement to the model. When using a computer to model any complex behaviour simplifications have to take place in order to gain an insight in the "trends" and/or important elements of the behaviour.

"Since physical models are often relatively expensive to build and unwieldy to move, mathematical models are often preferred. In a mathematical model, mathematical

symbols or equations are used (instead of physical objects) to represent the relationship in the system. To perform a simulation using a mathematical model, the calculations indicated by the models' equations are performed iteratively to represent the passage of time (in one second intervals, for example)" (Roberts et al. 1983)

In order to simulate the behaviour of a complex relationship, it is necessary to determine the important elements and to combine these into a simplified representation. Using this simplified representation it is possible to calculate with a reasonable degree of accuracy the probable outcome of different theoretical combinations of the relationship.

3.3.1 Finite Element Analysis

As stated earlier finite element analysis was an intensive approach in solving multiple simultaneous equations relating to a model. Due to the repetitive nature of finite element analysis, which is very time consuming if carried out manually, it is ideally suited to a computer. With the introduction of new, advanced computer programs, especially those developed for the researcher, finite element analysis has increased in popularity as a research tool over the years. More and more complex programs are being written and used by the new breed of researchers.

Finite element modelling is normally carried out in one of two ways using either elastic or plastic analysis.

3.3.2 Elastic Analysis

The elastic limit of a material can be defined as the following:

"the maximum stress that may be developed during a simple tension test such that there is no permanent or residual deformation when the load is entirely removed" (Nash, 1998, P4)

In an elastic loading regime the stress within the material is directly proportional to strain and when the loading is removed the original shape of the structure would return and there would be no residual strains present. In finite element analysis elastic modelling is easier and quicker to carry out. However the main disadvantage of

this type of analysis is that the behaviour of the structure to model is normally limited to a short range in the loading cycle of a structure. It does not throw any light into the post-elastic behaviour of the structure leading to failure. Therefore an analysis in the post-elastic or plastic domain is preferred.

3.3.3 Plastic Analysis

Plastic analysis can be defined as that carried out in:

"the region of the stress-strain extending from the proportional limit to the point of rupture which is called the plastic range"(Nash, 1998, P5)

The strain is not completely removed upon unloading i.e. residual strain would be present after the load is removed giving rise to permanent distortion of the structure. In order to conduct the analysis in the plastic domain where the stress-strain relationship is non-linear, the associated material properties must be taken into account.

Non-linear modelling is therefore far more complex and consequently more time consuming to produce satisfactory results. The power of the computer is therefore vitally important for this type of analysis, far more so than the elastic analysis. A further complication arises when three-dimensional analysis is used and this is the case for bolted connections.

3.3.3.1 Types of Dimensional Analysis

Two types of dimensional analysis can be used by the researcher: two dimensional and three dimensional analysis. The following gives a brief outline of the types of dimensional analysis.

Many of the older papers deal with two dimensional analysis, as three dimensional analysis requires much more computing power, because of non-availability of powerful computing hardware

3.3.3.2 Two Dimensional Analysis

Two dimensional analysis involves considering the behaviour of a three dimensional object such as a T-stub, in only two dimensions: length and height. Modelling using this method requires introducing constraints to the loading and boundary conditions in order to produce satisfactory results.

The advantage of this type of analysis is the speed; less powerful computers were normally used by researchers in the past but they were still able to produce reasonable results. Two dimensional modelling while not representing the true behaviour of the structure, still provides a reasonable estimate.

3.3.3.3 Three Dimensional Analysis

Three dimensional analysis is used to model the whole or part of a structure: length, breadth and height. Due to the extra data required for the geometry and the material properties, it is much harder for the researcher to develop a satisfactory model of the structure using this type of analysis. Computer power becomes more important and processing time becomes much longer. As the stresses and strains can now move in three dimensions, a complex interaction between the various components of the structure would now be present. Fewer boundary constraints are now required to be placed on the computer model, if the whole structure is modelled in a realistic and accurate fashion.

Krishnamurthy and Graddy (Krishnamurthy and Graddy, 1976; Krishnamurthy, 1976) encompassed both 2 and 3 dimensional analyses in the hope of obtaining a correlation between the two models. They analysed 13 different connections using finite element analysis, both 2D and 3D, in order that correlation factors could be derived. The authors found various correlation factors relating to the stress and displacement. They found that the 3-D models were more flexible, i.e. more freedom of movement was possible. Satisfactory results were observed when comparisons were made with experimental results using the derived correlation factors. Prying forces were not acknowledged, with no direct calculations given by the authors.

Krishnamurthy et al (Krishnamurthy et al. 1979) produced a follow-up paper on the on-going investigations using finite element analysis for the study of steel bolted connections. The authors used bi-linear stress/strain approximation to define the material behaviour in their models. The models constructed related only to symmetrical sections, the column web was therefore limited in movement, which limited the scope of the investigation as buckling in the web was unable to develop due to boundary conditions applied.

Using 3-dimensional analysis was part of the study carried out by Tarpy and Cardinal (Tarpy and Cardinal, 1981) into semi-rigid end plate behaviour. The authors conducted the research in three ways, physical testing (16 tests), parametric and analytical studies. The model took account of the nodes having three degrees of freedom each for displacement and rotation, i.e. 6 degrees of freedom per node (now standard for any three dimensional modelling). The introduction of bolts modelled as springs was also included in the model. The interaction between the end plate and column flange was included by using a form of contact analysis. The elements were not allowed to overlap but were able to separate. This was carried out using theoretical spring elements, with infinite stiffness in compression and zero in tension. The complex representation of this model allowed a reasonable prediction of the behaviour of the model.

With any type of modelling the researcher must define the depth of study as steel bolted connections are complex structures. Therefore certain assumptions are required. This is how Maxwell et all (Maxwell et al. 1981) carried out their study:

"A connection is made up of small components each capable of a significant influence on the overall deformation pattern" (Maxwell et al. 1981, P2.49)

"The behaviour of the connection is often non-linear even when the component remains in an elastic state of stress" (Maxwell et al. 1981, P2.50)

The finite element models were compared with test results and the authors predicted cost savings of up to 20% if their recommendations from the study were followed by the designer.

Using a general purpose finite element package, NONSAP (NONlinear Structural Analysis Program), Patel and Chen (Patel and Chen, 1984) investigated interior connections. Limitations on computing hardware, meant that only 2D analysis was carried out by the researchers. The results reflected the problems inherent in using 2D modelling to define a 3D structure. Slippage occurred during the physical tests, but this was not taken account of in the model and thus another reason for the difference i.e. friction between the components, was not included.

Bose et al (Bose et al. 1991) modelled various three dimensional steel bolted connections using the commercially available finite element package LUSAS (London University Structural Analysis System). Contact analysis was included in the model to define the interaction between the end plate and the column flange. As the section was symmetrical, only a quarter of the connection was modelled (figure 3.15), this was mainly due to the hardware and software limitations. The LUSAS program was unable to handle non-linear buckling. In spite of these problems, a reasonable representation and results were produced.

The model in the above paper (figure 3.15) was based on the work carried out by Bahrami (Bahrami, 1991) in the completion of his Ph.D. studies, which was an in-depth study of the behaviour of unstiffened beam to column EEP connections, utilising finite element analysis techniques. Twelve full scale tests were conducted, in order to compare physical test and finite element analysis results

The authors utilised three dimensional modelling using joint elements to model the contact between the column flange and end plate. The joint elements were non-linear in nature with the finite stiffness in one direction i.e. no overlapping but could separate if required. Figure 3.16 shows how the contact analysis is undertaken.

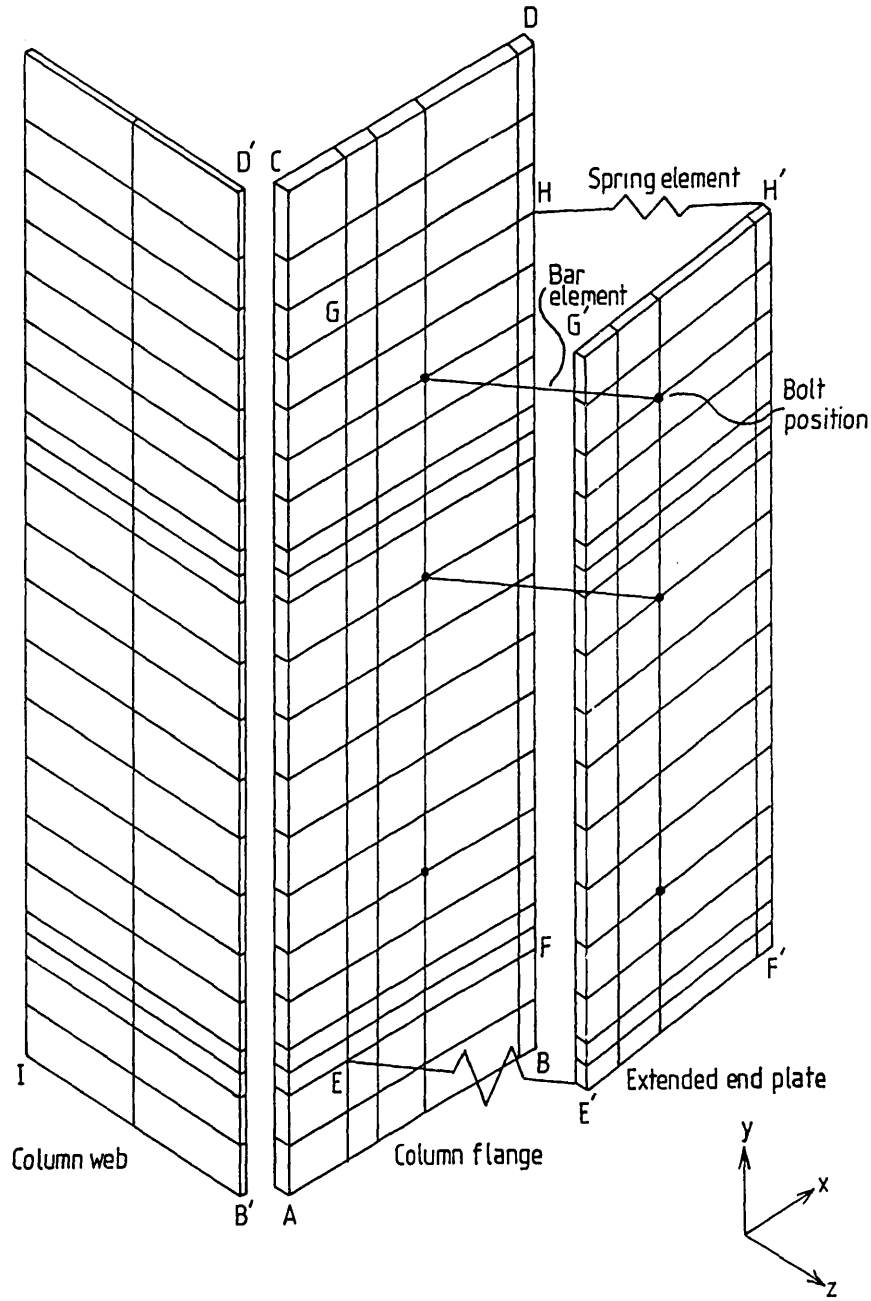

Figure 3.15: 3 Dimensional model as used by Bahrami (Bahrami, 1991)

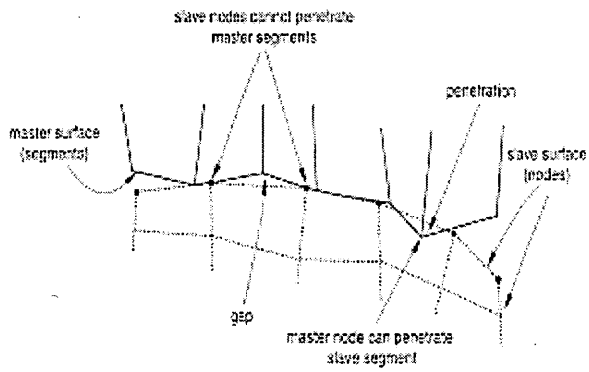

Figure 3.16: Showing method incorporated for contact analysis

Sherbourne and Bahaari (Sherbourne and Bahaari, 1994; Sherbourne and Bahaari, 1994) used the commercial finite element analysis package ANSYS for their study. The authors used 3D analysis techniques in order to define the behaviour of the connection. The different aspects of the connection are discussed with emphasis on the effects of boundary conditions, material properties and the type of loading. The authors state that their research was limited due to only 4 connections being compared but "the predicted results are within the range of accuracy of experimental values".

Wang's research (Wang, 1996) followed on from Bahrami's (Bahrami, 1991) but he investigated FEP only (Figure 3.17). The author also investigated the effect boundary conditions have on the structure and what the minimum effective length is required for the column. Six FEP bolted connections were modelled in conjunction with 6 experimental results.

The author found during his study that 2x D, where D is the length of the end plate, was sufficient for the boundary conditions not to affect the behaviour of the connection. Due to the limitations of the software (LUSAS), non-linear buckling effects were not taken account of in the analysis.

The benefits and disadvantages of certain types of elements were also discussed with relevance to accuracy, specifically 8, 16 or 20 noded elements. The author concluded that 16 noded elements combined the benefits of 20 noded elements without the

computational expense, and were more accurate than the lower order 8 noded elements.

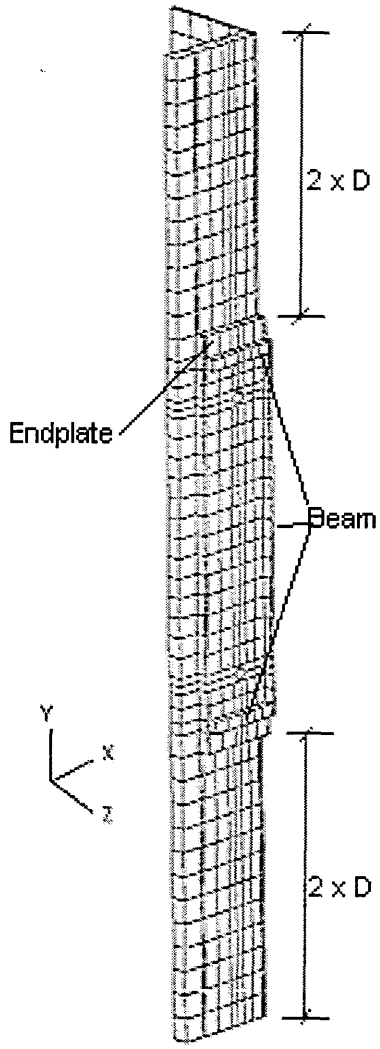

Figure 3.17: Model used by Wang (Wang, 1996)

A follow-up paper by Bose et al (Bose et al. 1997) based on Wang's (Wang, 1996) and Bahrami's (Bahrami, 1991) work discussed the various problems relating to finite element analysis and suggestions in overcoming them. The problems with defining the boundary conditions was of major importance especially when only a quarter of the connection is modelled.

The authors discuss how to model a connection with emphasis on the material properties of the connection, i.e. Young's modulus, Poisson's ratio and the limits of plastic stresses and strains. Some simplifying assumptions are required in any finite element model, otherwise the model itself will become too complex but care must be taken. The authors mention that welds, bolt heads and column fillets were not modelled; they felt that the contribution from these components was minimal. In their summing up, the authors conclude that for successful results using finite element modelling, the more complex and time consuming 3D analysis techniques have to be used.

A refined 3 dimensional model was produced by Choi et al (Choi and Chung, 1996) to develop a better understanding of connection behaviour. Figure 3.18 details the model used, only half of the connection was modelled, as the authors were interested in understanding the interaction between the column flange and end plate. The authors discuss the complexity of the mesh required for successful analysis, with emphasis on the effects that this has on the outputs.

In their first of two papers (Sherbourne and Bahaari, 1996) on the subject of 3-D modelling, the authors modelled the basic T-stub using the commercial package ANSYS (V 4.4). They mentioned that they only modelled a quarter of the T-stub, due to the symmetrical nature of the connection and displacement and prying forces were also discussed. The results obtained for the analytical models compared well with experimental results.

Bahaari and Sherbourne (Bahaari and Sherbourne, 1996) in their second paper on the subject of 3-D simulation of connections were interested in the behaviour of full bolted connections. (ANSYS was again used for the modelling.) A symmetrically loaded model was developed, therefore the column web was held using boundary conditions to allow the model to converge. A good representation was reported.

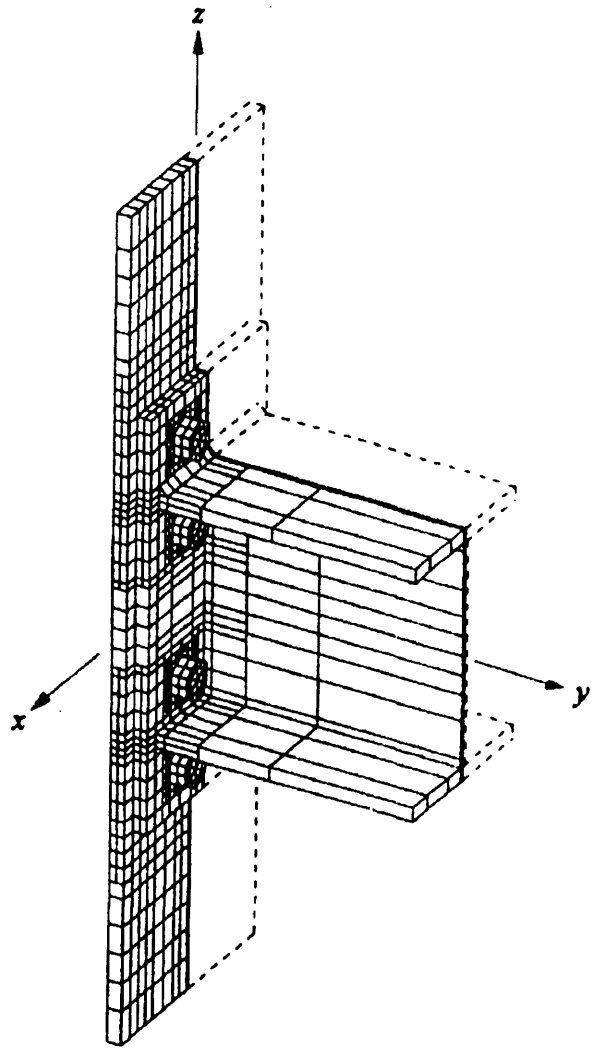

Figure 3.18: Refined 3 Dimensional model as used by Choi (Choi and Chung, 1996)

The more recent paper by Bose et al (Bose et al. 1997) reported the results using the commercial package ABAQUS to model a basic T-stub connection. The T-stub model itself included a fully detailed bolt model comprising the bolt head and shank (figure 3.19). Defining the bolt as detailed as this allowed the researchers to obtain good correlation between experimental and theoretical results for the basic T-stub. See Chapter 7 for detailed discussions of T-stub behaviour.

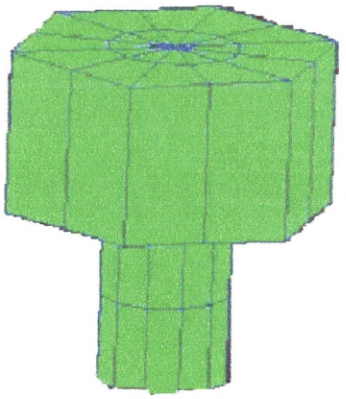

Figure 3.19: Details of the 3D bolt model used by Bose et al (Bose et al. 1997)

Bose et al (Bose et al. 1998) had instigated a study using finite element model into the behaviour of full scale steel bolted connections based on experimental results (Bose, 1993; Bose, 1994). The authors were addressing the problem of column web buckling and how this non-linear failure could be modelled. They discussed the use of eigenmodes and eigenvalues in order to obtain the critical vibration of the structure (See Chapter 8 on modelling full scale connections). The model encompassed all the usual attributes required for complex modelling, contact analysis, non-linear material properties etc. The discussions also centred on obtaining the final failure loads of the connection, by using the eigenvalues in another analysis.

As can be seen with most of the above models, the assumptions relate to the column web being able to withstand the loading and not buckle i.e. most researchers use boundary conditions to control the movement in the web in their finite element models. The current researcher is therefore investigating the phenomenon of buckling of the web in semi-rigid connections using finite element analysis in order that current methods of design can be improved. This should lead to a more complete picture of steel bolted semi-rigid end plate connections.

Discussion on Physical Testing

Chapter 4

4.0 History

At the University of Abertay-Dundee, a considerable number of steel bolted beam to column endplate connections were tested as part of a consultancy for the Steel Construction Institute. In total 18 full scale connections were tested, of those 12 were extended endplates and 6 were flush endplates. These were mainly standard ductile connections developed by the Steel Construction institute (figure 4.1). Of the 18 connections tested, there were 3 non-standard connections with thicker end plates, 20 mm instead of the usual 15 mm. The results of these tests were also used by a postgraduate student for his research project. (Wang, 1996).

4.1 Description of the Tests

4.1.1 Test Rig

The 18 full scale destructive tests were carried out in one of the loading frames in the heavy structures laboratory within the School of Construction and Environment. A 1000 kN capacity hydraulic jack was used to apply the load to the various connections.

4.1.2 Test Programme

The connections were made up of a combination of 5 beams types, 3 columns types, various end plates and two types of bolts. For more details on the type and size of the connection the reader is referred Table 5.3 (Chapter 5 on Comparison of Eurocode 3-Annex J and tests).

4.1.3 Bolt Types

In the tests, two types of bolts were used, either M20 or M24, both grade 8.8. There was little or no pre-tensioning of the bolts prior to their being locked down before loading commenced.

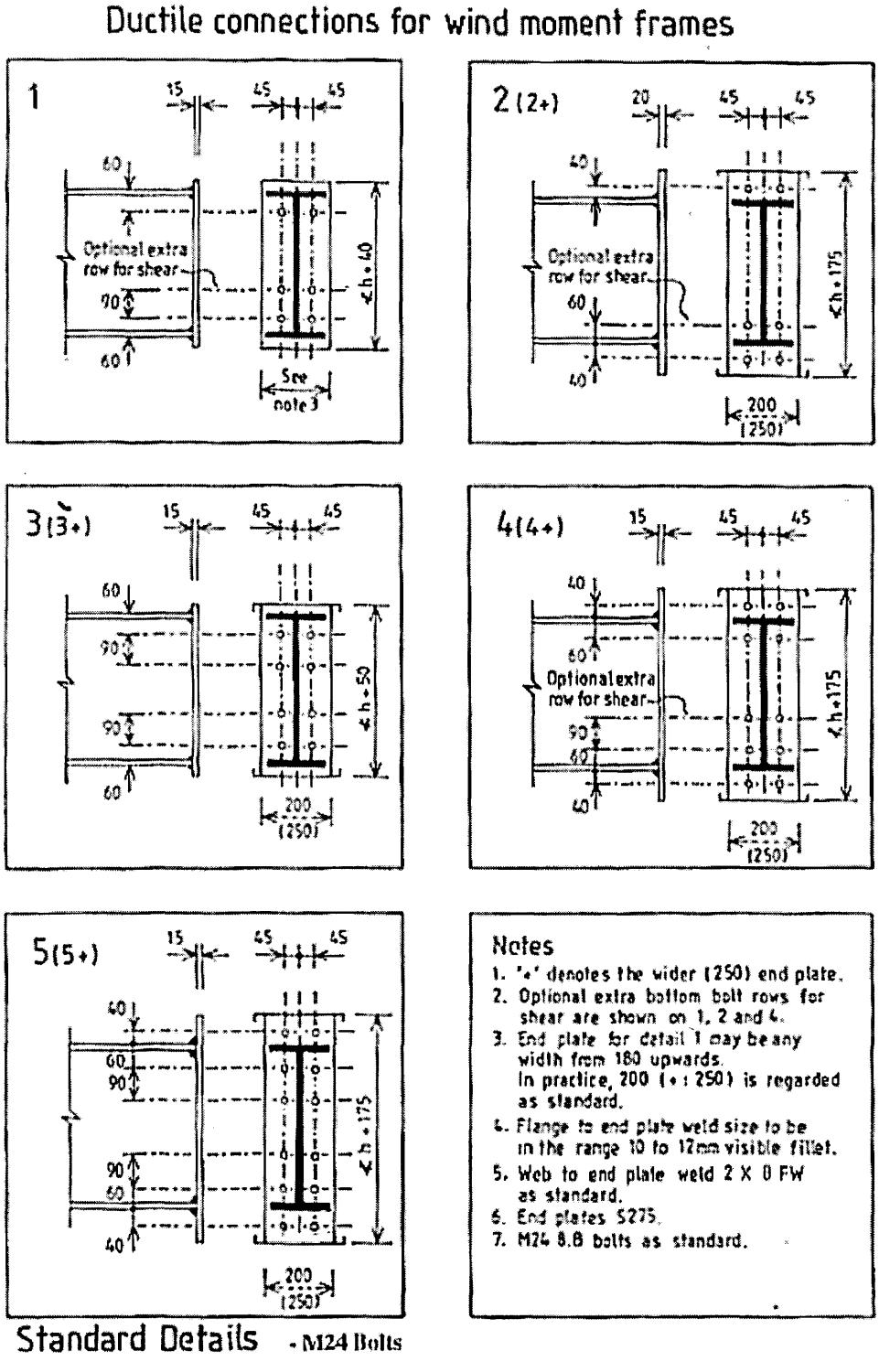

Figure 4.1: showing standard Steel Construction Institute details for steel bolted connections

All the connections were supplied by two local steel fabricators, Macintosh Steel Structures and Jackson Steel fabrications. The fabricators were told to punch the holes in the components i.e. not to drill them. This only applied to the end plates, the holes in the column flanges having to be drilled. The workmanship of the connections was left up to the fabricator themselves, subject to inspection by the researchers.

Grade 43 steel was used for all components. The welds used between the end plate and the beam sections were all 10 mm fillet welds. The heat required during the welding process caused some distortion which was expected, but this appears not to have affected the overall behaviour of the connection.

A podger spanner was used to tighten the bolts in-situ; several circuits of tightening the various bolts was required to bring the end plate and column flange in to contact before the testing began. The circuits were required due to the distortion caused by the welding process.

4.1.4 Instrumentation and Measurement during the Experiment

In order to understand the behaviour of the connection, the rotation of the connection has to be measured during physical testing. Rotation was defined as the "*change of angle between column and beam centre lines.*"

These measurements (rotations) are vital in understanding the behaviour of the connection but there is still no standard method of measurement to define the afore-said angles. Researchers have adopted various means of measurement but there is no uniform agreement amongst them on the best methodology.

4.1.5 Procedures for measurement of Rotation

Two independent methods of measurement were employed. This ensured that duplicate results were available and if a problem arose during the test with one of the measuring devices then the test could still proceed. As the testing system employed was symmetrical, the gauges and transducers used were mirrored on each side.

Figure 4.2 outlines the setup for taking various measurements during the tests. A steel bar was rigidly connected to the column web at position A and a steel angle section was attached to each of the beam webs at B. Point A was located on the column at the intersection of column and beam centre lines, and point B was positioned on the beam

centre line very close to the welded end plate. Two dial gauges were set-up on the beam attachment 300 mm apart, with their pointers resting on the column attachment. A pair of transducers were supported using a rigid steel frame with the pointers resting on the beam attachment, also 300 mm apart.

The steel frame used to hold the transducers in place, was fixed to the heavy structures laboratory floor in front of the testing rig itself, using large bolts anchored to the laboratory floor i.e independent of the test specimen (figure 4.2b). This method was reproduced on the other side of the column, to allow both sides to be measured during the loading process. This ensured that an average value could be obtained if required and minimise the potential error. At any applied load, the difference between the two dial gauge readings or the two transducers in mm divided by 300 mm represented the rotation of the connection at that point.

To obtain the total moment applied to the connection, the support reaction (half of the applied load) is multiplied by the distance between the roller support and the face of the column flange.

During the tests the strains at different points were also measured using strain gauges, the output from the gauges were recorded using a data logger; the data logger was calibrated before commencement of each test.

In order to understand the interaction between the end plate and the column flange, carbon paper was interposed between the two components. The imprints on the paper indicate the area and severity of the contact pressure between the two components. The higher the prying force the more discolouration on the carbon paper (figure 4.3).

4.1.6 Loading the Connection

The loads were applied at the top of the column stub using a hydraulic jack. Each specimen was initially loaded and unloaded in the elastic region, in order to check if the overall test set-up was functioning as it should i.e gauges were working, loggers were recording etc. Loading was applied in uniform increments while in the elastic range of the material. When the material started to yield (plastic range reached) the load increments were reduced.

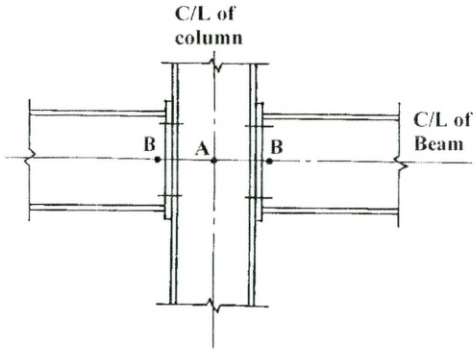

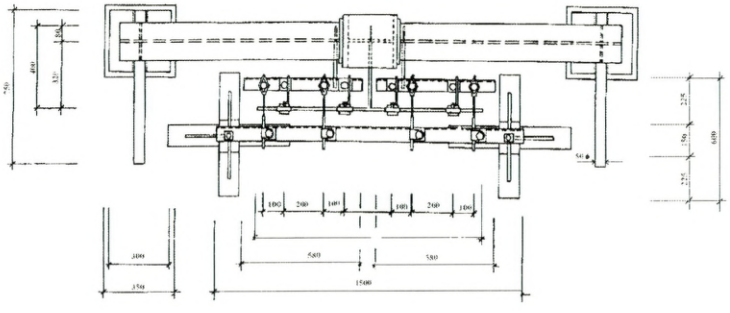

Figure 4.2a: Showing setup for instrumentation

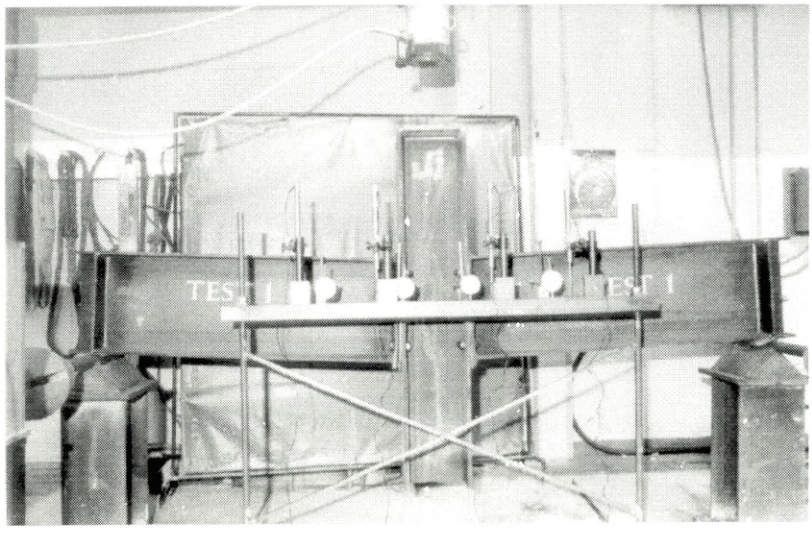

Figure 4.2 b: Rigid frame used for transducers

Figure 4.2: Showing the setup used for taking measurements during the tests.

Figure 4.3: Prying pattern during one of the tests

Once the load increment had been applied, all the relevant readings were taken. When yielding started to occur in the material problems arose with recording the readings from the gauges and the transducers. Due to the yielding of the material, the gauges would not stop moving and time was allowed for this to "settle down", i.e the loading was held at the value until most of the movement had stopped. This problem also occurred in the transducer reading. The connection was inspected after each load increment for plumbness, physical state of all instrumentation and any visible signs of deformation and any anomalies were noted before the next load increment.
When the testing was completed photographs were taken and the type of connection failure was also noted.

4.2 Summary of experiments

From the considerable amount of data obtained during the tests, various graphs could be drawn to show the overall behaviour of the connection. This was especially true of the moment-rotation curves (figure 4.4).
During some of the tests, bolts failed as a result of thread stripping. This problem of bolt stripping can be resolved by adopting European standards of practice(British Standard Institution, 1998) for bolts. The bolts were tested beforehand using a specially built testing rig (figure 4.5) However the testing rig for bolts does not produce a true representation of what occurs in the connection during loading. The bolt is not just subjected to pure tension in the connection but also experiences moments due to the distortions that develop as the connection is loaded to failure.
The device used to check the bolts comprised two interlinked boxes with a central hole through the two inner plates. A bolt with various strain gauges attached to it was placed in the above apparatus. A compression force was applied to the device forcing the two boxes to separate and thus creating a tensile force within the bolt. The strain gauge readings were averaged to eliminate any problems with bolts bending etc. All failures during these tests were either due to fracture which occurred in the threaded region of the bolt or due to thread stripping.

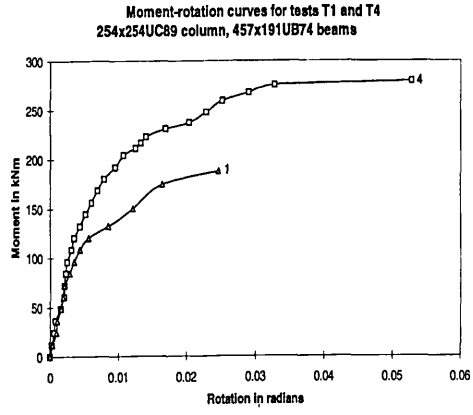

Test T1: Single row M20 bolts. Test T4: Double rows M20 bolts.

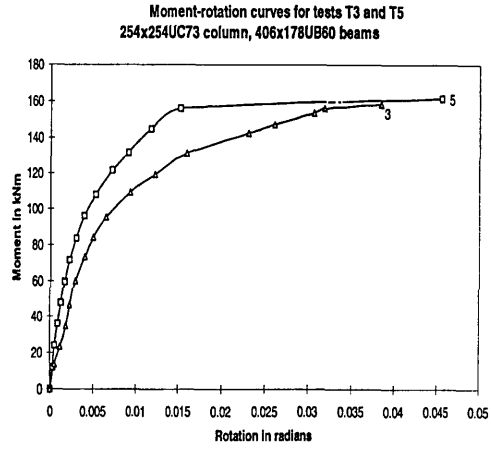

Test T3: Single row M20 bolts. Test T5: Double rows M20 bolts.

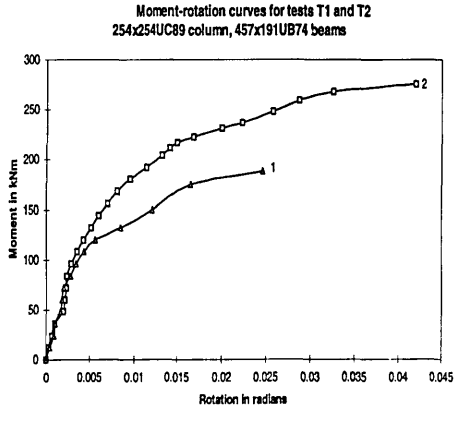

Test T1: End plate 12 mm, single row M20 bolts. Test T2: End plate 15 mm, single row M24 bolts.

Figure 4.4: Examples of Moment/Rotation curves.

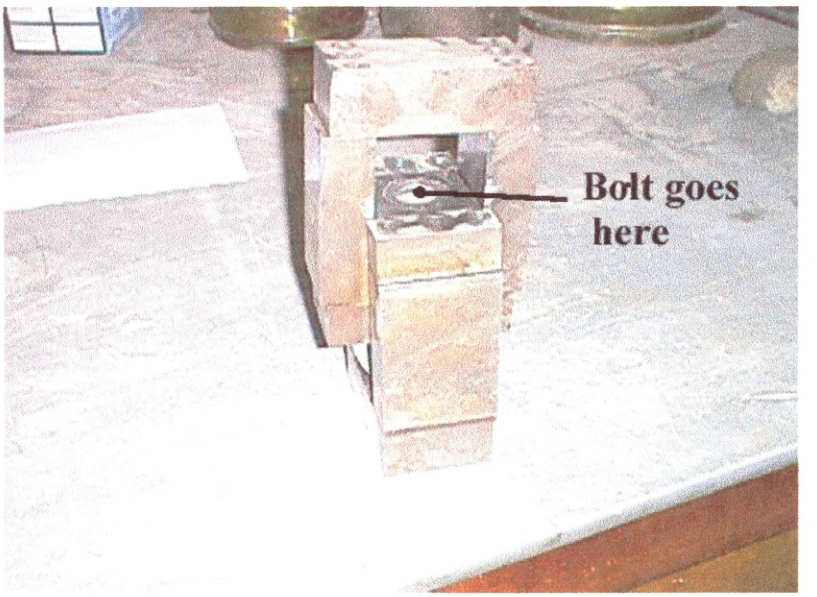

Figure 4.5a: Showing the original testing rig for bolts

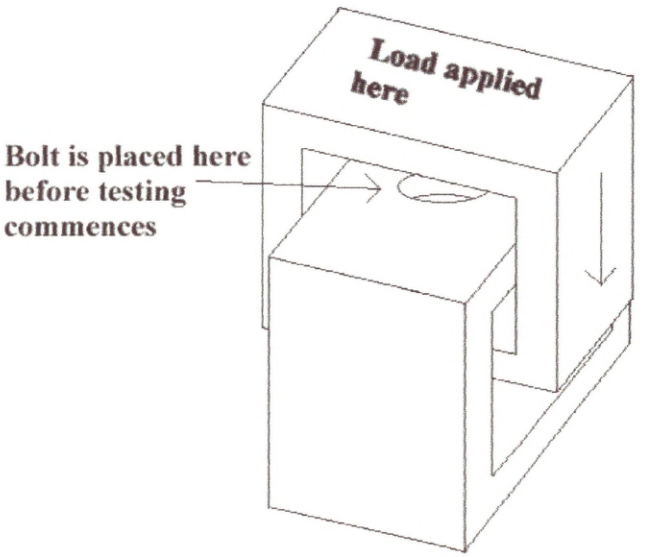

Figure 4.5b: Schematic of the testing rig

Figure 4.5: Bolt Testing Apparatus

As can be seen in the tests deformation occurred in some of the components. In many tests there was considerable deformation in the column flange due to the applied loading (figure 4.6).

4.3 Material Testing

For finite element analysis of the connection, using computers, a true picture of the connection has to be obtained for all relevant components. Therefore, material tests were carried out on parts of the connection, the testing of which carried out to the relevant standards, namely BS EN 10 002-1(British Standard Institution, 1998). During the testing of some of the specimens there was a problem with the testing machine, thus the value of E for the specimens was much lower than expected. They were ignored and a standard E value of 200 kN/mm^2 was used in the finite element models for some of the components when the test data was unavailable.

4.4 Conclusion

Full scale testing is costly and very time consuming. The preparation of specimens including placement of gauges, data loggers etc require careful study and experience. With practice and understanding, accurate data relating to the connection behaviour can be obtained. This can be used for further study by the researcher and is a valuable research tool.

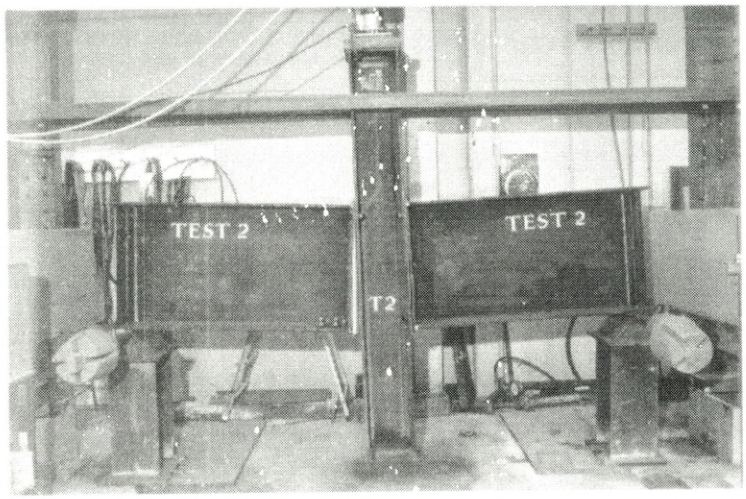

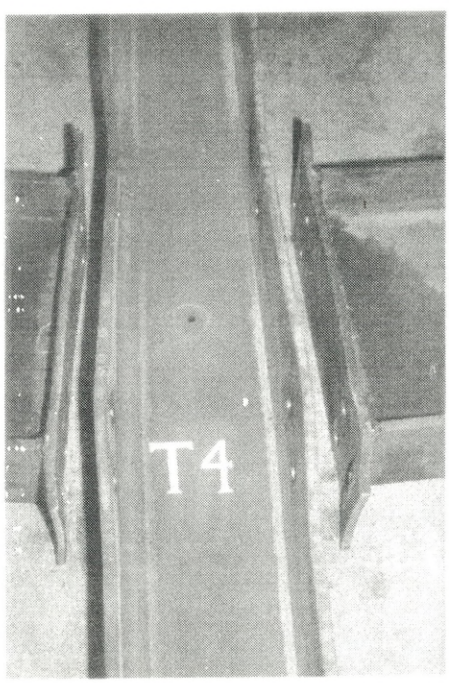

Figure 4.6a: Showing failures of tests 2,3 and 4

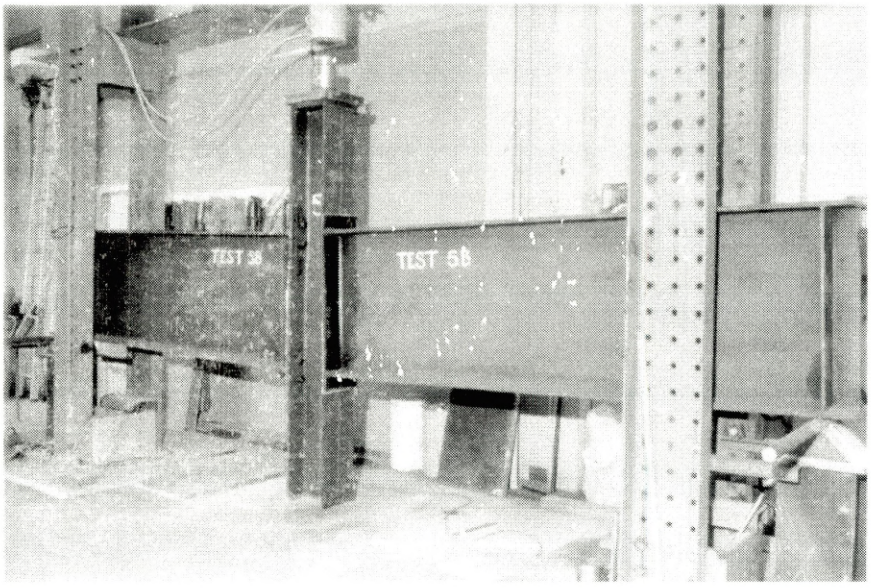

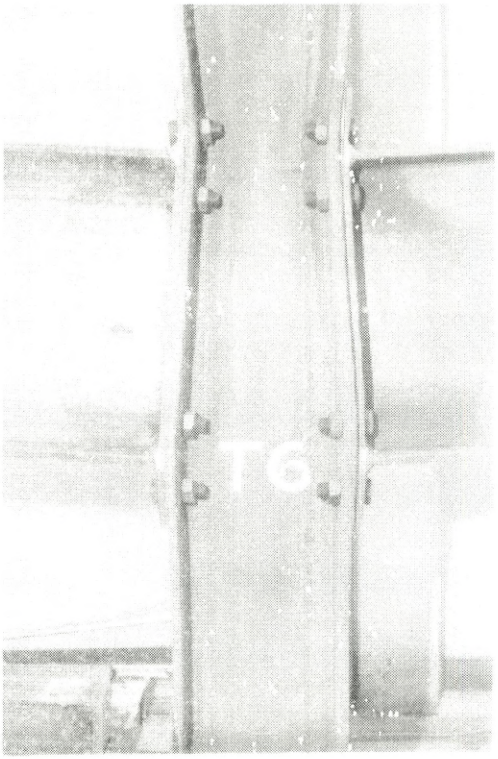

Figure 4.6b: Showing failure of tests 5b and 6

Figure 4.6: Pictures of some of the test specimens after testing has finished

EUROCODE 3- ANNEX J: COMPARISON WITH EXPERIMENTAL RESULTS

Chapter 5

5.0 Background: What is Eurocode 3- Annex J ?

Eurocode 3- Annex J is a draft European code on structural steelwork which will eventually replace all existing National codes in Europe, including the British Code BS5950. In Annex J an attempt has been made to produce a standard method for designing steel bolted connections by applying yield line method.

5.1 History

"The Commission of the European Communities initiated the work of establishing a set of harmonised technical rules for the design of building and civil engineering works which would initially serve as an alternative to the different rules in force in the various Member states and would ultimately replace them. These technical rules became known as the Structural Eurocodes" [Foreword of Eurocode 3, (British Standard Institution, 1995)]

During his Ph.D. study, Dr Jaspart (University of Liege, Belgium) initiated the development of the component method of analysis for steel bolted connections (Jaspart and Maquoi, 1994). Over the last twelve years these models have been refined and backed up by extensive testing (over 100 physical tests to date by the researchers). Therefore, a large store of experimental information exists for the formation of theoretical models.

The component method attempts to separate the whole connection into individual parts. The following is the list of parts that Eurocode 3 Annex J uses to check the bolted connection:

- column web panel in shear;
- column web in compression;
- beam flange and web in compression;
- column flange in bending;
- column web in tension;

- end-plate in bending;
- beam web in tension;
- flange cleat in bending;
- bolts in tension;
- bolts in shear;
- bolts in bearing;
- plate in tension or compression.

Each component is checked for various criteria, using the relevant equation, the weakest component is then derived from these equations. Not all of the above components are relevant to each type of connection. Various factors have to be noted i.e. type of loading, connection design, the type of connection: interior or exterior etc.

5.2 Eurocode 3- Annex J

Eurocode 3 Annex J investigates three main characteristics of connection behaviour:

1. Moment resistance
2. Rotational stiffness
3. Rotation capacity.

The following sub-sections give a brief outline of the various criteria stated above; for more detailed information, Eurocode 3- Annex J (British Standard Institution, 1995) will need to be consulted.

5.2.1 Classification by Strength (Moment Resistance)

Within Eurocode 3-Annex J, the remit is to obtain the "weakest link" in a single bolt row and/or combination of bolt rows. The values for each component within the connection are derived from the equations. The lowest value is calculated, then multiplied by the lever arm, to ascertain the overall moment which the connection can withstand. Thus the maximum moment that the connection can attain is based on the weakest component in the connection.

Moment of resistance of the connection can be defined according to three classifications:

1. Nominally pinned.

2. Partial strength.
3. Full strength.

Section J 2.5.2, Eurocode 3-Annex J details the relevant criteria.

"A beam to column joint may be classified as full strength ,nominally pinned or partial strength by comparing its design moment resistance with the design moment resistances of the members which it joins." (British Standard Institution, 1995)

The following equations from Eurocode 3-Annex J are used to obtain the "weakest" component of the connection for the strength check i.e. the moment capacity of the section.

5.2.2 *Column web panel in shear*

$$V_{wp,Rd} = \frac{0.9 f_{y,wc} A_{vc}}{\sqrt{3}\gamma_{MO}}$$

$f_{y,wc}$ is the characteristic strength of steel in the column web.

A_{vc} is the shear area of the column defined by 5.4.6

γ_{MO} is the factory of safety.

5.2.3 *Column web in compression*

$$F_{c,wc,Rd} = \frac{\rho b_{eff} t_{wc} f_{y,wc}}{\gamma_{MO}}$$

ρ is the reduction factor found from table J5

b_{eff} (effective width) for above equation is found using the following

$$b_{eff} = t_{fb} + 2\sqrt{2}a_p + 5(t_{fc} + s) + s_p$$

a_p is given by Table J23 [Eurocode 3- Annex J (British Standard Institution, 1995)]

t_{fc} is the thickness of the column flange

s is r_c for rolled I or H sections or $\sqrt{2}a_c$ for welded I or H sections

t_{wc} is the thickness of the column web

5.2.4 *Column web in tension*

$$F_{t,wc,Rd} = \frac{\rho b_{eff} t_{wc} f_{y,wc}}{\gamma_{MO}}$$

The effective width, b_{eff} for bolted end plate connection (Rolled I or H section), in the above equations is given by:

$$b_{eff} = t_{fb} + 2\sqrt{2a_b} + 5(t_{fc} + s)$$

5.2.5 Equivalent T-stub Assumption in Eurocode 3- Annex J

The column flange and end plate are designed as an equivalent T-stub for single bolt rows and combination of bolt rows depending on the design of the connection.

Designs of the above two components are similar, but the values of m, n ,e, $l_{eff,1}$ and $l_{eff,2}$ are derived in a slightly different manner (figure 5.1). These use the equivalent t-stub models to simplify the complex behaviour of the component in question.

Mode 1: Complete yielding of Flange

$$F_{T,Rd} = \frac{4M_{pl1,Rd}}{m}$$

Mode 2: Bolt failure with yielding of the flange

$$F_{T,Rd} = \frac{2M_{pl2,Rd} + n\Sigma B_{t,Rd}}{m+n}$$

Mode 3: Bolt failure

$$F_{T,Rd} = \Sigma B_{t,Rd}$$

$$M_{pl,1,Rd} = \frac{0.25\Sigma l_{eff,1} t_f^{\,2} f_y}{\gamma_{MO}}$$

$$M_{pl,2,Rd} = \frac{0.25\Sigma l_{eff,2} t_f^{\,2} f_y}{\gamma_{MO}}$$

where,

$B_{t,Rd}$ is the design tension resistance of a bolt-plate assembly.

$\Sigma B_{t,Rd}$ is the total value of $B_{t,Rd}$ for all the bolts in the T-stub.

$\Sigma l_{eff,1}$ is the value of $\Sigma leff$ for mode 1.

$\Sigma l_{eff,2}$ is the value of $\Sigma leff$ for mode 2.

γ_{MO} is a factor of safety, usually 1.1.

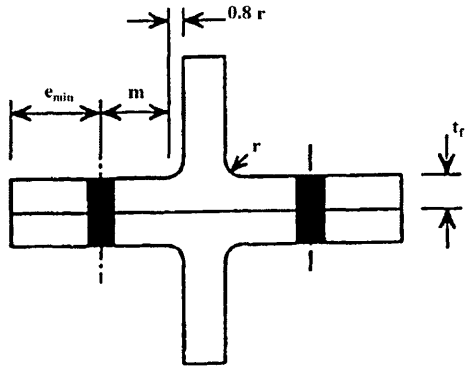

Figure 5.1a: Showing dimensions of equivalent T-stub flange

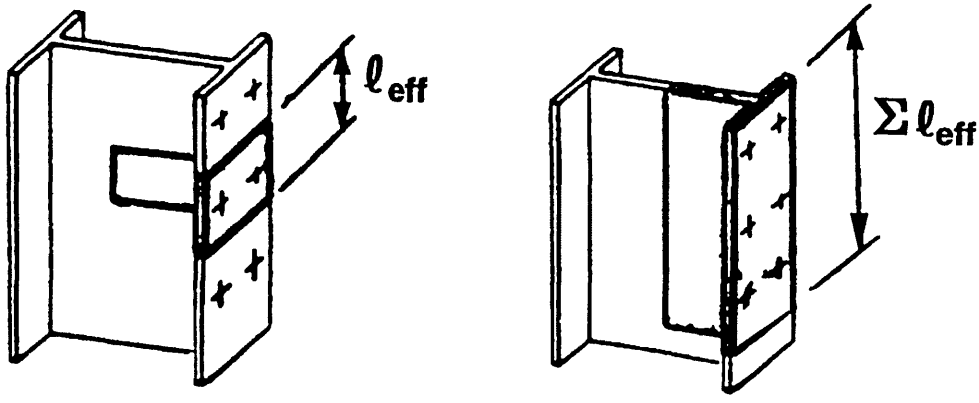

Figure 5.1b: Showing effective lengths

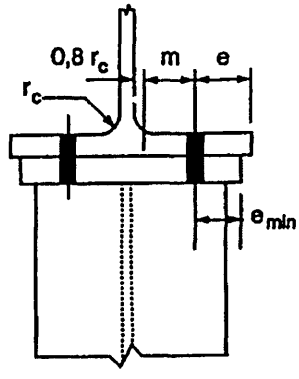

Figure 5.1c: Dimensions for a column flange

Figure 5.1: Detailing different dimensions used in Eurocode 3-Annex J

5.2.6 *Derivation of Bolt Strength*

$$B_{t,Rd} = F_{t,Rd} = \frac{0.9 f_{ub} As}{\gamma_{Mb}}$$

where,

A_s is the tensile stress area of bolt

γ_{Mb} is the factor of safety, normally taken as 1.25 for bolts in the U.K.

5.2.7 *Beam flange and web in compression*

$$F_{c,fb,Rd} = \frac{M_{c,Rd}}{(h_b - t_{fb})}$$

h_b is the overall depth of the beam

t_{fb} is the thickness of the beam flange.

5.2.8 *Rotational Stiffness*

Three main classifications exist within Eurocode 3-Annex J for bolted connections:

1. Pinned.
2. Semi-rigid.
3. Rigid.

Rotational stiffness classification of the connection, can be obtained by calculating the initial stiffness from test results. The moment rotation graphs (test results) are used to find the initial stiffness.

The value of rotational stiffness from Eurocode 3- Annex J are based on the contribution of the different components of the connection, known as the "k_i "value, for each component. The rotational stiffness, S_j, of the connection is obtained from the k_i values, as indicated below:

5.2.9 *Stiffness coefficients for basic components*

$$S_j = \frac{Ez^2}{\mu \sum_i \frac{1}{k_i}}$$

where,

k_i is the stiffness coefficient representing component i

z is the lever arm

μ is the stiffness ratio $S_{j,ini} / S_j$

$S_{j,ini}$ is the value S_j when the moment $M_{j,Sd}$ is zero

Table J.10 [Eurocode 3-Annex J] is used to find k_i and states which coefficients to take into account for particular loading conditions. The table below (table 5.1) is an extract from TABLE J.10. for interior connections, with moments equal and opposite as in test set-up.

Number of Bolt-rows in tension	Stiffness coefficient k_i to be taken into account
one	k_2; k_3; k_4; k_5; k_7
Two or more	k_2; k_{eq}

Table 5.1: Extract from table J.10 of Eurocode 3-Annex J

Stiffness ratio μ should be determined from:

$$\mu = \left[\frac{1.5 Mj,Sd}{Mj,Rd}\right]^{\Psi}$$

Where

Ψ= 2.7 for bolted end plates

5.2.10 General method

The general method is used when there is more than one bolt row in tension, in order to obtain one equivalent stiffness value, which is used in the above equation for Sj.

$$k_{eq} = \frac{\sum_r k_{eff,r} h_r}{z}$$

where,

h_r is the distance between bolt row r and the centre of compression, if more than one bolt row then this is calculated for each bolt row (figure 5.2).

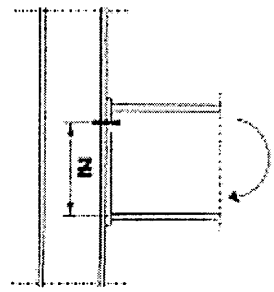

Figure 5.2a: Bolted end-plate connection with only one bolt-row in tension

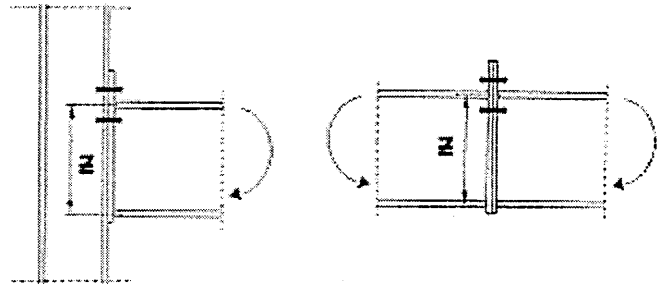

Figure 5.2b: Bolted end-plate connection, simplified method

Figure 5.2: Showing how z is obtained for each bolt row from Eurocode 3(1995)

5.2.11 *Effective stiffness coefficient*

$$k_{eff,r} = \frac{1}{\sum_i \frac{1}{k_{ir}}}$$

k_{ir} is the stiffness coefficient representing component i relative to bolt row r.

The lever arm z is derived from the following equation when the connection has more than one bolt row in tension.

$$z = \frac{\sum_r k_{eff,r} h_r^2}{\sum_r k_{eff,r} h_r}$$

The next set of equations are used to find the overall "k" value (stiffness coefficient).

5.2.12 *Double-sided joint in which the beam depths are similar*

$$k_1 = \frac{0.38 A_{vc}}{\beta Z}$$

A_{vc} is the shear area of column.

Z is the lever arm

For a symmetrically loaded beam [test set-up], the transformation parameter β is usually zero, therefore k_1 is infinity. Table 5.2 shows the different β values that can be used.

Transformation parameter β	Reduction factor ρ
$0 \leq \beta \leq 0{,}5$	$\rho = 1$
$0{,}5 < \beta < 1$	$\rho = \rho_1 + 2(1 - \beta)(1 - \rho_1)$
$\beta = 1$	$\rho = \rho_1$
$1 < \beta < 2$	$\rho = \rho_1 + (\beta - 1)(\rho_2 - \rho_1)$
$\beta = 2$	$\rho = \rho_2$

$$\rho_1 = \frac{1}{\sqrt{1 + 1{,}3(b_{eff}\, t_{wc}/A_{vc})^2}} \qquad \rho_2 = \frac{1}{\sqrt{1 + 5{,}2(b_{eff}\, t_{wc}/A_{vc})^2}}$$

A_{vc} is the shear area of the column, see J.3.5.2;

β is the transformation parameter, see J.2.6.3.

Table 5.2: β parameter from Eurocode 3- Annex J

5.2.13 *Unsitffened column web in compression*

$$k_2 = \frac{0.7 b_{eff} t_{wc}}{d_c}$$

where,

b_{eff} is the effective breadth of the column web in compression.

d_c is the clear depth.

5.2.14 *Column flange, single bolt row in tension*

$$k_3 = \frac{0.85 l_{eff} t_{fc}^3}{m^3}$$

where, l_{eff} is the smaller of the effective lengths either from table J6 or J7 - Eurocode 3 Annex.

m is from Figure 5.1c

5.2.15 ***Column web in tension, for a stiffened or unstiffened bolted connection with a single bolt row in tension***

$$k_4 = \frac{0.7 b_{eff} t_{wc}}{d_c}$$

5.2.16 ***End plate, single row in tension***

$$k_5 = \frac{0.85 l_{eff} t_p^{\,3}}{m^3}$$

5.2.17 ***Bolts, single bolt row in tension***

$$k_7 = \frac{1.6 A_s}{L_b}$$

where, A_s is the tensile stress area of the bolt.

L_b is the elongation length of the bolt.

5.2.18 Rotation Capacity

The rotation capacity is governed by what type of failure mode is predicted by the code. The following extract is taken from Eurocode 3 Annex J Section J. 5.

"A joint with a bolted connection with end plates or angle flange cleats may be assumed to have sufficient rotation capacity for plastic analysis if both the following conditions are satisfied.

a) The design moment of resistance of the joint is governed by the resistance of either:
   - the column flange
   - the beam end-plate or tension flange cleat
b) the thickness t of either the column flange or the beam end-plate or tension flange cleat (not necessarily the same component as in (a)) satisfies:

$$t \leq 0.36 d \sqrt{f_{ub} / f_y}$$

Where:

d is the nominal diameter of the bolts;

f_{ub} is the nominal tensile strength of the bolts;

f_y is the yield strength of the relevant basic component.

5.3 Test Programme

For detailed discussions of tests, the reader is referred to Chapter 4, Physical Testing

5.3.1 Comparisons of Test Results and Eurocode 3-Annex J.

The comparison was carried out according to the various criteria defined in Eurocode 3- Annex J. These are

1. Strength.
2. Rigidity.
3. Ductility.

As the method employed in Eurocode 3 separates the connection into individual components to find the weakest link, equations are developed to find the weakest member.

5.3.2 Classification by Strength (Moment Resistance)

The most noticeable difference between the results of physical tests and Eurocode 3-Annex J, is that the moment resistance indicated in the tests is higher than the values predicted by Eurocode 3-Annex J (table 5.3).

Economy is a vital component in the design of connections, as cost is one of the major concerns for any designer. There is little point in designing a connection, that in practice will take twice the design load as its relative cost might be prohibitive. The range of results varied between 1.09 and 1.96, when a comparison is made between the test specimens and the predicted values (a large spread of results). As a norm strengths obtained by tests should be higher than that predicted by design and thus result in a safer design.

Test	Detail	Column	Beam	End plate	Failure load kN	Failure moment kNm	Predicted moment resistance Eurocode 3 Annex J kNm	Ratio = Test/ Predicted	Rotation at failure rad	Failure mode
1	W1/20	254 x 254 UC 73	406 x 178 UB 60	460 x 200 x 12	264	158.4	91.2	1.74	0.038	Thread stripping
2	W1/20	254 x 254 UC 89	406 x 178 UB 60	450 x 200 x 12	209	125.4	85.2	1.47	0.036	Thread stripping
3	W1/20	254 x 254 UC 89	457 x 191 UB 74	510 x 200 x 12	313	187.8	104.6	1.80	0.025	Thread stripping
4	W1/24	254 x 254 UC 89	406 x 178 UB 60	450 x 200 x 15	385	231.0	119.7	1.93	0.050	Thread stripping
5	W1/24	254 x 254 UC 89	457 x 191 UB 74	510 x 200 x 15	459	275.4	140.4	1.96	0.042	Thread stripping
6	W1/24	254 x 254 UC 89	686 x 254 UB 125	720 x 250 x 15	709	425.4	228.4	1.86	0.034	Bolt fracture
7	W2/24	254 x 254 UC 89	457 x 191 UB 74	640 x 200 x 20	417	250.2	164.9	1.52	0.031	End plate fracture
8	W3/20	254 x 254 UC 73	406 x 178 UB 60	460 x 200 x 12	269	161.4	121.2	1.33	0.046	Column web buckling
9	W3/20	254 x 254 UC 89	457 x 191 UB 74	510 x 200 x 12	465	279.0	142.5	1.96	0.053	Column web buckling
10	W3/24	254 x 254 UC 73	406 x 178 UB 60	460 x 200 x 15	276	165.6	152.3	1.09	0.051	Column web buckling
11	W4/24	254 x 254 UC 73	457 x 191 UB 74	640 x 200 x 15	470	282.0	223.4	1.26	0.033	Column web buckling
12	W4/24	254 x 254 UC 89	457 x 191 UB 74	640 x 200 x 15	688	412.8	235.0	1.76	0.061	Column web buckling & end plate fracture
13	W4/24	254 x 254 UC 89	762 x 267 UB 147	930 x 250 x 15	574	688.8	462.3	1.49	0.019	Column web buckling
14	W4/24	254 x 254 UC 132	457 x 191 UB 74	640 x 200 x 15	689	413.4	240.7	1.72	0.039	Bolt fracture
15	W4/24	254 x 254 UC 132	762 x 267 UB 147	930 x 250 x 15	554	664.8	462.3	1.44	0.009	Bolt fracture, thread stripping and end plate fracture
16	Note (i)	254 x 254 UC 89	457 x 191 UB 74	640 x 200 x 15	308	184.8	102.5	1.80	0.034	Bolt fracture and end plate fracture
17	Note (ii)	254 x 254 UC 89	457 x 191 UB 74	640 x 200 x 15	412	247.2	208.6	1.18	0.013	Thread stripping
18	Note (iii)	254 x 254 UC 89	686 x 254 UB 125	860 x 250 x 20	929	557.4	444.7	1.25	0.007	Column web buckling

All flange welds 2 x 10 FW; all web welds 2 x 8 FW. All material S275. All bolts 8.8 (i) As detail W2/24 except that end plate is 15 (not 20) thick (ii) As detail W4/20 except that end plate is 15 (not 12) thick (iii) As detail W5/24 except that end plate is 20 (not 15) thick

Table 5.3: Summary of test results

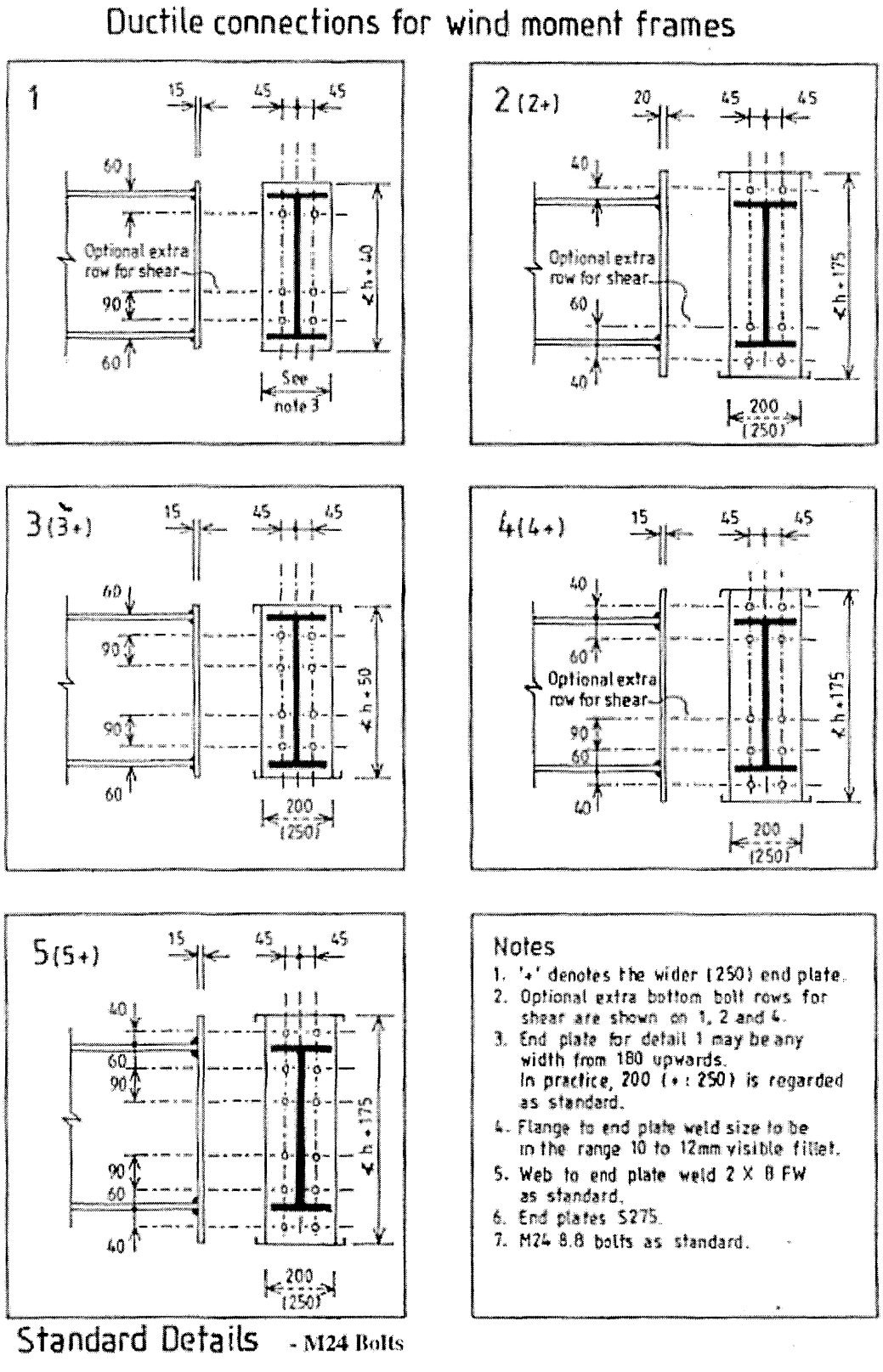

Figure 5.3: Connection details of SCI standard details

5.3.3 Comparison of Failures

As Eurocode 3- Annex J attempts to assess the type of failure that would occur in the various connections, a comparison can be made with the test results. This is shown in table 5.4 which indicates that the failure types noted in the tests and predicted by Eurocode 3 are not in agreement. The first 6 tests failed by bolt stripping or bolt fracture, whilst the failure of the end plate in either mode 1 or mode 2 was predicted (See Chapter 3, Figure 3.12).

Tests 8 to 13 and 18 with two bolt rows, (FEP or EEPs) failed by column web buckling, while failures either in the end plate, column web or column flange were predicted by Eurocode 3- Annex J. Column web buckling accounted for most of the failures in end plates with two or more bolt rows in the test specimens.

The connection with three bolt rows has been shown by the Eurocode 3- Annex J to have zero force in the third bolt row, therefore seen as redundant by the code.

Column web buckling was the most common failure derived practically from physical testing but the most common type of failure predicted by Eurocode 3 -Annex J was end plate failure in either mode 1 or mode 2.

The worrying aspect is that the column web in compression has been included in the code as a possible failure, while column web buckling has been discounted. The difference between column web crushing (compression) and buckling is very small (table 5.5) but this is still a serious oversight by the producers of Eurocode 3-Annex J as the physical tests exemplify. The buckling resistance shown in Table 5.5 was calculated by using Section 5.7.5 of Eurocode 3

5.3.4 Bolt forces

With Eurocode 3-Annex J, an estimation of the bolt force at failure can be carried out, table 5.5 shows the values obtained using the relevant equations from Eurocode 3-Annex J. Using the equation $2f_{ub}A_s$, where f_{ub} is the tensile strength of the bolts from the material tests and A_s is the tensile area, Annex J solutions are much lower than the values from the above equation.

Test	Detail	Failure type	
		Test	Predicted
1	W1/20	Thread stripping	End plate in mode 1
2	W1/20	Thread stripping	End plate in mode 2
3	W1/20	Thread stripping	End plate in mode 1
4	W1/24	Thread stripping	End plate in mode 2
5	W1/24	Thread stripping	End plate in mode 2
6	W1/24	Bolt fracture	End plate in mode 2
7	W2/24	End plate fracture	End plate in mode 2
8	W3/20	Column web buckling	Row 1- End plate in mode 2 Row 2- End plate in mode 1 (group failure)
9	W3/20	Column web buckling	Row 1- End plate in mode 2 Row 2- End plate in mode 1 (group failure)
10	W3/24	Column web buckling	Row 1- End plate in mode 2 Row 2- Column web in compression
11	W4/24	Column web buckling	Row 1- End plate in mode 1 Row 2- Column flange in mode 1
12	W4/24	Column web buckling and end plate fracture	Row 1- End plate in mode 1 Row 2- End plate in mode 2
13	W4/24	Column web buckling	Row 1- End plate in mode 1 Row 2- End plate in mode 2
14	W4/24	Bolt fracture	Row 1- End plate in mode 1 Row 2- End plate in mode 2
15	W4/24	Bolt fracture, thread stripping and end plate fracture	Row 1- End plate in mode 1 Row 2- End plate in mode 2
16	NON-STANDARD	Bolt fracture and end plate fracture	End plate in mode 1
17		Thread stripping	Row 1- End plate in mode 1 Row 2- End plate in mode 2
18		Column web buckling	Row 1- End plate in mode 2 Row 2- Column web in compression Row 3- Zero force

Mode 1 - complete yielding of flange

Mode 2 - bolt failure with yielding of flange

Table 5.4: Failure types

Test	Detail	Failure type	Force in each bolt row kN	Total force acting on bolts kN	Column web in compression $F_{c,wc,Rd}$ kN	Buckling resistance kN	Force required to induce bolt failure in each row kN
1	W1/20	End plate in mode 1		268.1	465.3	445.5	532.1
2	W1/20	End plate in mode 2		250.6	614.2	617.5	435.1
3	W1/20	End plate in mode 1		268.1	619.2	618.1	532.1
4	W1/24	End plate in mode 2		352.0	721.4	687.7	650.9
5	W1/24	End plate in mode 2		360.1	637.0	620.3	670.0
6	W1/24	End plate in mode 2		374.5	732.9	689.2	650.9
7	W2/24	End plate in mode 2		336.5	761.0	693.3	650.9
8	W3/20	Row 1 - End plate in mode 2 Row 2 - End plate in mode 1 (group failure)	268.1 120.1	388.2	465.3	445.5	532.1 532.1
9	W3/20	Row 1 - End plate in mode 2 Row 2 - End plate in mode 1 (group failure)	268.1 126.5	394.6	619.2	618.1	532.1 532.1
10	W3/24	Row 1 - End plate in mode 2 Row 2 - Column web in compression	358.7 121.2	479.9	479.9	447.1	670.0 670.0
11	W4/24	Row 1 - End plate in mode 1 Row 2 - Column flange. in mode 1	198.4 323.7	522.1	552.5	491.9	650.9 650.9
12	W4/24	Row 1 - End plate in mode 1 Row 2 - End plate in mode 2	191.4 353.4	544.8	727.1	688.4	650.9 650.9
13	W4/24	Row 1 - End plate in mode 1 Row 2 - End plate in mode 2	261.5 375.0	636.5	645.9	621.6	640.3 640.3
14	W4/24	Row 1 - End plate in mode 1 Row 2 - End plate in mode 2	209.2 354.2	563.4	1263.6	1234.8	640.3 640.3
15	W4/24	Row 1 - End plate in mode 1 Row 2 - End plate in mode 2	261.5 375.1	636.6	1278.5	1237.0	640.3 640.3
16	NON-STANDARD	End plate in mode 1		209.2	637.0	620.3	640.3
17		Row 1 - End plate in mode 1 Row 2 - End plate in mode 2	209.2 272.2	481.2	637.0	620.3	435.1 435.1
18		Row 1 - End plate in mode 2 Row 2 - Column web in compression Row 3- Discounted	350.9 320.8 0	671.7	671.7	625.6	640.3 640.3 640.3

Table 5.5: Component forces for moment resistance

5.3.5 Classification by Strength

All connections apart from one, can be termed partial strength from the test results. The exception is the connection with a large beam and a small column, using an EEP. This connection has full-strength characteristics according to Eurocode 3-Annex J. A similar situation occurs when the predicted strength capacity is used from Eurocode 3- Annex J. Only two connections failed to achieve the partial strength extension, the others have a lower moment and according to the strength classification are nominally pinned [see table 5.6].

5.3.6 Classification by Rotational stiffness

This is a difficult property to measure, as the M-θ curves are very irregular due to the movement of the connection initially e.g. slippage between the various components. Therefore, finding the initial stiffness from the test results will be open to some inaccuracies. There is still a considerable difference however between test results and the values predicted by Eurocode 3- Annex J.

Various factors can affect the rotational stiffness of the connection, e.g. thickness of end plate, the bolt size , column flange to web thickness and the size of the lever arm.

Annex J checks if the connection is suitable for plastic design at ultimate limit state. The rotation is the main factor that can be used to verify this. Rotation behaviour is discussed in great detail by Bose and Hughes (Bose and Hughes, 1995) in their paper. They state that any value above 0.02 rad can be suitable for ultimate limit design. The values of rotation obtained from the tests and Eurocode 3-Annex J are detailed in table 5.7. There is some difference with the Eurocode 3 Annex J results; some of the test specimens which exhibited the required rotation are not accepted by Eurocode 3. The physical tests that failed the 0.02 rad cut off point, also failed Eurocode 3 Annex J.

Test	Detail	$M_{c,pl,Rd}$ kNm	$M_{b,pl,Rd}$ kNm	Moment required for full strength appellation kNm	Failure moment kNm	Predicted moment resistance kNm	Strength classification	
							Test	Predicted
1	W1/20	272	327	327	158.4	91.2	PS	PS
2	W1/20	326	327	327	125.4	85.2	PS	PS
3	W1/20	326	456	456	187.8	104.6	PS	NP
4	W1/24	326	327	327	231.0	119.7	PS	PS
5	W1/24	326	456	456	275.4	140.4	PS	PS
6	W1/24	326	1060	652	425.4	228.4	PS	PS
7	W2/24	326	456	456	250.2	164.9	PS	PS
8	W3/20	272	327	327	161.4	121.2	PS	PS
9	W3/20	326	456	456	279.0	142.5	PS	PS
10	W3/24	272	327	327	165.6	152.3	PS	PS
11	W4/24	272	456	456	282.0	223.4	PS	PS
12	W4/24	326	456	456	412.8	235.0	PS	PS
13	W4/24	326	1370	652	688.8	462.3	FS	PS
14	W4/24	496	456	456	413.4	240.7	PS	PS
15	W4/24	496	1370	992	664.8	462.3	PS	PS
16	NON- STANDARD	326	456	456	184.8	102.5	PS	NP
17		326	456	456	247.2	208.6	PS	PS
18		326	1060	652	557.4	444.7	PS	PS

FS = Full strength; PS = Partial strength; NP = Nominally pinned

Table 5.6: Strength classification

5.4 Conclusions

Eurocode 3 Annex J is a step forward in the design of steel bolted connections but from the tests and the comparisons carried out, it appears that the code has to be modified before it can be used safely. One of the problems with Eurocode3- Annex J is in underestimating of the strength of the connection, this method must be modified to produce a more economic design. Another problem that has to be overcome is the mode of failure prediction in Eurocode 3. The most common prediction from Eurocode 3 Annex J was end plate failure but in reality column web buckling was the most common type of failure. This leads on to the main concern, that there is no provision in the code for column web buckling and this is a serious oversight that must be corrected. The problem with bolts in the tests can be resolved easily with the introduction of the European Codes for bolts. Bolts that failed due to stripping complied with the British Standard, BS 3693 (British Standard Institution, 1967) and not the new BS EN 24014, 24016, 24032, 24034, 10002 codes (British Standard Institution, 1992;). Eurocode 3 Annex J is the way forward with its innovative method of connection design. However there are still major issues that require resolution.

Test	Detail	Initial rotational stiffness MNm/rad		Ratio = Test/ Predicted	Stiffness Classification			
					Test		Predicted	
		Test	Predicted		Braced	Unbraced	Braced	Unbraced
1	W1/20	21.3	29.8	0.71	SR	SR	SR	SR
2	W1/20	21.6	42.4	0.51	SR	SR	R	SR
3	W1/20	30.4	46.1	0.66	SR	SR	SR	SR
4	W1/24	37.5	53.9	0.70	R	SR	R	SR
5	W1/24	36.0	55.2	0.65	SR	SR	R	SR
6	W1/24	83.3	177.0	0.47	SR	SR	R	SR
7	W2/24	60.0	116.1	0.52	R	SR	R	SR
8	W3/20	40.0	32.6	1.23	R	SR	SR	SR
9	W3/20	46.7	53.6	0.87	SR	SR	R	SR
10	W3/24	21.3	37.6	0.57	SR	SR	R	SR
11	W4/24	65.0	107.2	0.61	R	SR	R	SR
12	W4/24	100.0	131.1	0.76	R	SR	R	SR
13	W4/24	220.0	355.2	0.62	R	SR	R	SR
14	W4/24	75.0	169.3	0.44	R	SR	R	R
15	W4/24	258.3	489.1	0.53	R	SR	R	R
16	NON STANDARD	35.0	96.1	0.36	SR	SR	R	SR
17		60.0	118.1	0.51	R	SR	R	SR
18		143.8	318.9	0.45	R	SR	R	SR

SR- Semi rigid; R- Rigid

Table 5.7: Stiffness classification

Finite Element Method and ABAQUS

Chapter 6

6.0 Introduction

Finite element analysis of structures is seen as one of the most powerful techniques to solve large complex and time consuming problems. This type of analysis can be used to solve problems ranging from analysing the behaviour of a structure to CFD (computational fluid dynamics) problems. There are many well written books on the subject and the following explanation of the theory is taken from a cross section of the following (Zienkiewicz, 1998; Rockey et al. 1998; Rao, 1988).

The first stage of the analysis is to define the elements being used, these range from the two-dimensional (tetrahedron) to the three dimensional (hexahedron) element. The following tables extracted from reference(Rao, 1988) detail the basic equations that must be used in determining solutions to finite element modelling problems:

Type of Equations	Number of Equations in 3-dimensional problems
Equilibrium equations	3
Stress-strain relations	6
Strain-displacement relations	6
Total number of equations	15

Table 6.1: Number and type of equations for each category that must be used. (Rao, 1988)

6.1 Hexahedron elements

Hexahedron elements are elements that have 8 nodes to create a cube (figure 6.1). The nodes are at the corner of the elements and each of these have three degrees of freedom (x, y and z directions); therefore the element has a total of 24 degrees of freedom.

The number of unknowns in table 6.2 must match the number of equations in table 6.1.

Unknowns	In 3-dimensional problems using Displacement method of Analysis
Displacements	u, v, w
Stresses	σ_{xx}, σ_{yy}, σ_{zz}, σ_{xy}, σ_{yz}, σ_{zx}
Strains	ε_{xx}, ε_{yy}, ε_{zz}, ε_{xy}, ε_{yz}, ε_{zx}
Total number of unknowns	15

Table 6.2: Number of unknowns to be obtained. (Rao, 1988)

Within each 3-D model there may exist, hundreds, maybe even thousands of elements. The individual elements and nodes within that element use their own co-ordinate system (local co-ordinate system) to define movement of their own nodes. In order to model the overall structure the individual elements must be related to each other. This is achieved by defining the elements in terms of a global co-ordinate system, which relates the displacement, rotation, stress etc of a single element to the rest of the structure. In order to carry this out the base state is selected (global co-ordinates) "Global co-ordinate system is one which is defined for the entire domain or body" (Rao, 1988, P125)

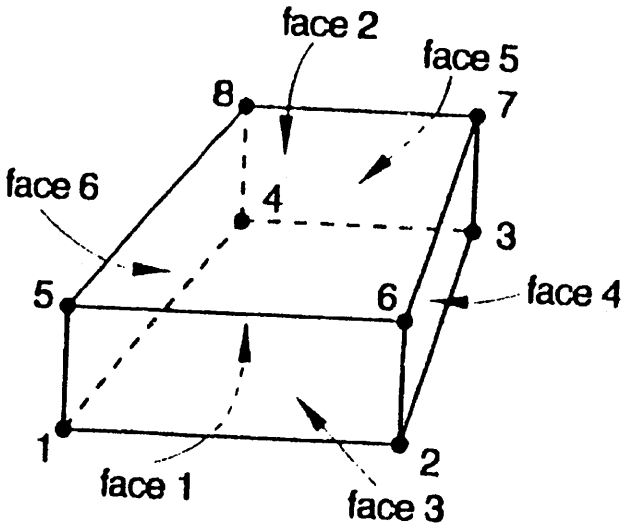

Figure 6.1: Typical example of a 8 node Hexahedron element

6.1.1 Co-ordinate system used for Hexahedron elements.

Figure 6.1 details the layout of the hexahedron element, which can be any six sided shape not necessarily a cube, but for ease of discussion a cube is selected. The same principle and method would still be valid for other six sided elements.

The first step is to relate the local co-ordinates of the element to the global co-ordinates of the structure. This can be achieved via a 'shape function' and expressed as:

$$\begin{Bmatrix} x \\ y \\ z \end{Bmatrix} == [N] \begin{Bmatrix} x_1 \\ y_1 \\ z_1 \\ x_2 \\ y_2 \\ z_2 \\ \vdots \\ z_8 \end{Bmatrix} \tag{6.1}$$

Where,

x_1, y_1 and z_1 are the displacements in the three directions at node 1 etc.

$$[N] = \begin{bmatrix} N_1 & 0 & 0 & N_2 & \vdots & 0 \\ 0 & N_1 & 0 & 0 & \vdots & 0 \\ 0 & 0 & N_1 & 0 & \vdots & N_8 \end{bmatrix} \tag{6.2}$$

Where [N] is the column matrix relating to the shape function for displacement. The shape functions relate to the different ways the element can distort due to loading and thus the movement of the nodes:

where

$$N_i(r,s,t) = \frac{1}{8}(1+rr_i)(1+ss_i)(1+tt_i) \quad , \mathrm{i} = 1, \mathrm{to}\ 8 \tag{6.3}$$

or

$$\mathrm{x} = \sum_{\mathrm{i}=1}^{8} \mathrm{N_i x_i} \qquad \mathrm{y} = \sum_{\mathrm{i}=1}^{8} \mathrm{N_i y_i} \qquad \mathrm{z} = \sum_{\mathrm{i}=1}^{8} \mathrm{N_i z_i} \tag{6.4}$$

i.e the total displacement in the x, y z direction is based on the sum of the displacements of the individual nodes in the relevant directions, be they positive or negative.

6.2 Static Analysis

For static analysis there is a requirement and relationship between three states, these are equilibrium, strain compatibility and natural relationship.

6.2.1 Formation of Equilibrium equations

There are six steps that are followed for successful completion of any analysis, in order that the relevant states can be obtained, which are:

i) The definition of the solid body using small elements i.e. finite elements (Figure 6.1)
ii) The development of displacement model within each element.
iii) The derivation of the element characteristic (stiffness) matrix and characteristic (load) vectors from the principles of minimum potential energy.
iv) The formation of the equilibrium equations of the overall structure of body.
v) The solution for the nodal displacements, and
vi) The solutions for the element stresses obtained

6.2.2 (i) Defining the model as small elements

Defining the model as finite elements is carried out by the designer/researcher. The elements can be of any size, but the smaller the elements the more equations generated.

6.2.3 (ii) Displacement Model

In order to use the displacement model an assumption that the "variation of the displacement between the various nodes is linear". This means an expression can be obtained similar to that used to describe the geometry of the section.

$$\begin{Bmatrix} u \\ v \\ w \end{Bmatrix} = [N] \begin{Bmatrix} u_1 \\ v_1 \\ w_1 \\ u_2 \\ \vdots \\ w_8 \end{Bmatrix} = [N]\vec{Q}^{(e)} \tag{6.5}$$

Where, $\vec{Q}^{(e)}$ is the vector of nodal displacement based on various polynomial expressions using u_i, v_i and w_i (displacements of node i, where i= 1 to 8, Hexahedron element as in figure 6.1)

With the geometry of the structure established it is necessary to transpose the local displacements to the global system. The next step therefore is to express the strain within in each element in terms of the whole model i.e combining the strains of the individual elements.

6.2.3.1 Strain-displacement

There are three normal strain components in the x, y and z directions and three shear strain components. The deformed shape of the structure due to the loading and or temperature change can be described by three displacement components, u, v and w. These are parallel to the directions x, y and z (global axes) and are functions of the co-ordinates x, y and z. The following expression gives the strain matrix of a given element.

$$\vec{\varepsilon} = \begin{Bmatrix} \varepsilon_{xx} \\ \varepsilon_{yy} \\ \varepsilon_{zz} \\ \varepsilon_{xy} \\ \varepsilon_{yz} \\ \varepsilon_{zx} \end{Bmatrix} = \begin{Bmatrix} \dfrac{\partial u}{\partial x} \\ \dfrac{\partial v}{\partial y} \\ \dfrac{\partial w}{\partial z} \\ \dfrac{\partial u}{\partial y} + \dfrac{\partial v}{\partial x} \\ \dfrac{\partial u}{\partial z} + \dfrac{\partial w}{\partial y} \\ \dfrac{\partial w}{\partial x} + \dfrac{\partial u}{\partial z} \end{Bmatrix} = \underset{6x24}{[B]} \quad \underset{24x1}{\vec{Q}^{(e)}} \tag{6.6}$$

where, $\underset{6x24}{[B]} = [[B_1][B_2].....[B_8]]$

$$\underset{6x3}{[B_i]} = \begin{bmatrix} \frac{\partial N_i}{\partial x} & 0 & 0 \\ 0 & \frac{\partial N_i}{\partial y} & 0 \\ 0 & 0 & \frac{\partial N_i}{\partial z} \\ \frac{\partial N_i}{\partial y} & \frac{\partial N_i}{\partial x} & 0 \\ 0 & \frac{\partial N_i}{\partial z} & \frac{\partial N_i}{\partial y} \\ \frac{\partial N_i}{\partial z} & 0 & \frac{\partial N_i}{\partial x} \end{bmatrix}, \text{ i = 1 to 8} \tag{6.7}$$

The derivatives within the matrix $[B_i]$ can be evaluated by using the chain rule of differentiation to obtain the following:

$$\begin{Bmatrix} \frac{\partial N_i}{\partial r} \\ \frac{\partial N_i}{\partial s} \\ \frac{\partial N_i}{\partial t} \end{Bmatrix} = \begin{Bmatrix} \frac{\partial N_i}{\partial x}\cdot\frac{\partial x}{\partial r} + \frac{\partial N_i}{\partial y}\cdot\frac{\partial y}{\partial r} + \frac{\partial N_i}{\partial z}\cdot\frac{\partial z}{\partial r} \\ \frac{\partial N_i}{\partial x}\cdot\frac{\partial x}{\partial s} + \frac{\partial N_i}{\partial y}\cdot\frac{\partial y}{\partial s} + \frac{\partial N_i}{\partial z}\cdot\frac{\partial z}{\partial s} \\ \frac{\partial N_i}{\partial x}\cdot\frac{\partial x}{\partial t} + \frac{\partial N_i}{\partial y}\cdot\frac{\partial y}{\partial t} + \frac{\partial N_i}{\partial z}\cdot\frac{\partial z}{\partial t} \end{Bmatrix} \tag{6.8}$$

$$= \begin{bmatrix} \frac{\partial x}{\partial r} & \frac{\partial y}{\partial r} & \frac{\partial z}{\partial r} \\ \frac{\partial x}{\partial s} & \frac{\partial y}{\partial s} & \frac{\partial z}{\partial s} \\ \frac{\partial x}{\partial t} & \frac{\partial y}{\partial t} & \frac{\partial z}{\partial t} \end{bmatrix} \begin{Bmatrix} \frac{\partial N_i}{\partial x} \\ \frac{\partial N_i}{\partial y} \\ \frac{\partial N_i}{\partial z} \end{Bmatrix} = [J] \begin{bmatrix} \frac{\partial N_i}{\partial x} \\ \frac{\partial N_i}{\partial y} \\ \frac{\partial N_i}{\partial z} \end{bmatrix} \tag{6.9}$$

Where [J] is the Jacobian matrix,

The numerical coefficients within this matrix are dependant on the size, shape and orientation of the elements, which is dictated by the node co-ordinates and element numbers assigned by the user.

$$[J]_{3x3} = \begin{bmatrix} \frac{\partial x}{\partial r} & \frac{\partial y}{\partial r} & \frac{\partial z}{\partial r} \\ \frac{\partial x}{\partial s} & \frac{\partial y}{\partial s} & \frac{\partial z}{\partial s} \\ \frac{\partial x}{\partial t} & \frac{\partial y}{\partial t} & \frac{\partial z}{\partial t} \end{bmatrix} = \begin{bmatrix} \sum_{i=1}^{8}\left(\frac{\partial N_i}{\partial r}x_i\right) & \sum_{i=1}^{8}\left(\frac{\partial N_i}{\partial r}y_i\right) & \sum_{i=1}^{8}\left(\frac{\partial N_i}{\partial r}z_i\right) \\ \sum_{i=1}^{8}\left(\frac{\partial N_i}{\partial s}x_i\right) & \sum_{i=1}^{8}\left(\frac{\partial N_i}{\partial s}y_i\right) & \sum_{i=1}^{8}\left(\frac{\partial N_i}{\partial s}z_i\right) \\ \sum_{i=1}^{8}\left(\frac{\partial N_i}{\partial t}x_i\right) & \sum_{i=1}^{8}\left(\frac{\partial N_i}{\partial t}y_i\right) & \sum_{i=1}^{8}\left(\frac{\partial N_i}{\partial t}z_i\right) \end{bmatrix} \tag{6.10}$$

The Jacobian matrix is used due to the possibility of "violent distortion" within the element (in this case Hexahedron) and thus using the matrix above allows a unique mapping / scaling between the various coordinates.

The derivatives of the interpolation functions can be obtained from

$$\left.\begin{aligned} \frac{\partial N_i}{\partial r} &= \frac{1}{8}r_i(1+ss_i)(1+tt_i) \\ \frac{\partial N_i}{\partial s} &= \frac{1}{8}s_i(1+rr_i)(1+tt_i) \\ \frac{\partial N_i}{\partial t} &= \frac{1}{8}t_i(1+rr_i)(1+ss_i) \end{aligned}\right\}, \text{ i = 1 to 8} \tag{6.11}$$

Where (r_i, s_i, t_i) are the natural co-ordinates (Figure 6.2) of node i and this can be defined using

$$\begin{Bmatrix} r_1 \\ r_2 \\ r_3 \\ r_4 \\ r_5 \\ r_6 \\ r_7 \\ r_8 \end{Bmatrix} = \begin{Bmatrix} -1 \\ 1 \\ 1 \\ -1 \\ -1 \\ 1 \\ 1 \\ -1 \end{Bmatrix} \quad \begin{Bmatrix} s_1 \\ s_2 \\ s_3 \\ s_4 \\ s_5 \\ s_6 \\ s_7 \\ s_8 \end{Bmatrix} = \begin{Bmatrix} -1 \\ -1 \\ 1 \\ 1 \\ -1 \\ -1 \\ 1 \\ 1 \end{Bmatrix} \quad \begin{Bmatrix} t_1 \\ t_2 \\ t_3 \\ t_4 \\ t_5 \\ t_6 \\ t_7 \\ t_8 \end{Bmatrix} = \begin{Bmatrix} -1 \\ -1 \\ -1 \\ -1 \\ 1 \\ 1 \\ 1 \\ 1 \end{Bmatrix} \tag{6.12}$$

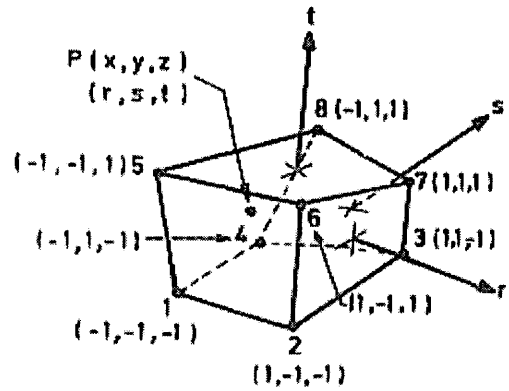

Figure 6.2: Determining the natural co-ordinate system for 3D element (Rao, 1988)

By inverting the matrix in equation 6.9, the following is obtained:

$$\begin{Bmatrix} \frac{\partial N_i}{\partial x} \\ \frac{\partial N_i}{\partial y} \\ \frac{\partial N_i}{\partial z} \end{Bmatrix} = [J]^{-1} \begin{Bmatrix} \frac{\partial N_i}{\partial r} \\ \frac{\partial N_i}{\partial s} \\ \frac{\partial N_i}{\partial t} \end{Bmatrix} \tag{6.13}$$

And then $[B_i]$ can be calculated.

6.2.3.2 Stress- Strain relationship

The stress- strain relationship can be expressed in general terms of Hooke's law (Elastic).

$$\sigma = E\varepsilon = \text{Young's Modulus x strain}$$

Stress at any point in a three dimensional element can be defined by the following vector comprising six components:

$$\vec{\sigma}^T = \left\{ \sigma_{xx} \sigma_{yy} \sigma_{zz} \sigma_{xy} \sigma_{yz} \sigma_{zx} \right\}$$

Stress-strain relationship for Three Dimensional elements can therefore be expressed as

$$\vec{\sigma} = [D]\vec{\varepsilon} \tag{6.14}$$

Where, [D] is the elastic matrix and is in the form:

$$[D] = \frac{E}{(1+v)(1-2v)} \begin{bmatrix} (1-v) & v & v & 0 & 0 & 0 \\ v & (1-v) & v & 0 & 0 & 0 \\ v & v & (1-v) & 0 & 0 & 0 \\ 0 & 0 & 0 & \left(\frac{1-2v}{2}\right) & 0 & 0 \\ 0 & 0 & 0 & 0 & \left(\frac{1-2v}{2}\right) & 0 \\ 0 & 0 & 0 & 0 & 0 & \left(\frac{1-2v}{2}\right) \end{bmatrix} \tag{6.15}$$

where v is Poisson's ratio and E is the Young's Modulus of Elasticity.

6.2.4 (iii) Element Stiffness Matrix

The element characteristic (stiffness) matrix for three dimensional eiements is given by:

$$[K^{(e)}] = \iiint_{V^{(e)}} [B]^T [D][B] \cdot dV \tag{6.16}$$

and it is also necessary to carry out the integration in natural co-ordinates using the following relationship. As matrix [B] was expressed in natural co-ordinates (Figure 6.2):

$$dV = dx\, dy\, dz = \det[J] \cdot dr\, ds\, dt \tag{6.17}$$

6.2.4.1 Element Characteristic (load) vector ($\vec{P}^{(e)}$)

To obtain the vector of element nodal forces, the following equation is used:

$$\vec{P}^{(e)} = \iiint_{V^{(e)}} [B]^T [D]\vec{\varepsilon}_v \cdot dV + \iiint_{V^{(e)}} [N]^T \vec{\phi} \cdot dV + \iint_{S_1^{(e)}} [N]^T \vec{\phi} \cdot dS_1 \tag{6.18}$$

Where

[D] is the elastic matrix;

[N] is the column matrix relating to the shape function for displacement;

$[B]^T$ is the transpose of equation 6.8;

ϕ is vector variable comprising components u, v and w

$\vec{P}_i^{(e)} = \iiint_{V^{(e)}} [B]^T [D] \vec{\varepsilon}_o \cdot dV$ = Vector of element nodal forces produced by the initial strain;

$\vec{P}_b^{(e)} = \iiint_{V^{(e)}} [N]^T \vec{\phi} \cdot dV$ = Vector of element nodal forces produced by body forces; and

$\vec{P}_s^{(e)} = \iint_{S_1^{(e)}} [N]^T \vec{\phi} \cdot dS_1$ = Vector of element nodal forces produced by surface forces.

6.2.4.2 Beam Elements

Beam elements are also vital in linking various components together and thus an understanding of their behaviour is vital, Figures 6.3 and 6.4 detail beam elements. The beam element has two nodes, at either end of the section. The nodes are called i and j and the variation of u (displacement) within the element is assumed to be linear. The local co-ordinate system assumes that the x axis is taken in the axial direction of the beam.

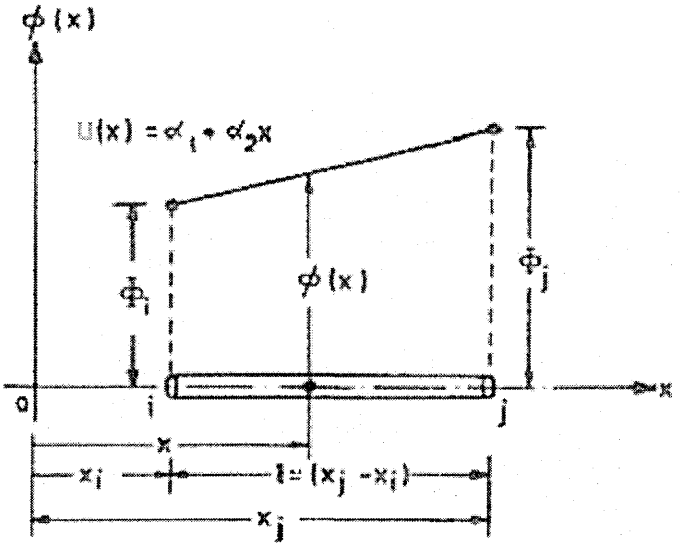

Figure 6.3: Bar element (Rao, 1988)

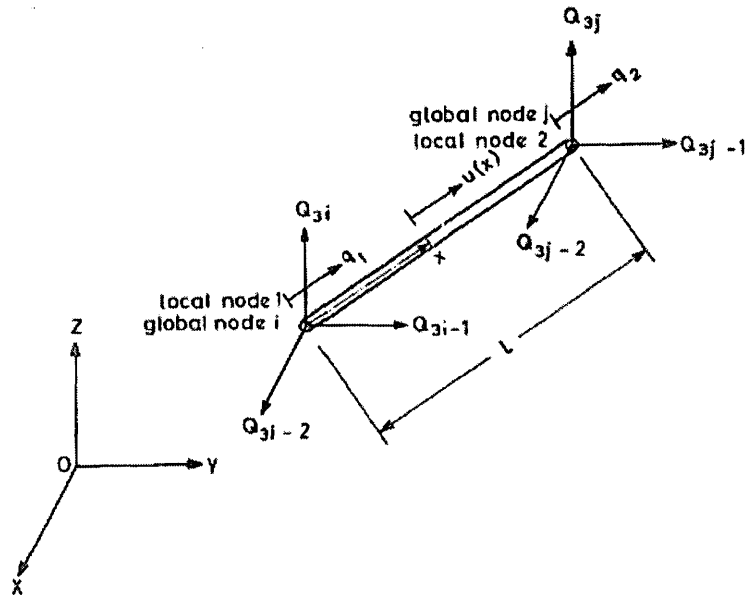

Figure 6.4: Example of the local co-ordinates system for a space truss (Rao, 1988)

Thus the equation can be written relating the displacement in the x direction:

$$u(x) = \alpha_1 + \alpha_2 x \tag{6.19}$$

based on the standard equation

$$u(x) = \alpha_1 + \alpha_2 x + \alpha_3 x^2 + \ldots + \alpha_{n+1} x^n \tag{6.20}$$

where n=1 in this case as it is assumed to be linear behaviour and α_1 and α_2 are constants.

The two constants α_1 and α_2 are the unknown co-efficients. By using the nodal conditions we can obtain:

$u(x) = q_1$ at $x = 0$

$u(x) = q_2$ at $x = 1$

With the above equations

$$u(x) = q_1 + (q_2 - q_1)\frac{x}{l} \tag{6.21}$$

This relationship is usually written as

$$\underset{1x1}{\{u(x)\}} = \underset{1x2}{[N]}\bar{q}^{(e)} \tag{6.22}$$

Where, N is shape function matrix $[N] = \left[\left(1-\frac{x}{l}\right) \quad \frac{x}{l}\right]$ and $\bar{q}^{(e)} = \begin{Bmatrix} q_1 \\ q_2 \end{Bmatrix}$

Using the basic equation for strain:

$$\varepsilon = \frac{\Delta L}{L} = \frac{\text{Change in length}}{\text{Original Length}} \tag{6.23}$$

in the form

$$\varepsilon_{xx} = \frac{\partial u(x)}{\partial x} = \frac{q_2 - q_1}{l} \tag{6.24}$$

This produces

$$\underset{1x1}{\{\varepsilon_{xx}\}} = \underset{1x2}{[B]}\bar{q}^{(e)} \tag{6.25}$$

Where $[B] = \left[-\frac{1}{l} \quad \frac{1}{l}\right]$

Thus the stress-strain relationship can be obtained

$$\sigma_{xx} = E\,\varepsilon_{xx} \tag{6.26}$$

and

$$\underset{1x1}{\{\sigma_{xx}\}} = \underset{1x1}{[D]}\underset{1x1}{\{\varepsilon_{xx}\}} \tag{6.27}$$

Using the above equations the stiffness of the beam can now be obtained in terms of the local co-ordinate system.

$$\underset{2x2}{\left[k^{(e)}\right]} = \iiint_{V^{(e)}} [B]^T [D][B] \cdot dV = A \int_{x=0}^{l} \begin{Bmatrix} -\frac{1}{l} \\ \frac{1}{l} \end{Bmatrix} E \begin{Bmatrix} -\frac{1}{l} & \frac{1}{l} \end{Bmatrix} dx = \frac{AE}{l} \begin{bmatrix} 1 & -1 \\ -1 & 1 \end{bmatrix} \quad (6.28)$$

Where, A is the cross sectional area of the beam

The equation now obtained defines a single finite element (a beam) but this only relates to the local co-ordinate system. Usually these types of elements are part of a larger structure and therefore they must be related to the global co-ordinate system. This is achieved by means of the transformation matrix which links the two systems of co-ordinates.

The various steps required to achieve this are as follows:

Let the local system of co-ordinates be nodes 1 and 2, and i and j in the global system of co-ordinates (Figure 6.4).

The displacement in the local system q_1 and q_2, which can be represented as $Q3_{i-2}$, $Q3_{i-1}$, $Q3_i$ and $Q3_{j-2}$, $Q3_{j-1}$, $Q3_j$, which are parallel to the x, y and z axes respectively

Thus the two sets of displacements can be represented by

$$q_1 = l_{ij} Q_{3i-2} + m_{ij} Q_{3i-1} + n_{ij} Q_{3i} \quad (6.29)$$
$$q_2 = l_{ij} Q_{3j-2} + m_{ij} Q_{3j-1} + n_{ij} Q_{3j}$$

or

$$\vec{q}^{(e)} = [\lambda] \vec{Q}^{(e)} \quad (6.30)$$

where

$$[\lambda] = \begin{bmatrix} l_{ij} & m_{ij} & n_{ij} & 0 & 0 & 0 \\ 0 & 0 & 0 & l_{ij} & m_{ij} & n_{ij} \end{bmatrix} \quad (6.31)$$ is the transformation matrix, and

$$\vec{Q}^{(e)} = \begin{Bmatrix} Q_{3i-2} \\ Q_{3i-1} \\ Q_{3i} \\ Q_{3j-2} \\ Q_{3j-1} \\ Q_{3j} \end{Bmatrix} \text{ is the vector of nodal displacements for a single element,} \tag{6.32}$$

and l_{ij}, m_{ij} and n_{ij} are the direction cosines of angles between the line i j and the directions OX, OY and OZ respectively.

The direction cosines can therefore be expressed in terms of global co-ordinates:

$$l_{ij} = \frac{Xj - Xi}{L}, m_{ij} = \frac{Yj - Yi}{L}, n_{ij} = \frac{Zj - Zi}{L} \tag{6.33}$$

where,

(X_i, Y_i, Z_i) and (X_j, Y_j, Z_j) are the global co-ordinates of nodes i and j respectively, and L is the length of the element i j which is given by

$$l = \left\{ \left(X_j - X_i\right)^2 + \left(Y_j - Y_i\right)^2 + \left(Z_j - Z_i\right)^2 \right\}^{\frac{1}{2}} \tag{6.34}$$

With transformation matrix obtained the stiffness matrix for the element **e** can now be obtained in the global co-ordinate system, and this is given by:

$$\underset{6x6}{\left[K^{(e)}\right]} = \underset{6x2}{[\lambda]^T} \underset{2x2}{\left[k^{(e)}\right]} \underset{2x6}{[\lambda]} = \frac{AE}{L} \begin{bmatrix} L_{ij}^2 & L_{ij}m_{ij} & L_{ij}n_{ij} & -L_{ij}^2 & -L_{ij}m_{ij} & -L_{ij}n_{ij} \\ L_{ij}m_{ij} & m_{ij}^2 & m_{ij}n_{ij} & -L_{ij}m_{ij} & -m_{ij}^2 & -m_{ij}n_{ij} \\ L_{ij}n_{ij} & m_{ij}n_{ij} & n_{ij}^2 & -L_{ij}n_{ij} & -m_{ij}n_{ij} & -n_{ij}^2 \\ -L_{ij}^2 & -L_{ij}m_{ij} & -L_{ij}n_{ij} & L_{ij}^2 & L_{ij}m_{ij} & L_{ij}n_{ij} \\ -L_{ij}m_{ij} & -m_{ij}^2 & -m_{ij}n_{ij} & L_{ij}m_{ij} & m_{ij}^2 & m_{ij}n_{ij} \\ -L_{ij}n_{ij} & -m_{ij}n_{ij} & -n_{ij}^2 & L_{ij}n_{ij} & m_{ij}n_{ij} & n_{ij}^2 \end{bmatrix} \tag{6.35}$$

6.2.4.3 Consistent Load Vector

The consistent load vectors can be found using equations 6.16, 6.18 and 6.27.

Load vector due to initial strains(temperature) can be expressed as:

$$\vec{p}_i^{(e)} = \iiint_{V^{(e)}} [B]^T [D]\vec{\varepsilon}_o \cdot dV = A\int_0^l \begin{Bmatrix} -\frac{1}{L} \\ \frac{1}{L} \end{Bmatrix} [E]\{\alpha T\} \cdot dx = A \;\; E \;\; \alpha T \begin{Bmatrix} -1 \\ 1 \end{Bmatrix} \tag{6.36}$$

Load vector due to constant body force can be expressed as:

$$\vec{p}_b^{(e)} = \iiint_{V^{(e)}} [N]^T \vec{\phi} \cdot dV = A\int_0^l \begin{Bmatrix} 1-\frac{x}{L} \\ \frac{x}{L} \end{Bmatrix} \{\phi\} \cdot dx = \frac{\phi_0 \;\; AL}{2} \begin{Bmatrix} 1 \\ 1 \end{Bmatrix} \tag{6.37}$$

As the beam is in one direction only i.e. p_x, (Applied force) must be applied at one of the nodal points. It is assumed that the stress is applied at node 1, therefore the load vector becomes:

$$\vec{p}_{s1}^{(e)} = \iint_{s_1^{(e)}} [N]^T \{p_x\} \cdot dS_1 = p_o \begin{Bmatrix} 1 \\ 0 \end{Bmatrix} \iint_{s_1^{(e)}} dS_1 = p_o \cdot A_1 \begin{Bmatrix} 1 \\ 0 \end{Bmatrix} \tag{6.38}$$

Therefore, the total consistent load vector in the local co-ordinate system can be given by

$$\vec{P}^{(e)} = \vec{P}_i^{(e)} + \vec{P}_b^{(e)} + \vec{P}_{s_1}^{(e)} + \vec{P}_{s_2}^{(e)} \tag{6.39}$$

Converting this to the global co-ordinate system in order to relate back to the other elements in the structure. This can be expressed as:

$$\vec{P}^{(e)} = [\lambda]^T \vec{P}^{(e)} \tag{6.40}$$

Where, $[\lambda]$ (Transformation matrix) can be obtained from equation (6.30)

The above discussion gives a general background to the finite element modelling but as a specific package was used in the investigation the following discussion will concentrate on in the finite element package ABAQUS.

6.3 ABAQUS

With any commercially available finite element package, an understanding of the fundamental equations used is essential in order that project is completed successfully. The theory behind the development of not just the equations to solve the models but also how the materials are defined, how loads are applied and how stress/strains are derived etc.

ABAQUS has a wide variety of elements and methods to select from and the following discussion will relate to particular methods employed by the author, within the various models used to validate the experimental results.

If the problem to be solved is non- linear in nature then an iterative procedure has to be used to find the solution. This is why the Newton Raphson Method of Analysis is used by ABAQUS.

6.3.1 Newton Raphson Method of Analysis

The standard Newton Raphson method is normally used by ABAQUS to solve most non-linear problems. This method is preferred over alternative methods (Modified Newton Raphson or quasi-Newton method) because of the faster convergence rate when modelling using finite element analysis.

However, the main reason why the Newton Raphson method is usually avoided for solving large finite element models is because the **Jacobian matrix** is difficult to formulate with large models. The other reason is that this method is expensive to run on the computer, because the "Jacobian matrix" must be formed and solved at each iteration . This is when the modified Newton Raphson method is often used (see section 6.4.2).

6.3.1.1 How the Newton Raphson method works

The Standard Newton Raphson method assumes that the computer makes an initial estimate of displacement by using the linear stiffness equation, with the stiffness value used from the previous load condition. The value of strain is then calculated and an equivalent stress is taken from the input for the material properties, i.e. the stress-strain curve data. This stress is then compared with the stress due to the applied load. If this is different then it means that a residual force is present within the structure; if this difference from is within a certain predefined limits then a satisfactory solution

has occurred. If the residual force is outwith the predefined limits (tolerance), then the above process is repeated for a new reduced displacement. The stiffness is updated from the calculations of each estimate and then taken as a tangent to the stress-strain curve at the point it previously considered [See figure 6.5].

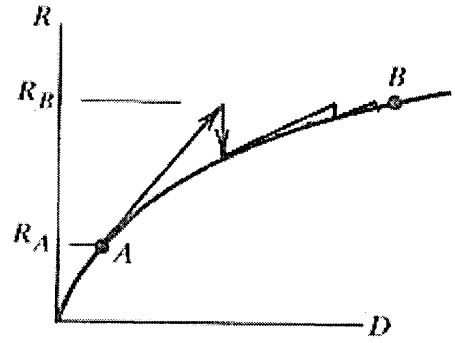

Figure 6.5: Newton Raphson method of Analysis.

This "guess work" is the reason that the initial increment takes some considerable time; time is required to narrow the limits of displacement. Once this is obtained then the number of iterations per increment will be less due to the software now having the approximate displacement, i.e. working from the first solution to find the next.
In the standard Newton Raphson procedure each iterative calculation is based upon the current **tangent stiffness**. The matrix produced during this type of analysis is large and can cause problems depending on the hardware i.e. large solver file. The Newton-Raphson method requires that the stiffness matrix [K] is derived for each cycle, making it slow. For a highly non-linear problem the Newton Raphson method is not efficient and therefore other methods have to be tried.

6.3.1.2 Example of Newton Raphson method

The example below explains how to obtain the solution for the following expression $x^2-4 = 0$.

Using basic Newton Raphson equation of $x_{n+1} = x_n - \frac{f(x_n)}{f'(x_n)}$

n	x_n	$f(x_n)$	$f'(x_n)$	x_{n+1}	dx
0	x_0=6	$f(x_0$=32)	$f'(x_0$=12)	x_1=3.33	
1	x_1=3.33	$f(x_1$=7.09)	$f'(x_1$=6.66)	x_2=2.27	dx=1.06
2	x_2=2.27	$f(x_2$=1.14)	$f'(x_2$=4.53)	x_3=2.02	dx=0.25
3	x_3=2.02	$f(x_3$=0.06)	$f'(x_3$=4.03)	x_3=2.00	dx=0.02

$f(x_n)= x^2-4$.

$f'(x_n)= 2x$ (Jacobian derivative)

Initial estimate is 6.

6.3.2 Modified Newton Raphson Method

Modified Newton method is very similar to the Newton Raphson method but the Jacobian matrix is not calculated as often. This means that the matrix will be used for several iterations and thus faster in some cases, when there are severe non-linear conditions are to be analysed. A non-symmetric Jacobian matrix is produced, but the user is allowed to choose to use a symmetric approximation of the Jacobian which allows quicker convergence.

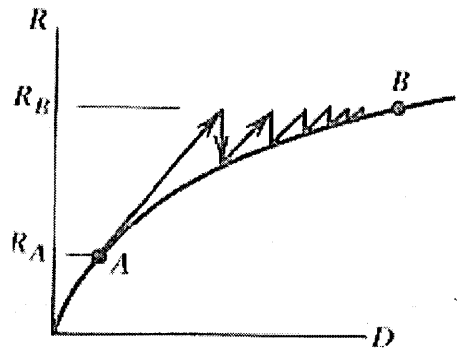

Figure 6.6 Example of Modified Newton Raphson method of Analysis

6.3.2.1 Example of Modified Newton Raphson

The example below explains how to obtain the solution for the following equation $x^2-4 = 0$.

n	x_n	$f(x_n)$	$f'(x_n)$	x_{n+1}	dx
0	$x_0=6$	$f(x_o=32)$	$f'(x_o=12)$	$x_1=3.33$	
1	$x_1=3.33$	$f(x_1=7.09)$	$f'(x_1=12)$	$x_2=2.74$	dx=0.59
2	$x_2=2.74$	$f(x_2=3.51)$	$f'(x_2=12)$	$x_3=2.45$	dx=0.29
3	$x_3=2.45$	$f(x_3=1.99)$	$f'(x_3=4.9)$	$x_3=2.04$	dx=0.41
4	$x_3=2.04$	$f(x_3=0.17)$	$f'(x_3=4.9)$	$x_3=2.01$	dx=0.03
5	$x_3=2.01$	$f(x_3=0.03)$	$f'(x_3=4.01)$	$x_3=2.00$	dx=0.01

$f(x_n)=x^2-4.$

$f'(x_n)= 2x$

Initial estimate is 6.

The example indicates that the Newton-Raphson method is faster than the Modified method in terms of number of steps used, but this does not take account of the time involved in calculating $f'(x_n)$. In the above example the calculation time is insignificant as this is such a simple example but for more complex problems (non-linear), the modified method can reduce the simulation time considerably.

6.3.3 Deformation

In any structural problem the analyst (researcher) describes the initial unloaded configuration of the structure. Each "material particle" located at some position "X" in space (given by the various co-ordinates) will move to a new position "x" under loading. This movement is known and therefore certain relationships between various points in the structure exist. The deformation gradient relationship of the various particles in the model can be expressed as:

$$F = \frac{\partial x}{\partial X}$$

This formula is for standard rigid body motions; however, material behaviour of component members must be taken into account which gives rise to straining of the material. Therefore, the "stretch ratio"(Ω) of the gauge length (distance between 'x' and 'X') can be obtained. If the value of Ω is 1, then there is no strain of this "infinitesimal gauge length", only rigid body motion has occurred in the model.

An example of this is if a rubber band was stretched then the length would increase and thus the stretch factor could be 2 or more.

This ratio can be compounded with the deformation gradient and then all deformation can be represented as a rigid body motion, plus a pure stretch in three orthogonal directions. This is called the polar decomposition theorem, expressed as:

$$F = V \times R$$

where,

" F defines the relative motions of material particles in the infinitesimal neighbourhood of the material particle that was at X in the reference configuration",

"V defines the deformation of the material particles at X ", and

"R defines the rigid body rotation of the principal direction of strain"

6.3.4 Strain

Uni-directional strain is usually calculated using the decomposition theorem once strain in a single direction is obtained; then strain in the other directions can be calculated.

When the stretch ratio(Ω), is equal to 1, the strain is assumed to be zero, i.e. unstrained, initial conditions of the structure prior to loading. Therefore strain is defined as a function of the stretch ratio.

$$\varepsilon = f(\Omega)$$

6.3.5 Stress

There are various types of stress that can be defined in ABAQUS:

- Cauchy stress
- Kirchhoff stress
- Piola-Kirchhoff stress

True stress (Cauchy) is the usual value for stress that the engineer requires, as it is a direct measure of the **traction being carried per unit area** by any internal surface in the body under study.

Normally materials are thought of as having a natural elastic state but this is not true for metals as they can yield and therefore modification is required to account for the inelastic deformations that can occur. This is where the concept of **work rate per unit of volume** for this elastic reference state is written as:

$$dW^0 = \tau : d\varepsilon$$

where, "W is the force*distance/ energy"

" ε is the choice of strain matrix"

"τ is the stress matrix that is work conjugate (product of the stress and strain rate defines work per current volume) to dε"

6.3.6 Elements within ABAQUS

ABAQUS has a wide variety of elements that can be used for different types of analysis; three dimensional elements are defined as "bricks" (hexahedral) within the program.

Within ABAQUS there are two types of descriptions for elements, first-order (linear) and second-order (quadratic) elements.

6.3.6.1 (i) First-Order Elements

These elements are essentially constant strain elements, and can represent certain important linear strain fields.

6.3.6.2 (ii) Second-Order Elements

These elements are used to represent all possible linear strain fields, which include elasticity, heat conduction and acoustics.

Second-order elements are ideal for members subjected to bending as first-order elements can sometimes suffer from **shear locking** (an element must shear in order to supply the necessary behaviour for bending), which makes the element response too stiff. The second-order elements are more reliable because the second-order interpolation contains linear stress fields (one element thick allows representation of bending behaviour). There is little benefit gained when more complex elements are used; the accuracy may increase but the computational power required will also increase which could mean that solving time can be excessive even for small models.

6.3.7 Geometrical Non-linearity

ABAQUS assumes that there is mostly inelastic behaviour within an element i.e. elastic strains are usually small compared to the overall behaviour of the material.

6.3.8 Solid Element Formulation

All the solid elements in ABAQUS allow for finite strain and rotation within the remit of large displacement analysis. When the strain and/or rotation are no longer small then, there are two ways for ABAQUS to compute the strain. The assumption that the elastic strains are small compared to unity i.e. the reference configuration and the current configuration are infinitesimally different, as to make the two values very similar. This assumption is incorrect when the stains are in the order of 20-30% which is possible in some of the materials that can be analysed using ABAQUS. This is not a problem with steel as strains will never reach the above order of magnitude.

6.3.9 Hexahedral Elements

Two types of integration used in solving problems using hexahedral elements are detailed below:

(i) Full integration.

(ii) Reduced integration.

6.3.9.1(i) Full Integration

In full integration, the stiffness matrix of an element with uniform material behaviour is integrated exactly. Parallel faces are needed in the element otherwise inaccuracies can occur; these small inaccuracies do not affect the element as to cause too inaccurate results. Reasonable values are still obtained when these assumptions are used.

6.3.9.2 (ii) Reduced Integration

In reduced integration, the integration scheme used is of an order one less than the full integration scheme and it is used to integrate the elements' internal forces and stiffness. This means that in the reduced integration the power of integration is 4 instead of the power of 5 (full integration). This method appears to be slightly less accurate than the full integration scheme but there are advantages. For first order

elements, the uniform strain method yields the exact average strain over the element volume. This produces a better representation of the true strains for the elements being modelled. With second order elements, the strains are calculated from the interpolation functions and thus a higher accuracy at these points is produced.
This method also reduces the "cost" of forming an element; full integration of second order elements requires integration at 27 points, whereas with reduced integration only 8 points are required. Therefore the overall size of the matrix is reduced for the solver file (ABAQUS Matrix file) and is extremely beneficial if long running times are required due to the complexity of the model (**the authors model**)
The problem with this method is that "hourglassing" can occur (zero energy modes can start propagating through the mesh, leading to inaccurate solutions); this is not a concern in second order elements but for first order elements this is a major problem. The artificial stiffness method is used to control the problem and is generally only suitable for linear and slightly non-linear problems. If the problem is extremely non-linear, then there maybe problems with convergence and reasonable results may not be obtained. In cases like these incompatible mode elements have to be used, such as C3D8I (**the authors model**) if the possibility of "hourglassing" occurring.

6.3.10 Continuum Elements with Incompatible Modes

These elements with incompatible modes have enhanced behaviour response to bending. The main effect of these extra freedoms is to eliminate the effect of "parasitic shear stresses" on the elements.
Another effect that the extra freedom has, is that artificial stiffening occurs due to the Poisson's effect during bending within the element. In normal elements, the linear variation of axial stress due to bending is accompanied by a linear variation of the stress which is perpendicular to the bending direction, which leads to incorrect stresses and an overestimation of the stiffness. The use of elements with incompatible modes prevents this occurring.
The time "cost" of these elements with incompatible modes is increased but the benefits outweigh any time disadvantages. For these elements to work at their best (i.e reliable results) the elements must be approximately rectangular, which is how the researcher's models were developed.

6.3.11 Formation of Geometric Non-linearity.

As these elements(C3D8I) can be used for any material type then the incompatible modes are expressed as a modification of the deformation gradient.

The usual approach is to add the incompatible mode to the deformation gradient:

$$\bar{F} = F + \tilde{F} = \frac{\partial x}{\partial X} + \tilde{F}$$

The above equation is not valid when the elements have distorted due to the deformation; therefore, a modification to the equation is required, which is obtained by the addition of an incompatible deformation rate to the standard rate of deformation.

$$\dot{\bar{\varepsilon}} = \dot{\varepsilon} + \dot{\tilde{\varepsilon}}$$

6.3.12 Contact Modelling

The small sliding option can be used to model the interaction between two deformable bodies; only small sliding is allowed but rotations are not limited to such an extent.

There are two methods for modelling the contact between the two bodies, these are as follows:

(i) Definition of possible contact conditions by identification and pairing of potential contact surfaces.

(ii) the use of contact elements.

The two contact surfaces do not have to match but for the best accuracy it is advantageous if they do i.e. nodes on the two surfaces having similar co-ordinates.

6.3.12.1 (i) Pairing of contact surfaces

This type of contact modelling is computationally less expensive, i.e. smaller matrix files etc. are produced compared with other methods such as finite sliding contact, which in ABAQUS has problems with 3D deformable bodies. Vectors are used to track the various nodes and how they interact with the other nodes. Unit vectors are calculated for all nodes on the contact surfaces.

At each node, calculations are carried out to verify if contact between the pair of nodes has occurred; the program (ABAQUS) then calculates the "measure of overclosure", i.e. how far have one set of nodes penetrated the other surface (figure 6.7). "h" is used as the overclosure constant of the various surfaces; if h< 0 then there is no contact (figure 6.7) and then no calculations take place at those nodes. If h > 0 then surfaces are in contact and then "h" is reset to zero and the multiplier for contact pressure is then obtained (See section 6.4.13.2 for more details).

6.3.13 Small Sliding Interaction

ABAQUS has the capability to model interaction between two bodies when contact occurs. Before the process of working out the behaviour of the slave and master surfaces, normal vectors (N) are computed for all nodes on the master surface (Figure 6.7) Then "anchor" points(X_o) are obtained for all slave nodes on the master surface. These are vectors based on the normal vectors of the master surface, but if there is no match then the anchor point could be between two nodes on the master surface(Figure 6.7). This produces the equation:

$$X_0=X(u_0)= (1-u_0)X_1+u_0X_2$$

X_1 – Coordinates of node 1

X_2 – Coordinates of node 2

u_0 – Distance along the segment

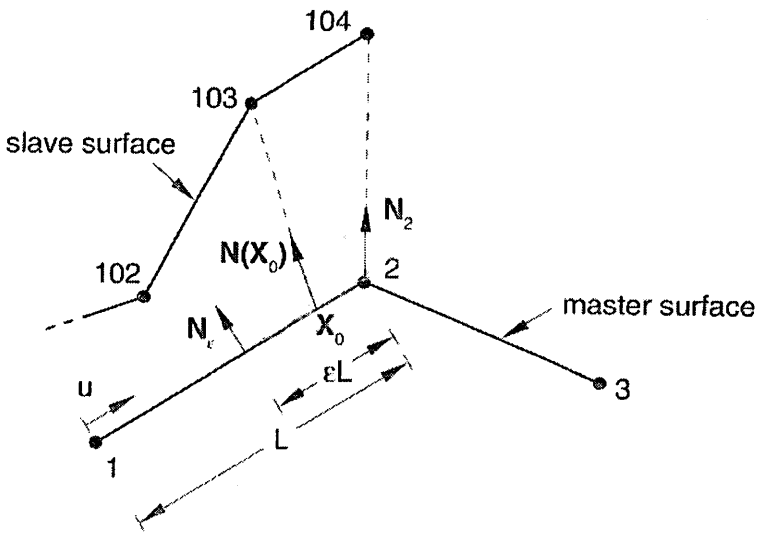

Figure 6.7: Contact between slave and master surfaces.

If during the creation of the small sliding contact a node (104 node) anchor point is coincident to master node 2 ,the following equation is obtained:

$$X_0 = N_2(u_0)X_2$$

6.3.13.1 Contact Plane tangent Direction.

The contact plane tangent is found at position X_0 for the node 103 so that it is perpendicular to line $N(X_0)$

$$V_0 = N(X_0) \times e_z = T.\frac{\partial X(u_0)}{\partial u} = T.(X_2 - X_1)$$

The equation for the tangent at node 2 (master) and node 104 (slave) is:

$$v_0 = N_2 \times e_z$$

6.3.13.2 Penetration of the master surface

As a slave node comes into contact with the master surface a measure of overclosure (h) and a measure of slip(s_i) is obtained.

The over closure (h) along the unit contact normal N (See Figure 6.7) between the slave point x_{N+1} and the master plane $p(\xi_1, \xi_2)$ can be determined by finding the vector $(p - x_{N+1})$ from the slave node to the plane that is perpendicular to the tangent vectors v_1 and v_2 at p.

This can be expressed as:

$$hn = p(\xi_1, \xi_2) - x_{N+1}$$

where

$$v_1.(p(\xi_1, \xi_2) - x_{N+1}) = 0 \text{ and}$$

$$v_2.(p(\xi_1, \xi_2) - x_{N+1}) = 0$$

If $h < 0$ there is no contact between the surfaces at the nodes but if $h \geq 0$ the surfaces are in contact. h is then set to zero and then to enforce the contact restraint, the first variation ∂h is found, also for the Newton Raphson iterations, the second variation $d\partial h$. The same is obtained for the slippage ∂s_i and $d\partial s_i$.

Using the above equations the three dimensional small sliding contact can be derived:

$$p(\xi_1,\xi_2) = x_0 + \xi_1 v_1 + \xi_2 v_2$$

where, x_0 is the planes anchor point (Figure 6.7) and the vectors v_1 and v_2 are functions of the current master node co-ordinates $x_1,\ldots x_N$.

6.3.14 Material properties definition

There is a wide variety of materials that can be used in any structural problem not just metals and these can be handled by ABAQUS, as the following show:

- concrete
- plastic
- foam
- rubber
- etc

Therefore a variety of models are required to be able to describe the relevant material behaviour. With different types of loading, it is vital to predict the behaviour of the material under all types of loading conditions.

As the wide range of material availability cannot be foreseen, the package has an option to allow user inputs for any type of material and the researcher can then specify the behaviour. The researcher can use their own code for their own models either using "UMAT" or "VUMAT".

ABAQUS separates the various responses for the type of behaviour being exhibited, by separating the deformation into recoverable (elastic) and non-recoverable (inelastic) parts. For the above to apply, the assumption that there is a relationship between the strain rates, is expressed in the form:

$$\dot{\varepsilon} = \dot{\varepsilon}^{el} + \dot{\varepsilon}^{pl}$$

"The elastic strains always remain fairly small for most materials of practical interest e.g. the yield stress of a metal is typically three orders of magnitude smaller than its elastic modulus, implying elastic strains of under 10^{-3}"(Hibbitt, et al, 1999)

There are several options available when using plasticity analysis for metals, the main choices are rate independent and rate dependent plasticity. These are either Mises

yield surface for isotropic materials or Hill's yield surface for anisotropic materials (Rate dependent).
In Rate Independent modelling there is a choice between isotropic and kinematic hardening.

6.3.15 Isotropic Elasto-Plasticity model for Materials

This is the most commonly used model for metal plasticity, with either rate dependent or rate independent models. As this method is easy to define, an efficient code is produced in describing the model, as the material stiffness matrix can be written explicitly.

6.3.16 Analysis Methods

ABAQUS uses various methods to define the loading on the structure, loads are applied using the CLOAD (applied to nodes within the elements) or DLOAD (applied to the face of the element) options. For the analysis of the models representing effect of buckling, another method was required; the modified RIKS method is usually used for these cases.

6.3.16.1 (i) Eigenvalue Bucking Prediction

This method is used to analyse "stiff" structures when the prebuckling response is almost linear. To obtain the buckling load, an estimate is obtained as the multiplier of the pattern of perturbation loads, this is added to the base state loads. The analysis produces the vibration of the structure, in order that further analysis can be carried out.

6.3.16.2 (ii) Modified RIKS method

The modified RIKS method is used to obtain non-linear static equilibrium solutions for unstable problems. The load and/or displacement may decrease as time progresses.(Figure 6.8) There are various assumptions including that the load is proportional (all load magnitudes vary with a single scalar parameter) Another assumption is that the response to the load is smooth in the model.
"The essence of this method is that the solution is viewed as the discovery of a single equilibrium path in a space defined by the nodal variable and the loading parameter"(Hibbitt, et al, 1999)

The method is still based on the Newton Raphson method but the load path instead of the displacement path is the control for the convergence of the model. The displacement can also be obtained similar to the Newton Raphson method i.e. comparing stress and strain in the material and adjust as required depending on the value of residual force. In the modified RIKS method the standard convergence rate dependent, automatic incrementation algorithm is used. The algorithm is implemented by moving the model over a given distance along the tangent to the current solution point. There it is solved to find equilibrium in the plane that passes through the point which is obtained and thus this is the orthogonal to the same tangent line.

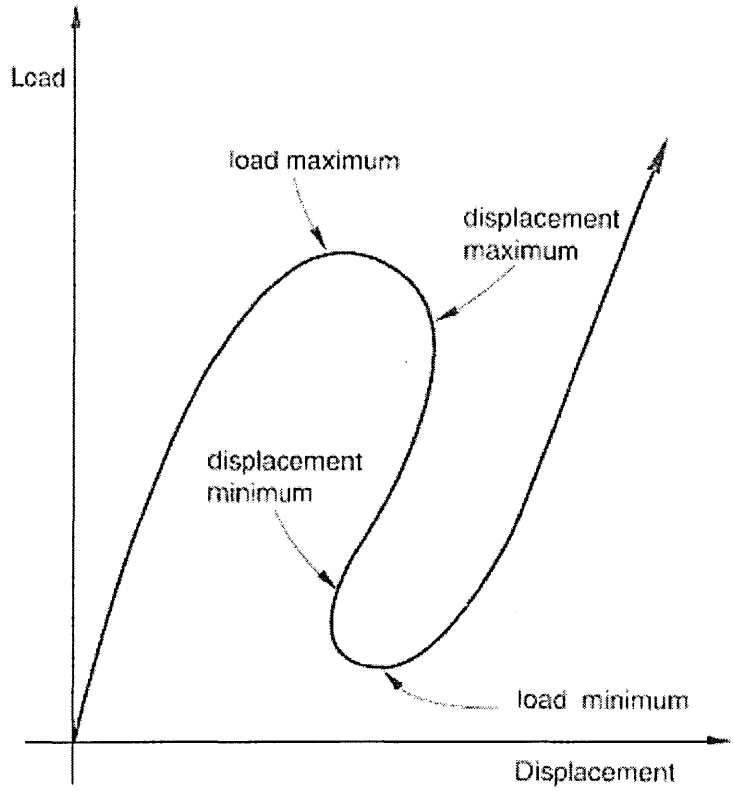

Figure 6.8: Riks typical response.

6.4 Conclusion

As can be seen in this chapter, finite element analysis is both complex and repetitive. Many different theoretical concepts from many different aspects of finite element theory have to be utilised in order to obtain the necessary solution for the model being analysed.

As the equations have to keep being generated until a suitable solution is found then this necessitates the use of a computer model, which can be readily produced to allow simulations to be undertaken in a realistic time frame.

Basic Model

Chapter 7

7.0 Introduction

Using a software package for the first time, one must begin with a smaller, more basic model. Once understanding is gained, then modelling of more complex structures can be undertaken. This is how the author proceeded. When carrying out this type of modelling, experimental data must be available, in order that the validity of the model constructed using finite element technique, can be assessed. For this investigation, test data on a series of full scale model tests were available to allow evaluation of the finite element model used (See Chapters 4 and 5)

7.1 T-stub Modelling

Why choose to model a steel bolted T-stub (figure 7.1) ? The "Numerical Simulations Group", one of many working groups under the European Research Project COST C1 intended to produce a standard method of analysing beam to column connections in steel structures(Jaspart and Bursi, 1995). Thus results from many different studies using several well known finite element software packages e.g. LUSAS, ABAQUS, ANSYS etc. could be compared.

The T-stub includes everything that a more complex bolted endplate connection would encompass, without needing to spend considerable time generating the model. Thus many research institutions in various Europeans Countries could be involved in the study, due to relative ease of its construction and testing. The important details to note for T-stub connection are:

(i) bolts.

(ii) boundary conditions.

(iii) contact limitations.

(iv) non-linear behaviour (both material and geometrical)

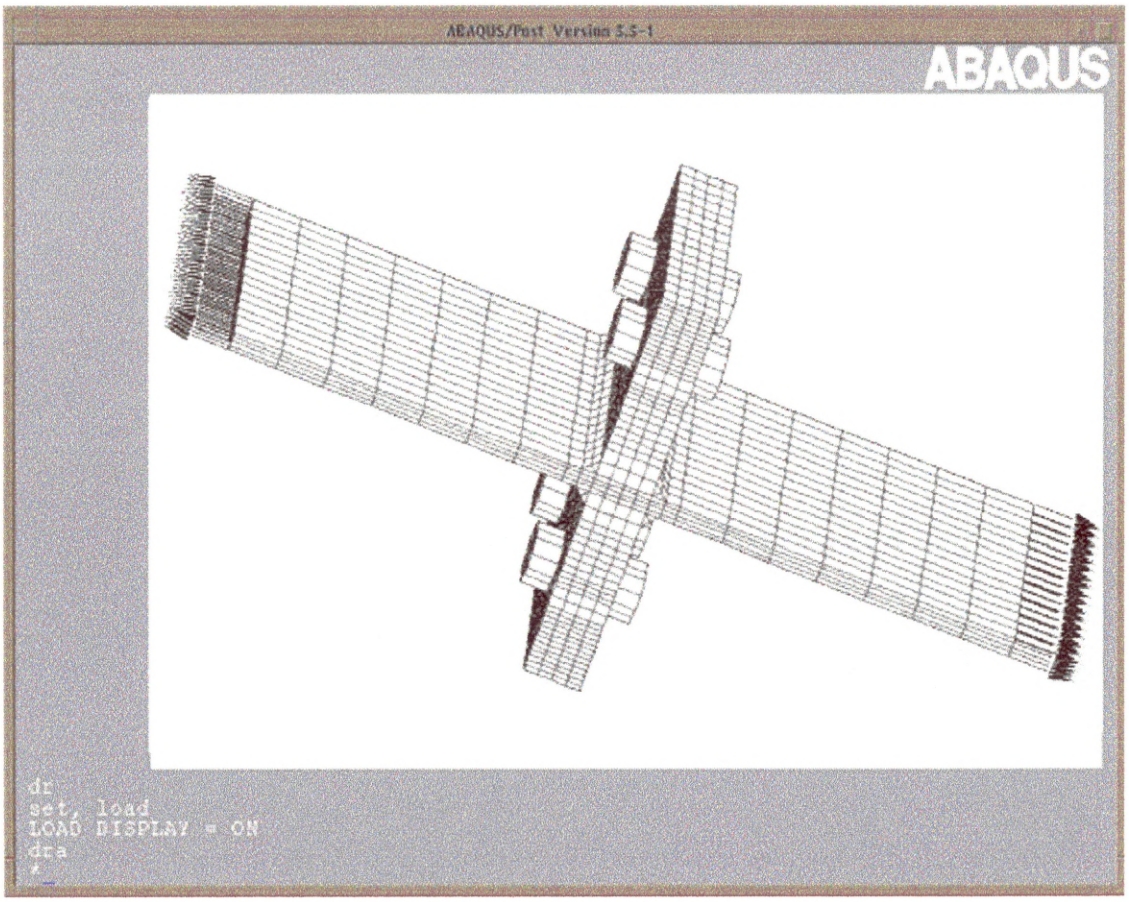

Figure 7.1: Full T-stub

7.2 Finite Element Modelling

7.2.1 ABAQUS Finite Element Software

ABAQUS is a finite element package sold by Hibbitt, Karlsson and Sorensen Ltd (HKS). This software is used world wide by many leading research institutions and multi-national companies e.g. Lockheed, Boeing and International Business Machines (IBM). ABAQUS can handle many complex problems, including material and geometric non-linearity, which are needed in understanding the behaviour of steel structures.

7.2.2 Element Selection

In order to discretize the structure and ascertain the best element for the finite element model, an understanding of the behaviour of the structure is essential. ABAQUS is an all embracing program, with many different element types suitable

for a myriad of applications. Therefore, investigations must be carried out to select the element types most suited for the successful completion of the research.

Other groups (Bursi and Jaspart, 1997) had carried out similar tasks and their findings are discussed below, together with the conclusions drawn by the author.

Two types of 3-dimensional continuum elements (figure 7.2a and 7.2b) were selected for the investigation of the 3-dimensional structure. These were as follows:

(i) C3D8, 8 noded linear brick.

(ii) C3D20, 20 noded quadratic brick.

The elements are solid 3D elements, the decription above is as follows

(i) C: Continuum Stress/ Displacement

(ii) 3D: Three Dimensional

(iii) 8 or 20 : Number of nodes required to create elements

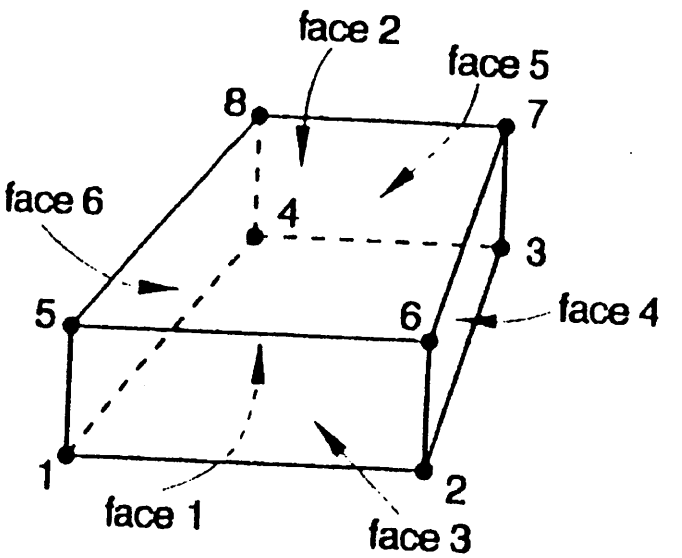

Figure 7.2a: C3D8: 8 node Solid Element

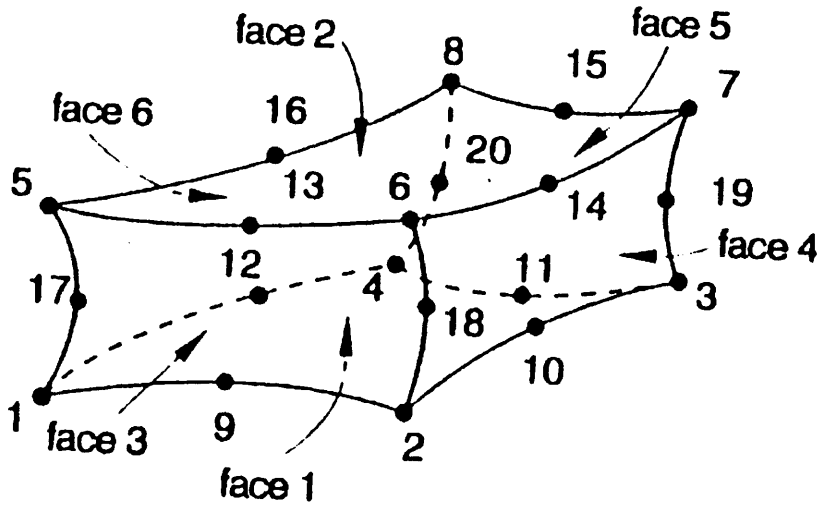

Figure 7.2b: C3D20: 20 node Solid Element

Figure 7.2: Showing Elements used in the modelling

There are several important considerations when choosing a particular type of element for the type of structure being modelled. These are:

(i) The percentage error induced.
(ii) Time to generate the model.
(iii) Computer analysis time and power of the computer.

For the first consideration a comparison between the results derived from these elements was made which indicated that there was very little difference in the result produced between the two types of elements.

The last two considerations are interlinked; these will therefore be discussed together. The C3D20 elements with 20 nodes per element, take longer to generate, due to an increased number of nodes requiring definition and the additional information required in specifying their shape. The input file is also larger due to the considerable increase in the number of co-ordinates that need specified.

C3D8 elements with 8 nodes, require considerably less information; fewer nodes result in a faster generation time and reduced convergence time.

Various bending related problems were modelled using both sets of elements by Bursi and Jaspart ((Bursi and Jaspart, 1997). It was found that there was very little difference (apart from time) in the results produced, from both sets of elements.
C3D8 element was therefore chosen as the most suited to the task in hand. Within the C3D8 family of elements, more specialised elements exist. The list below shows the various sub-group of elements which were investigated.

(i) C3D8.

(ii) C3D8I.

(iii) C3D8R

The coding for the above is as follows

(i) I: Incompatible mode

(ii) R: Reduced integration

The elements above were tested against a standard bending test, physically carried out at the University of Liege (Bursi and Jaspart, 1997), in order to determine the validity of the elements. Throughout the calibration procedure C3D8I was the most satisfactory performer. Hence this element was chosen for use in the bending related structural problem; the other two types are usually used for other types of analysis problem, as they were deemed unsuitable for this type of analysis.

7.3 Mesh Generation

Generating the correct type of mesh is vital (Ragupathy and Virdi, 1995) and an understanding of the behaviour of the structure being modelled is extremely important. The type of mesh depends on the information required for the study. As the author required a wide range of results, a fine mesh was necessary (figure 7.3). With a fine mesh, a more detailed picture of the behaviour of the structure under loading can be obtained. The percentage error will also be smaller utilising a finer mesh but due to greater number of elements needed, time considerations become important. Where most of the bending occurs, a finer mesh may be required to capture the necessary data.

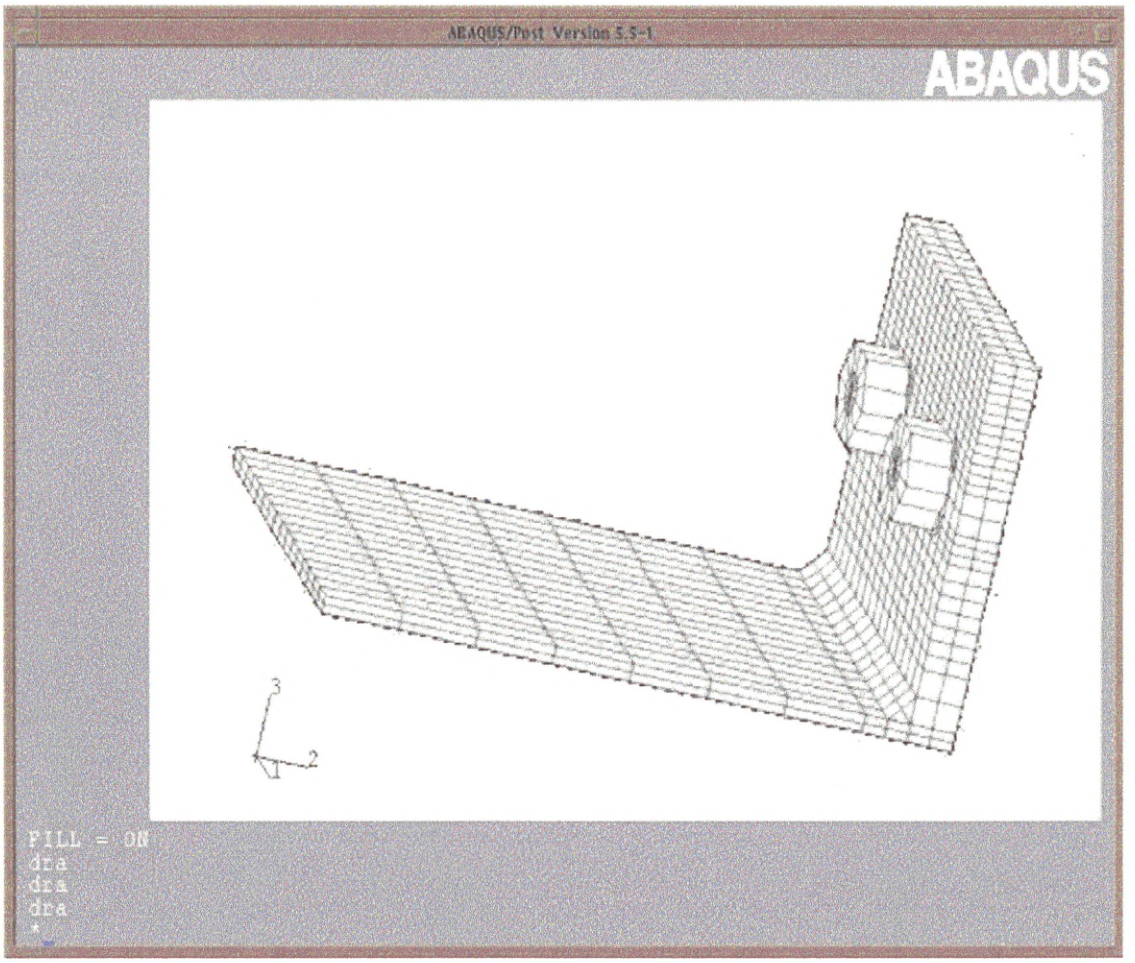

Figure 7.3: Showing the fine mesh required for T-stub

7.4 Bolts

Bolts add stiffness to the overall T-stub but are complex to model successfully within the computer environment. As the bolt shank is circular in nature, another type of element was used, the element recommended for use in conjunction with C3D8 elements was C3D6 by the ABAQUS manual. This was the element selected by the author. As before for C3D8 element, there exists sub groups for C3D6 (Figure 7.4) and therefore C3D6I was chosen as the element to use in the study.

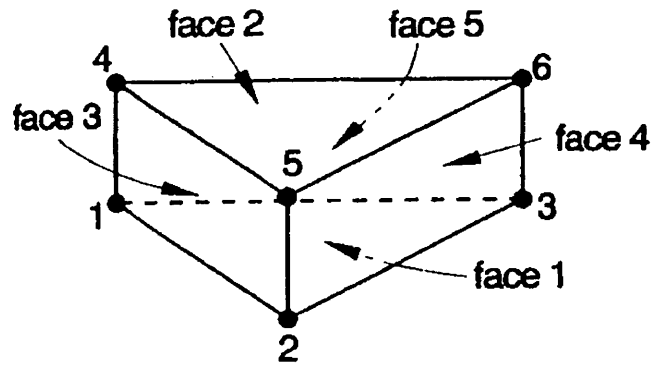

Figure 7.4: C3D6 node Element

7.5 Boundary Conditions

Boundary conditions are used to specify the different values of all "basic solution variables" i.e. displacements, rotations, pore pressures, temperature, electrical potentials, normalised concentrations or acoustic pressures etc. Boundary conditions can also be used to simulate missing parts of a connection. With the connection symmetrical about two axes only a quarter of the connection needs to be modelled. Boundary conditions can stop the connection being able to move in a particular direction, i.e. all movement can be stopped in either X, Y, Z or combinations of axes depending on the input. An understanding of how boundary conditions operate is necessary. There are many advantages in using the reduced model which are listed below:

(i) less time is needed to develop the model, i.e. fewer nodes and elements are required to produce the mesh,

(ii) less computer time to analyse,

(iii) less computing power required in order to obtain similar results in an equivalent time frame.

The main concern is that appropriate boundary conditions must be as applied; any discrepancy might render the results worthless.

7.5.1 Boundary Conditions at each node

The standard movements and restrictions for each node are shown below. At each node 6 main conditions can exist (Figure 7.5). The ability to move in X, Y, Z directions and the ability to rotate about X,Y,X axes.

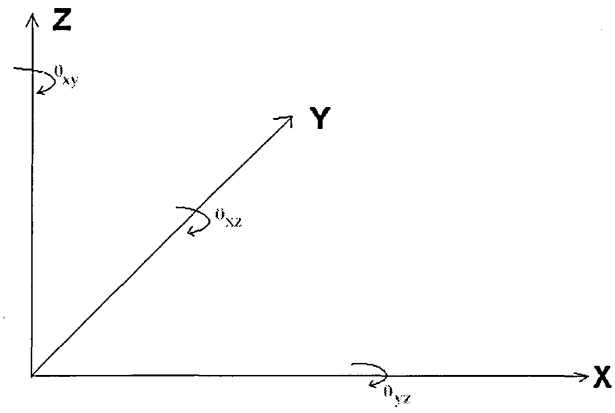

Figure 7.5: Sign Convention and movements for ABAQUS nodes

7.5.2 Boundary Conditions (Bolts)

Boundary conditions applied to the bolts were also modified in this manner. Certain limitations were applied to the bolt shank to limit the movement in the connection. The restrictions to the base of the bolt shank stopped the movement in any direction and rotation about any axis (figure 7.6).

7.5.3 Boundary Conditions (T-stub)

The T-stub was limited in its movement by applying boundary conditions to the web of the T-stub as shown in figure 7.7. The main reason for applying boundary conditions is that in the real structure there are other parts of the T-stub which affect the behaviour of the connection

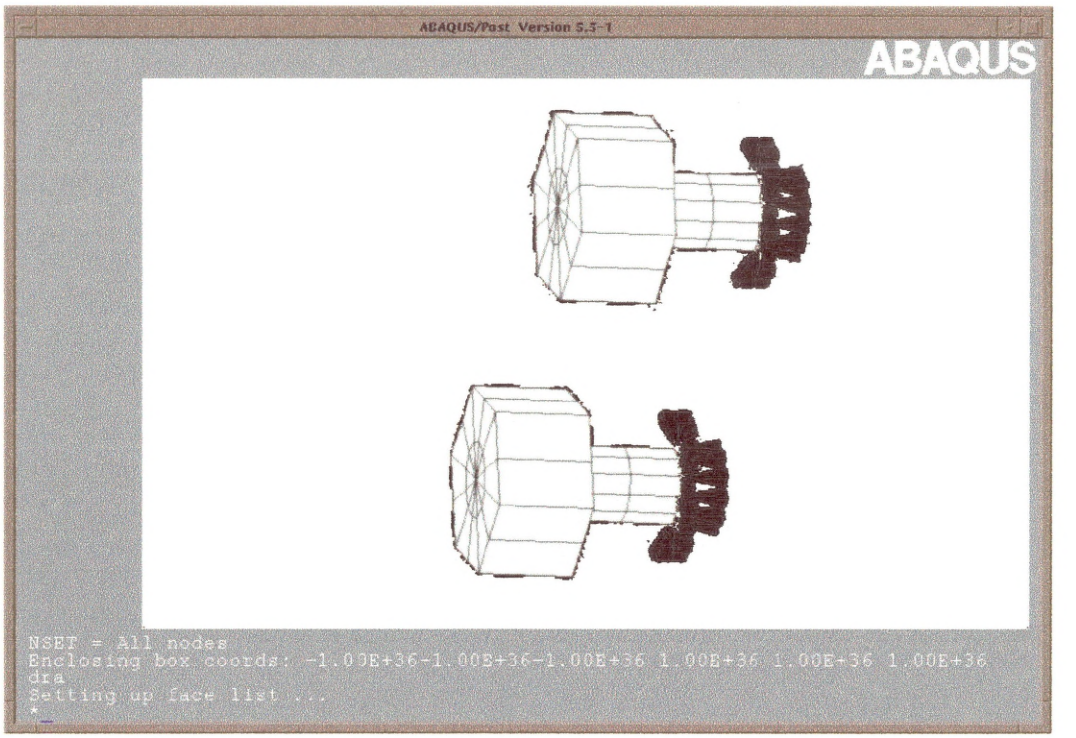

Figure 7.6: Bolt shank boundary conditions

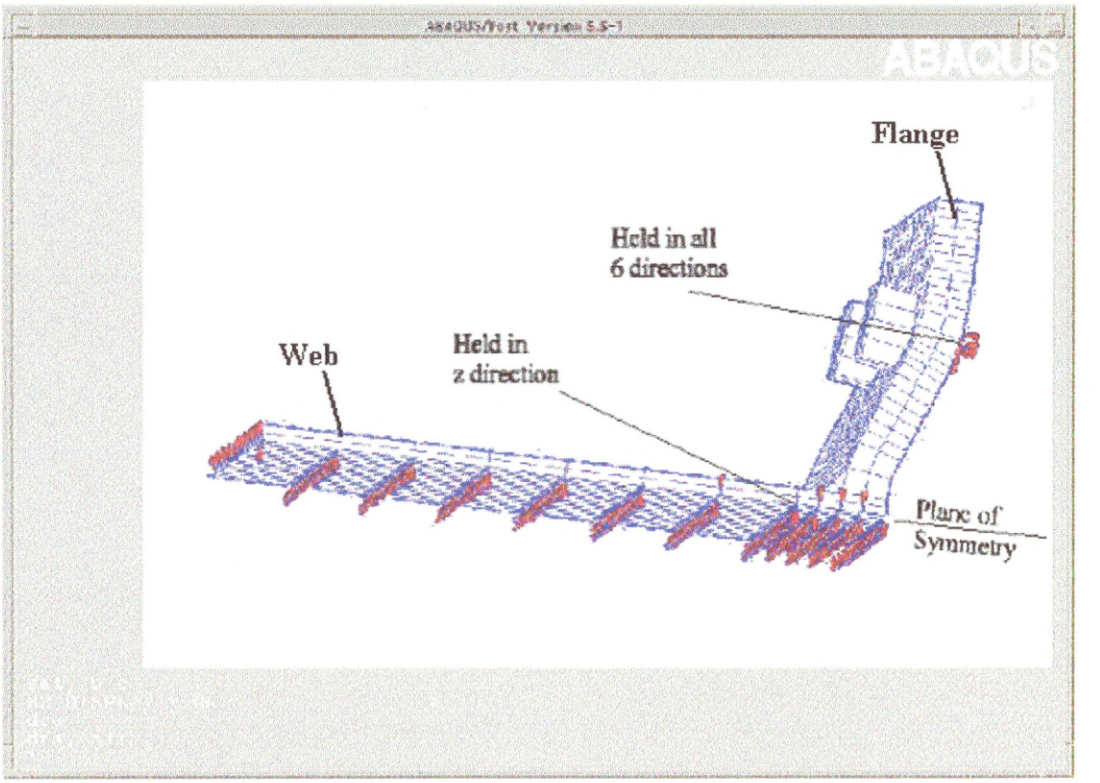

Figure 7.7: Boundary Conditions applied to the T-stub

7.5.4 Gap elements (GAPUNI)

Where boundary conditions are insufficient in describing the behaviour of the structure, gap elements (figure 7.8) can be utilised. Fully restricted boundary condition stops movement in any direction, whereas gap elements allow movement in one part of the axis i.e. able to move in a positive x-direction but not in a negative x-direction or vice-versa. Node 1 is part of element 1 (Figure 7.8) and node 2 is part of element 2, h is the current clearance distance between the two nodes and n is contact direction.

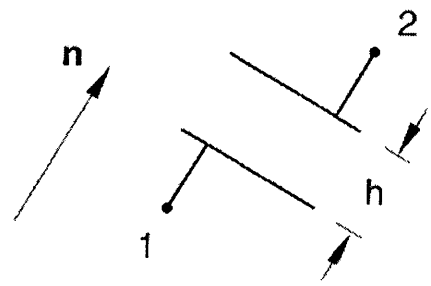

Figure 7.8: GAPUNI element

7.6 Loading

Loads are applied at the web end of the T-stub and the whole connection attempts to move in the direction being pulled. The load itself was applied to each node on the face of the elements and thus the combined load from all the nodes, produced the total load applied. Loads are not applied all at once due to convergence problems arising. Control parameters are used to increment the loading in a step by step fashion. This produces still more data and can create extra problems, which can be overcome by limiting the output to specific elements.

Within ABAQUS, loads can be defined in a variety of ways, concentrated or distributed (CLOAD or DLOAD). There are many types of distributed loading that can be applied depending on the type of elements that are being used by the researcher.

The model is loaded throughout the timestep which begins initially at zero progressing through to one, which is the end of the timestep. The load can be applied in one increment but this usually causes difficulties with the solver matrix, i.e. convergence problems.

Concentrated loads are applied as either force or moment using the CLOAD option, the loads being applied to the nodes themselves that make up the element. They can either be fixed in direction or able to rotate as the load is applied depending on the options selected. The loads can also be specified to move in any of the three directions; in this case they were all allowed to move in the y-direction, both positive or negative, applied as ENDS1, 2, 1000 or ENDS2, 2, -1000 etc. This allows the user to understand the way the loads are operating within the model. The values this specified are the total load that is to be applied to each node at the end of the time increment; this will never actually occur as the total load will be far above what the connection can take, it will therefore be a percentage of the value.

7.7 Control Parameters

Control parameters are used to allow the load to be incremented in time steps, which are initially zero progressing to one at the finish. The smaller the time step, the larger the output files and thus more information gained, which is very important for non-linear behaviour.

ABAQUS automatically adjusts the size of the time increments during the analysis to solve non-linear problems efficiently. Using the control parameters option the initial time increment is suggested by the researcher and after this the program modifies the increment to suit the analysis. If there are problems with the increment then the increment is reduced by 75 % and the analysis is tried again with the new time step; this continues until the increment chosen is smaller than the minimum time increments, the model will then stop. If the solution to the two consecutive increments is less than 5 attempts, there is a 50 % increase in the time step of the analysis.

7.8 Material properties

Material properties are needed in order that the realistic behaviour can be modelled accurately. The material properties are defined using stress/strain graphs (figure 7.9). The graphs are initially linear but soon become non-linear (curved section). The linear section of the graph is defined using Young's modulus of elasticity and Possions ratio. The non-linear section of the graph has to be generated using plastic

stress/ strain graph (figure 7.10) as many points on the curved part of the graph has to be defined as necessary. This is termed a "piecewise linear approximation".

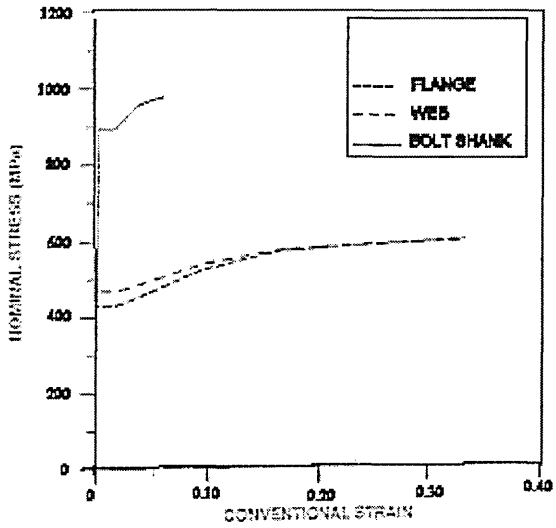

Figure 7.9: Material Properties used to define the behaviour of the T-stub

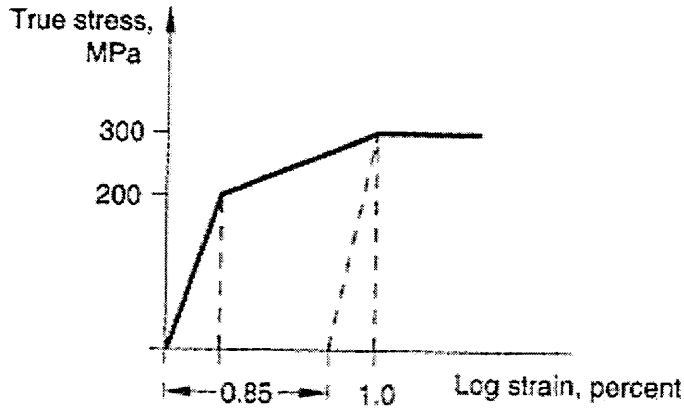

Figure 7.10: Plastic stress/strain derivation graph

7.9 The model

The T-stub has been generated as accurately as is possible. There are three types of elements used in the model; the list below shows the number of each type of element

Type of Element	Number of elements	Use
C3D8I	1272	Main body of T-stub
		Defining part of the bolt head
C3D6	104	Bolt shank
		Defining part of the bolt head

		The fillet
GAPUNI	579	Modelling the other parts of the structure

7.10 Results

Physical tests were conducted at the University of Liege (Jaspart and Bursi, 1995) to establish the performance of the T-stub. Researchers also constructed finite element models (Ragupathy and Virdi, 1995; Bursi and Jaspart, 1997; Mistakidis et al. 1996) which could be compared with the author's finite element model.

The attached graph (figure 7.11) shows the results obtained from the testing and results from the authors finite element analysis. Reasonable results were obtained from modelling the T-stub, but the finite element model results are slightly lower than those obtained from physical testing. The T-stub appears to have a higher stiffness and thus a higher strength at the conclusion of the test. The load at which the specimen failed, agreed reasonably accurately with the finite element model's predictions. As stated before, it is usually better to slightly underestimate the strength of the connection than overestimate it resulting in a safe design.

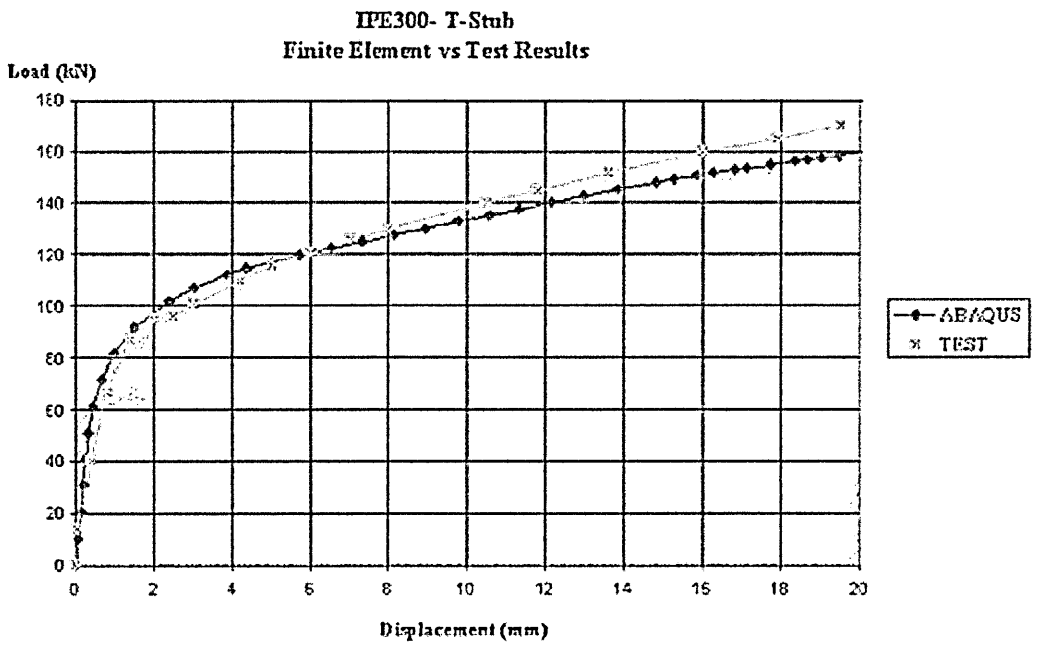

Figure 7.11: Comparison of results between physical testing and ABAQUS modelling

The initial linear section of the analytical curve compares well with the test results. Before the onset of yielding, the finite element model is able to sustain a higher load for the equivalent displacement. Where considerable yield occurs both in the test and in the finite element model, the point of occurrence can be seen clearly on the graphs. Within ABAQUS there is another program called ABAQUS/Post, which allows the user to view the output files in a graphical format; figures 7.12a to 7.12e show the difference in the T-stub stresses over the timestep and how the displacement increases.

The most noticeable is the fillet between the web and the flange of T-stub which is very highly stressed. This shows the need for fillets to be included in T-stub finite element analysis. Otherwise the values of displacement will be higher and thus a lower load will be obtained from the model run.

7.10.1 Linear Behaviour

Linear behaviour occurs when the load and the displacement are proportional i.e. as the load increases the displacement increases proportionately. Linear behaviour will occur initially in the T-stub as the load increases.

7.10.2 Non-Linear Behaviour

Due to the material property of steel, linear behaviour will not continue ad infinitum. When the yield point is reached non-linear behaviour will commence. As the material is non-linear in nature, properties entered must reflect this. A standard stress-strain curve (figure 7.10) is required to input the relevant values required by ABAQUS. The material properties diagram is split into the relevant sections i.e. where the curve changes gradient. A piecewise linear approximation is used to describe the material behaviour of the T-stub.

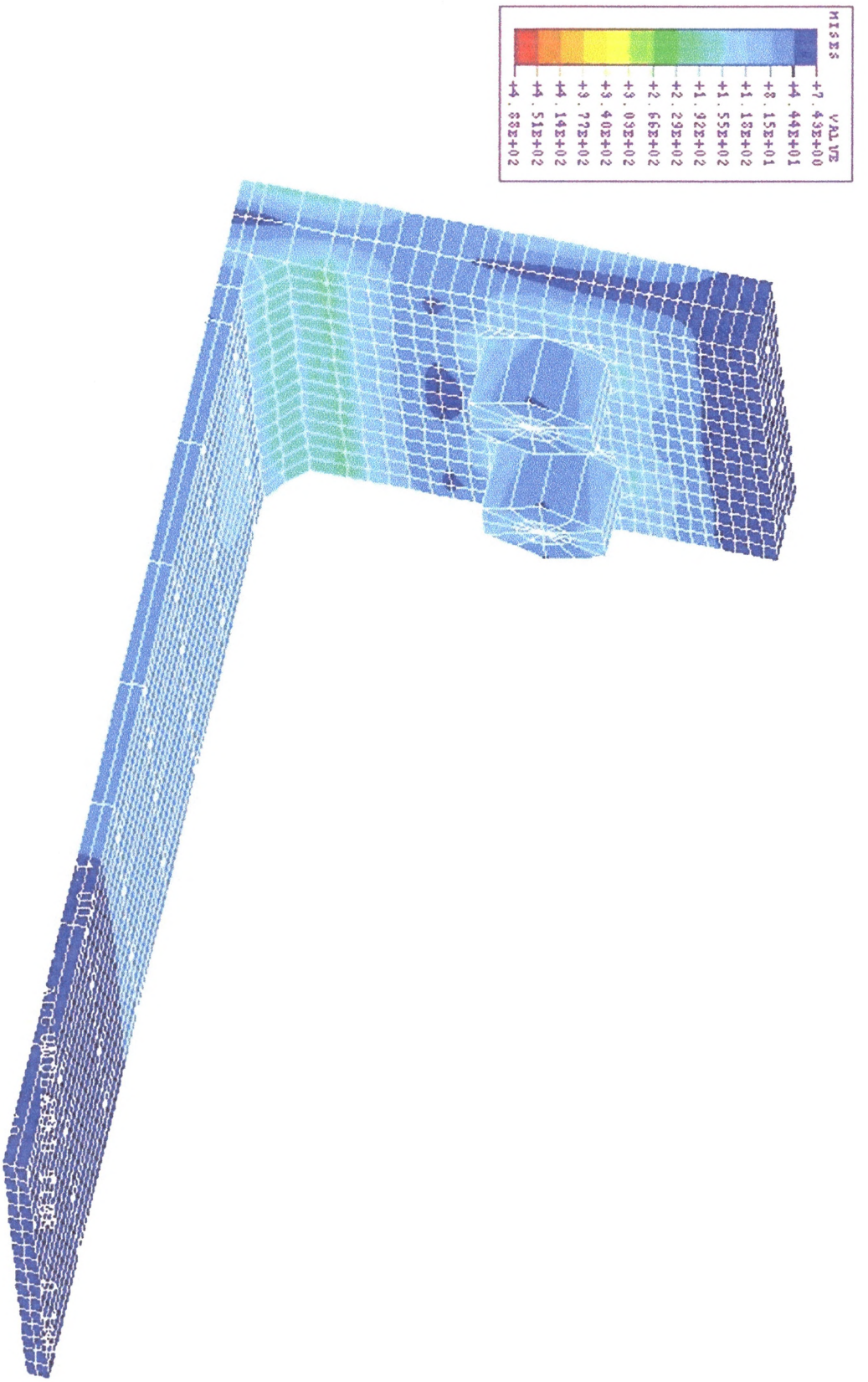

Figure 7.12a: Showing change in Stress over time and load

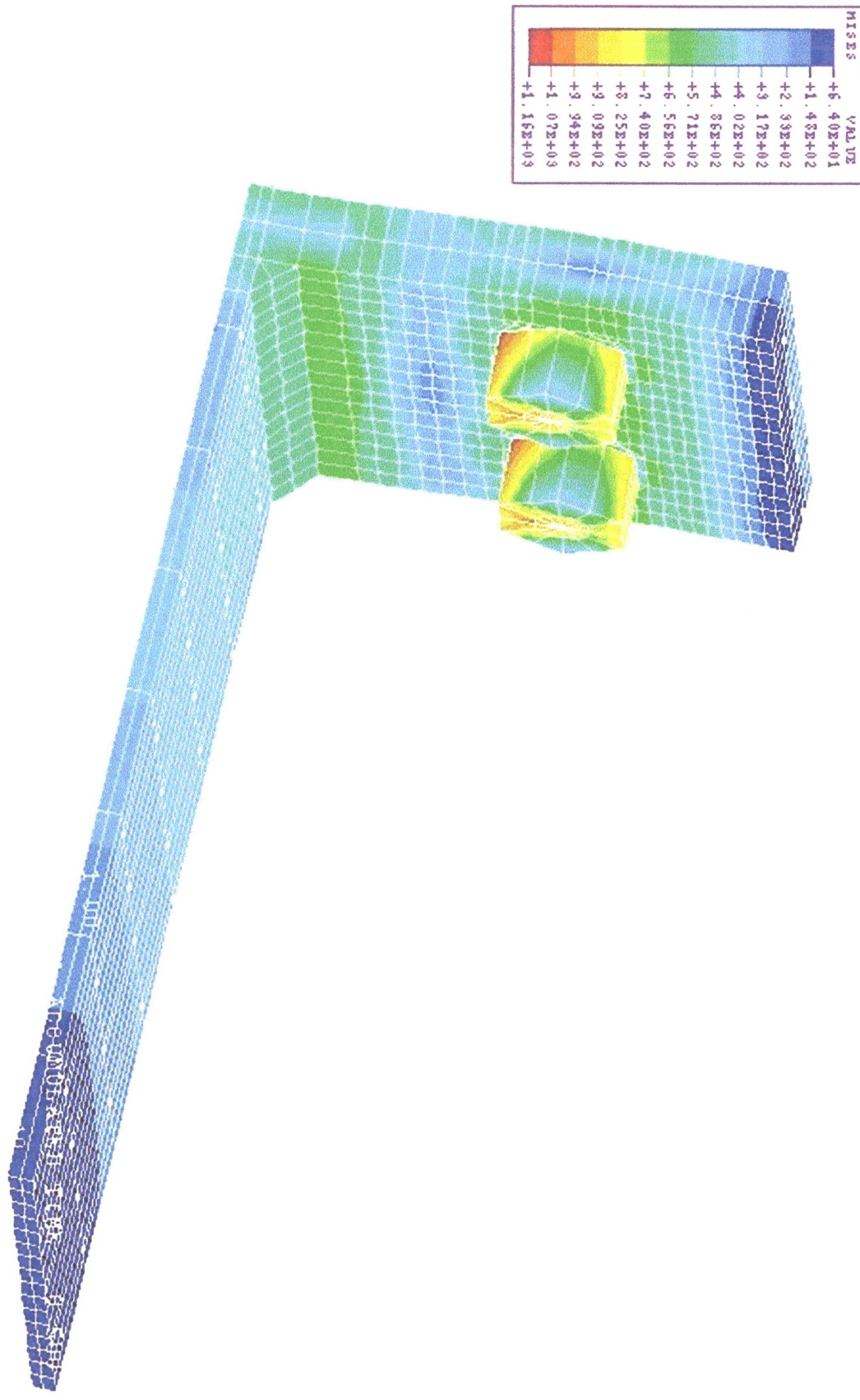

Figure 7.12b: Showing change in Stress over time and load

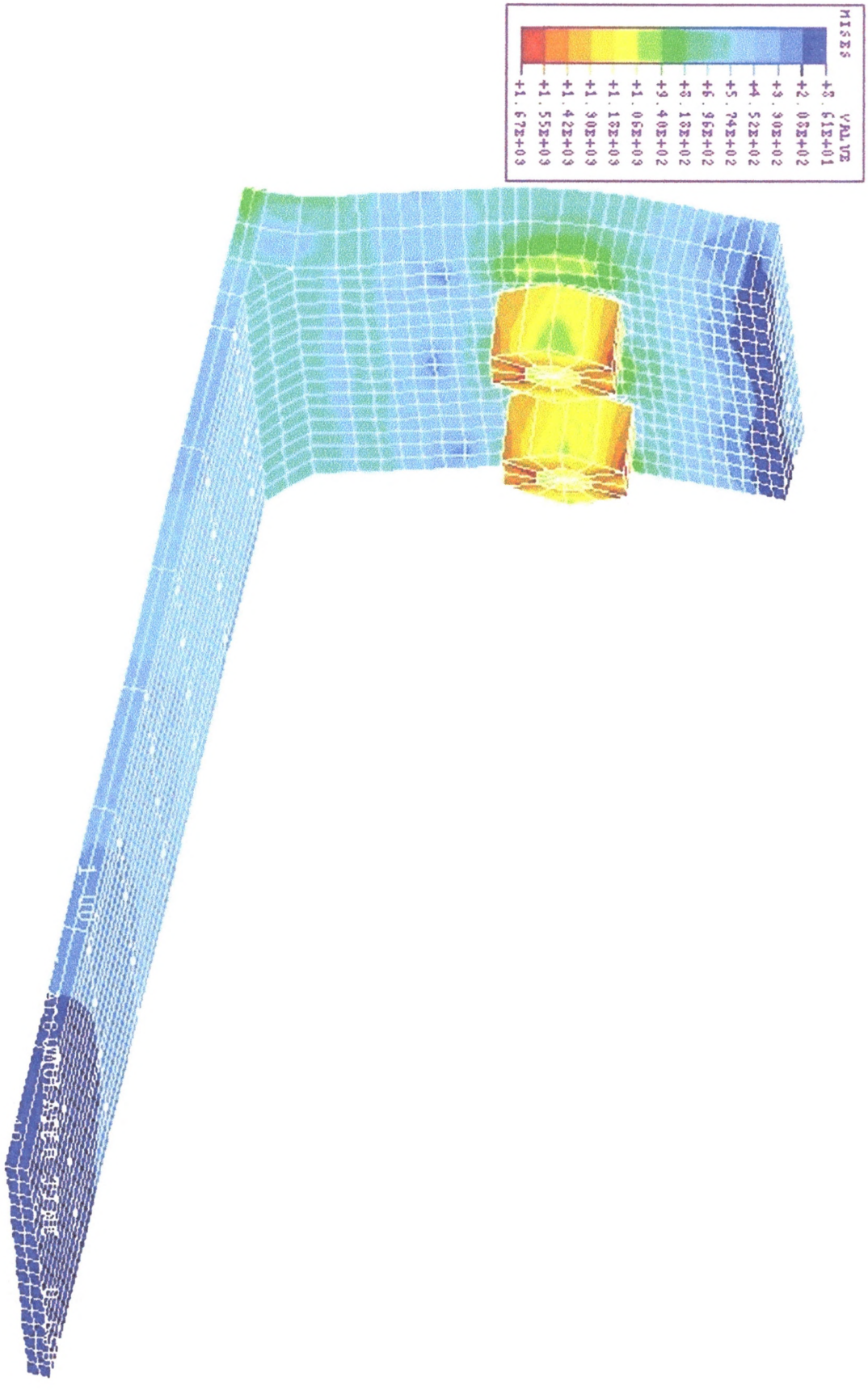

Figure 7.12c: Showing change in Stress over time and load

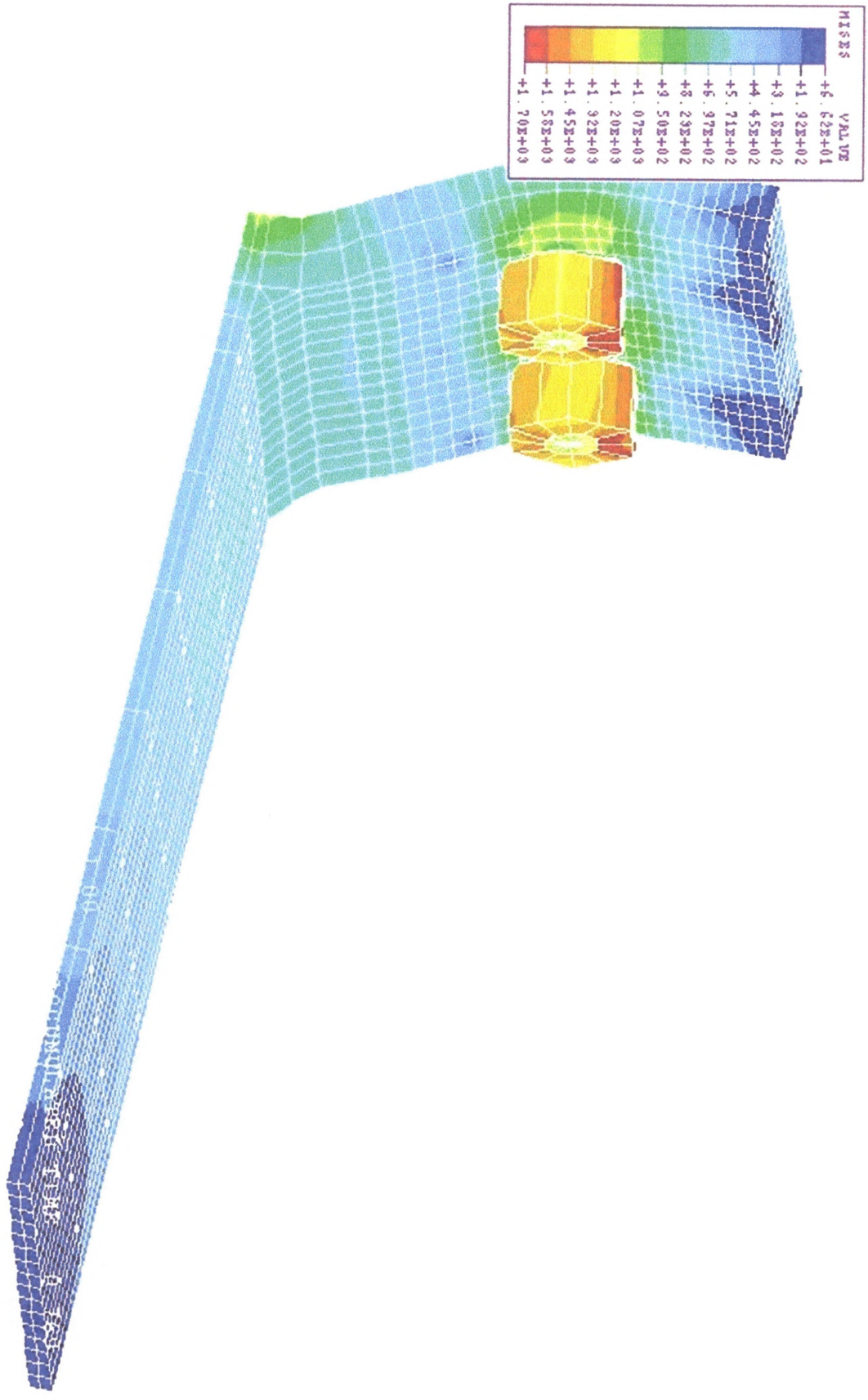

Figure 7.12d: Showing change in Stress over time and load

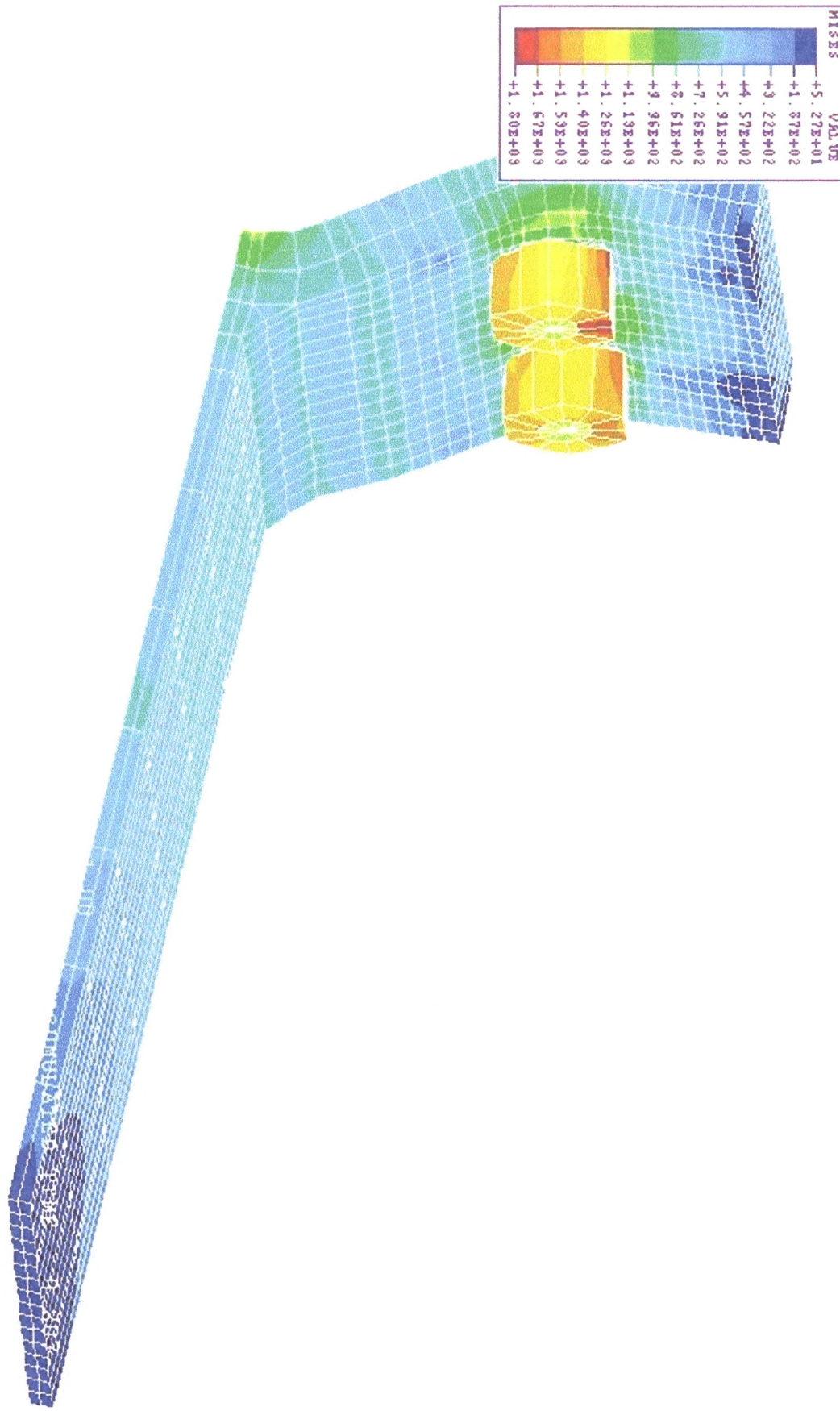

Figure 7.12e: Showing change in Stress over time and load

7.11 Conclusion

The task involved in the modelling of any steel beam to column connection using finite element analysis is daunting. Understanding how the ABAQUS program operates and the relative merits of different types of elements available is vital. Mesh generation depends on several factors including the power of the hardware (computer) being used. Using too fine a mesh will considerably increase the time taken for the completion of the model but inaccurate results can transpire if the mesh is not well defined. The correct material properties must be obtained otherwise the results will be meaningless. With time, effort and experience, finite element modelling can produce an accurate representation of a physical structure, with the added advantage that individual components can be investigated without resorting to more expensive and time consuming testing.

Small details that appear not important like the fillet, eventually are proven by analysis to be vital in obtaining an accurate picture of the behaviour of the T-stub in this type of displacement analysis.

Modelling a Full Scale Connection
Using ABAQUS
Chapter 8

8.0 Background

As stated earlier of the eighteen full scale connections (Bose, 1993; Bose, 1994) tested to destruction at UAD, seven of the eighteen connections failed due to column web buckling.

As discussed earlier buckling is an extremely complex failure node to comprehend and model, due mainly to the interaction between the various components of the connection. (Chapter 3 for details of buckling in column webs, Section 3.3.2)

Finite element modelling was considered as one of the most productive and accurate method for modelling this phenomenon, without resorting to the very expensive and time consuming physical tests.

The connection chosen by the author, for the initial investigation was from a series of tests carried out by Wang, from his Ph.D. thesis (Wang, 1996) which constituted FEP connections. These had the following components:

1. 16 Bolts.
2. 4 Beams flanges.
3. 2 Beam web.
4. 2 End plates.
5. 2 Column flanges.
6. 1 Column web.

8.1 Full Connection Modelling

The elements used previously by the author to model the T-stub, were again used for the full connection. The full connection behaviour is similar to that of the T-stub, which was dominated by bending and displacement, thus C3D8I and C3D6I elements were again used. A review of selection procedure of element types is dealt within Chapter 7 on Basic Modelling of a T-stub.

8.1.1 Bolts

The bolts were defined in a manner similar to that employed by Wang (Wang, 1996) using bolts as bar elements (figure 8.1) with a high yield stress. In the full model, the bolt head was included in the model. Six bar elements were used to define the bolt shank, with an area totalling the area of the bolt.

Figure 8.1: Bar element used to define bolt shank

8.1.2 The Beam Components

As the researcher was mainly interested in the column web behaviour, the beam component was modelled in sufficient detail (Figure 8.2) to allow for its effect upon the structure. This meant that only part of the beam was modelled. The material properties were modified to allow almost infinite stiffness (Wang, 1996), which would limit the bending within the endplate itself. This was to allow stresses and strains due to the load to be transferred to the column endplate interface. This involved adjusting the elastic properties in ABAQUS, to create a high Young's Modulus of Elasticity. This step reduced the need for more elements to define the beam, thus allowing a smaller model to be produced and therefore a faster convergence time for analysis.

8.1.3 End Plates

The end plate plays an important part in transferring the load from the beam to the column flanges; with this in mind the end plate was modelled using a fine mesh. This included modelling the circular bolt holes as detailed in figure 8.2.

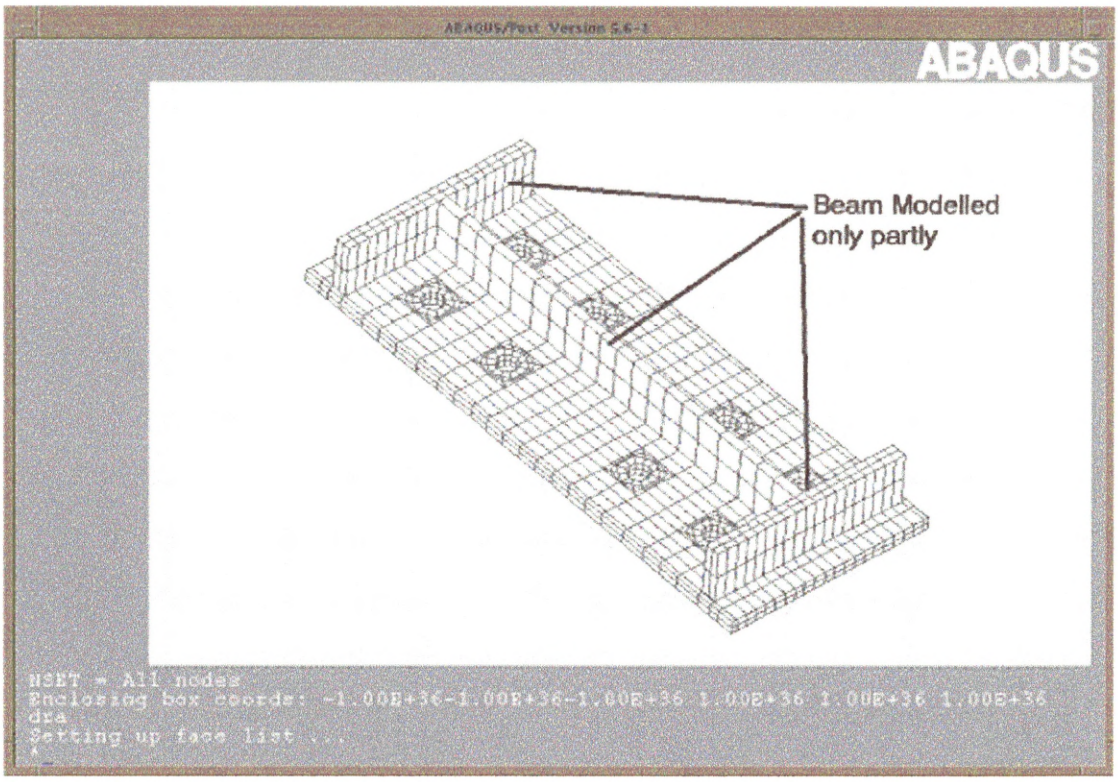

Figure 8.2: Model showing how single beam and endplate were modelled

8.1.4 Columns

The column was the most important element of the connection and as such was modelled using a fine mesh (figure 8.3) to obtain as much information about the area of the column web that would buckle. The difference in the mesh size can clearly be seen in figure 8.3, the area that was expected to fail due to buckling had a smaller more refined mesh.

8.1.5 Boundary Conditions

Very little boundary conditions were required to be imposed as the whole connection was being modelled. The only boundary conditions being applied were at the ends of the column flanges and web to stop the model moving in space i.e. held in place. These nodes were not allowed to move or rotate in any of the three directions using the "ENCASTRE" option.

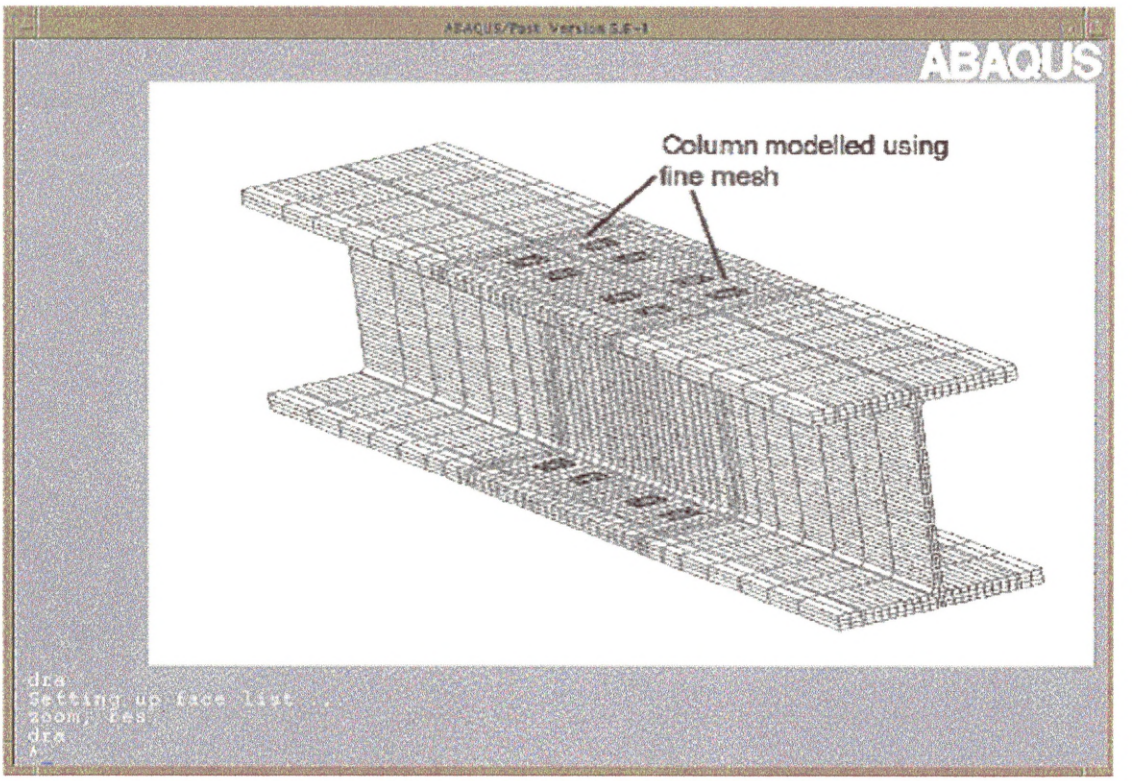

Figure 8.3: Example of the fine mesh used in defining the column.

8.1.6 Material Properties

The material properties were obtained from tests carried out by Bose (Bose, 1993; Bose, 1994) and Wang (Wang, 1996). Similar to the T-stub model a "*piecewise linear approximation*" (See Chapter 6 on Basic Modelling) of the graphs produced was used in order to obtain material properties. (Figure 8.4) Due to a large number of different components e.g beam, column, end plate, bolts etc, a considerable number of stress-strain curves were required to define the material properties of all the components.

8.1.7 Loading

The loads were applied at the ends of the beam flanges, opposite in direction at top and bottom and thus inducing an applied moment to the connection. The loads were applied longitudinally through the beam flange (Figure 8.5), to each node, as in the T-stub; therefore the summation of the individual loads on the nodes produced the total load applied. Control parameters were required to limit large changes in the loading. Loads are required to be increased incrementally throughout the time step, which begins initially at zero progressing through to one (end of step).

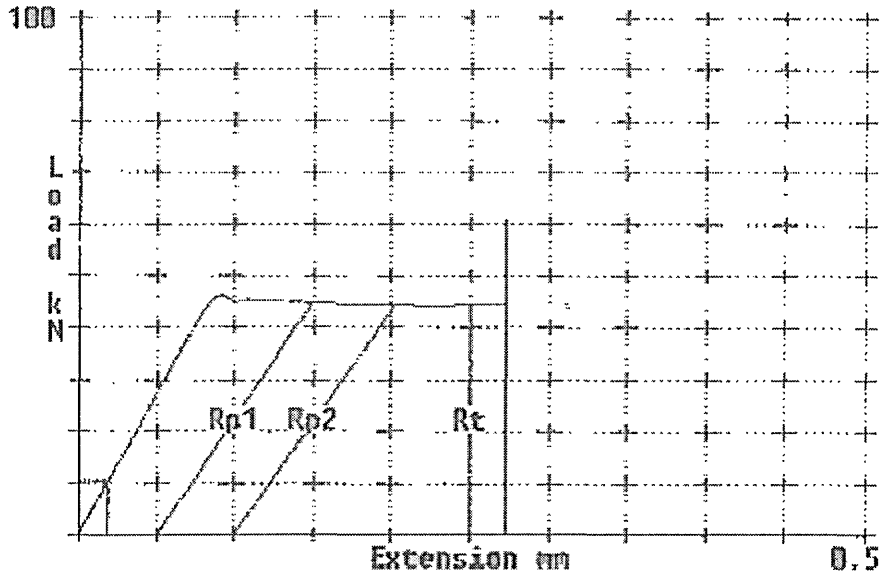

Figure 8.4: Example graph produced using tensile test

The initial attempt to load the structure using this method caused major convergence problems. The models themselves produced solutions that were unsuitable. The failure in the model was neither expected, nor as predicted (See later for details on eigenvalue extraction). The model predicted a failure by yielding of the end plate and not by buckling. This was caused, according to ABAQUS technical support, due to the unstable nature of the connection during loading. Another method had therefore to be found to load the structure in an appropriate way.

8.1.7.1 Alternative loading method

Due to buckling being an unstable failure mode, the loading applied to the structure using the CLOAD option was deemed unsuitable by Technical support at ABAQUS after lengthy discussions. Suggestions by them included adding extra elements to stiffen the beam flanges, thus allowing modification to the loading conditions. Figure 8.6 (supplied by Technical Support at ABAQUS) shows the alterative method of loading. Using the Multi-Point Contact (MPC) (figure 8.7) option with "TYPE=BEAM", produced rigid beam elements that are connected to a central point, a single node

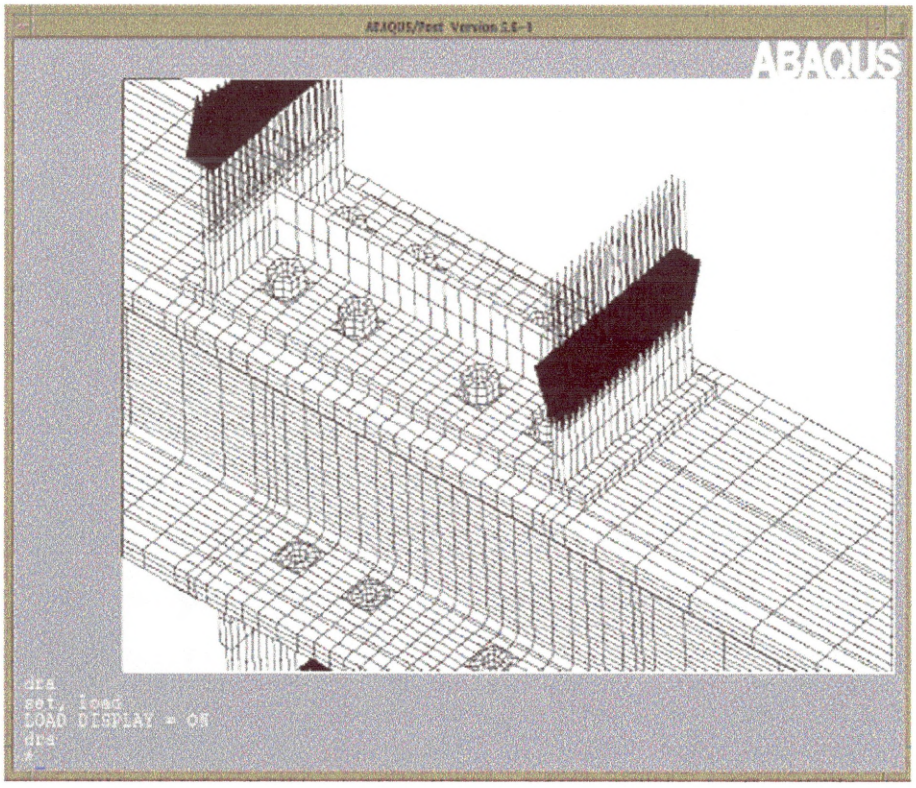

Figure 8.5: How connection is loaded

8.1.7.2 Multi-Point Contact (MPC)

These provide contact between two surfaces; in this case of the full model the BEAM option was used which "provides a rigid beam between two nodes to constrain the displacement and rotation at the first node to the displacement and rotation of the second node" (Page 20.2.2-12, Hibbitt, Inc, 1999) .

8.1.7.3 Applying Loading

The BOUNDARY option is then used to produce a rotation to the single node. Thus the rigid beam elements attached to the top of the section pull the beam flange, while the other MPC beam elements push the flange. The beam flanges on the other side of the connection are detailed in the same manner, apart from the rotation applied to the other node which was opposite in direction. This is to force the web to compress during the model analysis.

The rotation was applied to the fourth degree of freedom (D.O.F), x being the first, y and z are second and third respectively. Therefore the rotation about the x-axis, causes the web to compress.

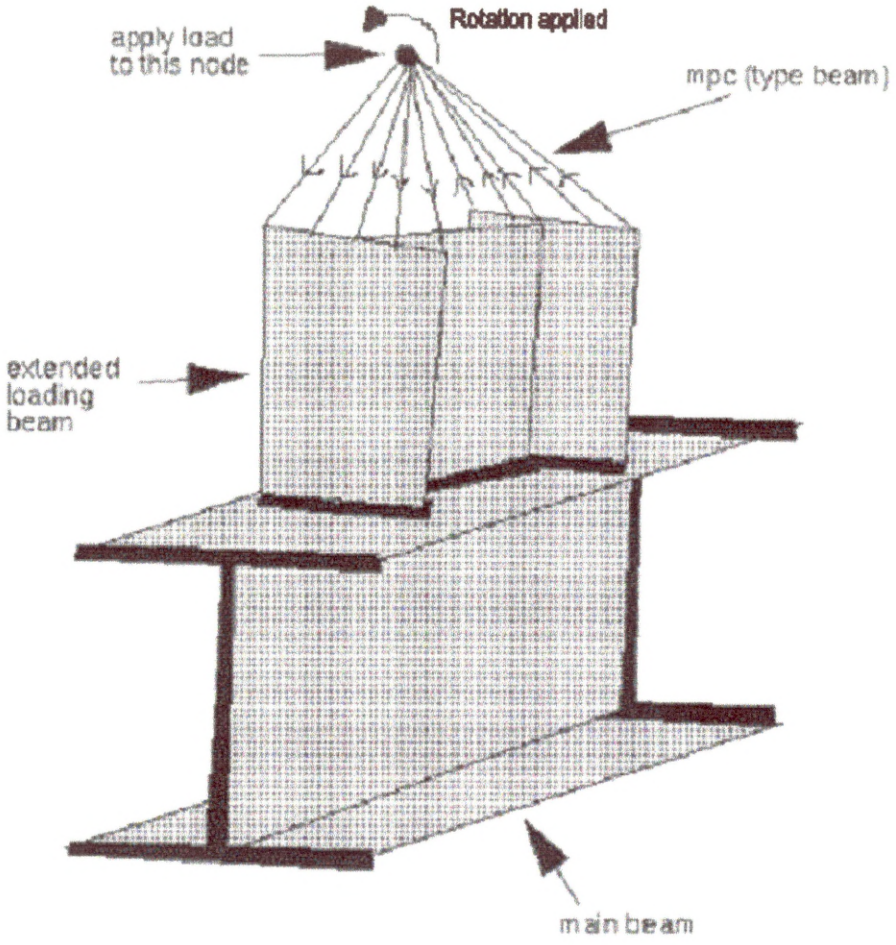

Figure 8.6: Showing the new method for loading

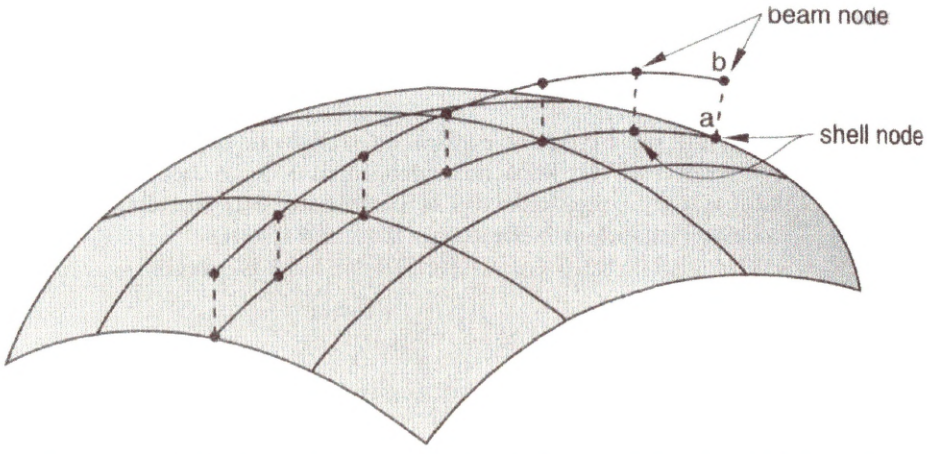

Figure 8.7: Details MPC BEAM constraints (Page 20.2.2-12, Hibbitt, Inc, 1999).

The extra elements (beam flange) included in the model are to allow connection behaviour to continue normally, without the rigid beam elements restraining the true behaviour of the structure (figure 8.6).
The rotation applied to the node must be in radians and a suitable value is selected. The rotation increases throughout the time step similar to that in the previous loading option.

8.1.8 Increments

Similar to modelling the T-stub, the time steps were modified to allow more data to be generated for the study (See Chapter 9 on Using ABAQUS). Therefore the number of equilibrium iterations had to be modified from the default values, to allow time for the connection matrix to converge.

8.2 Mesh Generation

The column web was the main area for investigation; therefore the mesh used had to reflect this. Many elements were used to create the web in detail i.e a fine mesh was used by the researcher to highlight this area for extensive examination. The other components of the connection were of less importance and the choice of a coarse mesh reflected this.

8.3 Behaviour of a Connection

8.3.1 Buckling of a Connection

As configuration of loading on the connection was symmetrical in nature, theoretically crushing of the connection would occur. A way had to be found to allow the connection to buckle and thus obtain an accurate representation. According to the Buckling and Collapse Course Notes (Hibbitt, Inc, 1997) produced by HKS Ltd, an imperfection must be introduced into the connection in order to allow buckling to occur. A perfect mathematical model would not allow buckling to take place.

8.3.2 Buckling using ABAQUS

Two types of analysis are needed when modelling non-linear structures using ABAQUS in order to derive the overall behaviour of the structure from the data obtained.

- Eigenvalue extraction
- RIKS analysis.

8.3.3 Eigenvalue Extraction

To carry out an eigenvalue extraction, various details are required to be entered into the initial model file. Using the "BUCKLE" option allows the researcher to define how many eigenvalues are to be obtained during the analysis. The author selected 8. To allow the second analysis to be run, a "fil" file is needed, the "fil" file is created using the NODE FILE command. This creates the eigenvalue data required for the second part of the analysis (RIKS), which allows the researcher to add imperfections to the perfect geometry of the model.

8.3.4 Imperfection modelling in ABAQUS

8.3.4.1 RIKS analysis

With version 5.6 of ABAQUS being used by the researcher, there is a command called "IMPERFECTION" within the program. This allows the researcher to create a mathematical imbalance in the model and thus allow the overall behaviour of the connection to be obtained. (See Chapter 5 for more details).This option is usually carried out with the RIKS method of analysis, under the STATIC option in ABAQUS. The IMPERFECTION option applies modifications to the output from the first run, using values obtained from the "fil" file. The IMPERFECTION command applies a percentage modification to the model co-ordinates. In this case a combination 0.01, 0.1 or 1, these are 1% 10% and 100% modifcation respectively, as recommended by the ABAQUS manuals (Hibbitt, Inc, 1999). The only co-ordinates affected are the ones written in the "fil" file (column web co-ordinates).

The following statement has to be remembered, when applying the IMPERFECTION option during RIKS analysis:

" The lowest buckling modes are assumed to provide the most critical imperfections, so usually these are scaled and added to the perfect geometry to create the perturbed mesh" [(Hibbitt, Inc, 1999) ABAQUS manual section 7.5.1-2 V5.7]

Another important point to note from the manuals when using this method is:

"imperfections based in a single buckling mode tend to yield non-conservative results"[(Hibbitt, Inc, 1999) ABAQUS manual section 7.5.1-3 V5.7]

An example below shows how to include the imperfection option in an analysis, with the lower eigenmodes having higher imperfection modifications applied:

```
*IMPERFECTION, FILE=/usr/local/disk2/swap1/swap1, step=1, nset=c-web
2, 1.0
4, 0.1
6, 0.01
8, 0.01
```

The top line reads the output from the first analysis, i.e. reads the "fil" file and the other lines apply the modification factor to the data before the analysis begins, as discussed previously.

The only imperfections applied to the models were the values obtained from the eignmode analysis, no other imperfections were applied during the course of the investigation.

8.4 Contact Options

Contact between the endplate and the column flange was also modelled using ABAQUS. Contact modelling of surfaces is used in order to prevent penetration of either surface. This also allows gaps to develop as if the structure is being pulled apart. This is how the end plates and column flanges behave due to the complex loading (tension and compression).

To accomplish this, the "CONTACT PAIR" option was used. This allowed the surfaces that had the possibility of being in contact or would be in contact to be defined. Figure 8.8 details how the basics of contact modelling are developed in ABAQUS.

8.5 Results of the Eigenmode Analysis

Eight different eignemodes (figure 8.9a-h) were selected by the author to be calculated during the analysis. Once the eigenvalues are obtained then the researcher verifies the validity of each result manually. Details in table 8.1 show the outputs obtained from the first analysis. The results show a combination of positive and negative eigenvalues, and pairs of values, but their signs are different. This means that if the loading was reversed these negative values would become the positive eigenvalues

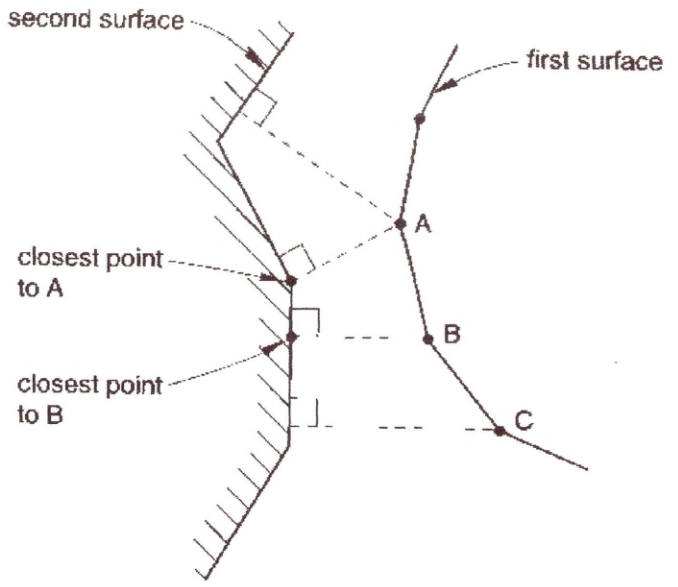

Figure 8.8: Contact between master and slave surfaces

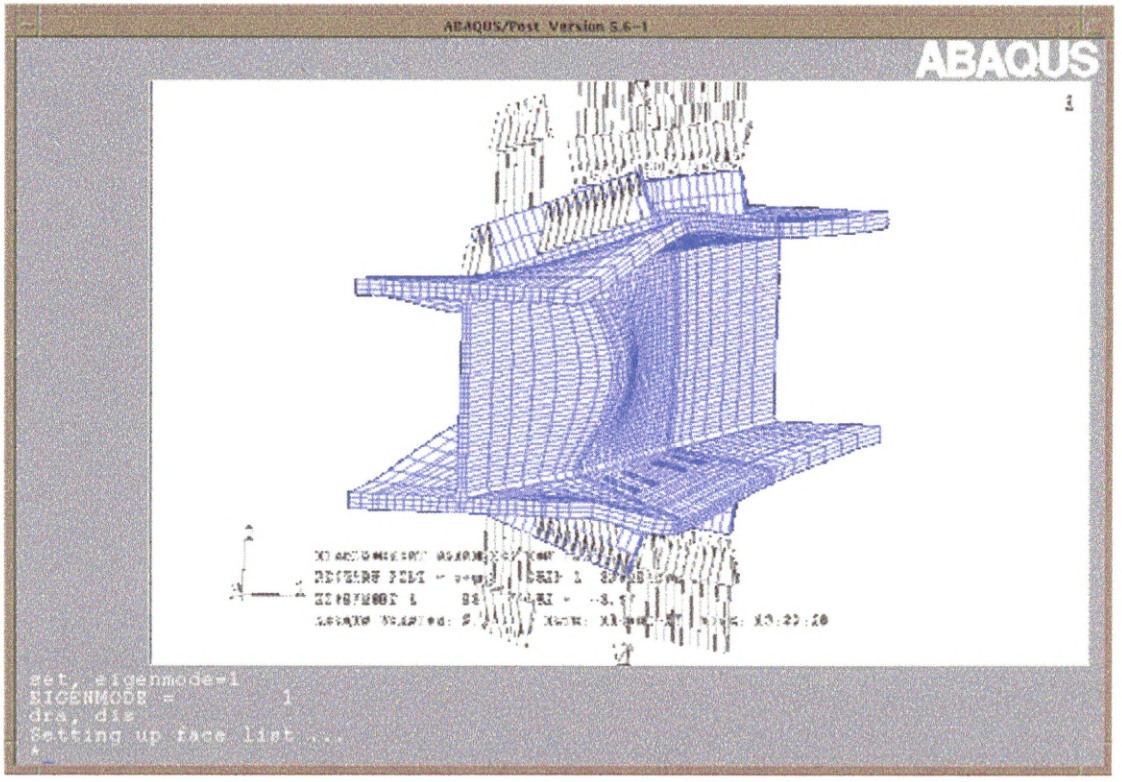

Figure 8.9a: Eigenmode 1

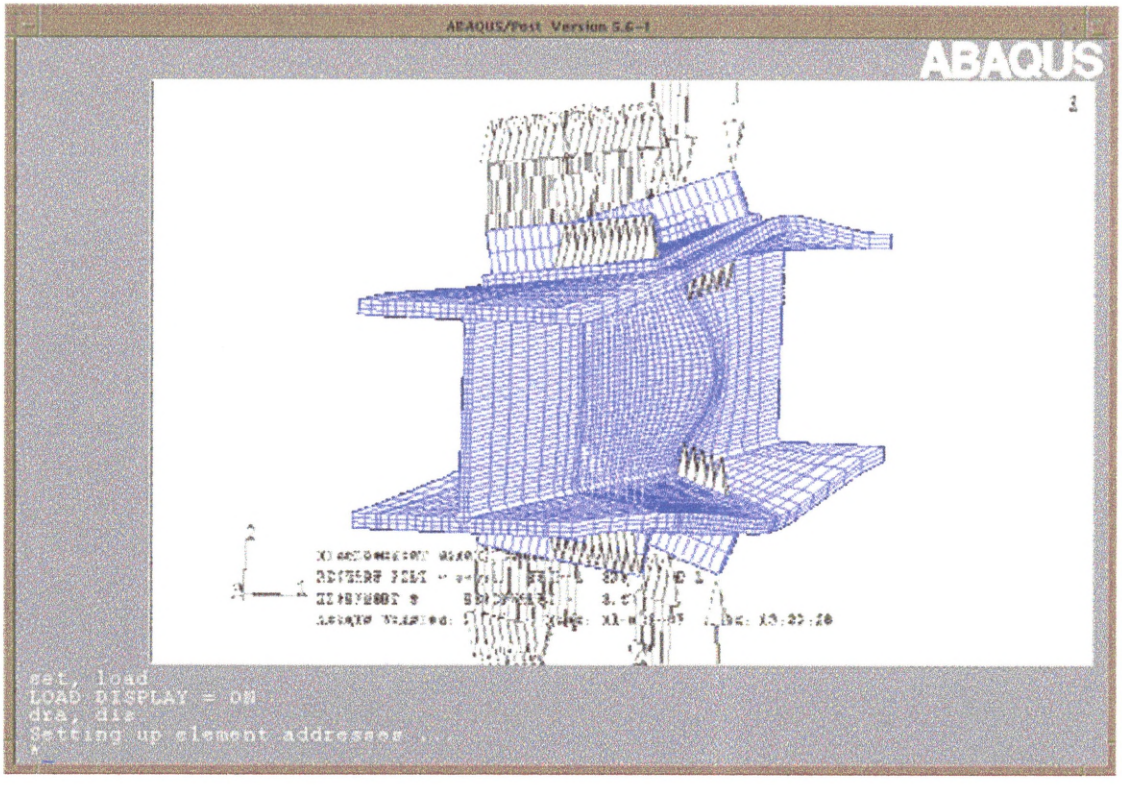

Figure 8.9b: Eigenmode 2

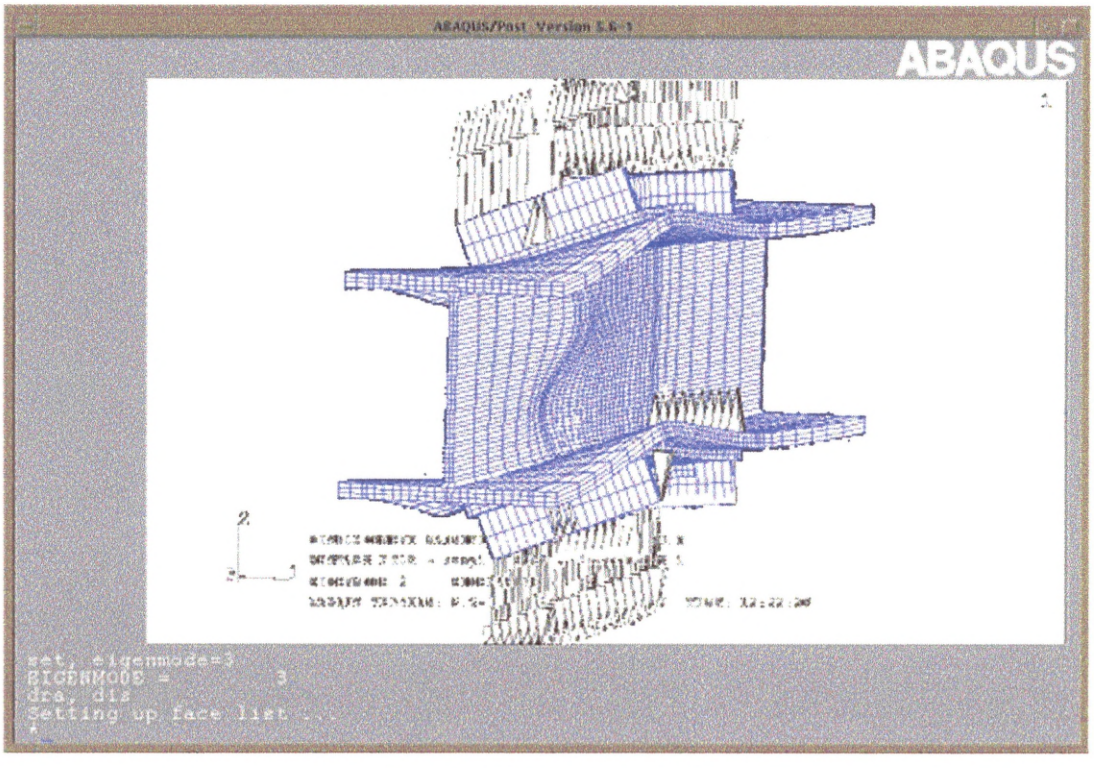

Figure 8.9c: Eigenmode 3

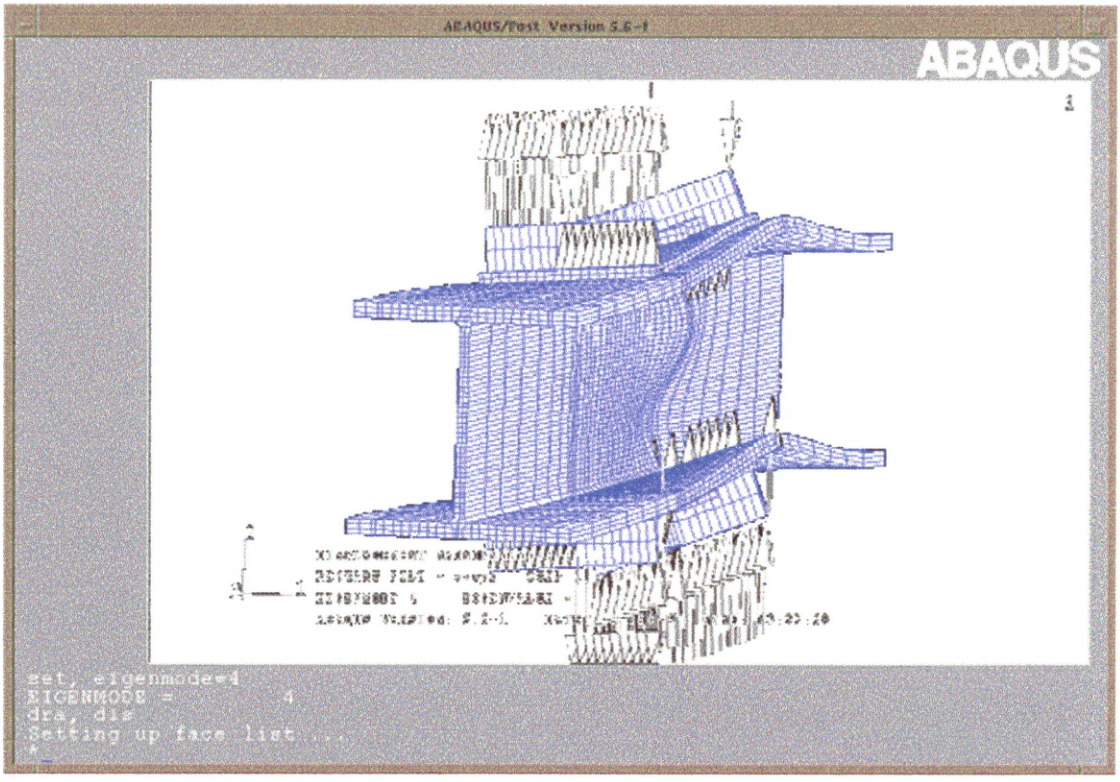

Figure 8.9d: Eigenmode 4

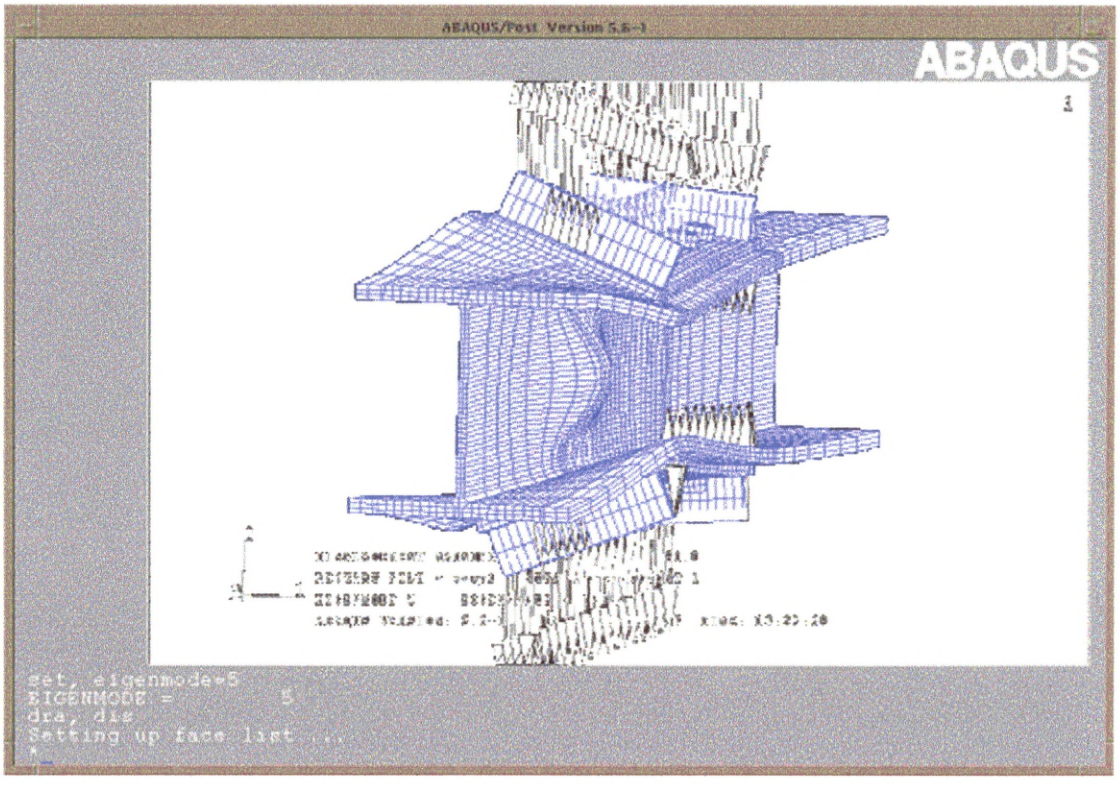

Figure 8.9e: Eigenmode 5

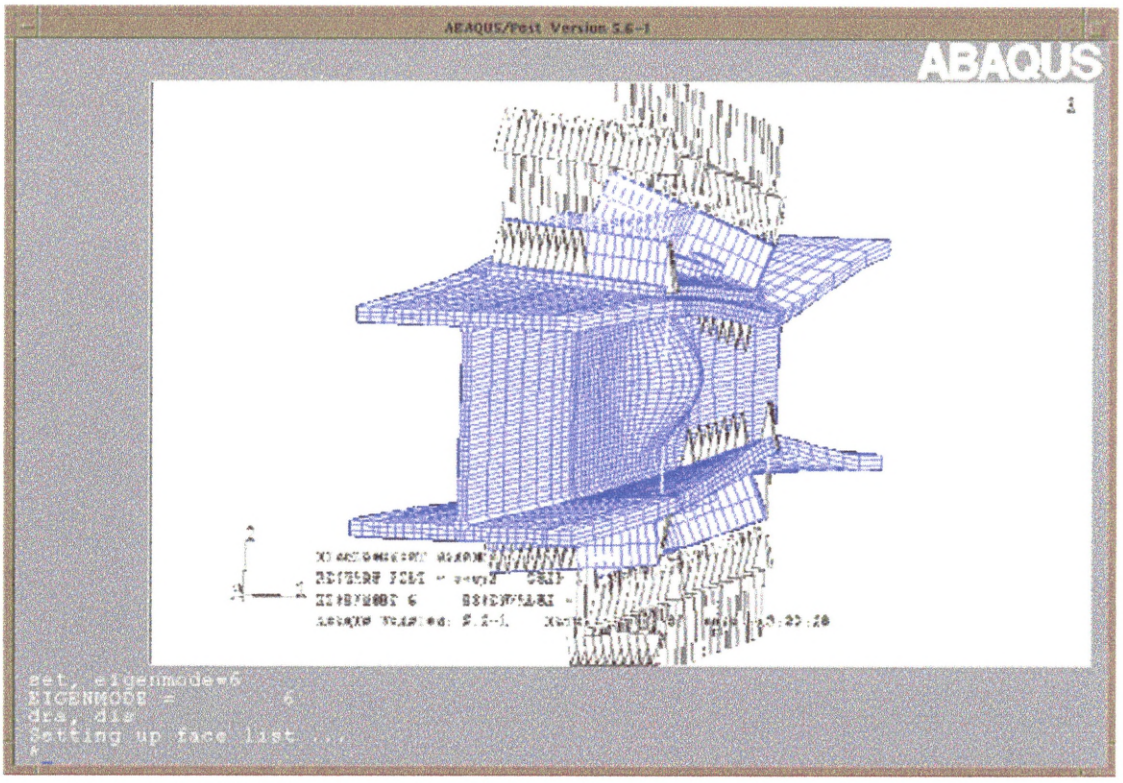

Figure 8.9f: Eigenmode 6

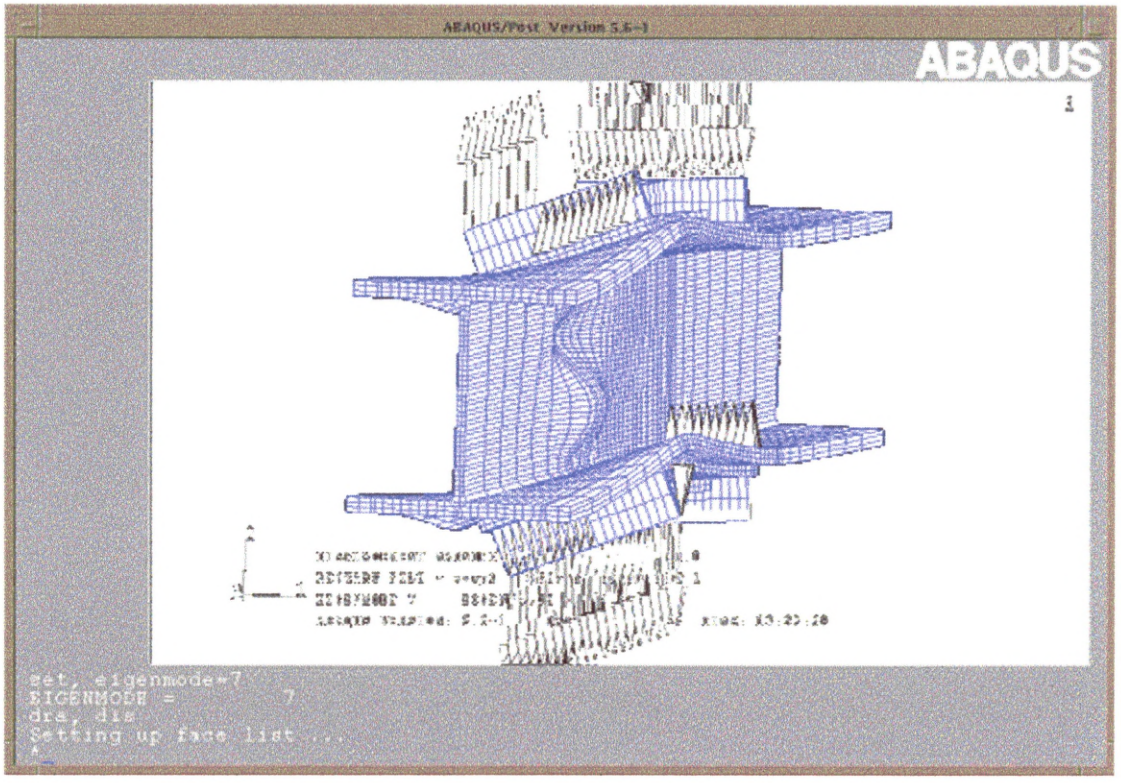

Figure 8.9g: Eigenmode 7

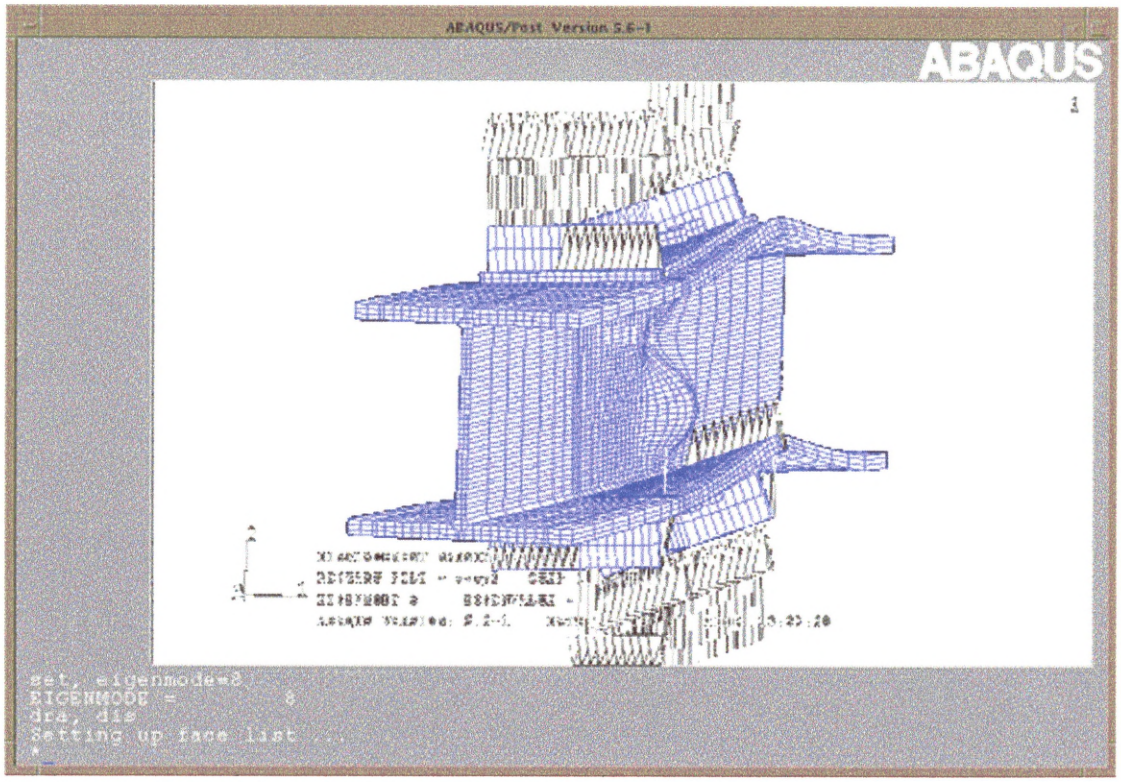

Figure 8.9h: Eigenmode 8

To understand and interpret the results, the ABAQUS manual has to be utilised extensively and part of relevant section is quoted below:

"In most cases such negative eigenvalues indicate that the structure would buckle if the load were applied in the opposite direction"((Hibbitt, Inc, 1999) Section 6.2.3-3 User Manuals).

All negative eignemodes are similar to the positive values apart from the sign. This means that if the loading on the model was reversed, then eigenmodes 2,4,6 and 8 would be negative while 1,3,5,7 would now be positive (Table 8.1)

Therefore all negative eigenmodes were ignored for this model as they occurred in the tension zone of the web.

8.5.1 Positive Eigenmodes

The eigenmodes that are left are therefore possible, as they occur in the compression zone of the web, as above figures show when taking account of the method and direction of loading

8.5.2 Eigenmode 2

This failure shows a single large failure of the web i.e. single curvature.

8.5.3 Eigenmode 4

This failure shows a double failure of the web i.e. double curvature.

8.5.4 Eigenmode 6

This failure shows a single failure of the centre section of the column web i.e. single curvature.

8.5.5 Eigenmode 8

This failure shows a double failure of the web i.e. double curvature.

Eigenmode	Eigenvalue	Failure Type
1	-1.27	Single Curvature
2	1.27	Single Curvature
3	-2.56	Double Curvature
4	2.56	Double Curvature
5	-3.28	Single Curvature
6	3.28	Single Curvature
7	-4.85	Double Curvature
8	4.85	Double Curvature

Table 8.1: Output from First connection model of eigenvalues

8.5.6 Modification Factors applied to Positive Eigenmodes

From Table 8.1 eigenmodes 2 is the more likely to occur, as this type of failure was similar to what was observed in the full scale tests, double curvature was not noted in the physical tests [modes 4 and 8].

The method employed by ABAQUS gives a weighting to the eigenmode failure; those that are more likely to occur will have a higher weighting. The range is from 0.01 to 1.

Therefore, modifications to mode 2 should be higher i.e. applying 1.0. The other modes will affect the behaviour less and can therefore have the lower factors. Table 8.2 details the weighting given to the different eigenmodes.

Eigenmode	Weighting
2	1
4	0.1
6	0.01
8	0.01

Table 8.2: Detailing the weighting given to each eigenmode

The lower the eigenmode, the more probable the outcome and the higher the modification factor that is applied. Eigenmode 2 was also the lowest eigenmode obtained during the analysis (table 8.1).

8.6 RIKS Analysis

The calibration of the models using different imperfections modification can only be verified by using these modifications with other connection models and applying similar imperfection to the various eigenmodes.

During the investigation it was noted that once peak loading was reached, problems with the RIKS analysis became evident. One of two possibilities should occur either the load stays constant as the time steps increase or the load slowly returns to the point of origin i.e zero load. With RIKS option selected the load decreases but keeps going and thus the load reverses (figure 8.10). The time step also became negative. This data should be ignored. The values are still valid up to and including peak load. Using an available post-processor should allow the researcher to view this strange occurrence and understand the problems that result. This problem is inherent in using the RIKS method of analysis according to ABAQUS technical support who stated that the values should be discounted.

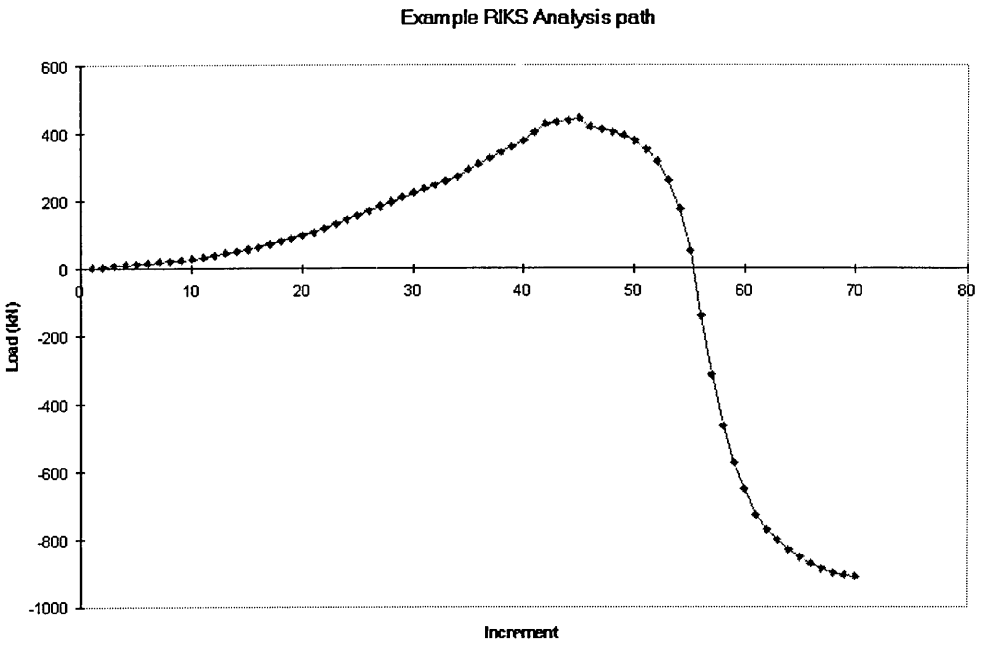

Figure 8.10: Showing the load reversal during the RIKS analysis

8.7 Conclusion

Full connection modelling is more time consuming and computer intensive when compared with basic T-Stub modelling. The techniques that were developed to produce the T-Stub were vital in the development of the much more complex models produced at a later date.

Problems With ABAQUS

Chapter 9

9.0 Introduction

In addition to its applicability for use in this research ABAQUS is utilised for a number of different applications worldwide. Specifically it can be used for mechanical, structural, civil, biomedical, and related engineering applications. Unfortunately whilst the software is capable of a wide range of tasks, the manuals and advice that accompany them does not cover all possible eventualities.

The worldwide use of the software further highlights this problem and there are numerous web pages and fora which detail issues and highlight potential solutions. Specifically it is worth mentioning the Finite Element USERS (FEUSERS) newsgroup which provided invaluable advice during this research. This particular group counts among its members the manufacturers of the software, experienced users and researchers..

This chapter details some of the main problems that were encountered and how they were resolved in order to proceed with the research. The following are discussed in this chapter and these relate to ABAQUS or UNIX [DEC Alpha running Digital UNIX]:

1. File space.
2. Memory.
3. Using the Abaqus.env file.
4. Disk space + time steps.
5. ABAQUS manuals.
6. Swap space
7. Using SPARSE SOLVER.

9.1 File Space

The sample programs were run successfully when ABAQUS was installed initially; yet there were problems with the author's own models. The T-stub model caused a failure which showed up as

"file system limits exceed on UNIT 2"

The error was traced to a problem with the scratch file and the location where the solver matrix information was being stored. All temporary file information was being written to the root directory of the main system. The size of this file exceeded the space available in the root section of the operating system. Modification to the "Abaqus.env" file were required. Additional lines were included to tell the program where the overflow was to be written; which enabled the author's modelling to continue. To accomplish this the "split_scratch" command is used to tell the program when to start using the other available space. This command relates to the temporary scratch file and when the file reaches a pre-determined size it then stops copying files to that particular directory (root), and begins to copy files to other specified directories. The location of these subsequent files is entirely open to nomination by the user.

9.2 Memory

The amount of system memory that can be utilised by ABAQUS both during analysis and display (ABAQUS/Post) can be specified in the "abaqus.env" file. The size was increased according to the error messages produced during the running of the various applications.

9.3 "Abaqus.env" file

This file is found in the ABAQUS directory on the computer and a copy should be transferred to the start-up directory of the account holder (UNIX operating system only). ABAQUS checks three places for this file:

1. The ABAQUS directory.
2. The start-up (Home) directory.
3. The directory that contains the program files.

Copying the file to the home directory enabled the author to modify the file as appropriate; once changes were made to this file, then all subsequent runs were affected. This would only have relevance to the researcher, the work of other people would be entirely unaffected.

9.4 Disk Space

Initially the output files, "*.res" and "*.dat" were too large for the disk space present (1 Gigabyte of free space). Various commands are available in ABAQUS, to limit the size of the following:

1. Number of times the files are written to.
2. The amount of data produced.
3. The type of data written to the data files.

"EL PRINT" and "EL FILE" are used to limit the data written to the "*.dat" file. These commands also control the type of data written; while information on specific areas can also be stored in these files if more data is needed.

Using the "RESTART, WRITE, FREQUENCY= **" will limit the size of the results file, i.e. the "FREQUENCY=**" command can be set at any figure the user wishes. The lower the number the more information written to the file and thus more information will be available for study at a later date.

The number of time steps will also affect the amount of data produced. Using the "STATIC" parameter to control loading increments, the smaller the time steps the more information produced. This is normally used in conjunction with the above parameters to limit the size of files produced.

9.5 ABAQUS Manuals

The ABAQUS manuals (which extend to several thousand pages) attempt to cover every eventuality. The shear volume of information that accompanies the software is daunting and results in "information overload". This situation is not aided by the poor quality of the referencing included in the manuals.

These two factors combined to hinder rather than assist the user and it meant that even when a specific methodology existed, it is not necessarily obvious. One such example of this, defining contact, is detailed below.

9.5.1 Defining Contact

This research attempted to use "CONTACT PAIR (under SURFACE DEFINITION ", "SURFACE INTERACTION") to define the interaction between the end plate and the

column. This seemed to be a reasonable solution as the manuals indicated that contact pair applied to the 2 surfaces would be sufficient to define the interaction between the two surfaces.

However, the result of this selection was that the end plate penetrated the column thus invalidating the results because this situation would never occur in reality. Further investigation indicated that it was necessary to also use the "SMALL SLIDING" option. This option prevents the penetration of one surface into the other and allows them to act as one at the boundary interface (resulting in bending which causes stress and strain in the components).

9.6 Control Parameters

Problems with the model not converging within the time may require modifications to the default control parameter. The defaults are limited to 12 increments (severe discontinuities) and 10 equilibrium iterations. Using "CONTROL, PARAMETER= TIME INC" and increasing the number of iterations resolved this particular problem. This was needed due to the complex nature of the problem being investigated by the researcher. If the "*.msg" file is checked then this would help determine if control parameters require alteration.

9.7 Temporary Hard Disk Memory

Temporary hard disk memory is required when the computer does not have enough physical memory and has to use the hard drive as extra storage space. The default is four times the amount of physical RAM i.e. if the computer had 32 MB physical Ram then 128 MB of virtual RAM (Swap space) would be available.

Due to the large model being used, warning messages appeared on the screen about the amount of swap space free:

"swap file space below ten percent"

This occurrence can start affecting the running of the computer. The swap space may need to be increased depending on the computer and the hardware configuration. A check can be obtained on how the system is performing using the "vmstat" command in UNIX. This gives details of system performance showing if the computer is paging continually [using disk space as imitation RAM] and is therefore working inefficiently.

Sometimes the only solution is to increase the amount of physical RAM. A comparison between running the models before adding new RAM and after the upgrade was made, for an example the tables for before (table 9.1) and after (table 9.2) the hardware upgrade (extra RAM) are presented. Two important sections needed investigation, which were "pages" and "cpu" and these are discussed in 9.8.1 and 9.8.2.

9.7.1 Pages

The important column to note is the "pin" which stands for 'pages in'. This relates to the information waiting to be processed by the computer. As can be seen this is very high (Table 9.1), due to the lack of available memory on the machine at this time. Investigating the other table (9.2), the values in this column are considerably lower; therefore less information is waiting to be processed by the processor (CPU). The information waiting to be processed is stored on the hard drive (Table 9.1), not in memory (RAM) (Table 9.2).

The speed of the hard drive is much slower than the speed of the physical RAM, milli seconds compared with nano seconds, a factor of 10^3. This meant that the T-Stub analysis was taking 3 weeks to converge before the upgrade. Following the upgrade results were able to be analysed in about a day. This example shows that RAM is extremely important in obtaining results in a reasonable timescale. It is imperative therefore that sufficient RAM is available in order that inefficiencies within the computer hardware does not slow the convergence time unnecessarily.

procs			memory			pages						intr			cpu		
R	w	u	act	free	wire	fault	cow	zero	react	pin	pout	in	sy	cs	us	sy	id
3	56	15	1480	28	1678	62	45K	163K	37M	61M	13M	248	92	618	7	5	87
2	57	15	1476	24	1686	390	3	56	245	310	17	487	43	1K	0	7	93
2	57	15	1470	21	1686	294	0	42	46	125	9	351	34	786	1	6	93
2	57	15	1472	27	1686	167	0	42	723	125	23	315	52	813	0	7	93
2	57	15	1454	22	1686	256	0	42	297	196	64	289	31	668	0	7	93
2	56	15	1472	28	1686	266	0	42	504	222	73	377	45	892	0	6	93
2	57	15	1480	20	1686	200	0	42	227	142	46	286	39	684	0	7	93
2	56	15	1488	12	1686	141	0	42	232	98	55	233	33	392	1	5	94

Table 9.1: Memory requirements before new RAM added.

procs			memory			pages						intr			cpu		
r	w	u	act	free	wire	fault	cow	zero	react	pin	pout	in	sy	cs	us	sy	id
3	50	15	15K	38	3563	1M	72K	307K	2M	1M	12K	43	159	309	84	6	10
3	50	15	15K	112	3559	131	19	53	0	18	0	33	63	297	93	5	1
3	50	15	15K	87	3556	36	0	36	0	0	0	26	66	276	94	6	0
3	50	15	15K	128	3556	36	0	36	0	0	0	21	49	266	95	4	1
3	50	15	15K	96	3556	36	0	36	0	0	0	25	71	272	95	5	0
3	50	15	15K	111	3551	36	0	36	0	0	0	26	68	272	93	5	2
3	50	15	15K	128	3550	36	0	36	0	0	0	27	54	269	95	5	0
3	50	15	15K	128	3554	36	0	36	0	0	0	31	70	285	91	6	3

Table 9.2: Memory requirements after new RAM added.

9.7.2 CPU

To verify if the machine is working at full efficiency, the section entitled CPU is investigated. The main figures to be compared is the "us" (usage) column. The processor in table 9.1 is running at a very low efficiency, between 0 and 8%, while the figures in a similar column in table 9.2 verify that with more RAM the processor efficiency is noticeably higher, the values obtained being between 85-95%, which are far superior to the original values i.e .before the upgrade. The investment in the upgrade can be shown to be beneficial, with considerably reduced convergence time and thus more models can be tried within a similar timescale.

Another method is to compare the times for the analysis runs of the various models. As can be seen with more physical RAM the completion time is reduced considerably for the T-stub model. The more details of the solver matrix stored in the physical memory of the computer and not in the virtual memory (Hard drive) the less time is taken to solve the matrix.

With more RAM available the large connection model will also run efficiently. Previously this model was unable to be run due to lack of memory, both physical and virtual, as the analysis being run is hardware dependent.

If the computer is running more than one ABAQUS application at any one time then the processor splits the time equally between the two tasks, i.e. both run at 49% CPU utilisation, if the hardware allows this(e.g. RAM, disk space etc.).

9.8 SPARSE Solver

Included in V5.6 of ABAQUS is the ability to reduce the model time, using the SPARSE solver option in the *HEADING option at the top of the input file. This enables more of the model to be loaded in the memory. The downside of this is that the computer hardware requirements increase considerably, especially the amount of memory required. The machine that the researcher used had 160 MB of RAM and 400 MB swap file and the model was unable to run using the SPARSE solver option, due to the swap file becoming full. The only way around this was for the system administrator to modify the computer settings to allow non-mirroring of the swap file and thus allow bigger models to be run in the available memory.

To do this, the user must be in superuser mode and go in to the "/etc/" directory and adjust the file called "swapdefault"; this needs to be renamed. The computer is

shutdown and re-booted to allow changes to take effect. This allowed more of the model to be stored in the memory and thus faster runs were effectively achieved. If this is still insufficient then the machine must be upgraded with more physical RAM required as a consequence or the swap file increased (normally not more than 3 times the amount of RAM).

9.9 Final Configuration of the Computer to run Full scale modes

Once the upgrades were completed the final specification of the computer was:

Upgrade carried out	Before	After
RAM (Mb)	32	288
Hard Drive (Gb)	2	10

Table 9.3: Upgrades carried out

The processor throughout the upgrade stayed as a DEC ALPHA 166 Mhz, 64 Bit processor.

9.10 Conclusion

Many unique challenges are created when ABAQUS is used to model complex connections and numerous problems are encountered.

Experience and perseverance will overcome most of these problems. However, this will only be possible if the right resources are available. Specifically; modelling complex connections requires, amongst other things, sufficient computing power. The computer must be able to analyse the solutions in a reasonable timeframe and then have sufficient disk space to store the results for later retrieval . The continual advancement of computer technology should minimise the problems encountered due to this problem for future researchers.

The problems encountered due to the manuals attempting (and failing) to cover every eventuality meant that it was not easy to determine the correct methodology for specific applications; this was not aided by the poor quality of the referencing.

Help for particular problems was sought from many sources, but by far the most helpful was the FEUSERS Newsgroup.

Discussion of results

Chapter 10

10.0 Introduction

This chapter will compare computer model results with actual physical results obtained from laboratory experiments. Additionally comparisons will be made with Eurocode 3 Annex J.

The discussion will therefore centre on these comparisons, highlighting the differences and any potential problems which may arise. It will also look at the best methodology to employ in different design scenarios.

The comparisons are all based on the information obtained in moment rotation curves and stiffness attributes of the steel bolted end plate connections.

10.0.1 Laboratory experiments

The physical tests are discussed in greater detail in Chapter 4, but suffice to say that full scale experiments (Bose, 1993, Bose, 1994 and Wang, 1996) were carried out on 18 steel bolted semi rigid end plate connections. This research specifically focuses on the 7 connections that failed due to column web buckling. These were the particular cases investigated in this study.

10.0.2 Eurocode 3 –Annex J

Eurocode 3-Annex J is discussed in greater detail in Chapter 5, Appendix C also shows examples of Eurocode 3- Annex J sample calculations. The code is a European standard code based on a significant number of experiments carried out throughout Europe. The results of these experiments have been converted into a mathematical model (Jaspart and Maquoi, 1994).

10.0.3 Finite Element Models

ABAQUS was used for the finite element modelling investigations, chapter 7 and 8 detail how these investigations were carried out. This research utilised both the shell model and the 3D model options as discussed below.

10.0.3.1 Shell Models

This involves 2D modelling of the connections with the third dimension (thickness) being defined as a constant. Shell elements were originally tested to increase the understanding of the software (ABAQUS) and to develop the methods required for modelling full scale 3D connection.

Shell models have a significant advantage over the 3D models in that both the design and analysis time is considerably reduced.

10.0.3.2 3D Models

A 3D model of the end plate connection is significantly more complex than its 2D equivalent, with a large number of additional variables. This research determined values for these variables from the tensile testing. A second model was also produced in accordance with the recommendations from other researchers (Gebheken and Wanzek, 1999) (Figure 10.1). This related to the high rate of strain produced during the tensile test affecting the behaviour of the specimen, therefore a 12% reduction was applied to the material properties.

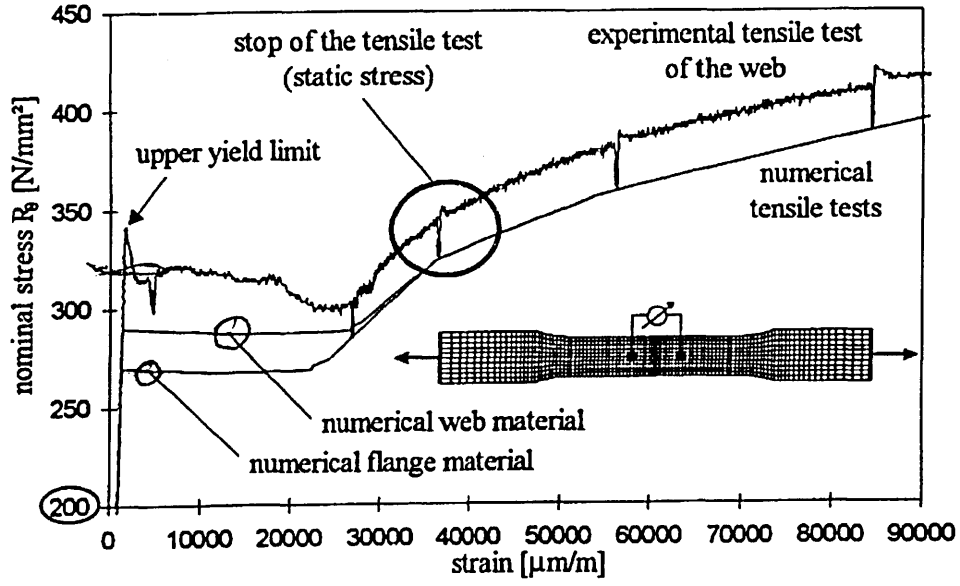

Figure 10.1: Example output of tensile testing of specimens

10.1 Discussion of Moment Rotation Curves

The moment rotation curves of a test specimen can tell the researcher much about the post elastic behaviour of steel bolted end plate connection and therefore provide

valuable information on the fundamental characteristics of the connection itself. Moment rotation curves are only obtained from the physical tests and ABAQUS, not Eurocode 3- Annex J.

Eurocode 3-Annex J classifies the connections according to various criteria. This methodology involves plotting Flexural rigidity (EI_b) against an assumed beam length (L_b) with a multiplication factor which varies depending on boundaries of the connection type. Specifically:

1. 0.5 EI_b /L_b : Nominally Pinned
2. 8 EI_b /L_b : Rigid (Braced)
3. 25 EI_b /L_b : Rigid (Unbraced)

In order to determine the connection type for the experimental results and ABAQUS it is necessary to plot moment rotation curve onto the Eurocode 3 graph. Examples of this are detailed in figure 10.2.

10.2 Original Physical Test Data.

As the discussion within in this chapter centres on the 7 physical connections that failed by column web buckling, the relevant data from Chapter 5 has been condensed and is repeated below to aid the reader (Table 10.1) . This information is considered to be the validation data and it is therefore referred to throughout the chapter to enable comparisons to the numerical and theoretical models to be made readily.

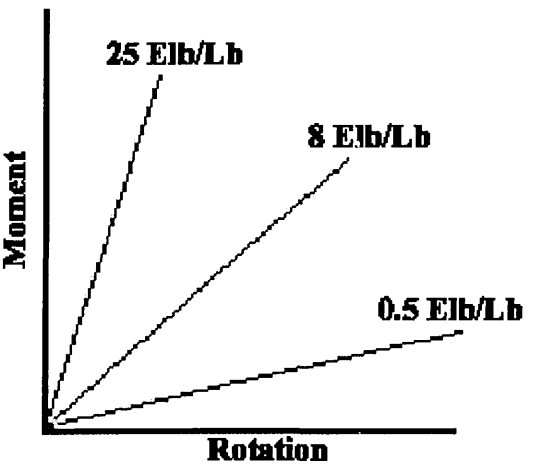

Figure 10.2a: Eurocode 3 – Annex J blank graph

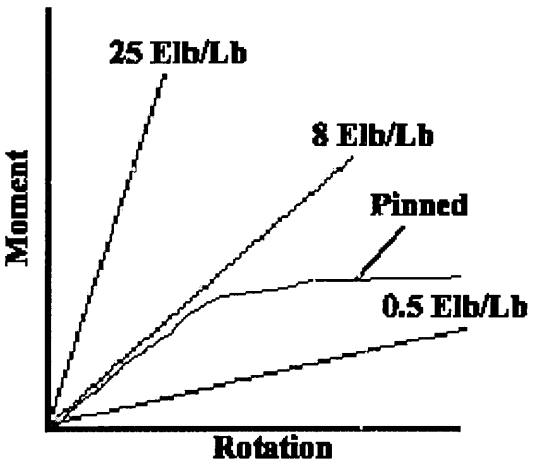

Figure 10.2b: Pinned example connection

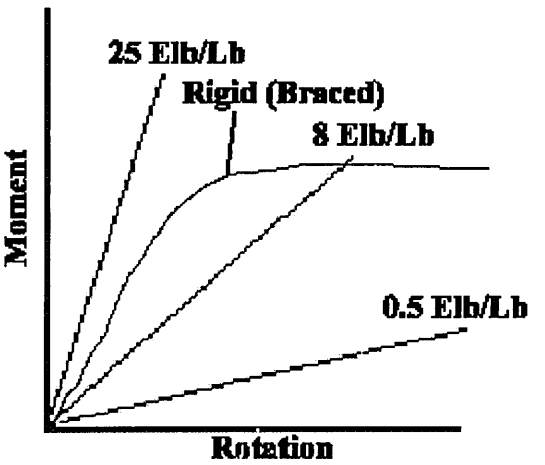

Figure 10.2c: Rigid(Braced) example connection

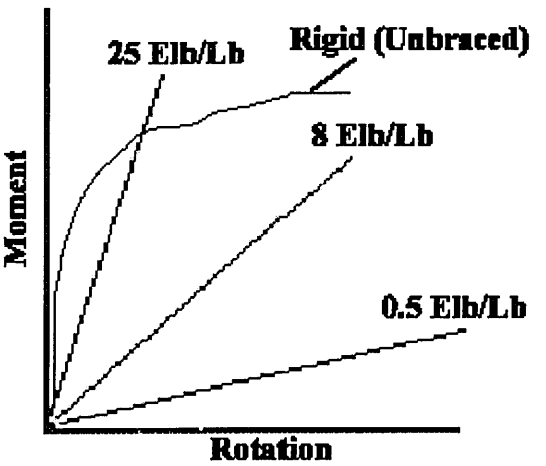

Figure 10.2d: Rigid(Unbraced) example connection

Figure 10.2: Example connection Types based on Eurocode 3 – Annex J.

10.3 Shell Models

These models were created using shell elements. Each element was given a thickness based on the location within the connection itself i.e. the shell elements that were used to describe the beam web were created with a thickness equal to the current beam being modelled.

10.3.1 Connections 1-7: FEP and EEPs (Shell)

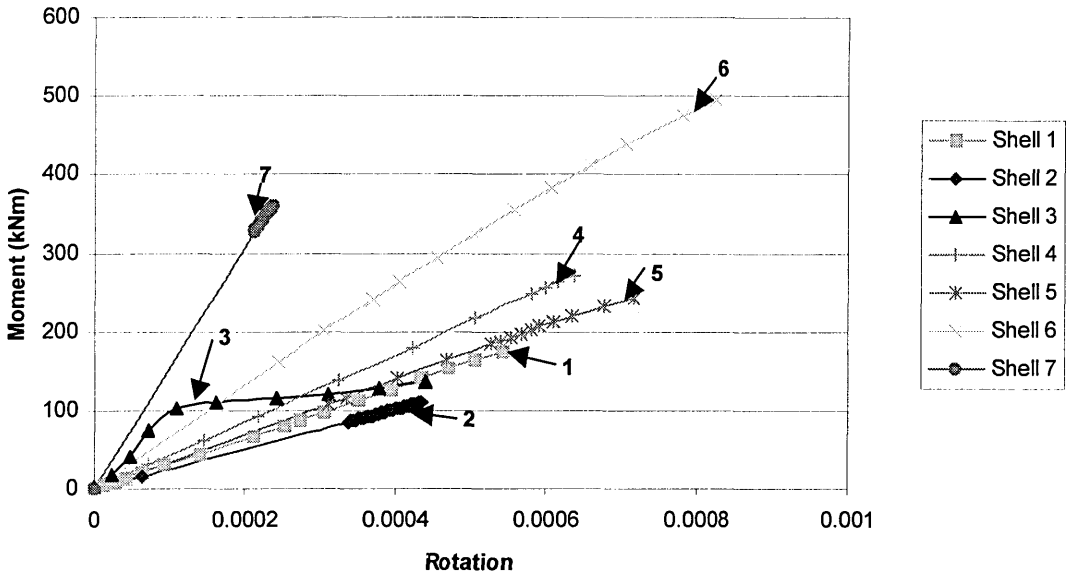

Figure 10.3: Moment Rotation curves for Shell Elements

All values selected for rotation and ultimate moment were selected on the basis of the above graph. Where the line ended for each model was assumed to detail the ultimate moment and rotation.

10.3.1.1 Connection 1(S1): (FEP)

As can be see in figure 10.3, rotation was very small. Consequently the scale was exaggerated to allow all 7 numerical results to be shown clearly on the graph. Rotation was 0.0005 and failure moment was 175 kNm.

Test	Detail	Column	Beam	End plate	Failure load kN	Failure moment kNm	Predicted moment resistance kNm	Ratio = Test/ Predicted	Rotation at failure rad	Failure mode
1	W3/20	254 x 254 UC 89	457 x 191 UB 74	510 x 200 x 12	465	279.0	142.5	1.96	0.053	Column web buckling
2	W3/20	254 x 254 UC 73	406 x 178 UB 60	460 x 200 x 12	269	161.4	121.2	1.33	0.046	Column web buckling
3	W3/24	254 x 254 UC 73	406 x 178 UB 60	460 x 200 x 15	276	165.6	152.3	1.09	0.051	Column web buckling
4	W4/24	254 x 254 UC 73	457 x 191 UB 74	640 x 200 x 15	470	282.0	223.4	1.26	0.033	Column web buckling
5	W4/24	254 x 254 UC 89	457 x 191 UB 74	640 x 200 x 15	688	412.8	235.0	1.76	0.061	Column web buckling & end plate fracture
6	W4/24	254 x 254 UC 89	762 x 267 UB 147	930 x 250 x 15	574	688.8	462.3	1.49	0.019	Column web buckling
7	Note (i)	254 x 254 UC 89	686 x 254 UB 125	860 x 250 x 20	929	557.4	444.7	1.25	0.007	Column web buckling

All flange welds 2 x 10 FW; all web welds 2 x 8 FW. All material S275. All bolts 8.8

(i) As detail W5/24 except that end plate is 20 (not 15) thick

Test numbers detailed above are only relevant for the detailed investigations undertaken by the researcher and do not necessarily correspond to those in chapter 5.

Table 10.1: Data for Physical Tests

10.3.1.2 Connection 2(S2): (FEP)

This was the second of the FEPs and obtained the lowest rotation and smallest ultimate moment. Rotation was 0.0004 and failure moment was 109 kNm.

10.3.1.3 Connection 3(S3): (FEP)

This followed, approximately the same gradient as connection 2, but with a rotation of 0.00053 obtained with a corresponding ultimate load failure of 136 kNm.

10.3.1.4 Connection 4(S4): (EEP)

This was the first EEP tested and the rotation obtained was larger that the three previous FEPs. Rotation was 0.0006 and ultimate load was 272 kNm.

10.3.1.5 Connection 5(S5): (EEP)

This connection follows approximately the same gradient as connection 1 as both use the same column and beams in the design, while the end plate was different, which would affect how the load was transferred to the other components. Rotation obtained was 0.00072 and ultimate moment was 242 kNm

10.3.1.6 Connection 6(S6): (EEP)

This connection attained the largest rotation and also the highest ultimate moment. Rotation obtained was 0.00083 and moment was 495 kNm.

10.3.1.7 Connection 7(S7): (EEP)

This connection used the thicker end plate (Table 10.1) and as such the rotation was the smallest obtained in the tests due to stiffness of the end plate. Rotation obtained was 0.00024 and the ultimate load failure was 359 kNm.

10.3.1.8 Comparison of connection moments capacity at failure. (Shell Models)

The ultimate moment capacity attained by experimental, Numerical (ABAQUS) and Eurocode 3 are summarised below:

	Experimental		Numerical (Shell)		
Test No	Ultimate Moment KNm	Rotation (Radians)	Ultimate Moment kNm	Rotation (Radians)	Eurocode 3 kNm
1	279	0.053	175	0.000544	142.5
2	161.4	0.05	109	0.000434	121.2
3	165.6	0.05	136	0.000526	152.3
4	412.8	0.06	272	0.0006	235
5	282	0.03	242	0.000718	223.4
6	688.6	0.019	495	0.000825	462.3
7	557.4	0.007	359	0.000236	444.7

Table 10.2: Failure moment and rotation values (Shell models).

10.4 3D Solid models(Non-Modified Material Properties – 3D SNMMP)

The full investigation of steel bolted end plate connections dealt with 3D solid models (See Chapter 8) and the following discussion centres on the moment rotation curves obtained.

10.4.1 Connection 1: FEP (3D SNMMP)

Test 1 is from a series of FEP connections tested by Wang (Wang, 1996) as part of his study of steel FEP connections. Due to the limitation of the software being used [LUSAS] the overall behaviour of these connections could not be fully determined. The software utilised by this researcher was able to model the behaviour of the connection more readily despite the non-linearity in the material and the geometry of the connection.

The value of the experimental failure moment is lower than that achieved by numerical modelling, as figure 10.4 shows. The rotation for the connection is higher for the experimental model than the numerical model. Once yielding occurred in the physical connection, it was still able to resist the applied loading for a longer period but this was not reflected to the same degree in the numerical results obtained. Failure moment was 317 kNm and rotation was 0.02 radians.

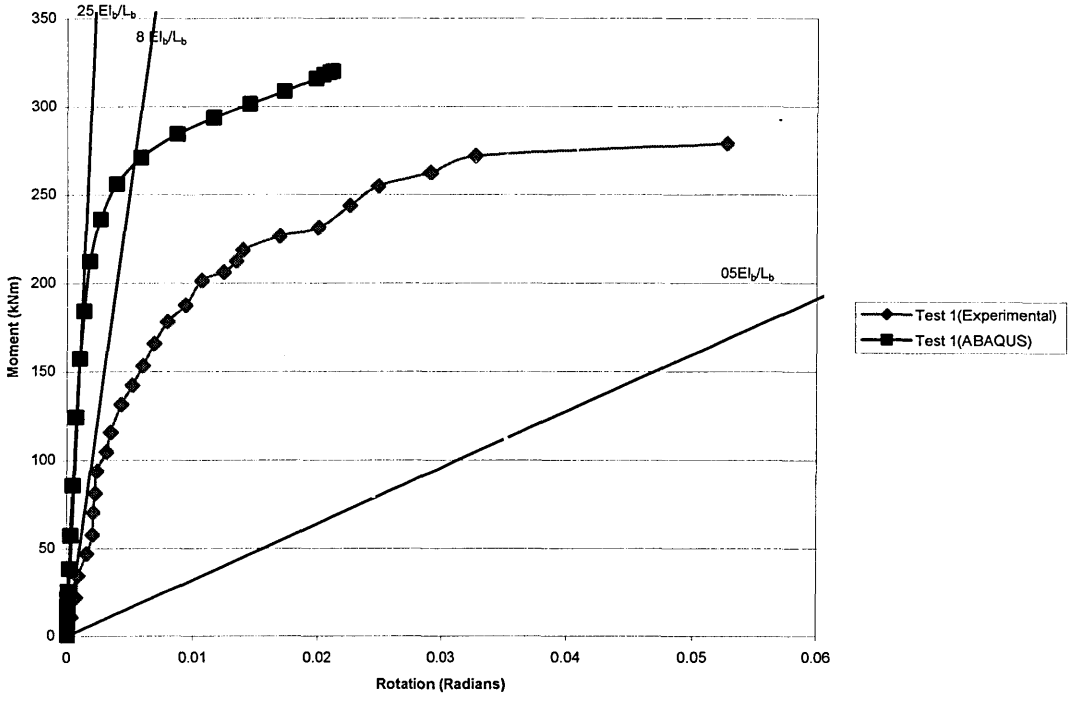

Figure 10.4: Moment Rotation curve for Test 1

10.4.2 Connection 2: FEP (3D SNMMP)

Test 2 (Figure 10.5) shows greater evidence of congruence in relation to the experimental behaviour than the previous connection. The numerical model follows a linear, elastic path. Yielding of the material then occurs and the rotation within the connection increases until failure is evident. The failure moments are broadly similar but the value estimated by the numerical model is once again higher than the experimental model.

Failure moment was 196 kNm and rotation was 0.05 radians.

10.4.3 Connection 3: FEP (3D SNMMP)

The numerical results for this FEP connection show a good representation of the behaviour for overall loading conditions. The numerical model shows a very clear linear path, followed by yielding and then a slow increase in moment capacity until failure occurred (Figure 10.6).

The value of the theoretical ultimate rotation was similar to that of the experimental model. Failure moment was 180 kNm and rotation was 0.04 radians.

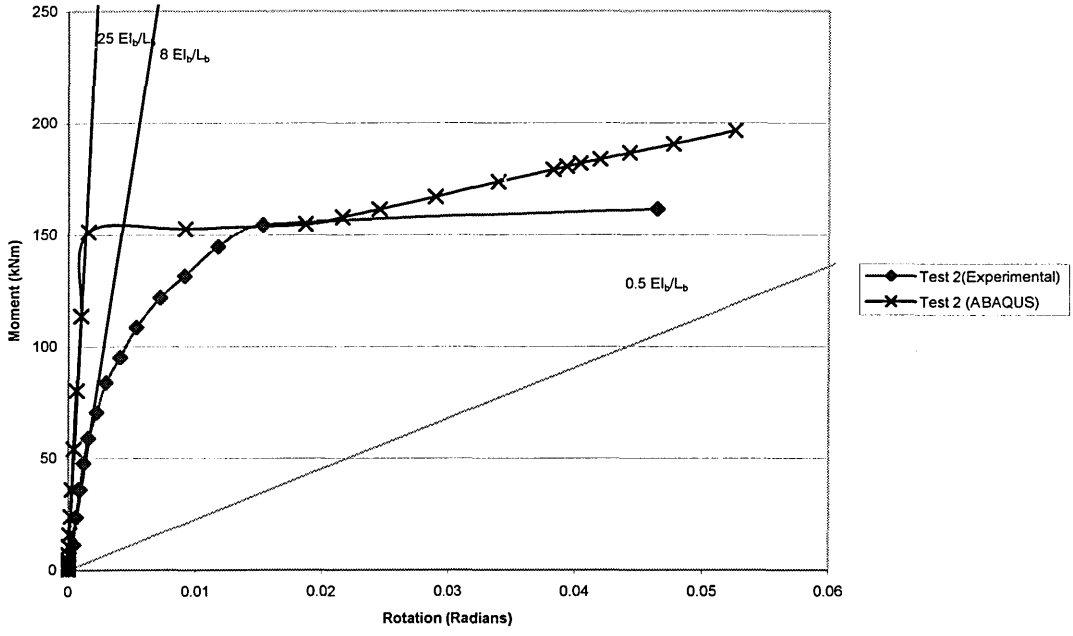

Figure 10.5: Moment Rotation curve for Test 2

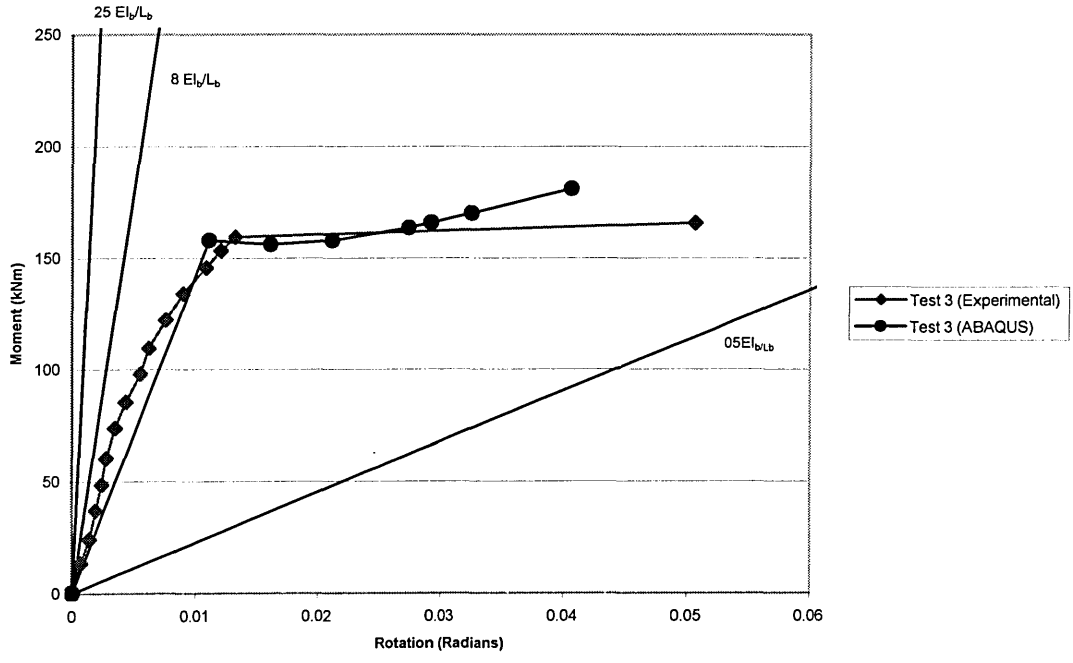

Figure 10.6: Moment Rotation curve for Test 3

10.4.4 Connection 4: EEP (3D SNMMP)

This test was chosen from a series of tests carried out by Bose (Bose, 1993, Bose, 1994) on behalf of the SCI. It was one of the first EEPs that failed by buckling during experimental testing. The moment rotation graph shows the results of the physical test, with a steady increase in the rotation as the load increased with the curve levelling out until failure occurred.

The numerical model demonstrates a much lower stiffness of the connection than that obtained by the experimental value as shown in figure 10.7. Predicted failure moment was 417 kNm and rotation was 0.01 radians.

10.4.5 Connection 5: EEP (3D SNMMP)

The experimental moment rotation curve (Figure 10.8) shows non uniform initial behaviour. The graph illustrates the rate of change in rotation when load was increased. This could be due to movement between the components during the initial stages of loading. It is difficult to establish the precise reason for this apparent movement due to the complexity of the connection. However, it would be reasonable to assume that this is due to the welding used on these particular connections, it may

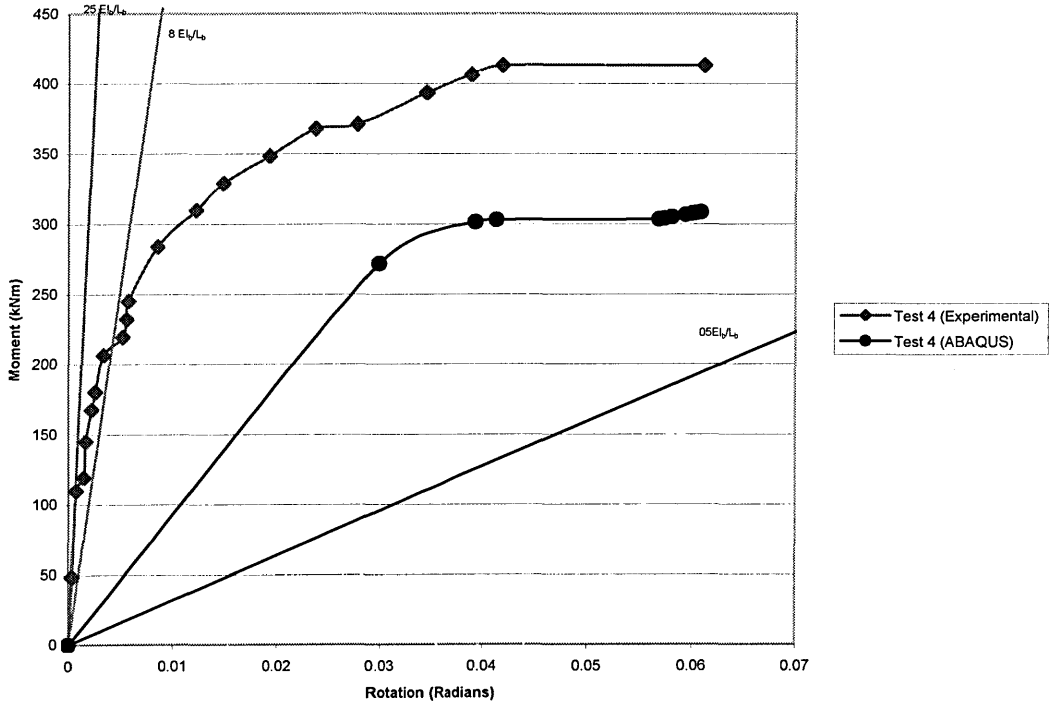

Figure 10.7: Moment Rotation curve for Test 4

have been that excessive heat was used during the fabrication of the connection. The failure moment predicted by the numerical model was significantly higher than that found by the experimental model. However, the value of the rotation for both methods compares reasonably well, with the experimental rotation being slightly higher. Failure moment was 391 kNm and rotation was 0.02 radians.

10.4.6 Connection 6: EEP (3D SNMMP)

The physical testing of this connection proved extremely difficult due to the high moments that the connection was able to withstand. For more detailed discussion of this and other tests see Chapter 4 on Physical testing.

Both experimental and numerical curves for this connection show a high initial stiffness, with the analytical curve having a slightly higher value (Figure 10.9). Failure moment was 818 kNm and rotation was 0.013 radians.

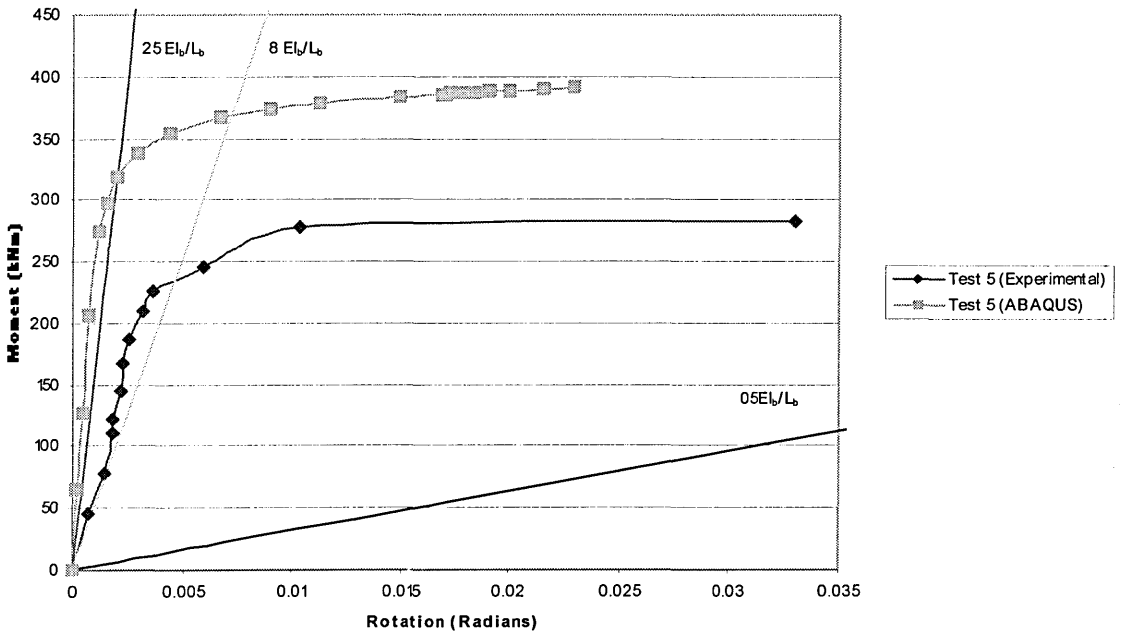

Figure 10.8: Moment Rotation curve for Test 5

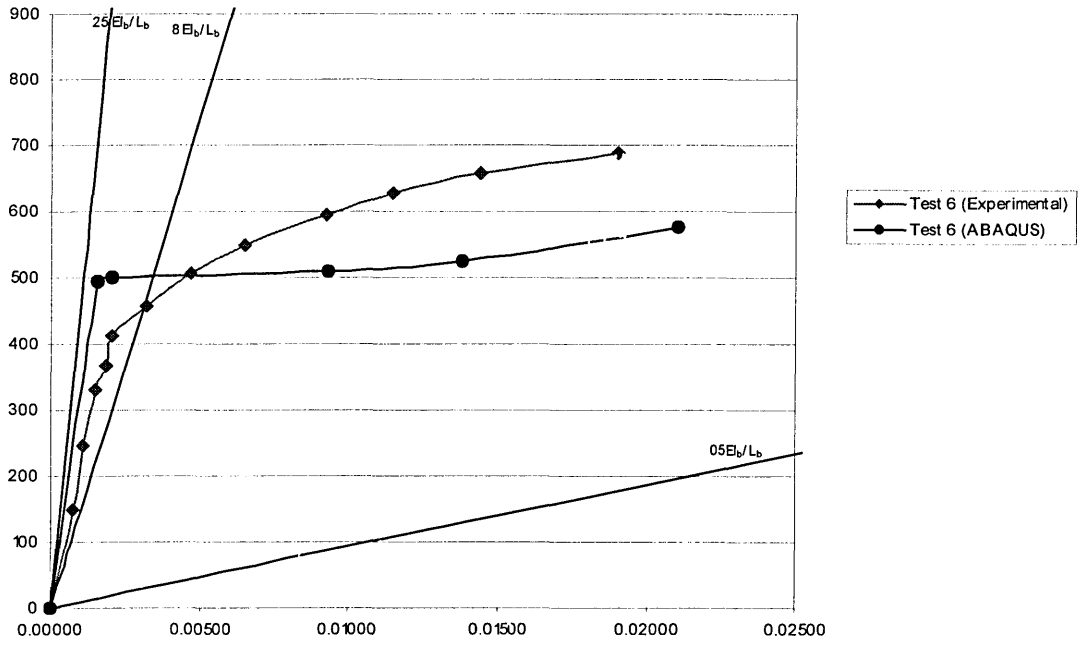

Figure 10.9: Moment Rotation curve for Test 6

10.4.7 Connection 7: EEP (3D SNMMP)

This connection was a non-uniform SCI connection utilising a thicker end plate of 20 mm instead of the normal 15 mm. With this thicker end plate the rotation of the connection and the subsequent distribution of the stress and strain throughout the other components was expected to be lower. In the physical test a low rotation was observed. The moment rotation graph (Figure 10.10) demonstrated a very high stiffness mainly due to the thickness of the end plate. The numerical model shows similar characteristics with very little rotation and a linear moment rotation curve up to yield point. Due to the lack of "give" in the end plate, a considerable prying action comes into play on the column flange, which is transmitted through to the column web. Failure moment was 616 kNm and rotation was 0.0005 radians.

10.4.8 Comparison of connection moments capacity at failure. (3D SNMMP)

In order to compare results in a consistent manner, the comparisons of the various connections in this section utilise the same method as the shell numerical models,

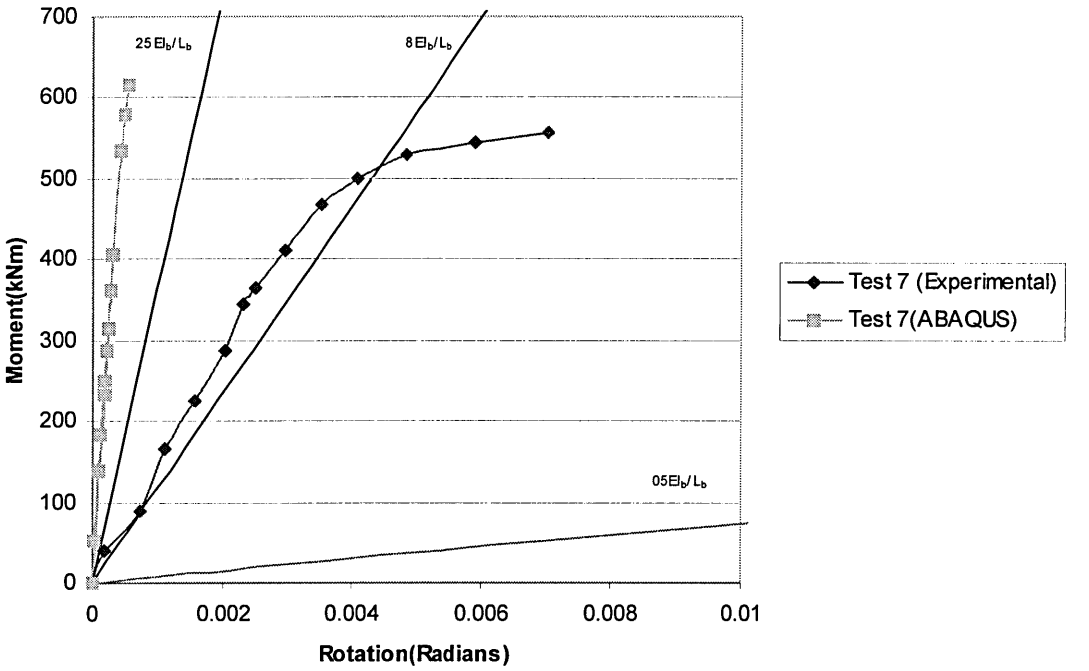

Figure 10.10: Moment Rotation curve for Test 7

specifically the use of line end values. Line end values are determined as the point immediately preceding the slope change to a negative gradient. This is equivalent to the connection failing as the rotation increased but the moment reduced.

Table 10.3 details the ultimate moment capacities for Experimental, 3D SNMMP and Eurocode 3, compiled into a readable and readily understood format.

10.5 3D Solid models(Modified Material Properties – 3D SMMP)

During the literature study (See Chapter 3 for more details) a paper was obtained which discusses the possible problems with the normal method of testing material properties (Gebheken and Wanzek, 1999) using the tensile test. This stated that during prolonged experimentation the properties of the material would be affected. The experimental test results utilised in this research, (Wang, 1996, Bose, 1993 and Bose, 1994) would be affected if Gebheken and Wanzek's theory is correct.

Therefore, all models were re-run, but only the material properties were changed, i.e. reduced in line with the recommendations in the above paper.

Table 10.4 details these new modified ABAQUS results.

	Experimental		Numerical (SNMMP)		
Test No	Ultimate Moment kNm	Rotation (Radians)	Ultimate Moment kNm	Rotation (Radians)	Eurocode 3 kNm
1	279	0.053	317	0.02	142.5
2	161.4	0.05	195.65	0.05	121.2
3	165.6	0.05	180	0.04	152.3
4	412.8	0.06	417	0.01	235
5	282	0.03	391.5	0.02	223.4
6	688.6	0.019	818	0.013	462.3
7	557.4	0.007	616	0.0005	444.7

Table 10.3: Failure moment and rotation values(3D SNMMP).

10.5.1 Connection 1: FEP (3D SMMP).

Values for moment and rotation from graph (Figure 10.11) were 279 kNm and 0.053 radians respectively.

10.5.2 Connection 2: FEP (3D SMMP).

Values for moment and rotation extrapolated from graph (Figure 10.12) were 161 kNm and 0.05 radians respectively

10.5.3 Connection 3: FEP (3D SMMP).

Values for moment and rotation from graph (Figure 10.13) were 166 kNm and 0.05 radians respectively.

10.5.4 Connection 4: EEP (3D SMMP).

Values for moment and rotation from graph (Figure 10.14) were 413 kNm and 0.06 radians respectively.

10.5.5 Connection 5: EEP (3D SMMP).

Values for moment and rotation from graph (Figure 10.15) were 282 kNm and 0.03 radians respectively.

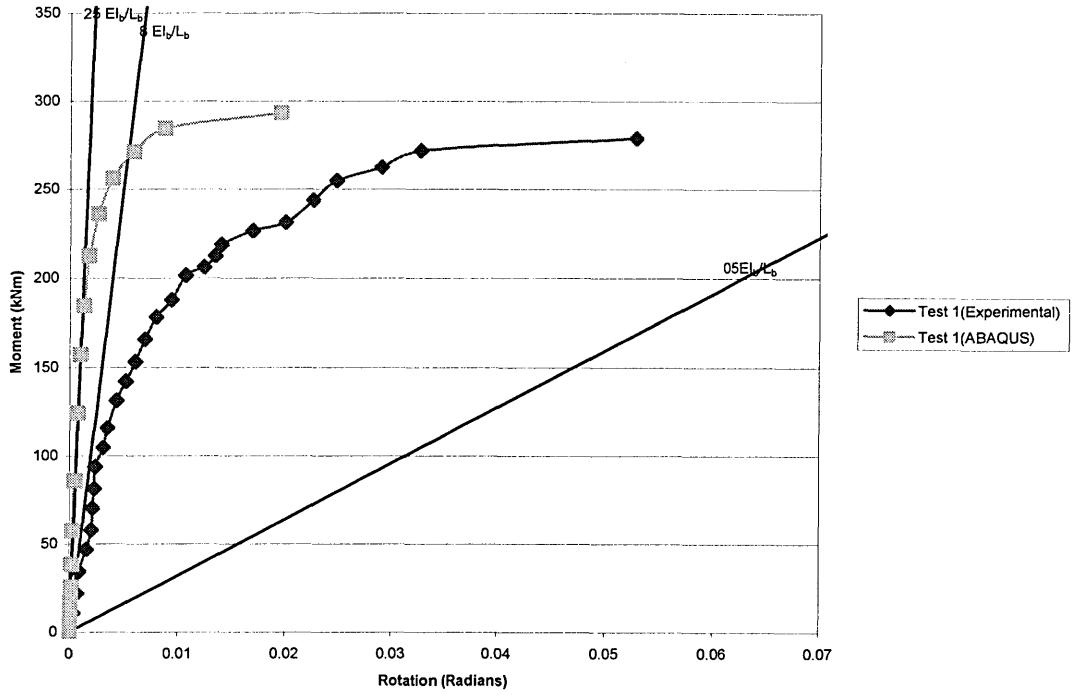

Figure 10.11: Moment Rotation curve for Test 1 (3D SMMP)

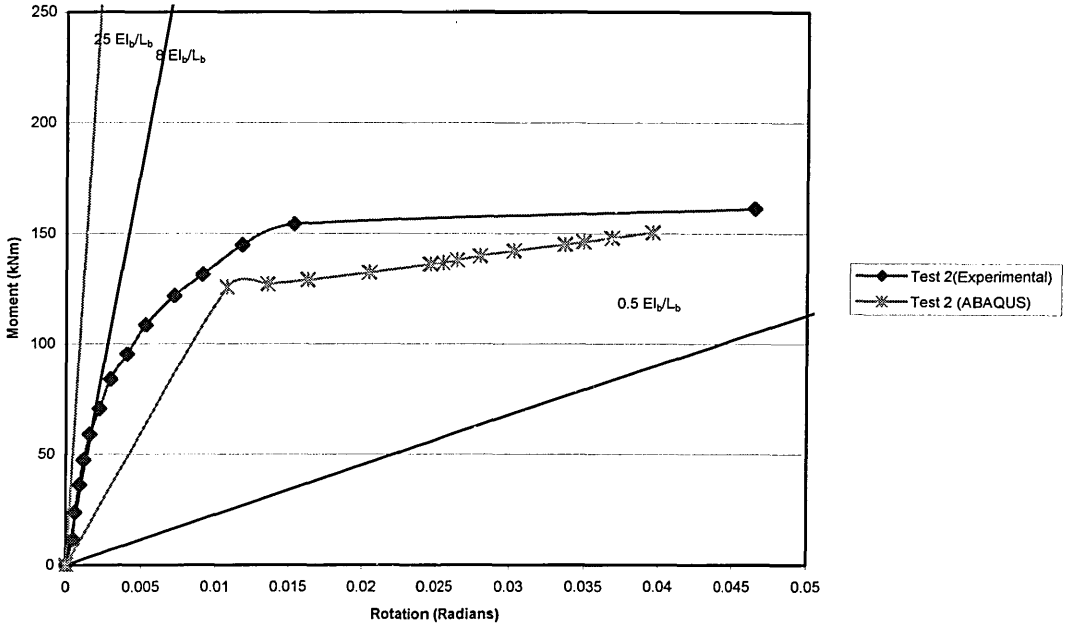

Figure 10.12: Moment Rotation curve for Test 2 (3D SMMP)

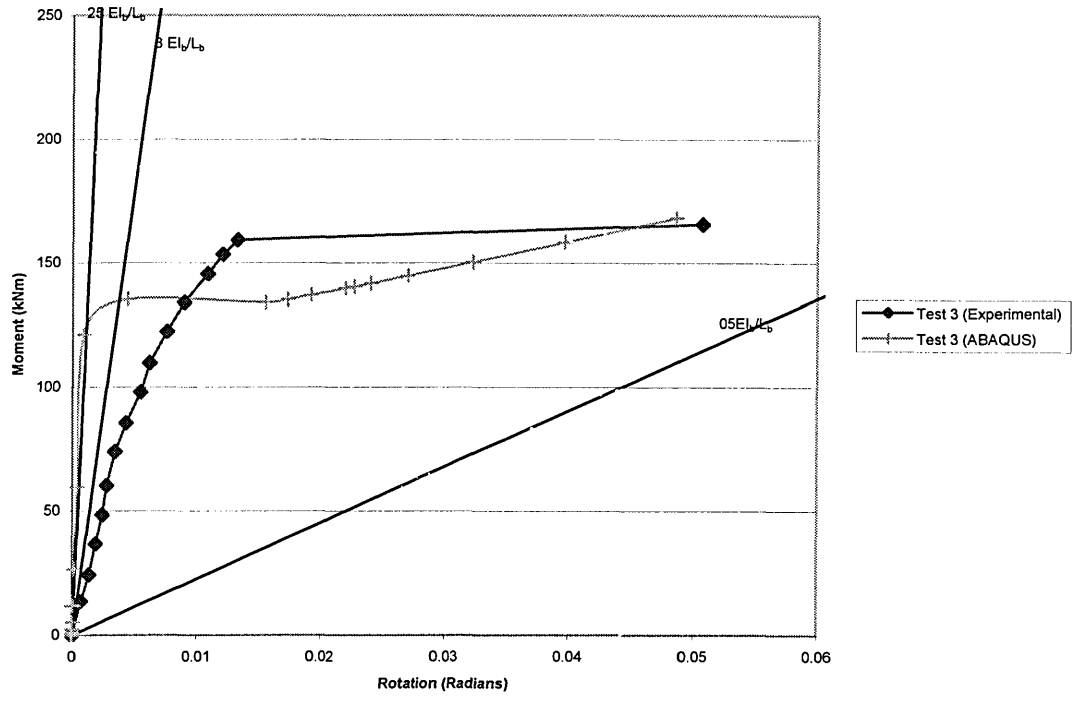

Figure 10.13: Moment Rotation curve for Test 3 (3D SMMP)

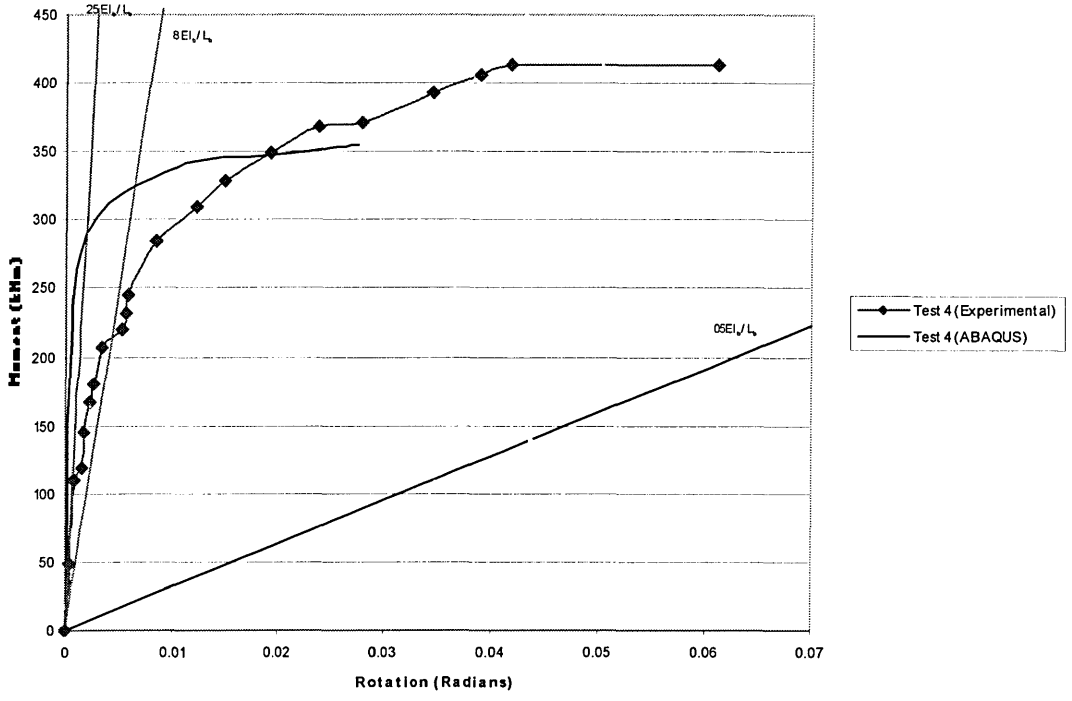

Figure 10.14: Moment Rotation curve for Test 4 (3D SMMP)

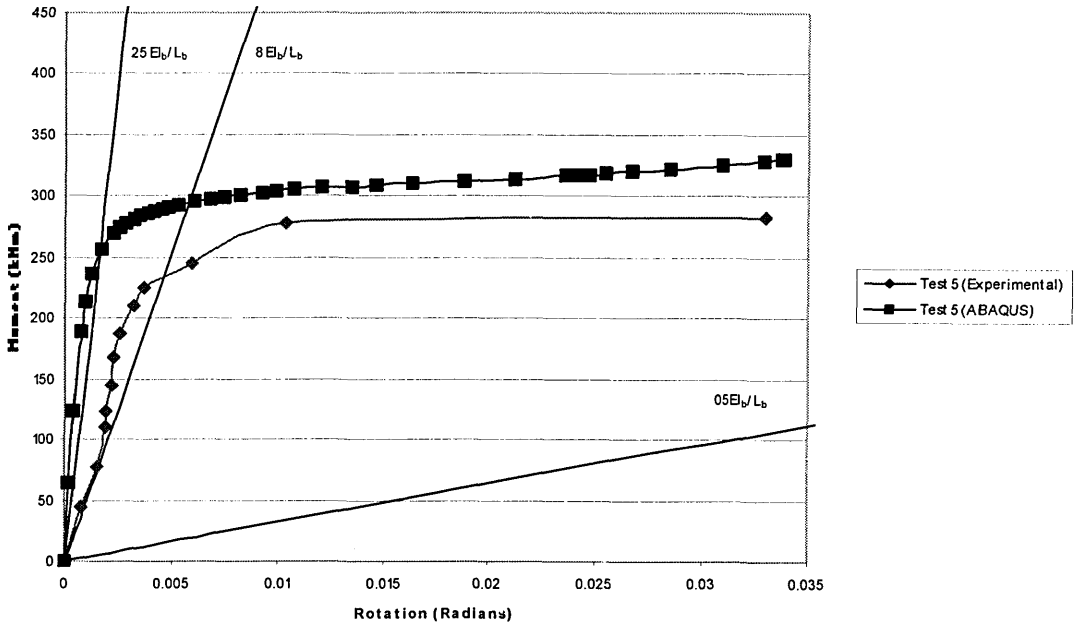

Figure 10.15: Moment Rotation curve for Test 5 (3D SMMP)

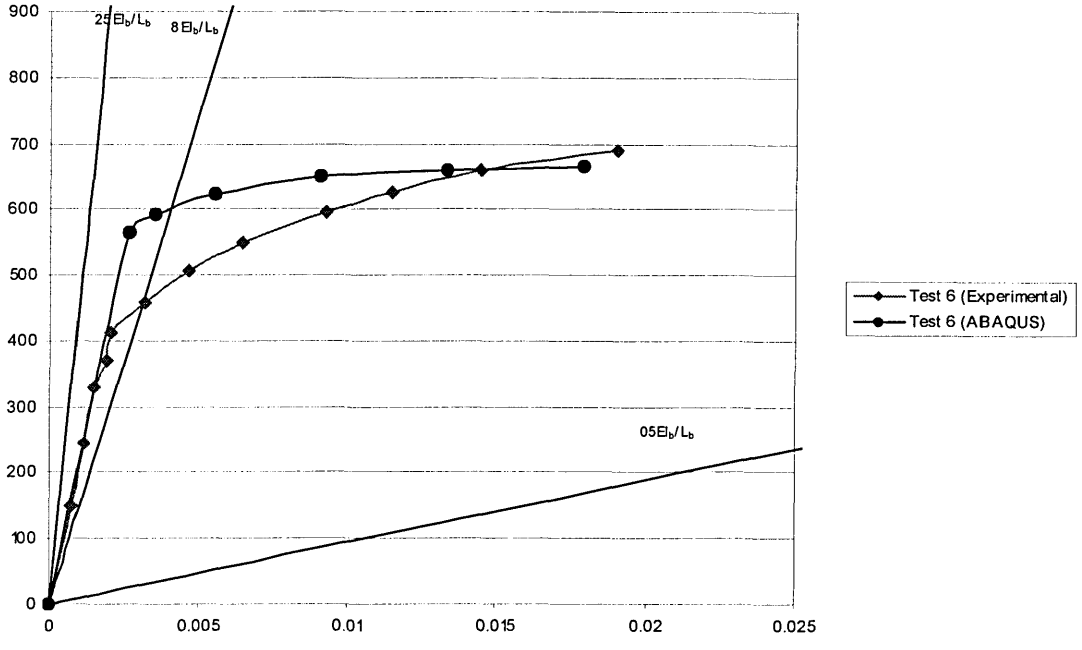

Figure 10.16: Moment Rotation curve for Test 6 (3D SMMP)

10.5.6 Connection 6: EEP (3D SMMP).

Values for moment and rotation from graph (Figure 10.16) were 689 kNm and 0.019 radians respectively.

10.5.7 Connection 7: EEP (3D SMMP).

Values for moment and rotation from graph (Figure 10.17) were 557 kNm and 0.007 radians respectively.

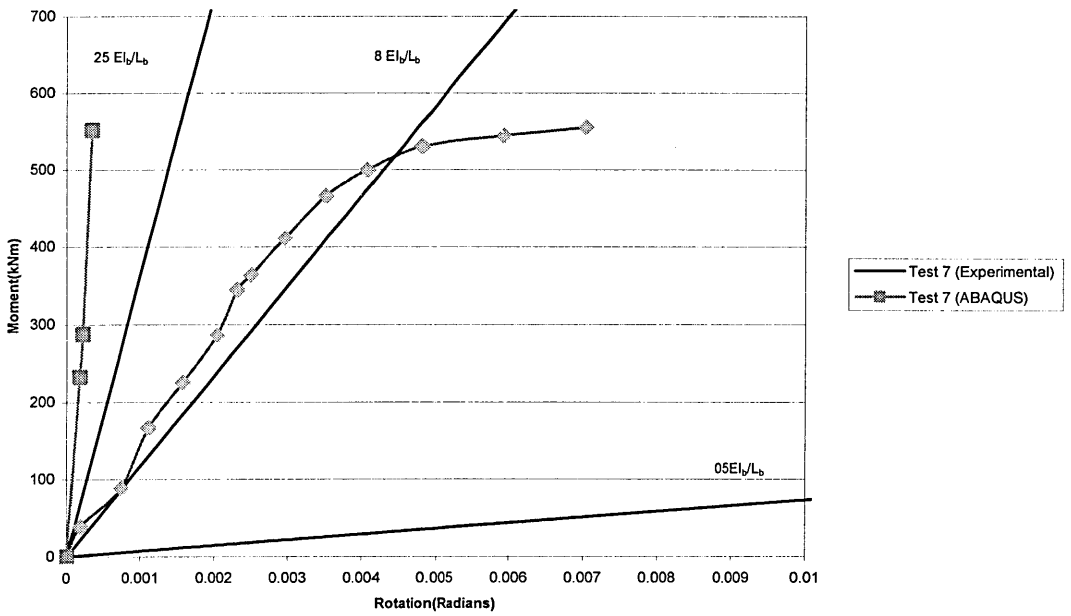

Figure 10.17: Moment Rotation curve for Test 7 (3D SMMP)

10.5.8 Comparison of connection moment capacity at failure (3D SMMP).

Table 10.4 details the Experimental, Eurocode 3-Annex J results and the numerical results, with modifications made to the material properties. The difference between Eurocode 3 and ABAQUS results are reduced. All the modified results show this, some more than the others. This shows that modifying the material properties do not have a uniform reduction on the strength of the connection, as would have been expected.

10.6 Combination Method

Eurocode 3-Annex J is uneconomical in its predictions of moment capacity as mentioned in Chapter 5, while ABAQUS is unsafe in some cases. Therefore, using a combination of both methods could result in a connection capacity that is both safe and economical. Using the initial results from ABAQUS (3D SNMMP), produced the results detailed in table 10.5.

	Experimental		Numerical (3D SMMP)		
Test No	Ultimate Moment KNm	Rotation (Radians)	Ultimate moment kNm	Rotation (Radians)	Eurocode 3 kNm
1	279	0.053	293	0.02	142.5
2	161.4	0.05	179	0.04	121.2
3	165.6	0.05	168.1	0.05	152.3
4	412.8	0.06	355	0.03	235
5	282	0.03	313.1	0.03	223.4
6	688.6	0.019	664.7	0.01	462.3
7	557.4	0.007	494.1	0.0004	444.7

Table 10.4: Failure moment and rotation values (3D SMMP).

The combination column was created by combining Eurocode 3 and ABAQUS (3D SNMMP) results and taking the average. As can be seen, combining the original ABAQUS results and Eurocode 3 results still produces unsafe connections. Connection 5 still produced ultimate moment value higher than that obtained by the physical test.

Therefore it appears that using the combination of the uneconomic Eurocode 3-Annex J results and the 3D SMMP results obtained from ABAQUS, produced results that are closer to those obtained from the physical tests.

This method could be the way forward using the two independent methods, which could also be used to verify each other. If any Eurocode 3-Annex J results produced were above those obtained from ABAQUS then there is a problem and the reverse is true for ABAQUS. Therefore, this is a check on the designs themselves.

Test No	Experimental Failure kNm	Eurocode 3 kNm	Numerical results (3D SNMMP) kNm	Numerical results (3D SMMP) kNm	Combination Average of ABAQUS (3D SNMMP) and Eurocode 3 kNm	Combination Average of ABAQUS (3D SMMP) and Eurocode 3 kNm
1	279	142.5	317	293	229.75	217.75
2	161.4	121.2	195.6 5	179	158.43	150.1
3	168	152.3	180	168.1	166.15	160.2
4	412.8	235	417	355	326	295
5	282	223.4	391.5	313.1	**307.45**	268.25
6	688.6	462.3	818	664.7	640.15	563.5
7	557.4	444.7	616	494.1	498.26	469.4

Unsafe values are in bold.

Table 10.5: Combination method summary

The overestimate of the failure moment (ABAQUS) is difficult to explain; a few connections vary quite widely and there are a few possible explanations which of these are offered below:

1. An overestimation of the material properties Gebbeken and Wanzek paper (Gebheken and Wanzek, 1999).
2. The non-linearity and non uniform properties of the connection means that under identical circumstances different results could be obtained (Chaos Theory).

The results obtained (ABAQUS) are more accurate than that of Eurocode 3-Annex J with some concern expressed about the overestimation of the strength of the connection. The economy is measurably greater with the failure moment being close to that of the physical test. In all cases the moment obtained was closer to the value in the physical test than those by Eurocode 3- Annex J.

10.6.1 3D Combination (3D SCMMP)

The combination method cannot be shown in graphical format but table 10.6 shows how averaging Eurocode 3 and ABAQUS modified results produces results that are both safe (greater than 1) and economic for all 7 connections.

10.7 Discussion of All Results

This section is devoted to the discussion of:

- Ultimate Moment discussion
- Rotation
- Stiffness

In table 10.6 the results obtained from all the methods discussed above are presented. In order to compare the results, ultimate moment ratios have been calculated and presented in a table format to highlight the differences between safety and economy. All methods have been compared with the experimental results obtained from previous analysis.

The table summarises the following information:

- Experimental ultimate moment denoted as (1)

- Experimental Rotation
- Numerical Shell – Non-Modified ultimate moment (2)
- Numerical Shell Rotation
- Numerical 3D – 3D SNMMP moment (3)
- Numerical 3D – 3D SNMMP Rotation
- Numerical 3D – 3D SMMP moment (4)
- Numerical 3D – 3D SMMP Rotation
- Numerical 3D – Combined (3D SCMMP) ultimate moment (5)
- Eurocode 3- Annex J ultimate moment.
- Ratio of Experimental / Shell ultimate moment ratio
- Ratio of Experimental/ 3D Numerical 3D SNMMP ultimate moment ratio
- Ratio of Experimental/ 3D Numerical 3D SMMP ultimate moment ratio
- Ratio of Experimental/ Combined (3D SCMMP) ultimate moment ratio

Values of ratios closer to but greater than 1 are those from the optimum design scenario which allow safe but economic design.

10.7.1 Shell Models

Tests 1-7 ((Figure 10.3) all show similar characteristics, non-linear behaviour was not observed in any of the numerical tests. The stiffness of the connections were all higher than that of the experimental results. Thus the rotation of the connection has been significantly affected, the rotations being significantly lower when compared those from with the experimental results. This observable phenomenon is mainly due to an appreciation of how shell elements are defined and their resulting behaviour. As they are only 2D the user defines the thickness and the various integration points throughout the element. This means that this type of element is not as effective in simulating bending and rotation as with 3D elements.

As can be seen in the table the ultimate moment ratios (1)/(2) are all safe but very uneconomical, ranging from 1.17 to 1.59. This means that in some cases the connection are some 59 % over-designed.

10.7.2 Solid Models

10.7.2.1 3D Solid (3D SNMMP)

For all the tests apart from test 7, the ratio's ((1)/(3)) indicate that all the predictions are unsafe (0.72- 0.99). The ABAQUS simulations suggest the physical results are too low and the connections should have been able to withstand a much larger load.

10.7.2.2 3D Solid (3D SMMP)

As figures 10.11- 10.17 show, the modified material properties have a significant impact on the behaviour of the structure. The stress was reduced by 20 % to implement the suggestions by Gebbeken and Wanzek (Gebheken and Wanzek, 1999). The above graphs show that if the stiffness of the connection is reduced, a higher rotation occurs in all connections. This in turn brings the results in line with those of the Eurocode 3 –Annex J.

The ratio's for these modified models (column (1)/(4)- Table 10.6) are much improved over the non modified models (column(1)/(3) – Table 10.6). A greater number of ratio's for the modified models are now safe (greater than 1) and thus economic (Ratio's are close to 1). Four of the seven connections are however, still unsafe as highlighted in table 10.6. This is still a major issue and worthy of consideration in the future.

10.7.2.3 3D Solid (3D SCMMP)

Combining the safe and economic Eurocode 3- Annex J results with the modified 3D models and taking the average of the two values obtained for each connection, a safe and economic ultimate capacity is obtained. (The ratio's obtained (column (1)/(5)- Table 10.6) are all above 1.)

	Experimental		Numerical (Shell)		Numerical (3D SNMMP)		Numerical (3D SMMP)		Numerical (3D SCMMP)	Eurocode 3	Ultimate moment ratios			
Test No	Ultimate Moment KNm (1)	Rotation (Radians)	Ultimate Moment KNm (2)	Rotation (Radians)	Ultimate Moment KNm (3)	Rotation (Radians)	Ultimate Moment KNm (4)	Rotation (Radians)	Ultimate Moment KNm (5)	Ultimate Moment KNm	(1)/(2)	(1)/(3)	(1)/(4)	(1)/(5)
1	279	0.053	175	0.000544	317	0.02	293	0.02	217.75	142.5	1.59	**0.88**	**0.95**	1.28
2	161.4	0.05	109	0.000434	195.65	0. 05	179	0.04	150.1	121.2	1.48	**0.82**	**0.90**	1.08
3	165.6	0.05	136	0.000526	180	0.04	168.1	0.05	160.2	152.3	1.22	**0.92**	**0.99**	1.03
4	412.8	0.06	272	0.0006	417	0.01	355	0.03	295	235	1.52	**0.99**	1.16	1.40
5	282	0.03	242	0.000718	391.5	0.02	313.1	0.03	268.25	223.4	1.17	**0.72**	**0.90**	1.05
6	688.6	0.019	495	0.000825	818	0.013	664.7	0.01	563.5	462.3	1.39	**0.84**	1.04	1.22
7	557.4	0.007	359	0.000236	616	0.0005	494.1	0.0004	469.4	444.7	1.55	**0.9**	1.13	1.19
										Average	1.42	**0.87**	1.01	1.18

Unsafe designs are in bold

Table 10.6: Summary of all results.

10.8 Rotations

Rotation is the key to plastic analysis. If sufficient rotation is not present then the assumption of using plastic design methods will be incorrect. The connection therefore must pass a predefined limit.

Many researchers have different ideas as to what this value should be but most agree the preferred value to be about 0.03 radians. Using the argument advanced by Bose et al (Bose and Hughes, 1995) of 0.03 radians and that anything less than 0.03 but greater than 0.02, will be the "grey area". This refers to a connection that might achieve sufficient rotation for plastic design assumptions to be valid. For detailed discussion of rotation relating to semi-rigid end plate connections, the reader is referred to Bose et al (Bose and Hughes, 1995).

Those that failed to achieve sufficient rotation are unsuitable for plastic design as insufficient rotation had developed and as such elastic design methods should be adopted. Plastic design produced connections that have a higher rotation capacity than those designed using elastic design methods.

10.8.1 Comparison of Rotations (Shell models)

The element chosen to model the shell elements behaved well in terms of bending but the rotations of the connections were always linear, which meant that rotations cannot be compared satisfactorily. The FE analytical predictions showed that all of the connections failed to achieve the minimum desirable rotation (0.02- 0.03) and therefore cannot be checked using plastic design methods as table 10.7 shows.

10.8.2 Comparison of Rotations (3D Solid models)

This section will assess if the connections are suitable or unsuitable for plastic design purposes based on the value of rotation obtained.

Eurocode 3-Annex J has not been included in this discussion as it does not provide rotation values but only indicates if the connection is suitable or unsuitable for plastic design purposes. Table 10.7 details the Eurocode 3-Annex J results.

Test No	Experimental Failure	Numerical Shell	Numerical (3D SNMMP)	Numerical (3D SMMP)	Eurocode 3
1	YES	NO	GREY	GREY	YES
2	YES	NO	YES	YES	YES
3	YES	NO	YES	YES	NO
4	YES	NO	NO	GREY	NO
5	GREY	NO	GREY	GREY	YES
6	NO	NO	NO	NO	NO
7	NO	NO	NO	NO	NO

Table 10.7: Comments on values with reference to 'grey areas'

10.8.2.1 3D SNMMP and 3D SMMP

The estimates of rotation given by ABAQUS compares reasonably well with those of experimental results apart from connection 4. There are two connections in the numerical model which predict rotation in the range of 0.02-0.03 radians and are thus shown as falling in to the GREY area. Connection 1 according to Eurocode 3 and experimental results is suitable for plastic design while the numerical methods have it in the "grey area", i.e. borderline. Connection 2 is passed by all four methods and is therefore suitable for plastic design. Connection 3 is passed by both experimental and numerical but according to Eurocode 3 is unsuitable for plastic design. The next four connections are all of the EEPs types. Connection 4 according to the numerical non-modified method failed to achieve sufficient rotation for plastic design but the value obtained experimentally prove otherwise. The numerical modified results places this connection's rotation in the grey area which is more representative of the true experimental result. Eurocode 3-Annex J also states that insufficient rotation will occur for plastic design assumptions to be valid. Connection 5 is similar to connection 1, it is passed by experimental and Eurocode 3 but is in the GREY area for both the numerical methods. The last two connections 6 and 7 do not achieve the required rotation for plastic analysis according to all of the methods.

Overall the numerical results (3D SNMMP and 3DSMMP) reflect the trend of physical tests, with the numerical modified values being slightly the better representation of the experimental results. This was not the case with Eurocode 3-Annex J, which failed connections 3 and 4.

10.9 Comparison of Stiffness

Stiffness is important in order to establish how the connection behaves during loading. Very stiff connections may fail suddenly under substantial load while those that have reduced stiffness may result in excessive distortion in the structure.

The initial stiffness of a connection is difficult to obtain due to the movement at the onset of loading. Therefore the experimental moment rotation graphs are not linear and an estimate of initial stiffness is required. This of course tends to imply that different researchers under slightly different conditions, would not achieve identical results.

It appears that due to the high stiffness estimated by the software (gradient of ABAQUS moment rotation curve), the numerical results are higher than the experimental results and thus some are classified as rigid for braced and unbraced frames (See Section 10.1). There is some similarity between the results (Experimental and Numerical) and the best results were obtained when the experimental value were compared with those using Eurocode 3. The values of stiffness obtained using the code and the numerical models were similar. The predictions from the code are similar to those of numerical modelling.

10.9.1 Stiffness of Connections from the graphs (Shell models).

The initial stiffness according to the numerical models (Table 10.8) show that the shell models have a very high stiffness level (all are classified as rigid). This is in keeping with the problems associated with modelling connections using the shell elements. Therefore this comparison is not valid, but has been carried out to highlight the difference between the shell elements and 3D elements.

10.9.2 Stiffness of Connections from the graphs (3D SNMMP)

Based on the moment rotation curves (Table 10.8) the connections are classified as Rigid (R), Semi-Rigid (SR) or Pinned (P). None of the connections tested were pinned and this is borne out with the numerical results, they are either Rigid or Semi-Rigid. The stiffness obtained using both in Eurocode 3 and the Numerical method are much higher than those obtained experimentally.

10.9.3 3D SMMP

Table 10.8 also shows a comparison between numerical models, with non-modified and modified rotational properties. Of particular interest are the stiffest connections 3 and 4 which are designated as rigid for both the braced and unbraced category, as opposed to their being designated semi-rigid by the numerical analysis using non-modified material properties. For other connections the modified material properties had much less of an impact, the connection type being designated similar to that observed by the non-modified material results.

10.10 Statistical Approach to Results

In order to properly assess the significance of the numerical results it is necessary to undertake a statistical analysis. The applicability of many statistical tools is negated by the small sample size available (7). The most applicable statistical tools that were available to the researcher were the sample mean (average) and range. This information was calculated by using the physical test, and analytical models. An example calculation is detailed in Appendix C. A summary of the results obtained are detailed in table 10.9

The percentage difference between the different analytical results (ABAQUS and Eurocode 3- Annex J) and the physical test results are detailed in column 2. Column 2 therefore illustrates the average numerical test as either safe or unsafe. Specifically, if the percentage difference detailed in column 2 is negative then the mathematical method is consistently calculating a ultimate moment that is higher than the experimental results, whilst a high positive number indicates that the ultimate moment from the mathematical models are on average less than the experimental results.

	Stiffness Classification									
	Physical Test		Numerical (Shell)		Numerical (3D SNMMP)		Numerical (3D SMMP)		Eurocode 3	
Test	Braced	Unbraced	Braced	Unbraced	Braced	Unbraced	Braced	Unbraced	Braced	Unbraced
1	SR	SR	R	R	R	R	R	SR	R	SR
2	R	SR	R	R	SR	SR	SR	SR	SR	SR
3	SR	SR	R	R	SR	SR	R	R	R	SR
4	R	SR	R	R	SR	SR	R	R	R	SR
5	R	SR	R	R	R	R	R	R	R	SR
6	R	SR	R	R	R	R	R	SR	R	SR
7	R	SR	R	R	R	R	R	R	R	SR

R-Rigid, SR-Semi Rigid

Table 10.8: Summary of Stiffness Classification Results.

However, the fact that the method's (mathematical) average is positive does not necessary indicate that the design will always be safe. In order to determine if the model is safe it is necessary to ensure that the percentage difference between the analytical results and the physical result always produces a positive value (ie the design indicates the connection will fail at a lower moment that the actual value obtained in the test). Column 3 of Table 10.9 details the ranges obtained for the researchers experiments. The ideal solution (a safe economic design) is a low positive number for the percentage difference in the mean with no negative numbers in the population range.

Test Type	Percentage difference between mean of analytical and mean of experimental results	Range of percentage differences between analytical and experimental results
Original ABAQUS results (Shell) compared with Physical test	28.5	14.2 to 37.4
Original ABAQUS results(3D SNMMP) compared with Physical test	-16.1	-39 to -9
Modified ABAQUS results (3D SMMP compared with Physical test	0.1	-11 to 14
Combination results (3D SCMMP) compared with Physical tests	**14.2**	**3 to 28.5**
Eurocode 3 compared with Physical tests	28.4	8 to 48

Table 10.9: Detailing the range and mean for all numerical results.

The original ABAQUS results when compared with experimental results indicate that ABAQUS consistently over estimates the capacity of the connection. The modified ABAQUS method produces a mean value of 0.1 but there is a negative value in the population range. As detailed above this means that the connection may fail unexpectedly and therefore, it is not an acceptable design methodology. Accepting a system which can over estimate connection capacity is at best unprofessional and at worst gross negligence. It may result in the structural failure of a building and potential loss of life and all the inherent bad publicity it engenders.

The results indicate that Eurocode 3 and Shell models always produces a safe design (population range 8 to 48 and 14.2 to 37.4 respectively) but the mean difference between Eurocode and the physical tests of 28 (28.5 for shell results) percent means that on average the connection will be significantly over designed. Whilst this is satisfactory from a safety point of view it is not ideal as it may have a significant economic impact on construction costs.

Table 10.9 indicates that the most suitable method of designing connections is the combined method (3D SCMMP) as the percentage difference between the physical test and the above method is always positive. However, whilst it can be argued that the connections are over designed, the results are significantly closer to the actual observed physical results than those produced by Eurocode 3.

10.11 Conclusion

10.11.1 Shell Models

2D models are useful tools as they allow designers to generate models to test assumptions and to determine if different modelling techniques work. When modelling complex interactions between different components, such as semi-rigid steel bolted end plate connections, shell models are unable to successfully model the full range of behaviour of the connection. This limitation is evident from this current research. Whilst the models performed reasonably well in obtaining the ultimate moment capacity of the connection they were unable to satisfactorily model the rotational behaviour.

10.11.2 Eigenvalue Analysis

Eigenvalue analysis allows the researcher to model the full non-linear behaviour of a steel bolted end plate connection. However, this means that the researcher has to guess the type of failure that will occur and assign percentage probabilities to each of the modes of failure that could occur. For a realistic solution experimental data has to be collected in order to accurately predict the behaviour of the connection in question. ABAQUS is a useful tool in modelling semi-rigid end plate connections but due to a tendency to under design, experiments must also be carried out to confirm any findings that have been produced. Therefore, the behaviour of any type of new connection must be fully tested in the laboratory in order to establish properties and then verified by simulations. Small modifications to the connection can be tested by numerical analysis and if required, confirmed by experimental analysis.

10.11.3 3D Models (3D SNMMP)

The use of 3D modelling for steel bolted connections is an extremely complex undertaking, the interaction between all the components is difficult to understand and model. This is readily understood because whilst steel in a section is uniform; a steel bolted connection is not.

Three key areas of the connection were modelled and the results were compared to the experimental results. The strengths (moment resistance) predicted by the numerical model were both lower and higher than those obtained by the experiments. The rotations obtained by the finite element models were all lower than the experimental results. Connections 4, 6 and 7 failed to achieve the minimum rotation (0.02 – 0.03) required for plastic design methods to be utilised. Only connection 4's failure rotation did not agree with the experimental results, which obtained a rotation in excess of 0.03. Connections 6 and 7 also failed to achieve the require minimum rotation in the physical tests. The rotation of connection 1 was in the "grey area" for the numerical results but the experimental minimum required rotation obtained was 0.05. Experimental and numerical rotations for connections 2, 3 and 5 are similar, two achieve required minimum rotation (Connections 2 and 3) and connection 5's rotation was in the "grey area" for both methods. These results are a major improvement over the shell model results.

In most cases the finite element models are more economical but are not necessarily safe when compared with Eurocode 3-Annex J results. All Annex J values are lower than the experimental results, sometimes by as much as half the value (Connections 1 and 4).

The comparison with the rotation estimates of Eurocode 3-Annex J and the ABAQUS results show that ABAQUS produces better estimates that Annex J. In particular, two of the connections failed to achieve sufficient rotation capacity (Test 3 and 4) according to Annex J, but attained a value greater than 0.03 according to ABAQUS. This matched the experimental results.

10.11.4 3D Model (3D SMMP)

Utilising the reduced material capacity in the models made a significant difference to the overall results. While finite element results are now a better estimate of the overall connection behaviour, there are still some problem results. This is because predicted failure occurs at a higher moment (Tests 1,2 and 5). However, overall test results are an improvement on the original finite element findings.

This emphasises the need to take account of how the material properties are obtained when developing finite element models. The tensile test is only an estimate and not a true reflection of the connection material behaviour.

The rotation of connection 4 is affected significantly by the modified material properties, as the original finite element model failed to achieve sufficient rotation, but the modified model is now in the grey area (0.02 –0.03)

10.11.5 3D Model (3D SCMMP)

Combining the two different numerical methods to produce a pragmatic approach (Eurocode 3 Annex –J and ABAQUS) might be the way forward for the design of a connection, utilising the uneconomic Eurocode 3 Annex-J and the sometimes unsafe ABAQUS results. The design produced a connection that was both economical and safe for all models investigated in this research.

Additionally the two methods (Numerical and Eurocode 3) can be used to verify each other, as ABAQUS results will always be higher than those of Eurocode 3 Annex-J.

The conclusions drawn from the combined methods show that taking account of the material properties is also vital in developing a better overall connection and a much

better appreciation of it behaviour. This would allow the designer to fully utilise the connection characteristics, both safely and economically.

Therefore, the use of ABAQUS combined with Eurocode 3 to model the behaviour of connections is generally satisfactory without being exceptional. Improvements to the models are required to reduce the wide range of results produced. Potential improvements to the models are:

1. Modelling the bolts in a more satisfactory manner, instead of just linear bar elements.
2. Using a more refined mesh to model the connection
3. More use of the C3D20 elements. However this would make the models much more time consuming to produce and consequently evaluate.

The worrying aspect is that the column web in compression has been included in the code as a possible failure, while column web buckling has been discounted. The difference between column web crushing (compression) and buckling is very small but this is still a serious oversight by the producers of Eurocode 3-Annex J as the physical tests exemplify. However, the review of Eurocode 3 showed that the designs are always uneconomic but never unsafe. This shows the need to modify Eurocode 3 in order to rectify the above problems.

11.3 Numerical models using the ABAQUS software package

The numerical modelling undertaken utilised the ABAQUS software package. ABAQUS is not the easiest program to use but with experience and time, results can be produced that reflect the physical connection being modelled.

The ABAQUS package allows the user to produce either shell models or 3D models.

7 full-scale models were developed in both these formats with variable results.

The shell models produced the most uneconomic designs but were never unsafe. Initial 3D models were all unsafe. However, subsequent methods developed using modified material properties were better with 3 out of the 7 models safe. However, there was still 4 models that predicted failure to occur with a greater load that the physical testing indicated and therefore these models were still unsafe. This research illustrated the need to modify the results obtained from this software package to ensure that designers are given more accurate information to ensure that building are safe.

11.4 Design Method

A new design philosophy was developed by combining the uneconomic Eurocode 3-Annex J results and the modified material results obtained from ABAQUS. The results produced from this combination were safe and more economic than Eurocode 3 for all connections investigated in this research.

This is proposed as a way forward. In addition to providing more accurate results the two independent design methods could also be used to verify each other. If any Eurocode 3-Annex J results produced were above those obtained from ABAQUS then there may be a problem and results should be checked and the reverse is true for ABAQUS.

11.5 Future Work

With a greater understanding of how to model and the importance of taking all measurements during physical testing and taking into account the above conclusions the author has a number of recommendations for future work.

1. Investigation of the effect of material properties over a long iteration testing, the difference between this and tensile tests and what effect this has on the overall results for the finite element model.
2. Modelling the whole connection with the correct loading, and not using assumptions relating to modified beam lengths and high Young's modulus of elasticity.
3. Modelling the bolt interaction better, using full three dimensional elements instead of single beam elements for each bolt. The bolt head could also be modelled as this was found to be of considerable importance in the T-stub. The bolt head affected the

bending properties of the T-stub and this might also affect the properties of the flush and extended endplate connections.

4. Obtain more information about the connection using more gauges in order that the comparison between numerical and experimental results can be improved.
5. Investigate the effect of non-uniform non-symmetrical loading.
6. A larger range of connections in order to verify the proposed design philosophy.
7. Investigating the effect of imperfects to the perfect geometry models, this would include detailed study of locations of imperfections and how large these imperfections are.

11.6 Improvements

11.6.1 Eurocode 3

1. Inclusion of column web buckling into the code.
2. Re-working of some of the equations in order to improve the values produced to create designs that are still safe but more economic.

11.6.2 ABAQUS

1. Re-working of the methods used in ABAQUS to obtain results that are safe.
2. Improvements to the layout of the manual with examples of the common techniques used for a whole design
3. Activity diagrams with the steps involved, this would add users in "getting up to speed" with the complex software.
4. Investigate the impact of initial imperfections in a full scale connection

References

Agerskov, H. (1976) High Strength Bolted Connections Subject to Prying. *Journal of the Structural Division* 161-167.

Agerskov, H. (1977) Analysis of Bolted Connections subject to Prying. *Journal of the Structural Division* 103, 2145-2163.

American Institute of Steel Construction (1969). *Specification for the design, fabrication and erection of structural steel for buildings, February 1969*

Bahaari, M.R. and Sherbourne, A.N. (1996) 3D Simulation of Bolted Connections to Unstiffened Columns- II. Extended End plate Connections. *Construction Steel Research* 40, 3. 189-223.

Bahrami, M. (1991) Behaviour of beam-to-column end late connections in structural steelwork. *University of Abertay-Dundee.*

Bailey, J.R. (1970) Strength and rigidity of bolted beam to column connections. *Conference on Joints in Structures, University of Sheffield* 4, A41-A429.

Bose, B. (1993) Tests to Verify the Performance of Standard Ductile Connections. *Heavy Structures Research Group, University of Abertay Dundee*

Bose, B. (1994) Additional Tests of Standardized Ductile Connections. *Heavy Structures Research Group, University of Abertay Dundee*

Bose, B. and Hughes, A.F. (1995) Verifying the performance of standard ductile connections for semi-continuous steel frames. *Proceedings of the Institute of Civil Engineers for publication in Structures and Buildings* 441-457.

Bose, B., Sarkar, S. and Bahrami, M. (1991) Finite Element analysis of unstiffened Extended End Plate Connections. *Structural Engineering Review* 3, 211-224.

Bose, B., Wang, Z.M. and Sarkar, S. (1997) Finite Element Analysis of Unstiffened Flush End-Plate Bolted Joints. *Journal of Structural Engineering*

Bose, B., Youngson, G.K. and Sarkar, S. (1997) Application of ABAQUS software for the finite element analysis of bolted T-stub connections in steel structures. *ABAQUS Users' Conference, Stresa, Lake Maggiore, Italy, May*

Bose, B., Youngson, G.K. and Sarkar, S. (1998) Application of Finite Element Technique to the Buckling Analysis of Unistiffened Column Web Bolted End Plate Connections. *Abaqus Users' Conference, Newport, Rhode Island, May*

Bose, B., Youngson, G.K. and Wang, Z.M. (1995) An appraisal of the design rules in Eurocode 3 for bolted end plate connections by comparison with experimental results. *Proceedings of the Institute of Civil Engineers for publication in Structures and Buildings*

Bose, S.K., McNeice, G.M. and Sherbourne, A.N. (1972) Column web in steel beam to column connections- Part 1. *Computers and Structures* 253-279.

Bose, S.K., McNeice, G.M. and Sherbourne, A.N. (1972) Column Webs in steel beam-to- column connections Part II- Design recommendations. *Computers and Structures* 2, 281-301.

British Standard Institution (1967) BS 3692: 1967. Specification for ISO Metric Precision Hexagon bolts, screws and nuts. *British Standards Institute*

British Standard Institution (1967) BS 3692: 1967. Specification for ISO Metric Precision Hexagon bolts, screws and nuts. *British Standards Institute*

British Standard Institution (1985) BS 5959: Part 1, Structural use of Steelwork in Buildings, Part 1, Code of Practice for design in simple and continuous construction: hot rolled sections. *British Standards Institute*

British Standard Institution (1992) BS EN 24032:. Hexagon nuts style 1. Product Grade A and B. *British Standards Institute*

British Standard Institution (1992) BS EN 24034:1992. Hexagon nuts. Product Grade C. *British Standards Institute*

British Standard Institution (1995) Eurocode 3: Design of steel Buildings. Part 1.1 General rules and rules for buildings. *European Committee for Standardisation*

British Standard Institution (1998) BS EN 10 002-1:1990. Tensile Testing of metallic materials, Part 1. Method of testing at ambient temperature. *British Standards Institute*

Bursi, O.S. and Jaspart, J.P. (1997) Benchmark for Finite Element Modelling of Bolted Steel Connections. *Construction Steel Research* 43, 17-42.

Bursi, O.S. and Jaspart, J.P. (1997) Calibration of a Finite Element Model for Bolted End plate Steel Connections. *Construction Steel Research* 44, 225-262.

Chen, W.F. and Newlin, D.E. (1973) Column Web strength in Beam-To-Column Connections. *Journal of Structural Engineering* 99, 1978-1984.

Chen, W.F. and Oppenhiem, I.J. (1970) Web Buckling strength of beam-to-column connections. *Report No 333. 10, Fritz Engineering Laboratory, Lehigh University*

Choi, C.K. and Chung, G.T. (1996) Refined three-dimensional finite element model for end plate connections. *Journal of Structural Engineering* 122, November. 1307-1316.

Douty, R.T. and McGuire, W. (1965) High Strength Bolted Moment Connections. *Journal of the Structural Division* 91, 101-129.

El-Ghazaly, H.A. and Sherbourne, A.N. (1987) Ultimate strength of stiffened symmetrical welded steel beam-to-column flange connections. *Computers and Structures* 749-760.

Gebheken, N. and Wanzek, T. (1999) Numerical Aspects For the Simulation of End Plate Connections. *ABAQUS Users' Conference, Stresa, Lake Maggiore, Italy, May*

Graham, J.D., Sherbourne, A.N. and Khabbaz, R.N. (1959) Welded Interior Beam-to-column Connections. *American Institute of Steel Construction Research at Lehigh University*

Hendrick, A. and Murray, T.M. (1984) Column web compression strength at end plate connections. *Engineering Journal/ American Institute of Steel Construction* 161-169.

Hibbitt, K.a., Inc (1997) Buckling and Collapse Course, *Hibbitt, Karsson and Sorensen Inc.*

Hibbitt, K.a., Inc (1999) ABAQUS User manuals. *Hibbitt, Karsson and Sorensen Inc.*

Jaspart, J.P. and Maquoi, R. (1994) Prediction of the semi-rigid and partial strength properties of structural joints. *COST C1 Working Group Meeting on "Steel Composite" held in Coinmbra (Protugal)*

Jaspart, J.P. and Bursi, O.S. (1995) Semi-rigid Behaviour, A refined finite element model for t-stub steel connections. *European Group on Numerical Simulations, Cost C1 Working Group Meeting on "Numerical Simulation", Trento, June 15*

Kalyanaraman, V., Pekiz, T. and Winter, G. (1976) Overall Buckling stability after local Buckling. *Journal of Structural Engineering* 757-771.

Kishi, N., Chen, W.F., Goto, Y. and Matsuoka, K.G. (1993) Design aid of semi-rigid connections for frame analysis. *Engineering Journal* 30, 90-107.

Kong, F.K. and Evans, R.H. (1990) Reinforced and Prestressed Concrete-Incorporating BS 8110 and microcomputer applications (3rd Edition), Chapman and Hall, 260

Krishnamurthy, N. (1976) Steel Bolted End Plate Connections. *Proceedings of the international Conference on Finite Element Methods in Engineering, Adelaide, Australia* 23.1-23.16.

Krishnamurthy, N. and Graddy, D.E. (1976) Correlation Between 2 and 3 Dimensional Finite Element Analysis of Steel Bolted Connections. *Computers and Structures* 6, 381-389.

Krishnamurthy, N., Huang, H., Jeffrey, P.K. and Avery, L.K. (1979) Analytical M-0 Curves for End Plate Connections. *Journal of the Structural Division* 105, 133-145.

Mann, A.P. (1968) Plastically Designed End-Plate Connections. *University of Leeds.*

Mann, A.P. and Morris, L.J. (1979) Limit Design of Extended End Plate Connections. *Journal of the Structural Division* 511-526.

Marshall, G. (1993) Connections types Survey of Structural Steelwork in Scotland, *University of Abertay-Dundee.*

Maxwell, S.M., Jenkins, W.M. and Howlett, J.H. (1981) Theoretical Approach to the analysis of connection behaviour, Joints in Structural Steelwork. *Proceedings of the international Conference Held at Teeside Polytechnic, Cleveland, U. K*

Mistakidis, E.S., Baniotopalos, C.C., Bisbos, C.D. and Panagiotopoulus, P.D. (1996) Numerical simulation of a T-stub connection. *European Group on Numerical Simulations, Cost C1 Working Group Meeting on "Numerical Simulation", Trento, June 15*

Morris, L.J. and Packer, J.A. (1977) A limit sate design method for the tension region of bolted beam-to-column connections. *Journal of Structural Engineering* 55, 446-458.

Nash, A.W. (1998) Theory and Problems of Strength of Materials, SI edition edn. McGraw Hill.

Patel, K.V. and Chen, W.F. (1984) Non-Linear Analysis of Steel Moment Connections. *Journal of Structural Engineering* 110, 1861-1875.

Ragupathy, P. and Virdi, K.S. (1995) Semi-rigid Behaviour, Numerical Simulation of a T-stub Connection using ANSYS. *European Group on Numerical Simulations, Cost C1 Working Group Meeting on "Numerical Simulation", Trento, June 15* 1-5.

Rao,S.S, (1988) *The Finite Element Method in Engineering*, Second edn, Pergamon Press

Roberts, N., Andersen, D., Deal, R., Garet, M.S. and Shaffer, W.A. (1983) *Introduction to Computer Simulations: The System Dynamics Approach*, London: Addison-Wesley.

Rockey, K.C., Evans, H.R., Griffiths, D.W. and Nethercot, D.A. (1998) The Finite Element Method, London: Granada.

Schutz, F.W. (1959) Strength of Moment Connections using High Strength Bolts. *American Institute of Steel Construction, National Engineering Conference Proceedings*

Sherbourne, A.N. (1961) Bolted Beam to Column Connections. *Structural Engineer* 203-210.

Sherbourne, A.N. and Bahaari, M.R. (1994) 3D simulation of End-plate Bolted Connections. *Journal of Structural Engineering* 3122-3136.

Sherbourne, A.N. and Bahaari, M.R. (1994) Computer modelling of an extended end-plate bolted connection. *Computers and Structures* 879-893.

Sherbourne, A.N. and Bahaari, M.R. (1996) 3D Simulation of Bolted Connections to Unistiffened Column-I: T-stub connections. *Construction Steel Research* 169-187.

Sherbourne, A.N. and El-Ghazaly, H.A. (1986) Plastic Buckling of Column Web in Symmetircal Stiffened Moment Connections. *Proceedings of the Pacific Structural Steel Conference* 55-71.

Sherbourne, A.N. and Murthy, D.N.S. (1978) Computer Simulation of Column Webs in Structural Steel Connections. *Computers and Structures* 8, 479-498.

Shi, Y.J. and Wong, Y.L. (1996) Modelling for Moment-Rotation Characteristics for Endplate connections. *Journal of Structural Engineering* 122, November. 1300-1306.

Stockwell, F.W. (1974) Yield line analysis of column webs with welded beam connections. *Engineering Journal* 11, 12

Surtees, J.O. and Mann, A.P. (1970) End Plate Connections in Plastically Designed Sructures. *Proceedings of The Conference of Joints in Structures* Vol 1, Paper 5

Tarpy, T.S. and Cardinal, J.W. (1981) Behaviour of Semi-Rigid Beam to Column End plate Connections. *Proceedings of the International Conference Held at Teesside Polytechnic, Cleveland, U. K* 2.3-2.25.

Toma, A., Sedlack, G. and Weynand, K. (1993) Connections in Cold Formed Steel. *Tin Walled Structures* 16, 219-237.

Tong, C.S. (1985) The Elastic-Plastic Behaviour of Semi-Rigid Connections in Steel Structures. *Hatfield Polytechnic.*

Wang, Z.M. (1996) Behaviour of Unstiffened Flush End Plate Beam to Column Connection in Structural Steelwork. *University of Abertay-Dundee.*

Yee, Y., L. and Melchers, R.E. (1984) Moment-Rotation Curves for Bolted Connections. *Journal of Structural Engineering* 615-635.

Zienkiewicz, O.C. (1998) The Finite Element Method, Third edn. McGraw Hill Book Company (UK) Limited.

Zoetermeijer, P. (1974) A Design Method for the Tension Side of Statically Loaded, Bolted Beam-To- Column Connections. *Heron 20,No 1,Delft,University of Delft,The Netherlands*

Zoetermeijer, P. (1981) Semi-rigid Bolted Beam to Column connections with stiffened Column flanges and Flush end plates. *International Conference on Joints in Structural Steelwork, Teesside Polytechnic* 2.99-2.118.

APPENDIX A

Proceedings of the Institute of Civil Engineers, 1995, Structures and Buildings (116) P221- 234.

The published article cited below has been removed from the e-thesis due to copyright restrictions:

Bose, B., Youngson, G.K. and Wang, Z.M. (1996). An appraisal of the design rules in Eurocode 3 for bolted end-plate joints by comparison with experimental results. In *Proceedings of the Institution of Civil Engineers - Structures and Buildings*, 116(2), 221-234.

Post Graduate Workshop, University of Abertay Dundee, 1996.

Validation of ABAQUS Software for Finite Element Modelling of Bolted Steel Connections.

G. K. YOUNGSON

School of Construction and Environment
University of Abertay Dundee

ABSTRACT
This paper relates to a study conducted at the University of Abertay-Dundee, to comprehend the complex behaviour of steel bolted connections, utilising finite element modelling techniques. Finite element modelling of complex structures requires expertise which can only be gained by experience. This paper discusses what is required for the successful completion of such an analysis. The finite element package discussed in this paper is the commercially available package ABAQUS.

1.0 INTRODUCTION

When using a software package for the first time, one must begin initially with a smaller, more basic model. Once understanding is gained, then modelling of more complex structures can be undertaken. This is how the author proceeded. When carrying out this type of modelling, experimental data must be available, in order that the validity of the model constructed, using finite element modelling, can be assessed.

2.0 FINITE ELEMENT MODELLING

2.1 ABAQUS Finite Element Software

ABAQUS is a finite element package sold by Hibbitt, Karlsson and Sorensen Ltd (HKS). This software is used world wide by many leading research institutions and multi-national companies e.g. Lockheed, Boeing and International Business Machines (IBM). ABAQUS can handle many complex problems, including material and geometric non-linearity, which are needed in understanding the behaviour of steel structures.

2.2 Element Selection

In order to discretize the structure and ascertain the best element for the finite element model, an understanding of the behaviour of the structure is essential. ABAQUS is an all embracing program, with many different element types suitable for a myriad of applications. Therefore, investigations must be carried out to select the element types most suited for the successful completion of the research.
Other individuals{#150, #132} had carried out similar tasks and their findings are discussed below, in association with the conclusions drawn by the author.
Two types of 3-dimensional continuum elements (figures 1 and 2) were selected for the investigation of the 3-dimensional structure. These are as follows:-

(i) C3D8:- 8 noded element.
(ii) C3D20:- 20 noded element.

There are other important considerations when choosing a particular type of element, than the type of structure being modelled. These are:-

(i) The % error induced.
(ii) Time to generate the model.
(iii) Computer analysis time and power of the computer.

A comparison between the results derived from these elements was made which indicated that there was very little difference between the two types of elements.
The last two considerations are interlinked, these will therefore be discussed together.
The C3D20 elements with 20 nodes per element will take a greater time to generate, due to an increased number of nodes requiring definition and the additional information in specifying their shape. C3D8 elements with 8 nodes, will require considerably less information. Fewer nodes results in a faster generation time and reduced convergence time.
C3D8 element was therefore chosen as the most suited to the task in hand. Within the C3D8 elements, more specialised elements exist. The list below shows the various sub-group of elements which were investigated.

(i) C3D8.
(ii) C3D8I.
(iii) C3D8R

The elements above were tested against a standard bending test.{#150, #132} in order to determine the validity of the elements. Throughout the calibration procedure, C3D8I was the most satisfactory performer. Hence this element was chosen for use in the bending related structural problem.

2.3 Mesh Generation

Generating the correct type of mesh is vital{#153} and an understanding of the behaviour of the structure being modelled is extremely important. Development of the mesh was carried out on a node by node basis, this enabled the author to modify the mesh as required. The type of mesh depends on the information required for the study. As the author required a wide range of results, stress, displacement etc, a fine mesh was necessary (Fig 4). With a fine mesh, a more detailed picture of the behaviour of the structure under loading can be obtained. The percentage error will also be smaller utilising a finer mesh but due to a greater number of elements needed, time considerations become important. Where most of the bending occurs, due to the loading applied, a finer mesh may be required.

2.4 T-stub Modelling

Why chose to model a steel bolted T-stub ? The "Numerical Simulations Group", one of many working groups under the European Research Project COST C1 intended to produce a standard method of analysing beam to column connections in steel structures. Thus results from different studies using several well known finite element software could be compared. With a standard method in existence the initial problem of knowing where and how to start the investigation is greatly facilitated.
The T-stub includes everything that a more complex bolted connection would encompass, without needing to spend considerable time generating the model. Thus many research institutions in various Europeans Countries could be involved in the study due to relative ease of its construction and testing.

The important details to note for a T-stub model are:-

(i) Bolts.
(ii) Boundary Conditions.
(iii) Contact limitations.
(iv) Non-linear Behaviour (Both material and geometrical)

Model Size
The input file, with the suffix "inp" will be large using this type of mesh generation procedure. The large temporary file space is due to the non-linear material properties and non-linear geometry being used for the analysis.
Analysis time was in the region of 3 weeks running on a DEC Alpha with one 166 MHz processor, 32 Mb ram and 6Gb drive space.

2.4.1 Bolts
Bolts (Fig 7) add stiffness to the overall T-stub and are very complex to model successfully within the computer environment. As the bolt shank is circular, another type of element is necessary (C3D8 is cubic in nature (Fig 2)) The element recommended by the ABAQUS manual for use in conjunction with C3D8 elements was C3D6 (Fig 3). Thus this element was selected for the investigation.
The bolts themselves were slightly modified, with the bolt head attached to the T-stub, to stop convergence errors. Two independent structures within one model can cause the model to fail and the "no rooted structure" error will occur in the output files. The shank was left separate from the bolt to allow some movement. This appeared to work successfully as the results show (See later section entitled results).

2.4.2 Boundary Conditions
Boundary conditions are used to simulate missing parts of a connection. With the connection symmetrical about two axes only a quarter of the connection needs to be modelled. Boundary conditions stop the connection being able to move in a particular direction, i.e. all movement can be stopped in either X, Y, Z or combinations of axis depending on input. Fig 5 shows the boundary conditions applied to the T-stub (the dark triangular sections on the web of the T-stub)
An understanding of how boundary conditions operate is necessary.
There are many advantages in using the reduced model which are listed below:

(i) less time is needed to develop the model, i.e. fewer nodes and elements are required to produce the mesh,
(ii) less computer time to analyse,
(iii) less computing power required.

The main concern is that appropriate boundary conditions must be applied and any discrepancy might render the results worthless.

Bolt boundary conditions
bolts were held at the base of the shank, the "ENCASTRE" option was used to stop any movement and rotation in any direction. Only the nodes at the end of the shank were limited using boundary conditions

T-stub boundary conditions

The web of the T-stub(Fig 5) was limited in its movement. The web was not allowed to move in the 3rd direction (i.e. the z-direction).

2.4.3 Gap elements

Where boundary conditions are insufficient in describing the behaviour of the structure. gap elements can be utilised. Boundary condition stop movement in any direction, while gap elements allow movement in one part of the axis i.e. able to move in a positive x-direction but not a negative x-direction or vice-versa.

The gap elements were initial set at zero, i.e. the T-stub was only allowed to move in a direction in which the gap opened. The three factors that can be used to control the gap were elements were set to zero.

2.4.4 Loading

Loads are applied at the end of the web of the T-stub and the whole connection attempts to move in the direction being pulled. The load itself was applied to each node on the face of the elements and thus the combined load from all the nodes, produced the total load applied. Loads are not applied all at once, due to convergence problems arising. Control parameters are used to increment the loading in a step by step fashion. This produces still more data and can create extra problems, which can be overcome by limiting the output to specific elements.

The T-stub model is made from approximately 2000 elements which include gap elements.

2.4.5 Modelling T-stub Behaviour

The behaviour of the T-stub falls into two categories:-

(i) Linear.
(ii) Non-linear.

2.4.5.1 Linear Behaviour

Linear behaviour occurs when the load and the displacement are uniform i.e. as the load increases the displacement increases proportionately. Linear behaviour will occur initially in the T-stub as the load increases.

Linear properties were defined using elastic definition with Young's modulus and Possions ratio.

2.4.5.2 Non-Linear Behaviour

Due to the property of steel, linear behaviour will not continue ad infinitum. When the yield point is reached non-linear behaviour will occur. As the material is non-linear in nature, properties entered must reflect this. A standard stress strain curve (Fig 6) is required to input the relevant values required by ABAQUS. The material properties diagram is split into the relevant sections i.e. where the curve changes gradient. A piecewise linear approximation is used to describe the material behaviour of the T-stub. Plastic strain was used for defining the material being used and was obtained from the stress/strain curves produced when a specimen was tested.

3.0 RESULTS

Physical tests were conducted at the University of Liege{#152} to establish the performance of the T-stub. Researchers also constructed finite element models{#153, #154, #156} which could be compared with the author's finite element model.

The attached graph (Fig 8) shows the results obtained from the testing and results from the authors finite element analysis. Reasonable results were obtained from modelling the T-stub, but the finite element model results are slightly lower than those obtained from physical testing. The T-stub appears to have a higher stiffness and thus a higher strength at the conclusion of the test. The load at which the specimen failed, agreed fairly accurately with the finite element model's predictions.
It is usually better to slightly underestimate the strength of the connection than overestimate it, resulting in this instance in a built in factor of safety.
The initial linear section of the curve compares well with the test results. Before the onset of yielding, the finite element model is able to sustain a higher load for the equivalent displacement. Where considerable yield occurs both in the test and the finite element model, the point of occurrence can be seen clearly on the graphs (fig 8) Yielding of the material i.e. when the material changes from elastic behaviour to plastic behaviour.

4.0 CONCLUSION

The task involved in the modelling of any beam to column steel connection, using finite element analysis, is daunting. Understanding how the ABAQUS program operates and the relative merits of different types of elements available is vital. Mesh generation depends on several factors including the power of the hardware (computer) being used. Using too fine a mesh will considerably increase the time taken for the completion of the model but inaccurate results can transpire if the mesh is not well defined. The correct material properties must be obtained otherwise the results will be meaningless. With time, effort and experience, finite element modelling can produce an accurate representation of a physical structure, with the added advantage that individual components can be investigated without resorting to more expensive and time consuming testing.

FUTURE

The author at present is trying to model a full scale steel bolted endplate connection using ABAQUS. The researcher is interested in the buckling of the column web, therefore contact analysis is being used to model specific behaviour between the end plate and the column flange.

Acknowledgements

The courtesy extended by the undernamed, and others named in the text, is gratefully acknowledged.

The Institute of Civil Engineers (ICE); The Department of Environment (DoE); The Steel Construction Institute (SCI); Dr B. Bose; Professor S. Sarkar; Dr R. Preston; Mr A. Hughes; Dr J. Jaspart (University of Liege); Dr O. Bursi (University of Trento); Professor R. Ashley; Dr Z.M. Wang; Mr A. M. Youngson; Dr N. Souter; Mr K. Thomson; Mr J. Galloway; Mr T. Wallace; Mr D. Husband; Mr J. Edwards; the technical staff of the School of Construction and Environment; the staff of the Information Services at the University of Abertay Dundee especially Mr P. Chapman; Mr F. Greig; Mrs J. Docherty.

ABAQUS Users Conference, Stresa Lake Maggiore, Italy May 1997.

The published papers cited below have been removed from the e-thesis due to copyright restrictions:

Bose, B., Youngson, G.K. and Sarkar, S. (1997). Application of ABAQUS software for the finite element analysis of bolted t-stub connections in steel structures. In *ABAQUS Users' Conference Proceedings*, June 4 - 6, 1997, Milan, Italy, 145-160.

Bose, B, Youngson, G.K. and Sarkar, S. (1998). Application of finete element technique to the buckling analysis of unstiffened column web in bolted end plate connections. In *ABAQUS Users' Conference Proceedings* : May 27 - 29, 1998, Newport, Rhode Island, 139-152.

Proceeding of Advances In Civil and Structural Engineering Computing For Practice, 1998. Edited by B.H.V Topping. Pages 125-134. Civil-Comp Press

The published paper cited below has been removed from the e-thesis due to copyright restrictions:

Bose, B., Youngson, G.K. and Sarkar, S. (1998). Finite element method for end-plate joints in steel frames: overview of applications at the University of Abertay Dundee. In Topping, B.H.V. (ed.), ***Proceeding of Advances In Civil and Structural Engineering Computing For Practice*****, 125-134.**

APPENDIX B

Example of Flush End Plate

Column **254 x 254 UC 89**	**Beam** **457 x191 UB 74**	**End Plate** **640 x 200 x 20**	**Bolts** **4M24-8.8**
$h_c = 260.4$	$h_b = 457.2$	$b_p = 200$	$d_n = 24$ mm
$b_c = 255.9$	$b_b = 190.5$	$t_p = 20$	$As = 353$ mm^2
$t_{fc} = 17.3$	$t_{fb} = 14.5$	$f_{yp} = 275$ N/mm^2	$f_{ub} = 800$ N/mm^2
$t_{wc} = 10.5$	$t_{wb} = 9.1$		
$t_c = 12.7$	$t_b = 10.2$		
$A_c = 114$ cm^2	Ab = 95 cm^2		
$f_{yc} = 275$ N/mm^2	$f_{yb} = 275$ N/mm^2		
	Wpl = 1660 cm^3		

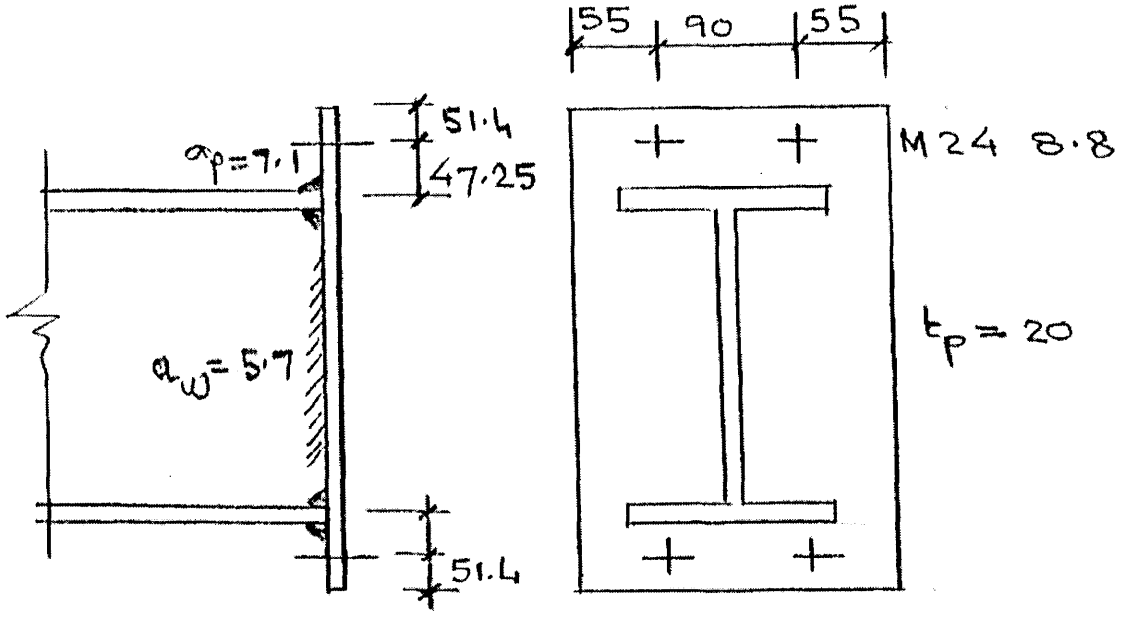

Design Moment resistance $M_{R,d}$ (J 5)

Column Web panel in Shear (J 3.5.2)

$$Vwp,Rd = \frac{0.9 f_{y,wc} A_{vx}}{\sqrt{3}\gamma_{Mo}}$$

$$A_{vc} = A_c = 2b_c t_{fc} + (t_{wc} + 2r_c)t_{fc} \qquad (5.4.6)$$

$= 11400 - 2 \times 255.9 \times 17.3 + (10.5 + 2 \times 12.7)17.3$

$= 3167$ mm^2

$$Vwp,Rd = \frac{0.9x275x3167x10^{-3}}{\sqrt{3}x1.1} = 411.4kN \qquad (5.1.1)$$

Column Web in Compression (J 3.5.3)

$$b_{eff} = t_{fb} + 2\sqrt{2}a_p + 2t_p + 5(t_{fc} + s)$$

$$= 14.5 + 2\sqrt{2}x7.1 + 2x20 + 5(17.3 + 12.7)$$
$$= 224.6 \text{ mm}$$

$\beta = 0$ (Table J4)
$\rho = 1$ (Table J5)

$$F_{c,wc,Rd} = \frac{\rho b_{eff} t_{ws} f_{y,wc}}{\gamma_{Mo}} = \frac{224.6x10.5x275x10^{-3}}{1.1} = 589.6kN$$

Beam Flange Web in Compression **(5.4.5.1)**

$$M_{c,Rd} = \frac{Wplf_y}{\gamma_{Mo}} = \frac{1660x10^3 x275x10^{-3}}{1.1} = 415000kNmm$$

$$F_{c,fb,Rd} = \frac{M_{c,Rd}}{h_b - t_{fb}} = \frac{415000}{457.2 - 14.5} = 937.4kN$$

Design Tension resistance of bolt row 1 **(J 3.6.2)**

(a) Column flange in bending (J 3.5.5)
e = 83
m = 29.6
e_{min} = 55
n = e_{min} but n less than or equal to 1.25 m
n = 1.25 x 29.6 = 37 mm

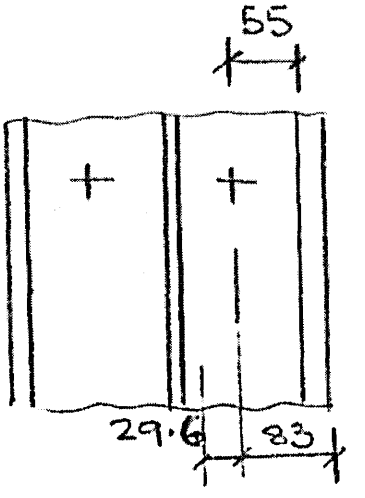

Effective Length::

$$l_{eff,cp} = 2\pi m = 2\pi x29.6 = 186.0mm$$

$$l_{eff,nc} = 4m + 1.25e = 222.2mm$$

For mode 1 $l_{eff,1} = 186.0mm$

For mode 2 $l_{eff,2} = 222.2mm$

Equivalent T-stub

$$M_{pl,1,Rd} = \frac{0.25\sum l_{eff,1} t_{fc}^{\ 2} f_{yc}}{\gamma_{Mo}} = \frac{0.25x186.0x17.3^2 x275x10^{-3}}{1.1} = 3479kNmm$$

$$M_{pl,2,Rd} = \frac{0.25 l_{eff,2} t_{fc}^{\ 2} f_{yc}}{\gamma_{Mo}} = \frac{0.25x222.2x17.3^2 x275x10^{-3}}{1.1} = 4156kNmm$$

$$B_{t,Rd} = \frac{0.9 f_{ub} A_s}{\gamma_{Mb}} = \frac{0.9x800x353x10^{-3}}{1.25} = 203.3kN \qquad \text{(Table 6.5.3)}$$

Design Tension Resistance
Mode 1:

$$F_{t,Rd} = \frac{4M_{pl,1,Rd}}{m} = \frac{4x3479}{29.6} = 470.1kN$$

Mode 2

$$F_{t,Rd} = \frac{2M_{pl,2,Rd} + n\sum B_{t,Rd}}{m+n} = \frac{2x4156 + 37x2x203.3}{29.6+37} = 350.7kN$$

Mode 3

$F_{t,Rd} = 2x203.3 = 406.6kN$

Therefore design resistance $F_{t1,fc,Rd} = 350.7kN(Mode2)$

(b) Column web in tension (J 3.5.6)

$$F_{t,wc,Rd} = \frac{\rho b_{eff} t_{wc} f_{y,wc}}{\gamma_{mo}} = \frac{1x186.0x10.5x275x10^{-3}}{1.1} = 488.3kN$$

(c) End plate in bending

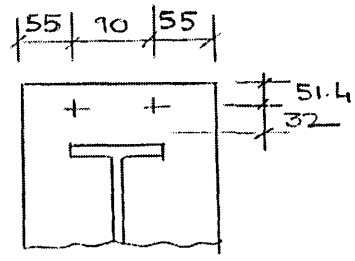

m_x = 40-0.8x10 = 32
e_x= 51.4
b_p = 200
w = 90
e = 55
e_{min}= e_x = 51.4 = n
n = less than equal to 1.25 m_x = 40

Effective length:

$2\pi m_x = 201.1$

$\pi m_x + w = 190.5$

$\pi m_x + 2e = 210.5$

Therefore $l_{eff,cp} = 190.5$ (Table J8)

$4m_x + 1.25e_x = 192.3$

$e + 2m_x + 0.625e_x = 151.1$

$0.5b_p = 100$

$0.5w + 2m_x + 0.625e_x = 141.1$

Therefore $l_{eff,nc} = 100$

$l_{eff,1} = 100$

$l_{eff,2} = 100$

Equivalent T-stub

$$M_{pl,1Rd} = M_{pl,2,Rd} = \frac{0.25\sum l_{eff,1} t_f^{\,2} f_y}{\gamma_{mo}} = \frac{0.25x100x20^2 x275x10^{-3}}{1.1} = 2500kNmm$$

$B_{t,Rd} = 203.3kN$

Design Tension Resistance

Mode 1

$$F_{t,Rd} = \frac{4x2500}{32} = 312.5kN$$

Mode 2

$$F_{t,Rd} = \frac{2x2500 + 40x2x203.3}{32 + 40} = 295.3kN$$

Mode 3

$F_{t,Rd} = 2x203.3 = 406.6kN$

Therefore design resistance $F_{t1,ep,Rd} = 295.3kN (Mode 2)$

Determination of $F_{t,Rd}$ **(Fig J 34)**

(J 3.6.2)

$V_{wp,Ed} / \beta = \frac{411.4}{0} = \alpha$ - No need to consider

$F_{c,wc,Rd} = 589.6kN$

$F_{c,fb,Rd} = 937.4kN$

$F_{t1,fc,Rd} = 350.7kN$

$F_{t1,wc,Rd} = 488.3kN$

$F_{t1,ep,Rd} = 295.3kN$

$F_{t1,Rd} = 295.3kN$ **(End Plate Failure)**

Design Moment Resistance **(J 32)**

$M_{j,Rd} = F_{t1,Rd} h_1 = 295.3x0.49 = 144.7kNm$

Stiffness Calculations

Elastic Stiffness Coefficient

Column web in compression (k_2)

$$k_2 = \frac{0.7b_{eff}t_{wc}}{d_c} = \frac{0.7x224.6x10.5}{200.4} = 8.24mm$$

$$b_{eff} = t_{fb} + 2\sqrt{2}a_p + 2t_p + 5(t_{fc} + s)$$

$$= 14.5 + 2\sqrt{2}x7.1 + 2x20 + 5(17.3 + 12.7)$$
$$= 224.6 \text{ mm}$$

Column flange in tension

$$k_3 = \frac{0.85l_{eff}t_{fc}^{\ 3}}{m^3} = \frac{0.85x186.0x17.3^3}{29.6^3} = 31.56mm$$

Column web in tension

$$k_4 = \frac{0.7b_{eff}t_{wc}}{d_c} = \frac{0.7x186.0x10.5}{200.4} = 6.82mm$$

End plate in tension

$$k_5 = \frac{0.85l_{eff}t_{fc}^{\ 3}}{m^3} = \frac{0.85x100x20^3}{32^3} = 20.75mm$$

Bolts in Tension

$$k_7 = \frac{1.6A_s}{l_b} = \frac{1.6x353}{54.75} = 10.32mm$$

$l_b = t_{fc} + t_p + t_{wb} = 17.3+20+17.45 = 54.75$

$$\sum \frac{1}{k_i} = \frac{1}{8.24} + \frac{1}{31.56} + \frac{1}{6.82} + \frac{1}{20.75} + \frac{1}{10.32} = 0.445mm^{-1}$$

Rotational Stiffness

$$S_{ji} = \frac{210000x490^2}{0.445} x10^{-9} = 113.3MNm/rad$$

$$S_j = \frac{113.3}{3} = 37.8MNm/rad$$

Rotation Capacity (J5 6a, 6b)

(a) Design moment resistance is governed by the resistance of the end plate

(b) $0.36d\sqrt{\frac{fub}{fy}} = 0.36x24x\sqrt{\frac{800}{275}} = 14.7mm$

t_{fc}=17.3 mm, t_p=20

$$t > 0.36d\sqrt{\frac{fub}{fy}}$$

Hence rotation capacity is inadequate for plastic analysis
Test results indicate adequate capacity

Example of Extended End Plate

Column **254 x 254 UC 89**	**Beam** **457 x191 UB 74**	**End Plate** **640 x 200 x15**	**Bolts** **8M24-8.8**
$h_c = 260.4$	$h_b = 457.2$	$b_p = 200$	$d_n = 24$ mm
$b_c = 255.9$	$b_b = 190.5$	$t_p = 15$	$As = 353$ mm^2
$t_{fc} = 17.3$	$t_{fb} = 14.5$	$f_{yp} = 275$ N/mm^2	$f_{ub} = 800$ N/mm^2
$t_{wc} = 10.5$	$t_{wb} = 9.1$		
$t_c = 12.7$	$t_b = 10.2$		
$A_c = 114$ cm^2	Ab = 95 cm^2		
$f_{yc} = 275$ N/mm^2	$f_{yb} = 275$ N/mm^2		
	Wpl = 1660 cm^3		

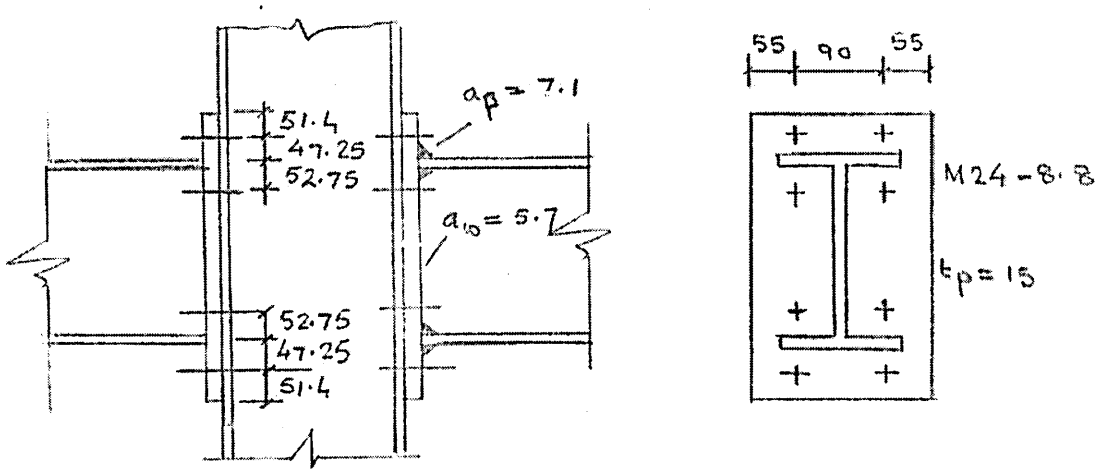

Design Moment resistance $M_{R,d}$

Determinataion of n_{bt}

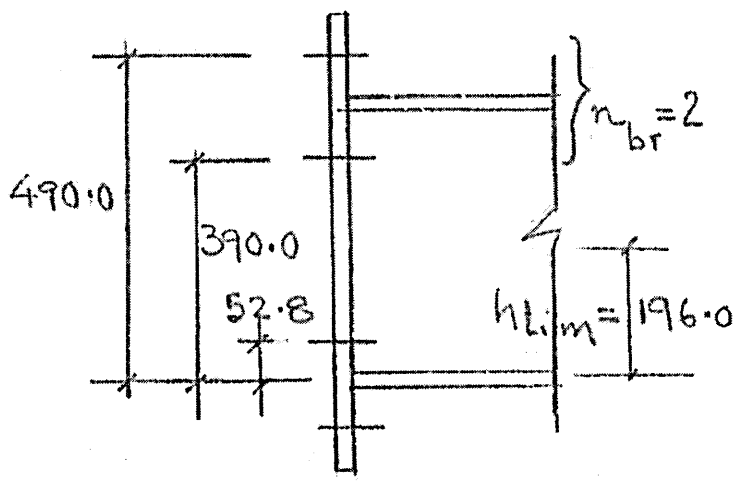

$h_{lim} = 0.4h_1 = 0.4 \times 490.0 = 196.0$

Column Web panel in Shear **(J 3.5.2)**

$$Vwp,Rd = \frac{0.9 f_{y,wcAvc}}{\sqrt{3}\gamma_{Mo}}$$

$$A_{vc} = A_c = 2b_c t_{fc} + (t_{wc} + 2r_c)t_{fc} \qquad (5.4.6)$$
$$= 11400 - 2 \text{ x } 255.9 \text{ x}17.3 + (10.5 + 2\text{x}12.7)17.3$$
$$= 3167 \text{ mm}^2$$

$$Vwp,Rd = \frac{0.9x275x3167x10^{-3}}{\sqrt{3}x1.1} = 411.4kN \qquad (5.1.1)$$

Column Web in Compression **(J 3.5.3)**

$$b_{eff} = t_{fb} + 2\sqrt{2}a_p + 2t_p + 5(t_{fc} + s)$$

$$= 14.5 + 2\sqrt{2}x7.1 + 2x15 + 5(17.3 + 12.7)$$
$$= 214.6 \text{ mm}$$

$\beta = 0$ (Table J4)

$\rho = 1$ (Table J5)

$$F_{c,wc,Rd} = \frac{\rho b_{eff} t_{ws} f_{y,wc}}{\gamma_{Mo}} = \frac{1x214.6x10.5x275x10^{-3}}{1.1} = 563.3kN$$

Beam Flange Web in Compression **(J 3.5.4)(5.4.5.1)**

$$M_{c,Rd} = \frac{Wplf_y}{\gamma_{Mo}} = \frac{1660x10^3 x275x10^{-3}}{1.1} = 415000kNmm$$

$$F_{c,fb,Rd} = \frac{M_{c,Rd}}{h_b - t_{fb}} = \frac{415000}{457.2 - 14.5} = 937.4kN$$

Design Tension resistance of bolt row 1 **(J 3.6.2)**

(a) Column flange in tension (J 3.5.5)
e = 83 mm
m = 29.5 mm
e_{min} = 55 mm
n = e_{min} but n less than or equal to 1.25 m
n = 1.25 x 29.5 = 36.9 mm

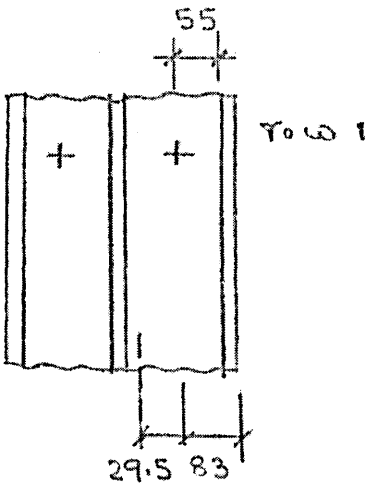

Effective Length:

$$l_{eff,cp} = 2\pi m = 2\pi x29.5 = 185.4mm$$

$$l_{eff,nc} = 4m + 1.25e = 4x29.5 + 1.25x83 = 221.8mm$$

For mode 1 $l_{eff,1} = 185.4mm$

For mode 2 $l_{eff,2} = 221.8mm$

Equivalent T-stub

$$M_{pl,1,Rd} = \frac{0.25\sum l_{eff,1} t_{fc}^{\ 2} f_{yc}}{\gamma_{Mo}} = \frac{0.25x185.4x17.3^2 x275x10^{-3}}{1.1} = 3468kNmm$$

$$M_{pl,2,Rd} = \frac{0.25 l_{eff,2} t_{fc}^{\ 2} f_{yc}}{\gamma_{Mo}} = \frac{0.25x221.8x17.3^2 x275x10^{-3}}{1.1} = 4149kNmm$$

$$B_{t,Rd} = \frac{0.9 f_{ub} A_s}{\gamma_{Mb}} = \frac{0.9x800x353x10^{-3}}{1.25} = 203.3kN$$ (J3.2.1)(Table 6.5.3)

Design Tension Resistance
Mode 1:

$$F_{t,Rd} = \frac{4M_{pl,1,Rd}}{m} = \frac{4x3468}{29.5} = 470.2kN$$

Mode 2

$$F_{t,Rd} = \frac{2M_{pl,2,Rd} + n\sum B_{t,Rd}}{m+n} = \frac{2x4149 + 36.9x2x203.3}{29.5 + 36.9} = 350.9kN$$

Mode 3

$F_{t,Rd} = 2x203.3 = 406.6kN$

Therefore design resistance $F_{t1,fc,Rd} = 350.9kN(Mode2)$

(b) Column web in tension **(J 3.5.6)**

$$F_{t,wc,Rd} = \frac{\rho b_{eff} t_{wc} f_{y,wc}}{\gamma_{mo}} = \frac{1x185.9x10.5x275x10^{-3}}{1.1} = 488.04kN$$

(c) End plate in tension

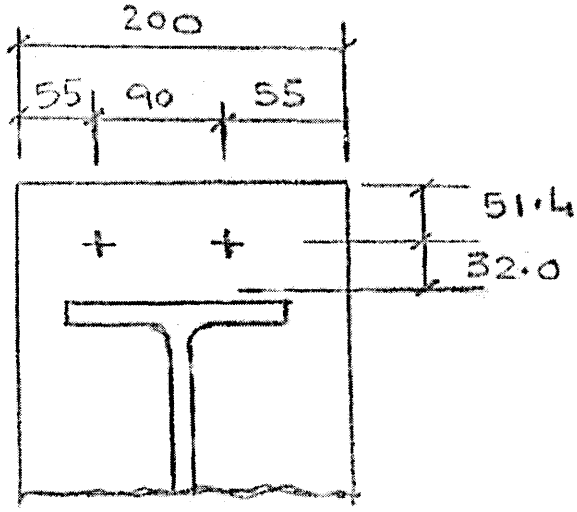

$m_x = 40\text{-}0.8x10 = 32$ mm
$e_x = 51.4$ mm
$b_p = 200$ mm
$w = 90$ mm
$e = 55$ mm
$e_{min} = e_x = 51.4 = n$ (J 3.2.1)
n = less than equal to $1.25\ m_x = 40$ mm

Effective length: Bolt row outside tension flange of beam (Table J8)

$2\pi m_x = 201.1$ mm

$\pi m_x + w = 190.5$ mm

$\pi m_x + 2e = 210.5$ mm

Therefore $l_{eff,cp} = 190.5$ mm

$4m_x + 1.25e_x = 192.3$ mm

$e + 2m_x + 0.625e_x = 151.1$ mm

$0.5b_p = 100$ mm

$0.5w + 2m_x + 0.625e_x = 141.1$ mm

Therefore $l_{eff,nc} = 100$

$l_{eff,1} = 100$

$l_{eff,2} = 100$

Equivalent T-stub

$$M_{pl,1Rd} = M_{pl,2,Rd} = \frac{0.25\sum l_{eff,1} t_f{}^2 f_y}{\gamma_{mo}} = \frac{0.25x100x15^2 x275x10^{-3}}{1.1} = 1406.3kNmm$$

$B_{t,Rd} = 203.3kN$

Design Tension Resistance

Mode 1

$$F_{t,Rd} = \frac{4x1406.3}{32} = 175.8kN$$

Mode 2

$$F_{t,Rd} = \frac{2x1406.3 + 40x2x203.3}{32 + 40} = 265.0kN$$

Mode 3

$F_{t,Rd} = 2x203.3 = 406.6kN$

Therefore design resistance $F_{t1,cp,Rd} = 175.8kN$ (Mode 1)

Beam web in tension **(J 3.5.8)**

$b_{eff} = l_{eff} = 100mm$

$$F_{t1,wb,Rd} = \frac{b_{eff} t_{wb} f_{y,wb}}{\gamma_{mo}} = \frac{100x9.1x275x10^{-3}}{1.1} = 227.5kN$$ (Eq. (J31))

Determination of $F_{t,Rd}$ **(Fig J34)**
(J 3.6.2)

$V_{wp,Ed} / \beta = \frac{411.4}{0} = \alpha$ - No need to consider

$F_{c,wc,Rd} = 563.3kN$

$F_{c,fb,Rd} = 937.4kN$

$F_{t1,fc,Rd} = 350.9kN$

$F_{t1,wc,Rd} = 488.04kN$

$F_{t1,cp,Rd} = 175.8kN$

$F_{t1,wb,Rd} = 227.5kN$

$F_{t1,Rd} = 175.8kN$ **(End Plate Failure, mode 1)**

Design tension resistance of bolt row 2

Bolt row 2 individually
Column flange in tension(as bolt row 1)
Therefore design resistance $F_{t2,fc,Rd} = 350.9kN(Mode2)$

Column web in tension(as bolt row 1) **(J 3.5.6)**
$F_{t2,wc,Rd} == 488.04kN$

End plate in tension

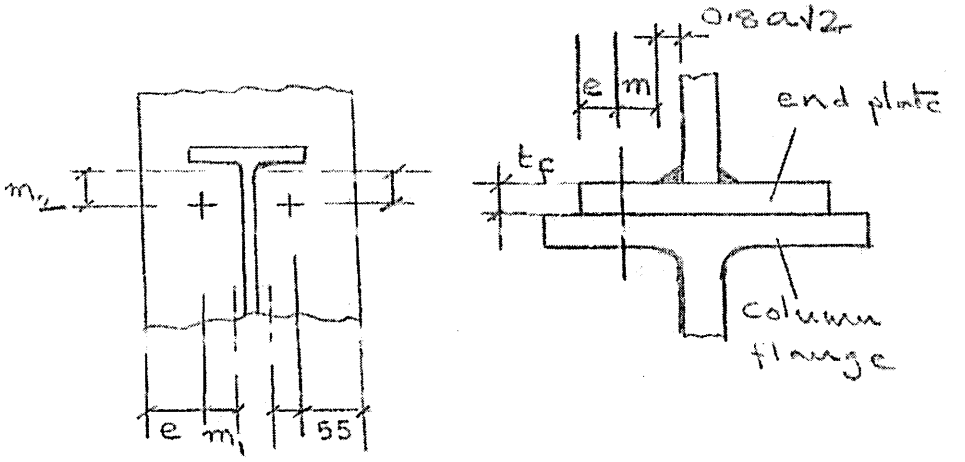

$$m_1 = 45 - \frac{9.1}{2} - 0.8x8 = 34.1mm$$

e = e_{min}= 55 mm
n = e_{min}= 55 mm
$n \le 1.25m = 1.25x34.1 = 42.6mm$
n = 42.6
m_2 = 60 –14.5-0.8x10 = 37.5 mm

$$\lambda_1 = \frac{m_1}{m_1 + e} = \frac{34.1}{34.1 + 55} = 0.38$$ (Fig J 27)

$$\lambda_2 = \frac{m_2}{m_1 + e} = \frac{337.5}{34.1 + 55} = 0.42$$

$\alpha = 6.7 > 2\pi$

$l_{eff,1} = \min(2\pi m, \alpha m) = 2\pi x34.1 = 214.3mm$
$l_{eff,2} = \alpha m = 6.7x34.1 = 228.5mm$

Equivalent T-stub

$$M_{pl,1Rd} = \frac{0.25\sum l_{eff,1} t_f^{\,2} f_y}{\gamma_{mo}} = \frac{0.25x214.3x15^2 x275x10^{-3}}{1.1} = 3014kNmm$$

$$M_{pl,2,Rd} = \frac{0.25\sum l_{eff,2} t_f^{\,2} f_y}{\gamma_{mo}} = \frac{0.25x228.5x15^2 x275x10^{-3}}{1.1} = 3213kNmm$$

Mode 1

$$F_{t,Rd} = \frac{4M_{pl,1,Rd}}{m_1} = \frac{4x3014}{34.1} = 353.5kN$$

Mode 2

$$F_{t,Rd} = \frac{2M_{pl,2,Rd} + n\sum B_{t,Rd}}{m_1 + n} = \frac{2x3213 + 42.6x2x203.3}{34.1 + 42.60} = 309.6kN$$

Mode 3

$$F_{t,Rd} = \sum B_{t,Rd} = 2x203.3 = 406.6kN$$

Therefore design resistance $F_{t,cp,Rd} = 309.6kN$ (Mode 2)

Beam web in tension **(J 3.5.8)**

$b_{eff} = l_{eff} = 228.5mm$

$$F_{t1,wb,Rd} = \frac{b_{eff} t_{wb} f_{y,wb}}{\gamma_{mo}} = \frac{228.5x9.1x275x10^{-3}}{1.1} = 519.8kN \qquad \text{(Eq. (J31))}$$

Bolt Groups, Row 1 and Row 2

Column flange in tension (Fig. J 25)

e = 83 mm
e_{min}=55 mm
m = 29.5
p = 100
n = e_{min}=55 mm

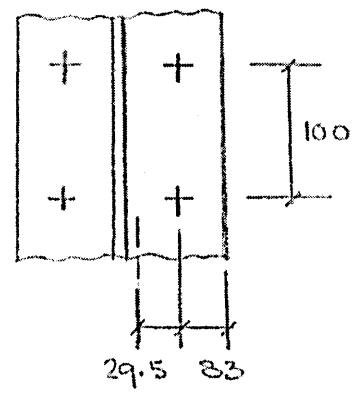

$n \le 1.25m = 1.25x29.5 = 36.9mm$

Effective length
Bolt rows as part of a bolt group
(Row 1 = Row 2= End bolt row)

$l_{eff,1} = \min(\pi m + p, 2m + 0.625e + 0.5p)$

$l_{eff,2} = 0.625e + 0.5p$

$\pi m + p = \pi x 29.5 + 100 = 192.7mm$
$2m + 0.625e + 0.5p = 2x29.5 + 0.625x83 + .5x100 = 160.9mm$

$l_{eff,1} = 2x160.9 = 321.8mm$
$l_{eff,2} = 2x160.9 = 321.8mm$

Equivalent T-Stub

$$M_{pl,1Rd} = \frac{0.25\sum l_{eff,1} t_{fc}^{\ 2} f_{yc}}{\gamma_{mo}} = \frac{0.25x321.8x17.3^2 x275x10^{-3}}{1.1} = 6019kNmm$$

$M_{pl,2,Rd} = 6019kNmm$

Mode 1

$$F_{t,Rd} = \frac{4M_{pl,1,Rd}}{m_1} = \frac{4x6019}{29.5} = 816.1kN$$

Mode 2

$$F_{t,Rd} = \frac{2M_{pl,2,Rd} + n\sum B_{t,Rd}}{m_1 + n} = \frac{2x6019 + 36.9x4x203.3}{29.5 + 36.9} = 633.2kN$$

Mode 3

$F_{t,Rd} = \sum B_{t,Rd} = 4x203.3 = 813.2kN$

Therefore design resistance =633.2 kN (Mode 2)

Column web in tension **(J 3.5.6)**

$b_{eff} = l_{eff} = 321.8mm$

$\rho = 1$ (Table J5)

$$F_{t2,wc,Rd} = \frac{\rho b_{eff} t_{wc} f_{y,wc}}{\gamma_{mo}} = \frac{1x321.8x10.5x275x10^{-3}}{1.1} = 844.7kN$$

End plate in tension
Not Relevant.

Determination of $F_{t2,Rd}$

$F_{t2,fc,Rd} = 350.9kN$

$F_{t2,wc,Rd} = 488.04kN$

$F_{t2,ep,Rd} = 309.6kN$

$F_{t2,wb,Rd} = 519.8kN$

Therefore $F_{t2,Rd}$ = 309.6 kN (End plate failure, mode 2) **(J 3.6.2) (4 & 5)**

$\sum F_{t,Rd} = 175.8 + 309.6 = 485.4$ kN (J 3.6.2) (6)

$V_{wp,Ed} / \beta = \frac{411.4}{0} = \alpha > 485.4$ kN

$F_{c,wc,Rd} = 563.3kN > 485.4$ kN

$F_{c,fb,Rd} = 937.4kN > 485.4$ kN

Bolt Group **(J 3.6.2) (7)**

$F_{t2,fc,Rd} = 633.2kN > 485.4$ kN

$F_{t2,wc,Rd} = 844.7kN > 485.4$ kN

$1.9B_{t,Rd} = 1.9x203.3 = 386.3kN$ (J 3.6.2) (8)

$F_{t1,Rd} = 175.8kN < 389.3$ kN

$F_{t2,Rd} = 309.6kN$ (End plate failure, Mode 2)

Design Moment Resistance **(J 32)**

$M_{j,Rd} = \sum_r h_r F_{tr,Rd} = 175.8x0.49 + 309.6x0.39 = 206.9 = 206.9kNm$

Design Shear Resistance V_{Rd} (J 3.1.2)

Bolt Rows (6.5.5) (Table 6.5.3)

$V_{b,Rd} = \frac{0.6 f_{ub} A_s}{\gamma_{Mb}} = \frac{0.6x800x353x10^{-3}}{1.25} = 135.6kN$ (6.1.1)

Bolt rows 1 and 2 are subjected to tension forces, bolt row 3 and 4 are not required to resist tension

$V_{b,Rd} = (4 + 4x\frac{0.4}{1.4})135.6 = 697.4kN$

Beam web (5.4.6)

$A_{vb} = A_b - 2b_b t_{fb} + (t_{wb} + 2\gamma_b) t_{fb}$

$= 9500 - 2x190.5 \times 14.5 + (9.1 + 2x10.2)\ 14.5$

$= 4403.3$ mm^2

Part of the beam web which is subjected to tension forces-

e = 55mm

m=34.1mm

L_1= 60+ 2x34.1+ 0.625x 55= 162.6mm (2.2.5.1 c)

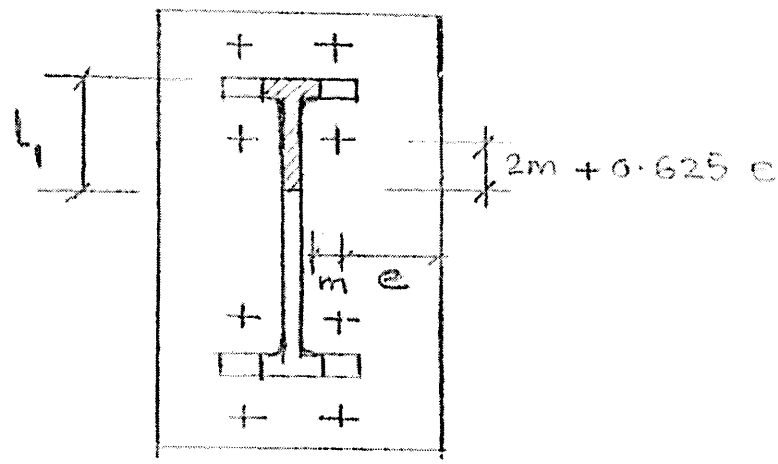

$$L_1 = \frac{162.6}{457.2} h_b = 0.36 h_b$$

L_2 =(1-0.36) h_b = 0.64h_b

$$V_{wb,Rd} = \frac{A_{vb} f_{ywb}}{v3\gamma_{Mo}} = 0.36 h_b$$

$$= (0.5x0.36 + 0.64)\frac{4403.3x275}{\sqrt{3}x1.1} X10^{-3}$$ (5.4.6)

=521.1kN

Determination of V_{Rd}

V_{Rd} = Smallest of $V_{b,Rd}$ &$V_{wb,Rd}$

= 521.2kN

Welds

Beam Flange – end plate in tension **(6.6.5.3)**

$$F_{w,Rd} = \frac{f_u a L_w}{v3\beta_w \gamma_{MW}}$$ (6.1.1)

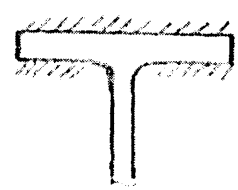

L_w = $2b_b - 2r_b - t_{wb}$

= 2 x 190.5- 2 x 10.2- 9.1 =351.5mm

$$F_{w,Rd} = \frac{390x7.1x351.5}{\sqrt{3}x0.8x1.25} x10^{-3} = 561.9kN$$

$F_{w,sd} = f_{t1,Rd} = 175.8$ kN < 561.9 kN therefore OK

Beam web – end plate in tension and shear

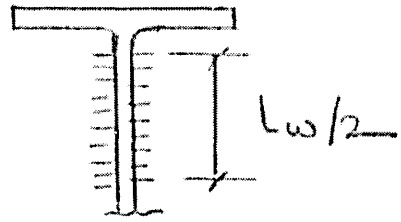

36% of the beam depth is subjected to tension and shear force

$l_w = 0.36(h_b - 2(t_{fb}+r_b))^2$
$= 0.36(457.2 - 2 x14.5 - 2 x10.2)^2$
$= 293.6mm$

$$F_{w,Rd} = \frac{f_u a l_w}{\sqrt{3}\beta_w r_{MW}} = \frac{390x5.7x293.6}{\sqrt{3}x0.8x1.25} x10^{-3} = 376.8kN$$

Maximum applied forces :

Tension: $F_{t2, Rd} = 309.6$ kN

Shear: Bolt row 1 and 2

$$V_{Rd} = 4x\frac{0.4}{1.4} x135.6 = 155.0kN$$

$$F_{w,Sd} = \sqrt{309.6^2 + 155.0^2} = 346.2kN < 376.8 \text{ kN therefore OK}$$

Bean web – end plate in shear

$L_w = 0.64 (457.2 - 2 x14.5 - 2x 10.2)^2$
$= 522.0$ mm

$$F_{w,Rd} = \frac{390x7.1x522}{\sqrt{3}x0.8x1.25} x10^{-3} = 834.5kN$$

$F_{w, Sd} = 4 x135.6 = 542.4$ kN . < 834.5 kN therefore OK

Beam Flange – end plate in compression

$F_{w, Rd} = 561.9$ kN

$F_{w, Sd} = F_{t1, Rd} + f_{t2, Rd}$
$= 175.8 + 309.6 = 485.4$ kn

Less than 561.9 kN therefore OK

Stiffness Calculations

Elastic Stiffness Coefficient

Column web in compression (k_2)

$$k_2 = \frac{0.7 b_{eff} t_{wc}}{d_c} = \frac{0.7x214.6x10.5}{200.4} = 7.87mm$$

$$b_{eff} = t_{fb} + 2\sqrt{2}a_p + 2t_p + 5(t_{fc} + s)$$

$$= 14.5 + 2\sqrt{2}x7.1 + 2x15 + 5(17.3 + 12.7)$$
$$= 214.6 \text{ mm}$$

Column flange in tension

$$k_3 = \frac{0.85 l_{eff} t_{fc}^{\ 3}}{m^3} = \frac{0.85x160.9x17.3^3}{29.5^3} = 27.58mm$$

Individually min l_{eff} for each bolt row = 185.4 mm (2.2.4)
As part of a bolt group min l_{eff} for each bolt row = 160.9 mm (2.2.5.2)

Column web in tension

$$k_4 = \frac{0.7 b_{eff} t_{wc}}{d_c} = \frac{0.7x160.9x10.5}{200.4} = 5.90mm$$

$dc = h_c - 2(t_{fc} + r_c)$

$= 160.4 - 2(17.3+12.7) = 200.4$ mm

End plate in tension

$$k_{5,1} = \frac{0.85 l_{eff} t_{fc}^{\ 3}}{m^3} = \frac{0.85x100x15^3}{32^3} = 8.75mm$$

Bolt row 1 l_{eff}= 100 mm 2.2.4 (c)
m = 32 mm

$$k_{5,2} = \frac{0.85 l_{eff} t_{fc}^{\ 3}}{m^3} = \frac{0.85x214.3x15^3}{34.1^3} = 15.50mm$$

Bolt row 2 l_{eff}= 214.3 mm 2.2.5.1 (c)
m = 34.1 mm

Bolts in Tension

$$k_7 = \frac{1.6A_s}{l_b} = \frac{1.6x353}{49.75} = 11.35mm$$

$l_b = t_{fc} + t_p + t_{wb} = 17.3+15+17.45 = 49.75mm$

Equivalent stiffness coeffficent

Bolt Row 1

$$\sum \frac{1}{k_i} = \frac{1}{\frac{1}{27.58}+\frac{1}{5.90}+\frac{1}{8.75}+\frac{1}{11.35}} = 2.45mm$$

Bolt Row 2

$$\sum \frac{1}{k_i} = \frac{1}{\frac{1}{27.58}+\frac{1}{5.90}+\frac{1}{15.50}+\frac{1}{11.35}} = 2.79mm$$

Lever arm

$$z = \frac{k_{eff,r1}h_1^2 + k_{eff,r2}h_2^2}{k_{eff,r1}h_1 + k_{eff,r2}h_2} = \frac{2.45x490^2 + 2.79x390^2}{2.45x490 + 2.79x390} = 442.5mm$$

$h_1 = 457.2+40-0.5x14.5 = 490.0$ mm
$h_2 = 457.2-60-0.5x14.5 = 390.0$ mm

$$k_{eq} = \frac{k_{eff,r1}xh_1 + k_{eff,r2}xh_2}{z} = \frac{2.45x490 + 2.79x390}{442.5} = 5.17mm$$

Design Rotational Stiffness **(J 4.1)**

$$S_{ji} = \frac{Ez^2}{\mu(\frac{1}{k_2}+\frac{1}{k_{eq}})} = \frac{210000x442.5^2}{\frac{1}{7.87}+\frac{1}{5.17}} x10^{-9} = 128.3MNm/rad$$

Initial stiffness $= \mu = 1$

$$S = \frac{128.3}{3} = 42.8MNm/rad$$

Secant stiffness
$M = M_{RD}$

$$\mu = (\frac{1.5M_{j,sd}}{M_{j,RD}})^{2.7} = (1.5)^{2.7} = 3$$

Rotation Capacity (J5 6a, 6b)

(a) Design moment resistance is governed by the resistance of the end plate

(b) $0.36d\sqrt{\frac{fub}{fy}} = 0.36x24x\sqrt{\frac{800}{275}} = 14.7mm$ (J48)

t_{fc}=17.3 mm, t_p=15

$$t > 0.36d\sqrt{\frac{fub}{fy}}$$

Hence rotation capacity is inadequate for plastic analysis

APPENDIX C

Appendix C

Example Statistical Calculations

Test No	Experimental Ultimate Moment KNm	Numerical 3D Non- Modified Ultimate Moment KNm	Percentage difference
1	279	317	-13.62
2	161.4	195.65	-21.22
3	165.6	180	-8.70
4	412.8	417	**-1.02 (Lowest)**
5	282	391.5	**-38.83 (Highest)**
6	688.6	818	-18.79
7	557.4	616	-10.51
		Total	**-112.69**

Example Calculation

Test 1

Percentage difference based on Experimental results

$$\frac{ExpeimentalMoment - NumericalMoment}{ExperimentalMoment} * 100 = \frac{279 - 317}{279} * 100 = -13.62$$

Mean (Average)

Total number of connections 7
Percentage difference total –112.68

$$mean = \frac{\text{Sum of all tests}}{\text{Sample population}} \frac{-112.69}{7.} = -16.1$$

Range

To obtain the range the lowest and highest values are found
Therefore the range is –38.83 to –1.02